An Investigation of Genetic Variation in Complex Disorders of the Pituitary Gland

Emanuela Spadoni

UCL

MPhil

Declaration

I, **Emanuela Spadoni**, confirm that the work presented in this thesis is my own. Where information has been derived from other sources, I confirm that this has been indicated in the thesis.

Abstract

Congenital hypopituitarism can be triggered by environmental insults, such as viral infections, vascular or degenerative damage and exposure to alcohol and drugs. Genetic mutations have been identified in genes responsible for pituitary development and function, however, only up to 10% of patients affected by hypopituitarism have recognised mutations in known genes. Clinical phenotypes may arise from gene dosage imbalance, but routine cytogenetic and molecular techniques can be insufficiently sensitive to detect chromosome rearrangements that are either submicroscopic in size or limited to a specific genomic locus or both.

In the present study, ten patients with a complex pathology of the pituitary gland of unknown aetiology were clinically pre-selected according to a criteria checklist, to undergo a genome-wide screening of copy number changes with high-resolution 250K SNP array. Genomic sequencing of three candidate genes, *BARX2*, *OTX2* and *BMP4*, was carried out in larger cohorts of selected patients.

Three pathogenic genomic imbalances, chromosome 6q terminal duplication, chromosome 11q terminal deletion, and an interstitial deletion of chromosome 22q were detected in two patients, and the breakpoints were defined at high resolution. A submicroscopic rearrangement in the chromosome region 1p36.33 was found in a patient presenting with the association of hypopituitarism and tetralogy of Fallot. Two CNVs were found at the location of the breakpoints of a cytogenetically visible translocation between chromosomes 11q and 22q in one patient. One region of genomic imbalance, identified in one patient, contained the whole length of the *ENG* gene. A novel amino acid change was identified in *BARX2* in a patient with isolated hypopituitarism. A novel nonsense mutation was found in *OTX2* in a patient with pathology of the pituitary gland associated wth severe eye defects.

These findings contribute to the understanding of the genetic bases of congenital hypopituitarism.

Table of Contents

List of Tables

List of Figures

List of Abbreviations

ACC: Agenesis of Corpus Callosum

ACTH: Adrenocorticotrophic Hormone

AP: Anterior Pituitary

APH: Anterior Pituitary Hypoplasia

ASD: Autism Spectrum Disorder

AVP: Arginine Vasopressin

BAC: Bacterial Artificial Chromosome

BARX2: BarH-like homeobox gene 2

BLAST: Basic Local Alignment Search Tool

BMP: Bone Morphogenetic Protein

bp: base pair

CACNG2: Calcium Channel, voltage-dependent, Gamma-2

CAH: Congenital Adrenal Hypoplasia

CDGP: Constitutional Delay of Growth and Puberty

CEU: Northern and Western European

CGH: Comparative Genomic Hybridisation

CHB: Chinese

CHD: Congenital Heart Defect

CN: Copy Number

CNAG: Copy Number Analyser for GeneChip

CNAT: Copy Number Analysis Tool

CNS: Central Nervous System

CNV: Copy Number Variation

CPHD: Combined Pituitary Hormone Deficiency

CS: Carnegie Stage

DI: Diabetes Insipidus

DD: Developmental Delay

ddH2O: double distilled water

DGV: Database of Genomic Variants

DLG: Discs Large, drosophila, homolog of

DLGAP2: Discs Large-Associated Protein 2

DM: Dynamic Model

DMSO: Dimethyl Sulfoxide

DNA: DeoxyriboNucleic Acid

DNAseI: Deoxyribonuclease I

dNTPs: deoxynucleoside riphosphates

dpc: days post coitum

DSB: Double-Strand Break

EDTA: EthyleneDiamineTetracetic Acid

EIF3D: Eukaryotic translation Initiation Factor 3, subunit D

ENG: Endoglin

EPP: Ectopic Posterior Pituitary

EtBr: Ethiudium Bromide

ExoI: Exonuclease I

FA: Fanconi Anemia

FAD: Flavin Adenine Dinucleotide

FGF: Fibroblast Growth Factor

FISH: Fluorescent In Situ Hybridisation

FLI1: Friend Leukemia virus Integration 1

FoSTeS: Fork Stalling and Template Switching

FOXRED2: FAD-dependent OxidoReductase 2

FSH: Follicle-Stimulating Hormone

Fshb: Follicle-stimulating hormone, beta polypeptide

GATA2: GATA-binding protein 2

GCOS: GeneChip Operating Software

GH: Growth Hormone

GHD: Growth Hormone Deficiency

GHNSD: Growth Hormone NeuroSecretory Dysfunction

GLI: GLI-Kruppel family member

GnRH: Gonadotropin-Releasing Hormone

GPR98: G Protein-coupled Receptor 98

GS: Genomic Smoothing

GTYPE: GeneChip Genotyping Software

HESX1: Homeobox gene expressed in ES cells

HH: Hypogonadotropic Hypogonadism

HHT1: Hereditary Hemorrhagic Telangiectasia type 1

HLA: Human Leukocyte Antigen

HMM: Hidden Markov Model

HPE: Holoprosencephaly

ID: Identification

IDDM: Insulin-Dependent Diabetes Mellitus

IGFBP3: Insulin-like Growth Factor Binding Protein 3

IGF1: Insulin-like Growth Factor 1

IGHD: Isolated Growth Hormone Deficiency

IRBP: Interstitial Retinoid-Binding Protein

IRF6: Interferon Regulatory Factor 6

IRGM: Immunity-Related GTPase family, M

ISCN: International System for human Cytogenetic Nomenclature

ISL1: ISL LIM homeobox 1

IUGR: IntraUterine Growth Retardation

JMML: Juvenile MyeloMonocytic Leukemia

JPT: Japanese

KALIG1: Kallmann syndrome Interval Gene 1

KIRREL: Kin of IRRE-Like

kb: kilobase

LCR: Low Copy Repeat

LH: Luteinizing Hormone

Lhb: Luteinizing hormone, beta polypeptide

LHX: LIM Homeobox gene

log: logarithmic

LOH: Loss Of Heterozygosity

LYSMD3: LysM, putative peptidoglycan-binding, Domain containing 3

Mb: Megabase

MC2R: MelanoCortin 2 Receptor

MCA: Multiple Congenital Anomalies

MCPH1: Microcephalin 1

MDS: MyeloDysplastic Syndrome

MHA: May-Hegglin Anomaly

MLPA: Multiplex Ligation-dependent Probe Amplification

MM: MisMatch

MMBIR: Microhomology-Mediated Break-Induced Replication

MMEJ: Microhomology-Mediated End Joining

MR: Mental Retardation

MRI: Magnetic Resonance Imaging

MSH: Melanocyte-Stimulating Hormone

MUSCLE: Multiple Sequence Comparison by Log-Expectation

MYH9: Myosin Heavy chain 9

NAHR: Non-Allelic Homologous Recombination

NCBI: National Center for Biotechnology Information

NHEJ: Non-Homologous End Joining

OMIM: Online Mendelian Inheritance in Man

ONH: Optic Nerve Hypoplasia

OTX2: Orthodenticle, drosophila homolog of, 2

PAX6: Paired Box gene 6

PCR: Polymerase Chain Reaction

PITX: Paired-like homeodomain Transcription Factor

PLXDC2: Plexin Domain-Containing protein 2

PM: Perfect Match

POMC: Proopiomelanocortin

POU1F1: POU domain, class 1, transcription Factor 1

PPM1K: Protein Phosphatase, PP2C domain-containing, 1K

PRL: Prolactin

PROP1: Prophet of Pit1

PTCHD1: Patched Domain-containing protein 1

PTPN11: Protein-Tyrosine Phosphatase, Nonreceptor-type, 11

REBASE: Restriction Enzyme data BASE

RNA: RiboNucleic Acid

RUNX1: Runt-related transcription factor 1

SAP: Shrimp Alkaline Phosphatase

SD: Standard Deviation

SF1: Steroidogenic Factor 1

SHANK2: SH3 and multiple Ankyrin repeat domains 2

SHH: Sonic Hedgehog

SIX: Sine oculis homeobox, drosophila homolog of

SNP: Single Nucleotide Polymorphism

SOD: Septo-Optic Dysplasia

SOX: SRY-BOX

SYNGAP1: Synaptic RAS-GTPase-Activating Protein 1

TBE: Tris/Borate/EDTA

TBX: T-BOX

TE: Tris-EDTA

Thr: Threonine

ToF: Tetralogy of Fallot

TRH: Thyrotropin-Releasing Hormone

TSH: Thyroid-Stimulating Hormone

TSHD: Thyroid-Stimulating Hormone Deficiency

Tshb: Thyroid-stimulating hormone, beta chain

TSPAN8: Tetraspanin 8

TXN2: Thioredoxin 2

UCSC: University of California Santa Cruz

UPD: UniParental Disomy

UTR: UnTranslated Region

UV: UltraViolet

WGTP: Whole Genome TilePath

VSD: Ventricular Septal Defect

WNT: Wingless-Type MMTV integration site family

VSD: Ventricular Septal Defect

YRI: Yoruban

Note: measure units were used according to The International System of Units (SI).

1. INTRODUCTION

1.1. Pituitary Gland

The pituitary gland is a central regulator of growth, reproduction, metabolism and stress responses, and functions to relay signals from the hypothalamus to peripheral organs. It is situated within the sella turcica, a recess in the sphenoid bone, at the base of the brain. The hypothalamus is the principal neural structure regulating homeostasis in vertebrates, coordinating complex signals from other regions of the brain and the periphery. The hypothalamus releases factors that control the endocrine activity of the pituitary cells. [1]

1.1.1. Anatomy and Physiology of the Pituitary Gland

The pituitary gland is formed by the juxtaposition of the adenohypophysis (anterior and intermediate lobes) and the neurohypophysis (posterior lobe).

The anterior pituitary consists of five different endocrine cell types secreting six hormones: somatotrophs that secrete growth hormone (GH), lactotrophs that secrete prolactin (PRL), thyrotrophs that secrete thyroid-stimulating hormone (TSH), gonadotrophs that secrete both gonadotrophins, follicle-stimulating hormone (FSH) and luteinizing hormone (LH), and corticotrophs that secrete adrenocorticotrophin (ACTH). [2]

Somatotrophs are the majority of adenohypophyseal secretory cells comprising nearly 50% of all anterior pituitary cells. Lactotrophs embryologically arise from GH-producing cells, and constitute about 15-20% of the anterior pituitary cell population, although pregnancy and lactation alter the number of maternal lactotrophs. Corticotrophs and gonadotrophs represent 15-20% and 10-15% of anterior pituitary

cells, respectively. The thyrotroph is the least common cell type in the anterior pituitary, accounting for less than 10% of the pituitary cell population. [3, 4]

The intermediate lobe secretes proopiomelanocortin (POMC), a precursor to melanocyte-stimulating hormone (MSH), and involutes in the adult. [2]

The neurohypophysis is formed from axonal terminals, projecting from two discrete groups of magnocellular neurones in the hypothalamus, surrounded by modified astrocytes called pituicytes. The two hormones secreted by the posterior lobe of the pituitary gland, arginine vasopressin (AVP) and oxytocin, are synthesized in the paraventricular and supraoptic nuclei within the hypothalamus. [2, 5]

The anatomical and functional relationships between the hypothalamus and the pituitary gland are described in Figure 1.

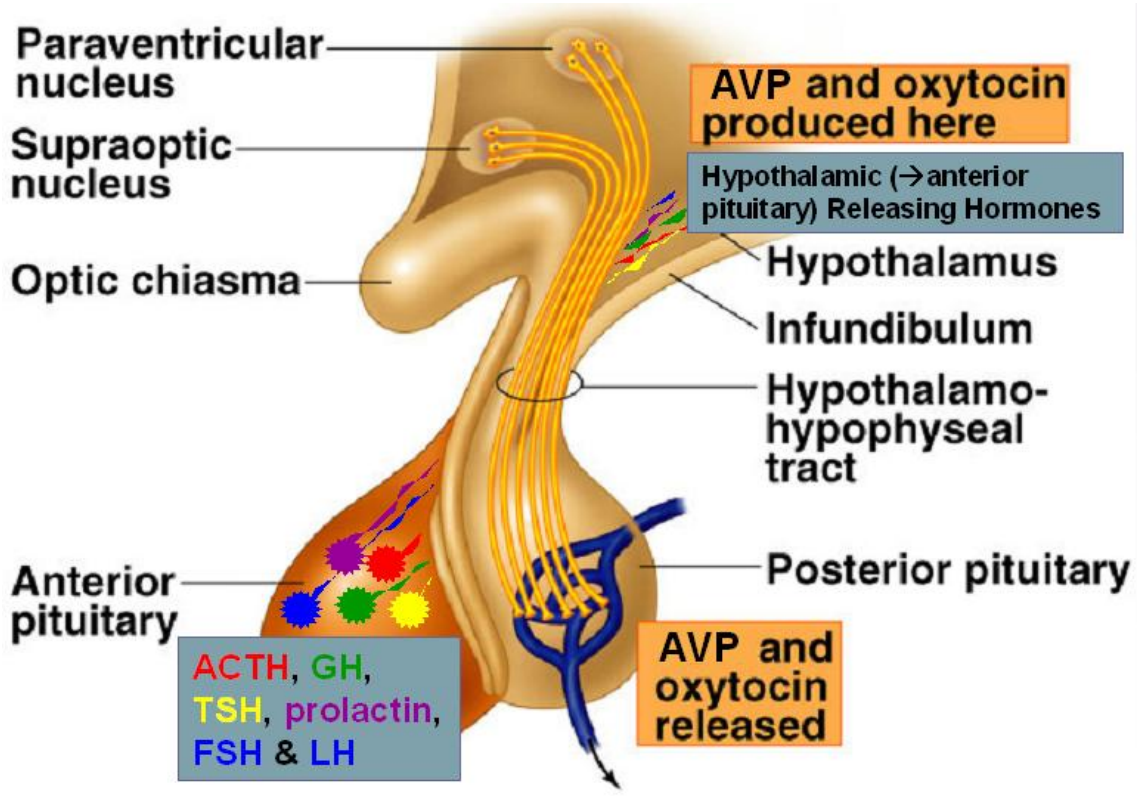

Figure 1. **Anatomical and functional relationship between the hypothalamus and the pituitary gland.** The hypothalamus is positioned above the pituitary gland in the basal part of the forebrain. The magnocellular neurons, within the paraventricular and supraoptic nuclei in the hypothalamus, produce AVP and oxytocin. Their axons form the hypothalamo-hypophyseal tract, and the hormones are released from the posterior pituitary into the general circulation in response to electrical excitation. The adenohypophysis is anatomically distinct from the hypothalamus. However, parvocellular neurons of the hypothalamus secrete releasing factors that, via a system of

hypophyseal portal vessels, act on the endocrine cells of the anterior lobe to stimulate or inhibit the synthesis and secretion of GH, prolactin, TSH, ACTH, and FSH and LH. The infundibulum (or pituitary stalk) carries both the portal blood delivering hypothalamic hormones to the anterior pituitary and the neural tract from the hypothalamic nuclei to the posterior pituitary. It is noteworthy that the optic chiasm lies above the hypophysis and anterior to the pituitary stalk. Thus, any mass lesion of sufficient size in the area of the pituitary gland will cause visual field defects. [1, 2, 4] ACTH: adrenocorticotrophin, AVP: arginine vasopressin, FSH: follicle-stimulating hormone, GH: growth hormone, LH: luteinizing hormone, TSH: thyroid-stimulating hormone.

The hormones secreted from the anterior pituitary regulate growth, puberty, metabolism, response to stress, reproduction, and lactation, while those from the posterior pituitary are required during parturition and lactation, and regulate water balance. [2]

GH stimulates insulin-like growth factor 1 (IGF1) gene expression and IGF1 synthesis in liver and bone, amongst other tissues, acting on growth. GH also regulates the hepatic production of insulin-like growth factor binding protein 3 (IGFBP3), acting as a gluco-counterregulatory hormone in metabolism. In muscle, GH increases protein synthesis, while in the adipocyte, GH induces lipolysis. [6, 7] PRL is the major hormone that simulates milk production, it inhibits LH and FSH secretion inducing lactation-related amenorrhea in the postpartum period. [5] ACTH binds with high affinity to the melanocortin 2 receptor (MC2R) in the adrenal gland and regulates steroidogenesis. [3] In the male, LH binds to a receptor on testicular Leydig cells and increases the synthesis of testosterone, [8] while FSH binds to testicular Sertoli cell and stimulates the production of proteins in the seminal fluid. [9] In females, LH binds to its receptor on ovarian theca cells and stimulates steroidogenesis; FSH stimulates ovarian follicular growth and facilitates generation of estrogen from thecal cells. [10] TSH binds to its receptor on thyrocytes, resulting in an increase in iodine transport, in the expression of thyroperoxidase and thyroglobulin, and ultimately in increased synthesis of thyroid hormones. [2, 3]

AVP acts on the V2 receptor in the renal collecting duct and increases water permeability to facilitate water reabsorption, and on V1 receptor in endothelial cells to promote vasoconstriction. [3] Oxytocin acts through its receptor, inducing intracellular calcium release that, in turn, results in smooth muscle contraction in the uterine

myometrial cells and mammary gland myoepithelial cells to cause uterine contraction and milk ejection, respectively. [11]

1.1.2. Pathology of the Pituitary Gland

Hypopituitarism is defined as a deficiency of one or multiple pituitary hormones. Congenital hypopituitarism is a syndrome with a wide variation in severity, age at presentation, from the early neonatal period to later in life (e.g. with abnormal pubertal development), and inheritance. It may manifest as isolated deficiency of GH, ACTH or TSH, hypogonadotropic hypogonadism (HH) or central diabetes insipidus (DI). Alternatively, several pituitary hormone axes may be defective, resulting in combined pituitary hormone deficiency (CPHD) syndromes. The hormonal deficits can be associated with extra-pituitary abnormalities, notably of the eye and midline forebrain, such as optic nerve hypoplasia (ONH), anophthalmia/microphthalmia, agenesis of corpus callosum (ACC) and absence of septum pellucidum. [1, 2]

The endocrinopathy can evolve to include other hormonal deficits, necessitating ongoing assessment, as these conditions are often associated with significant morbidity and occasional mortality. Neonates with congenital hypopituitarism may present with nonspecific symptoms, such as hypoglycaemia, lethargy, seizures, failure to thrive, cholestasis and prolonged jaundice, with or without associated developmental defects. Alternatively, they may be initially asymptomatic but at risk of developing pituitary hormone deficiencies over time. Males may present with undescended testes and a micropenis. Growth failure in severe growth hormone deficiency (GHD) can occur early in infancy, while bone maturation may be delayed for the chronological age but this is usually evident later in life. DI is characterised by polyuria and polydipsia. [2, 12] Moreover, neonates with optic nerve hypoplasia and/or midline abnormalities or syndromes known to be associated with hypopituitarism will need, in the first instance, assessment of their endocrine status, as well as long term follow-up even if the initial endocrine investigations are normal. Early diagnosis of hypopituitarism in the neonatal period is difficult due to the immaturity of the hypothalamic-pituitary axis, and the contraindication for some GH provocation tests at this age. More than 50% of patients with eye/forebrain and pituitary abnormalities have ACTH deficiency, and the resulting cortisol deficiency can be life threatening. Neonates with TSH deficiency may also

present with temperature instability. [12]

Investigations of hypopituitarism include the use of combined pituitary function and provocative testing of the hypothalamo-pituitary axis. GHD may be confirmed on the basis of low concentrations of IGF1 and IGFBP3 in combination with a poor growth rate, while GH provocation tests are contraindicated in children less than one year of age. The diagnosis of TSH deficiency is made in the presence of a low concentration of free thyroxine and basal TSH, and central hypothyroidism is associated with additional pituitary hormone deficiencies in 78% of cases. A thyrotropin-releasing hormone (TRH) test may be useful for the diagnosis of prolactin deficiency. A poor response to gonadotropin-releasing hormone (GnRH) stimulation within the first 12-18 months of life is suggestive of gonadotropin deficiency, which provides a window of opportunity for the early detection of HH, although patients will require repeat investigations at puberty. In neonates, multiple random cortisol measurements may point towards the integrity of the hypothalamo-pituitary-adrenal axis, but requires frequent blood sampling, while hypoglycaemia-inducing tests are contraindicated at this age. The cortisol response to an exogenous ACTH test is safe, but it has a sensitivity of 80%. Once the circadian rhythm has been established, an 08:00 am cortisol, a 24-hour plasma cortisol, and a mean cortisol may represent a more sensitive tool to confirm ACTH deficiency. Finally, early morning paired plasma and urine osmolarities point towards the diagnosis of DI. [2, 12]

Neuroimaging also plays an important role in the diagnosis and monitoring of patients with congenital hypopituitarism, as there is a correlation between the neuroradiological abnormalities and the severity and evolution of the endocrinopathy. Signs to look for at the magnetic resonance imaging (MRI) of the brain and pituitary include the size of the anterior pituitary, the presence and location of the posterior pituitary (absent or ectopic/undescended), the presence and morphology of the infundibulum, the presence and morphology of the corpus callosum and septum pellucidum, the appearance of the optic nerves and chiasm, as well as associated brain abnormalities. [13] The risk of hypopituitarism is 27.2 times greater in patients with an undescended posterior pituitary as compared with those with a normally positioned posterior pituitary, and midline forebrain defects are up to 5.2 times more prevalent in patients with CPHD as compared with isolated growth hormone deficiency (IGHD). [12, 13]

The mainstay of treatment of hypopituitarism is replacement therapy with appropriate hormones, which entails the use of subcutaneously administered recombinant human

growth hormone, oral hydrocortisone, thyroxine, and intramuscular or transdermal testosterone or oestrogen. [14]

1.1.3. Embryology of the Pituitary Gland

In the developing human embryo, the prosencephalon consists of two secondary brain vesicles: the diencephalon and the telencephalon. The diencephalic lateral walls form three swellings that develop into the thalamus, hypothalamus and epithalamus. In particular, the hypothalamus arises by proliferation of neuroblasts in the intermediate zone of the diencephalic walls, and the nuclei develop within its structure concerned with homeostasis, endocrine regulation, and the activity of the pituitary gland. [15, 16] The embryological development of the pituitary gland is described in Figure 2.

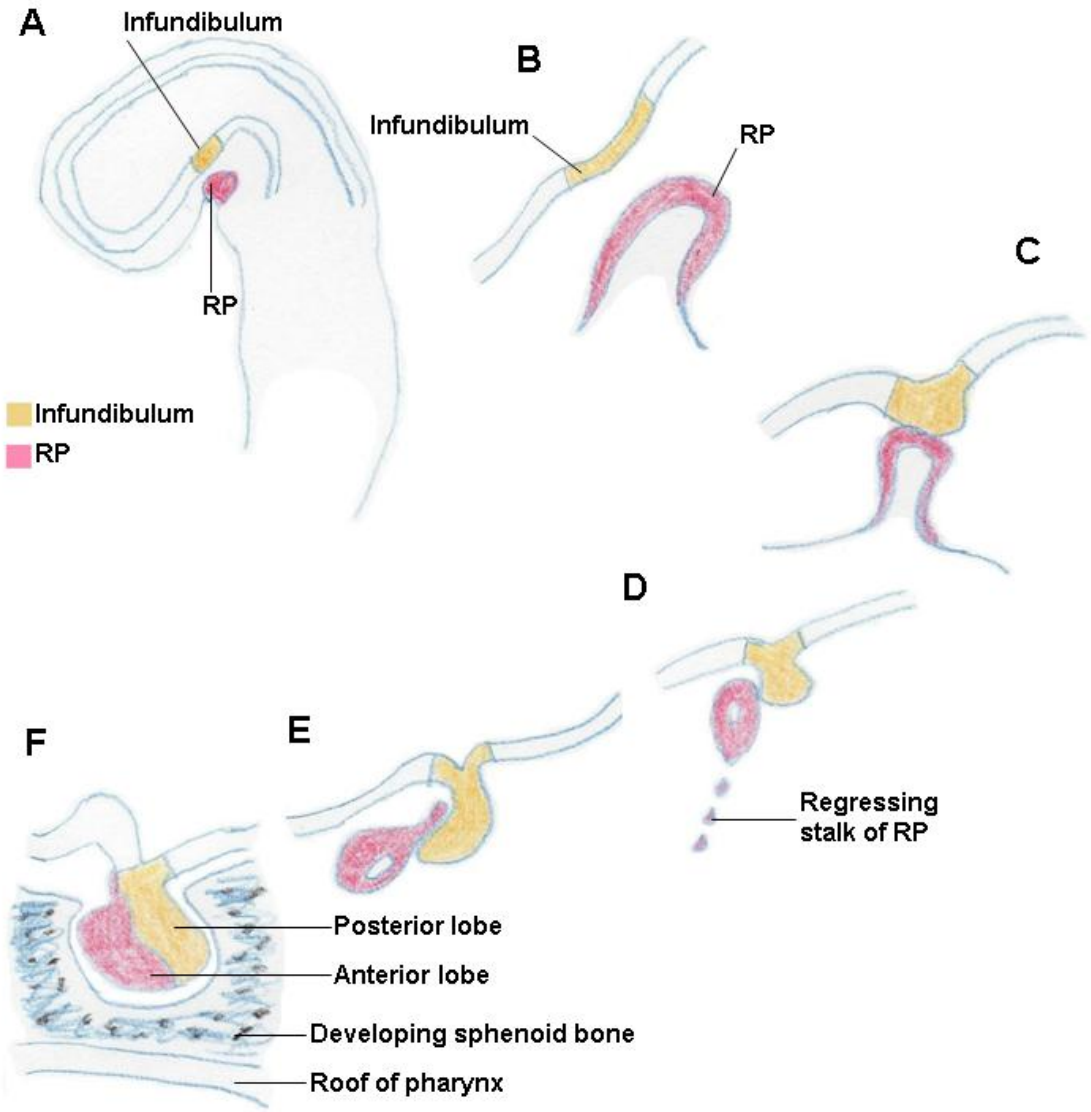

Figure 2. **Stages of embryological development of the pituitary gland.** A) Sagittal section of the cranial end of a human embryo of circa 36 days of gestation, showing the genesis of the pituitary gland, as a compound structure of the infundibulum and the Rathke's pouch, driven by morphogenetic transformations of the developing brain. B) Development of the adenohypophysis begins in week 4, Carnegie Stage (CS) 12a (25-26 days post-ovulation), of embryonic growth: an ectodermal placode appears in the roof of the stomodeum (the primary oral cavity) and outgrows dorsally to form a diverticulum, called Rathke's pouch. [17] C) At CS 13-14, the Rathke's pouch appears as a thin tube anteroposteriorly flattened to the lower posterior wall of the diencephalon, and opens into the cavity of the pharyngeal intestine with a blind terminating upper end. A separating mesenchymal layer appears between its anterior wall and the lower inferior wall of the diencephalon. [17] The rudiment of the hypothalamic infundibulum and neurohypophysis forms at CS 15 (33-36 days post-ovulation), as a thickening of the posterior wall of the floor plate of the diencephalon. During CS 17-18 (41-46 days

post-ovulation), the neuroectodermal thickening grows ventrally and the infundibulum, flexing above the floor of the Rathke's pouch, occupies the position characteristic of the neurohypophysis. Joining of the epithelial and neural rudiments of the pituitary gland into a single organ occurs during week 7 of embryo development. [5, 17] D) The epithelium of the lateral parts of the Rathke's pouch overlaps the growing infundibulum, and the growth and placement of the neurohypophysis leads to deformation and gradual separation of the Rathke's pouch from the roof of the stomodeum. [5, 17] E) The lumen of the Rathke's pouch is reduced to a small cleft that demarcates the boundary between the anterior and posterior lobes of the pituitary gland (CS 19; 47-49 days post-ovulation). By CS 20 (50-51 days post-ovulation), all component parts of the hypophysis occupy positions corresponding to those of the definitive pituitary gland. A developing capillary bed appears around the epithelial rudiment, this being absent only at the point of contact of the epithelial and neural elements of the organ. [5, 17] F) The degeneration of the connection between the Rathke's pouch and the stomodeum is complete by week 8 of embryonic development, and Rathke's pouch forms a discrete sac, separated by the growing sphenoid bone. [5, 17] RP: Rathke's pouch.

From week 5 of embryonic development, the walls of the Rathke's pouch contain numerous cells in different stages of mitosis, with proliferation mostly evident at the luminal border. Ultrastructurally, these cells display typical epithelial features and are interconnected by junctional complexes. In the diencephalon opposite the wall of the Rathke's pouch, numerous mitotic figures are also seen. At week 6, proliferation becomes more extensive in the developing adenohypophysis than in the neurohypophysis and adjacent mesenchyme, but mitotic cells decrease significantly after week 6 in the adenohypophysis, as well as in the neurohypophysis and in the mesenchyme. [18] From week 8 CS 21-23 (51-57 days post-ovulation), proliferation remains intense around the residual lumen of the Rathke's pouch only. Epithelial cords invaginate from the wall of the adenohypophysis to form a gland-like primordium, the structural-functional units of the organ, separated by deep and branching strands of mesenchymal tissue. Mitotic cells become less numerous in more differentiated gland-like structures of adenohypophysis, but they are very numerous in the mesenchyme penetrating the gland, prior to vascular invasion of the mesenchyme itself. A gradual increase in the volume of the organ is observed, and the increase in the length of the Rathke's pouch, between its appearance and the moment of formation of the posterior

lobe of the hypophysis, is proportional to the rapid growth of the diencephalon. [17, 18]
Using in vivo foetal MRI, Schmook et al. (2010) looked at prosencephalic development for anatomical landmarks before gestational week 27. The pituitary gland was detectable, overall, in 60% of the foetuses. The detection rate increased significantly with gestational age (30% between gestational week 16-21 and 77% after week 21). If delineable, the maximum diameter of the pituitary gland ranged from 2 to 6 mm [mean±Standard Deviation (SD): 3.9±0.9 mm] and increased with gestational weeks. Differentiation between adeno- and neurohypophysis was not reliably possible. The infundibulum was visible, overall, in 87% of the foetuses. [19]
Concurrently with the growth of the embryonic pituitary gland, cytological differentiation into endocrine cells proceeds, along with the onset of the active functioning of the organ and signs of secretion. [17, 18] By week 16 the adenohypophysis is fully differentiated, and the hypothalamo-pituitary axis is established by week 20. GH, ACTH and TSH are detectable in the foetus by week 12. Between weeks 20 to 24, serum GH levels peak, then decline gradually to term. [20]

1.1.4. Molecular Basis of Pituitary Development and Disorders

Isolated growth hormone deficiency (IGHD) is the most common endocrinopathy with an incidence ranging from 1 in 3,500 to 1 in 10,000 births, with the majority of cases being idiopathic in origin. [21-23] However, familial inheritance, which can be dominant or recessive, accounts for between 5 and 30% of all cases, suggesting a genetic aetiology for the condition. [24] At the more severe end of the spectrum, septo-optic dysplasia (SOD) is a rare congenital anomaly with a prevalence of approximately 1 in 10,000. It is a heterogeneous disorder characterized by a clinical triad of midline forebrain abnormalities, ONH and hypopituitarism. Each of these components can occur in isolation or in combination. Although the condition is generally sporadic, familial cases have been described. [25-26]

While the aetiology of congenital hypopituitarism remains unknown in the majority of cases, mutations have been found in genes encoding both transcription factors and signalling molecules important for the normal development of the hypothalamo-

pituitary axis, closely related to that of the forebrain. The clinical phenotype is extremely variable, depending upon the expression patterns of the molecule/s implicated in the aetiology of hypopituitarism. [1, 2, 12-14, 27, 28] Mutations in genes involved in the early development of the pituitary gland and patterning of the forebrain (homeobox gene expressed in ES cells 1: *HESX1*, SRY-box 2: *SOX2*, GLI-Kruppel family member 2: *GLI2*, SRY-box 3: *SOX3*, LIM homeobox gene 3: *LHX3*, LIM homeobox gene 4: *LHX4* and orthodenticle, drosophila homolog of, 2: *OTX2*) tend to result in syndromic forms of congenital hypopituitarism, in association with extrapituitary defects of the midline forebrain structures and of the eye. [29, 30] Mutations in genes involved in the initial stages of pituitary cell differentiation (prophet of Pit1: *PROP1* and POU domain, class 1, transcription Factor 1: *POU1F1*) often result in isolated/non-syndromic CPHD. [12]

The phenotype and pattern of inheritance of disorders of the pituitary gland, associated with mutations in developmental genes, are compared in Table 1.

Gene	**Loss of Function Phenotype in Mouse**	**Phenotype in Human**	**Inheritance in Human**
HESX1	Anophthalmia or microphthalmia, agenesis of corpus callosum, absence of septum pellucidum, pituitary dysgenesis or aplasia. [32, 35]	Variable: SOD, CPHD, IGHD with EPP. Anterior pituitary hypoplastic or absent. Posterior pituitary ectopic or eutopic. Frequency of mutations: approximately 1%. [31-34]	Dominant or recessive. Heterozygous mutations with incomplete penetrance or rare homozygous mutations. [35, 36]
OTX2	Lack of forebrain and midbrain, olfactory placode, optic placodes. [38]	Anophthalmia, APH, ectopic posterior pituitary, absent infundibulum. Frequency of mutations: 2-3% of anophthalmia/microphthalmia cases. [37, 38]	Dominant. Heterozygous mutations with haploinsufficiency or dominant negative effect. [39, 40]

SOX2	Poor growth, reduced fertility, central nervous system abnormalities, anophthalmia; pituitary hypoplasia with reduction in all cell types. Homozygous null mutants: embryonic lethal. [44, 45]	Hypogonadotropic hypogonadism; APH, abnormal hippocampi, bilateral anophthalmia/microphthalmia, abnormal corpus callosum, learning difficulties, oesophageal atresia, sensorineural hearing loss, hypothalamic hamartoma. Frequency of mutations: 3.5-10%. [41-43]	Dominant. De novo heterozygous mutations, as well as gene deletions, with haploinsufficiency effect. [44, 45]
SOX3	Poor growth, weakness, craniofacial abnormalities, ACC, hypothalamic and infundibular abnormalities. [47]	IGHD and mental retardation, hypopituitarism; APH, infundibular hypoplasia, EPP, midline abnormalities. Frequency of mutations: 6% (duplications), 1.5% (mutations). [46]	X-linked recessive. [47]
GLI2	N.A.	Holoprosencephaly, hypopituitarism, craniofacial abnormalities, polydactyly, single nares, single central incisor, partial ACC. Frequency of mutations: 1.5%. [48]	Dominant. Heterozygous mutations with incomplete penetrance, variable phenotypic expression, and with haploinsufficiency effect. [48]

LHX3	Hypoplasia of Rathke's pouch. [52]	GH, TSH, gonadotropin deficiency with pituitary hypoplasia. ACTH insufficiency variable. Short, rigid cervical spine. Variable sensorineural hearing loss. Frequency of mutations: 1.3%. [49-51]	Recessive. Homozygous and compound heterozygous mutations, as well as gene deletions. [52]
LHX4	Mild hypoplasia of anterior pituitary. [53]	GH, TSH, cortisol deficiency, persistent craniopharyngeal canal and abnormal cerebellar tonsils; APH, ectopic/eutopic posterior pituitary, absent infundibulum. Frequency of mutations: 1.2%. [53, 54]	Dominant. [55, 56]
PROP1	Hypoplasia of anterior pituitary with reduced somatotropes, lactotropes, thyrotropes, corticotropes and gonadotropes. [60, 65]	GH, TSH, PRL, and gonadotropin deficiency. Evolving ACTH deficiency. Enlarged pituitary with later involution. Frequency of mutations: 1.1% sporadic cases, 29.5% familial cases. [57-62]	Recessive. Homozygous mutations and gene deletions. [63-65]

POU1F1	Anterior pituitary hypoplasia with reduced somatotropes, lactotropes and thyrotropes. [66, 67]	Variable anterior pituitary hypoplasia with GH, TSH, and PRL deficiencies. Frequency of mutations: 3.8% sporadic cases, 18% familial cases. [66-69]	Dominant or recessive. [70-72]

Table 1. **Comparison of disorders of the pituitary gland: phenotype and pattern of inheritance.** ACC: agenesis of corpus callosum; APH: anterior pituitary hypoplasia; CPHD: combined pituitary hormone deficiency; EPP: ectopic posterior pituitary; IGHD: isolated growth hormone deficiency; SOD: septo-optic dysplasia; N.A.: not available.

Genetic mutations are more commonly found in familial, rather than sporadic, cases of hypopituitarism, however, the overall incidence of mutations in any known transcription factor or signalling molecule involved in the embryology and physiology of the pituitary gland and axis is low. Causative genetic mutations are found in only 5-10% of patients with hypopituitarism, indicating that several genes involved in the pathways of pituitary gland development remain to be identified. [1, 73, Dattani, personal communication] An overview of the complex network of transcription factors and signalling molecules emanating both from the ventral diencephalon and the developing Rathke's pouch is presented in Figure 3.

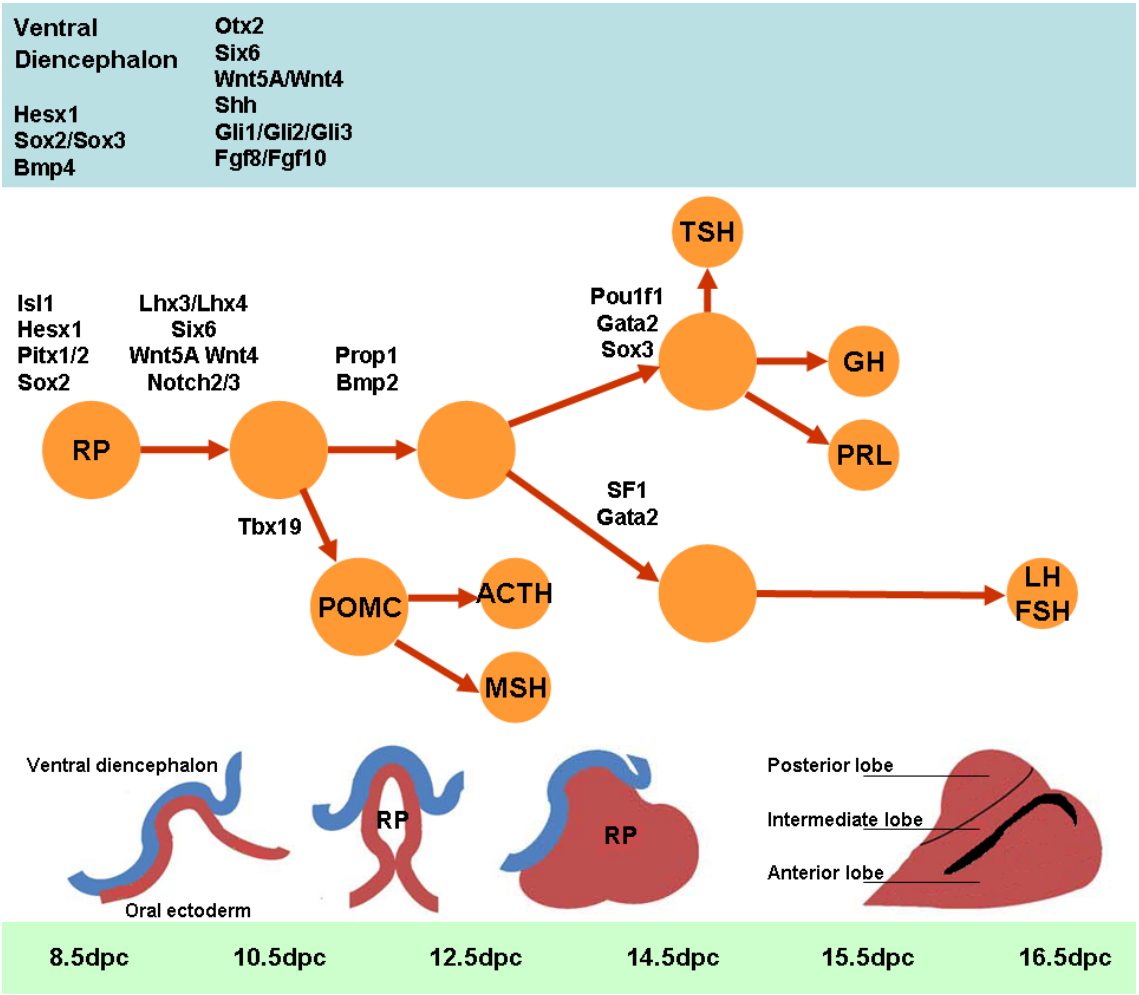

Figure 3. **Schematic representation of the developmental cascade of genes implicated in mouse and human pituitary development.** In the mouse, the first sign of pituitary development occurs at 7.5 days post coitum (dpc) with the development of the hypophyseal placode, a thickening of the ectoderm in the midline of the anterior neural ridge. At approximately 9 dpc, the placode forms a rudimentary Rathke's pouch. By 10.5 dpc, a region of the ventral diencephalon above the Rathke's pouch gives rise to the infundibulum from which the posterior pituitary and pituitary stalk will derive. At 12.5 dpc, the Rathke's pouch is juxtaposed to the diencephalon and completely separated from the underlying oral ectoderm, its lumen persists as the cleft separating the anterior and intermediate lobes. [1] Corticotrope cells expressing *Pomc* begin to be detected in the intermediate lobe. [74] Thyrotropes are observed at 14.5 dpc, characterised by the expression of thyroid-stimulating hormone, beta chain (*Tshb*), within the anterior lobe. The expression of *Gh* and *Prl* marks the differentiation of somatotrope and lactotrope lineages, respectively, beginning at 15.5 dpc. The gonadotropes are the last cell type to emerge, beginning at 16.5 dpc with the onset of luteinizing hormone, beta polypeptide (*Lhb*) expression, followed by follicle-

stimulating hormone, beta polypeptide (*Fshb*). [75, 76] Bone morphogenetic protein 4 (*Bmp4*) is the earliest secreted signalling molecule expressed in the ventral diencephalon, arising at 8.5 dpc. It is required for induction and maintenance of the Rathke's pouch, and for its regionalisation that allows the emergence of the different endocrine cell types. [75, 77] *Bmp4* also regulates early expression of Isl LIM homeobox 1 (*Isl1*) and *Lhx3* in the developing anterior pituitary, [78, 79] *Isl1* being the first LIM protein to be expressed during pituitary development at 8.5 dpc. [75] In human, both *LHX3* and *LHX4* are also expressed along the rostro-caudal length of the neural tube. [80] *Lhx3* activates *Hesx1* promoter to ensure its early expression. *Hesx1* is one of the earliest markers of the Rathke's pouch, it functions as a transcription repressor and its down-regulation is required for cell determination, and in particular for *Prop1* to function as activator. [81] The switch of expression from the repressor *Hesx1* to the activator *Prop1* is an important step during development of the pituitary gland because it is required for emergence of both the *Pou1f1* (*Gh*, *Prl* and *Tsh*) and gonadotrope lineages, and therefore cell determination. [82-84] *Sox2* and *Sox3*, are expressed throughout the central nervous system with particularly high levels in the ventral diencephalon. [85, 86] *Sox2* is also expressed in the early ectoderm including the Rathke's pouch. Its expression is down-regulated as endocrine cell differentiation proceeds, but it is maintained in the progenitor proliferative zone around the lumen. [85] In human, *SOX2* has a critical role in the development of the hypothalamo-pituitary axis. Between weeks 4.5-9, *SOX2* is expressed throughout the embryonic central nervous system, including strong expression within the Rathke's pouch which is maintained during the development of the anterior pituitary, as well as in the overlying presumptive hypothalamus. *SOX2* also shows an overlapping domain of expression with *LHX3* within the Rathke's pouch and the developing anterior lobe, and acts as a regulator and activator of *LHX3* during pituitary development. [87] By 14.5 dpc, expression of *Sox3* is also initiated in the developing pituitary, in a small subset of *Pou1f1*-positive cells. [86] Expression of Paired-like homeodomain transcription factor 1 (*Pitx1*) is first detected in the anterior ectoderm at 8.0 dpc, and in the Rathke's pouch by 9.5 dpc, where its expression is maintained in all hormone-producing cell types. *Pitx1* interacts with *Pou1f1* and GATA-binding protein 2 (*Gata2*) resulting in synergistic activation of the promoters of the *Prl* and *Gh* genes. [88, 89] Moreover, *Pitx1* synergizes with T-box 19 (*Tbx19*) and with Steroidogenic Factor 1 (*SF1*) to activate *Pomc* and *Lhb* expression, respectively. [74, 90] *Pitx2* exhibits a large degree of sequence identity with *Pitx1* and is similarly capable of activating the promoters of

most of the pituitary hormone genes, suggesting functional redundancy. [91, 92] Also, *Bmp2*, first expressed at 10.5 dpc, seems to induce the proliferation and determination of the *Pou1f1* lineage and gonadotropes. [75, 93] Early signalling includes Sonic hedgehog (*Shh*) and Gli pathways, [94, 95] while terminal differentiation requires fibroblast growth factors (*Fgfs*) and *Bmp* signalling down-regulation. [75, 96, 97] Moreover, a pathway involving signalling via Wingless-type MMTV integration site family (*Wnt*) and *Notch* genes appear to be essential for *Prop1* maintenance and to prevent early differentiation and allow the generation of diverse endocrine cell types (particularly, of *Pou1f1*-dependent lineages). [98-100] *Otx2* is expressed early in development, and is required for maintenance of the forebrain and correct *Hesx1* expression. [101, 102] As early as week 7 of gestation, strong expression of *OTX2* is detected in the diencephalon of the human foetal brain, and later in the hypothalamus and pituitary gland. [103] Both *OTX2* and sine oculis homeobox, drosophila homolog of, 6 (*Six6*) are also expressed in the developing eye and human foetal retina. [104, 105] RP: Rathke's pouch.

The advent of the high-throughput high-resolution genome-wide array technology has provided new instruments for the screening of patients with complex and/or specific clinical phenotypes, whose (genetic) aetiology remains undisclosed. Amongst them, up to 90% of patients with pathology of the pituitary gland lack an aetiological diagnosis. [106-108]

1.2. Copy Number Variations (CNVs)

Structural variations involve large stretches of human genomic deoxyribonucleic acid (DNA). They account for at least 12% of the human genome in which hundreds of genes reside, conceivably playing a role also in functional variability. [109, 110]

1.2.1. Definition and Origin of CNVs

A copy number variation (CNV), a form of structural variation, is defined as a DNA segment, longer than 1 kilobase (kb) to several megabases (Mb), with a variable copy number compared with a reference genome and/or amongst individuals. [111-113] CNVs may either be inherited or sporadic, caused by de novo mutations, and they arise both in the germline and in somatic cells. [114] CNV appears to be a major driving force and enhancing mechanism in evolution. [115-117]

There are at least two main mechanisms for formation of CNVs: non-allelic homologous recombination (NAHR) and non-homologous end joining (NHEJ). [115]

NAHR mediates the vast majority of recurrent CNVs, where the breakpoints are located within low copy repeats (LCRs). [118] LCRs are region-specific sequences that occur twice or a few times in a genome, with a degree of identity >95% and length >1 kb. [119] In particular, LCRs longer than 10 kb and with sequence identity equal or greater than 97% can lead to local genomic instability, and provide extensive homology for NAHR. [120] Homologous recombination is used in repair of DNA breaks and gaps, in particular double-strand break (DSB), including during chromosome segregation and recombination at meiosis. Homologous recombination is a mechanism of accurate DNA repair, that utilises another identical sequence as a template to repair the damaged DNA strand. [121] However, the presence of LCRs can lead to misalignment of chromosomes or chromatids, recruitment of a template sequence in a non-allelic position, and mediate NAHR. In turn, NAHR can result in unequal crossing-over and structural genomic rearrangements. [115, 122]

In contrast to NAHR, NHEJ is a pathway of DNA DSB repair that does not require homology or uses very short microhomology of 2 to 25 complementary base pairs (bp); the latter repair mechanism is also referred to as microhomology-mediated end joining (MMEJ). [115, 123] In NHEJ, the DNA break ends are directly ligated without the need for a homologous template to guide repair. Therefore, the product of repair often contains additional nucleotides and complex DNA end junctions, and NHEJ is prone to errors that lead to genetic change including CNV. [115, 122, 123] NHEJ mediates non recurrent genomic rearrangements where structural changes can be complex, and most non recurrent CNVs occur at sites of very limited homology. [124]

More recent models focus on perturbation of DNA replication as the origin of CNV. Fork stalling and template switching (FoSTeS) is a mechanism based on DNA

replication error, where the DNA replication fork stalls; the lagging DNA strand disengages from the original template and anneals, or switch, to another replication fork in physical proximity, by virtue of microhomology, priming or reinitiating DNA synthesis. [125] FoSTes is now superseded by the new microhomology-mediated break-induced replication (MMBIR) model. In MMBIR, when a single double-strand end results from replication fork collapse, the broken end from the collapsed fork can anneal to any single-stranded template with which it shares microhomology and that occurs in physical proximity, and repair and restart DNA synthesis in a new replication fork. [115, 126] If, instead of a sister molecule, the broken end invades the homologous chromosome and/or a homologous sequence in a different chromosomal position, MMBIR can result in the genesis of CNVs. [122, 126] FoSTeS and MMBIR appear to be major mechanisms for generating, particularly, non recurrent CNVs that have a complex structure in the human genome. [127, 128]

1.2.2. Effects of CNVs in Complex Disorders

The total number, position, size, type, and population distribution of CNVs in the human genome remain elusive. [129, 130] Between 9 and 18% of heritable variation could be associated to changes in copy numbers. [131] CNVs may be responsible for genetic heterogeneity and human phenotypic variability by modifying the expression levels of a single dosage-sensitive gene or a contiguous set of dosage-sensitive genes that map within the aneuploid segments. [122, 130, 132, 133] Alternatively, a structural variation could affect the expression of the gene/s that map in its flanking regions and/or of neighbouring normal copy-number genes that lie outside the boundaries of the CNV interval. [131, 133] The influence of genes that vary in dosage due to copy number change on the relative transcription levels of neighbouring genes may be mediated by regulatory elements. Moreover, if enhancer or repressor sequences map within a dosage-sensitive genomic interval, a CNV can disrupt the appropriate level of ribonucleic acid (RNA) and thus the protein production from that transcription unit. [116, 117, 122] CNVs could also induce a modification of the positioning of a genomic region and dissociate, especially long-range, enhancer and repressor elements from their controlled transcription unit. Therefore, CNVs can exert an effect on gene regulation and expression via position effect. [134-136]

A number of disorders and human phenotypes associated with CNVs have been described, as well as disease susceptibility or resistance to disease conferred by CNVs. [133, 137-141]

In the complex disorder Cri-du-chat syndrome, the DNA copy-number changes were mapped in 94 patients who had been carefully evaluated for the presence of the characteristic cry, speech delay, facial dysmorphisms, and degree of mental retardation (MR). The study localised the region associated with the cry to 1.5 Mb in distal 5p15.31, speech delay to 3.2 Mb in 5p15.32-15.33, and facial dysmorphic features to 2.4 Mb in 5p15.2-15.31. Three regions, MRI-III, were identified that differently affect the presentation of MR amongst patients with different size 5p deletions. Moreover, a significant percentage of patients with severe MR were found to have copy number changes in addition to the 5p deletion. [142]

In a study of 26 patients with clinical features of growth pathology Sotos syndrome, 4 potentially pathogenic copy number changes were detected. They involved 4 different chromosome regions: deletions of 10p12.32-p12.31, 14q13.1, Xq21.1-q21.31 and a duplication of 15q11.2-q13.1, and they varied in size from 155 kb to 13.36 Mb. The overall detection rate of novel abnormalities was 15%, and the chromosome region 10p12.32-p12.31 contained a candidate gene for overgrowth, plexin domain-containing protein 2 (*PLXDC2*), to be screened in a larger cohort of patients. [143]

A cohort of individuals with midline defects, consisting of 83 patients with syndromic cleft lip and cleft palate and of 104 cases of non-syndromic cleft lip and cleft palate, were analysed with the aim of identifying deletions and duplications of candidate gene loci. One subject was identified with a 2.7 Mb deletion at the 22q11.21 chromosome region. Five patients had deletions encompassing the interferon regulatory factor 6 (*IRF6*) gene, associated with midline disorder Van der Woude syndrome. One individual was found to harbour a 3.2 Mb de novo deletion at chromosome 6q25.1-25.2, and another individual a 2.2 Mb deletion at chromosome 10q26.11-26.13 inherited from the mother who also had cleft lip. Both deletions were considered to be causally associated with the phenotypes of the patients. [144]

In patients presenting with a pathological phenotype and constitutional de novo apparently balanced chromosome rearrangement, complex cryptic genomic imbalances have been found at or near the breakpoints, and also on chromosomes unrelated to the originally diagnosed rearrangement. [145-148] In a 16-year old patient affected with severe mental retardation and a cytogenetically visible rearrangement at the end of the

long arm of chromosome 9, a duplication of ~400 kb upstream of a ~2.4 Mb triplication followed by a duplication of ~130 kb of chromosome 9q34.3 were detected. [149] Amongst patients with various degrees of developmental delay (DD) and/or dysmorphic features and congenital malformations, deletions on chromosome 1q44 and 13q31.1 were detected in one individual, and loss of heterozygosity (LOH) of the entire chromosome 2 was identified in another. These findings also provided further evidence of the presence of a critical region for the development of microcephaly and corpus callosum abnormalities in children with distal 1q deletions, and represented the fourth report of inheritance of two copies of the whole chromosome 2 from one parent (father) only and no copies from the other parent, i.e. paternal uniparental disomy (UPD) of chromosome 2. [150]

The phenotypic effects of CNVs and their mechanisms of pathology still remain to be fully clarified, and more complex scenarios can be envisaged, like the inheritance of two or more CNVs at different loci from two healthy parents by an affected child. [122, 151]
Finally, it is possible that detected CNVs might not be associated with the pathology under investigation, but might equally represent at-risk alleles for late-onset disorders or recessive diseases. The implications must be considered when informed consent is requested. [152]

1.3. Single Nucleotide Polymorphisms (SNPs)

Data on the occurrence of sporadic genomic disorders have shown a rate of arising of CNV at least 2 to 4 orders of magnitude higher than that of point mutations. [138, 153] CNVs are estimated to encompass more total nucleotides than single nucleotide polymorphisms (SNPs), that represent another source of variation and contribute to determining phenotypic variability in humans. [109, 122]

1.3.1. Definition of SNPs

A SNP is a genome position in the DNA sequence at which there are, typically, two or more different nucleotide residues (alleles) in the population. [154] Each variant, or polymorphism, occurs at a minor allelic frequency (the lowest allele frequency at a locus) of at least 1% in the given population, and one allele is usually more common than the other/s. A SNP allele that is common in one geographical or ethnic group may be much rarer in another. [154, 155]

SNPs are widespread throughout the genome. There are an estimated 15 million SNPs in the human genome. [156] If SNPs lie in a coding region of a gene, they are distinguished into non-synonymous or synonymous depending on whether they do or do not change the protein amino acid sequence, respectively. SNPs lying in non-coding regions of genes or intergenic regions between genes may have an impact on gene splicing processes or transcription factor binding and hence on human genetic and phenotypic diversity. [154-156]

SNPs are introduced into the genome by spontaneous germline mutation of single nucleotides in the course of evolution. [156] Although genomic diversity during human reproduction is maintained by genetic recombination during meiosis, chromosomal segments tend to be transmitted as specific combinations of linked SNP alleles referred to as haplotypes. [154, 157] This implicates that a single SNP (also referred to as tag SNP) can act as a genomic marker within a given haplotype to predict the genotype of the surrounding region, which is described as linkage disequilibrium. [154, 156]

SNPs that are biallelic, or binary, are well suited to automated, high-throughput genotyping (determine which allele is present at a given genomic polymorphic position). Operationally, the two alleles of a SNP are often arbitrarily labelled as A and B. Therefore, when each individual inherits one copy of a SNP position from each parent, the genotype at a SNP site can be represented by either AA, AB or BB. [154, 155]

1.3.2. Role of SNPs in Disease Gene Discovery

Any two copies of the entre human genome share 99.9% of DNA sequence. Within the 0.1% of nucleotide sites where human genomes differ from one another, common

patterns exist, and approximately 90% of sequence variation among individuals is due to common variants. [154]

The HapMap is a genome wide catalogue of the common patterns of genetic variants that occur in humans, based on the identification of SNPs in haplotypes with a frequency of 5% or higher, and the way they are distributed amongst four population samples of different ancestral geographic origin: Yoruban (YRI) of Nigeria, Japanese (JPT), Han Chinese (CHB), and northern and western European (CEU). [154, 158, 159]

The DNA samples were extracted from cell lines established from blood samples collected from a total of 270 individuals. In the first stage of the construction of the HapMap database, all SNPs were genotyped in the full set of 270 DNA samples. In the second step, the common haplotypes, each with a frequency of at least 5%, were defined. Eventually, in the third phase, the tag SNPs were identified. Common haplotypes, within which SNPs are strongly associated and therefore tend to be inherited together, were characterised, and tag SNPs, that uniquely identify each one of these haplotypes via linkage disequilibrium, were recognised. [154, 158, 159]

Detecting tag SNPs allows to genotype only a percentage (300,000 to 600,000) of the whole of the 15 million common SNPs in the human genome, that is sufficient to identify each of the common haplotypes uniquely. Moreover, the tag SNPs contain much of the information about the common patterns of variation in the genome to predict the remainder of the common SNPs in that region and the pattern of genetic variation. As a result, only a few tag SNPs are genotyped directly, while the other SNPs are captured through linkage disequilibrium correlations with the tag SNPs. [160]

A set of sequence variants in the genome can, therefore, serve as genetic markers to detect associations between a particular genomic region and a disease, whether or not the markers themselves have functional effects. [161] While hundreds of genes for human rare diseases, in which mutation of a single gene is necessary and sufficient to cause disease, have been discovered, for common complex diseases, linkage studies have been much less successful in locating causative genetic variants, consistent with a more complex genetic architecture where each variant locus individually contributes only modestly to disease risk and aetiology. [155] Such conditions include diabetes, cancer, stroke, autoimmune pathology, schizophrenia, depression and asthma. [162, 163]

The HapMap dataset, that represents a SNP map of the common haplotypes and their tagging SNPs, constitutes a platform for disease association studies, where the haplotypes in individuals with a disease are compared to the haplotypes of a

comparable group of individuals without a disease (the controls). If a particular haplotype occurs more frequently in affected individuals compared with controls, a gene influencing the disease may be located within or near that haplotype. The search for the causative variants/genes can then be limited to the region/s showing association with the disease. [158, 161] This aims, in particular, at facilitating genome wide association studies, as well as analysis where a gene has been implicated in causing disease by chromosomal position relative to linkage peaks, known biological function or expression pattern. [155]

With the increasing number of SNPs genotyped by the HapMap project, it has become possible to correlate structural and SNP variation. However, because the frequency of individual, polymorphic and rare, CNVs in the general population has not yet been determined and the HapMap collection is intended to sample common SNPs and haplotypes, it is not known how well these samples reflect copy-number variability in humans. The structural variation may also vary among different populations to an extent yet unknown, and the sample size may be too small for discovering CNV genotypes that represents each of the four HapMap populations. Moreover, no clinical information are obtained by the HapMap project, therefore the structural variation ascertained from the HapMap samples is not necessarily benign or neutral. Finally, it is noteworthy that, since the source of the DNA for HapMap samples is transformed lymphoblastoid cell lines, it may be impossible to assess true germline CNVs. [154]

Recently, a study has confirmed that common CNVs are tagged by SNPs and so have been indirectly explored through SNP studies. [163] To address the issue of the role of common CNVs in genetic susceptibility to common disease, a genome-wide study of association between CNVs and eight common human diseases was undertaken in ~19,000 individuals at 3,432 polymorphic CNVs. It was concluded that common CNVs are unlikely to contribute greatly to the genetic basis of common human diseases. However, three loci were identified, where CNVs were associated with disease: immunity-related GTPase family, M (*IRGM*) for Crohn's disease, human leukocyte antigen (HLA) for Crohn's disease, rheumatoid arthritis, and type 1 diabetes, and transmembrane glycoprotein tetraspanin 8 (*TSPAN8*) for type 2 diabetes. [163] In each case the locus had previously been identified in SNP-based studies. [129, 164, 165] Significantly, systematic CNV differences between DNAs derived from blood and cell-lines were also confirmed. [163]

The more commonly occurring CNVs that show a lack of linkage disequilibrium with nearby SNPs might indicate that the structural variants have arisen repeatedly. [109] Ancestral non-recurrent structural variants are expected to show linkage disequilibrium with SNPs on their original haplotype, as they arise only once. [130, 166] If so, their presence or absence may be inferred by typing selected tagging SNPs. [167, 168] Flanking SNPs can potentially be combined into a more informative haplotype to be used as a proxy for simple CNV events. [130] However, CNVs associated with rare sporadic genomic disorders often arise in regions of complex genomic structure, and this limits the extent to which these variants can be genotyped using tagging SNPs. [169]

1.4. Array Techniques

Chromosome abnormalities detected by routine karyotyping are a known cause of spontaneous abortions and growth pathology including developmental delay, multiple congenital anomalies (MCA) and dysmorphic features. Chromosome abnormalities are observed in 50% of spontaneous first trimester abortions and 1% of all liveborn babies. Clinical phenotypes may arise from gene dosage imbalance, but routine cytogenetic and molecular techniques can be insufficiently sensitive to detect chromosome rearrangements that are either submicroscopic in size (<3 Mb) or limited to a specific genomic locus or both. [170] Fluorescent in Situ Hybridisation (FISH) using probes which localise at the subtelomeric regions of the chromosomes identifies a submicroscopic rearrangement, considered causative of the clinical phenotype, in approximately 5% of patients with DD/MCA, growth impairment, facial dysmorphic features, and a family history of DD. [171, 172]

Array-based technologies have enabled high resolution screening of the whole human genome in one experiment, for the diagnosis of copy number changes and genomic disorders in patients with DD and MCA. These platforms have the potential to improve the diagnostic yield of genetic abnormalities, and to replace the more time-consuming and less cost-effective, sequential locus-specific testing for microdeletion and microduplication syndromes. [173]

1.4.1. Bacterial Artificial Chromosome (BAC) Based Arrays

Array comparative genomic hybridisation (CGH) allows the genome wide screening of CNVs in a single overnight hybridisation. [174-177] The technique was largely developed based on the use of bacterial artificial chromosome (BAC) clones spotted on a glass slide array grid. The principles of the methodology are described in Figure 4.

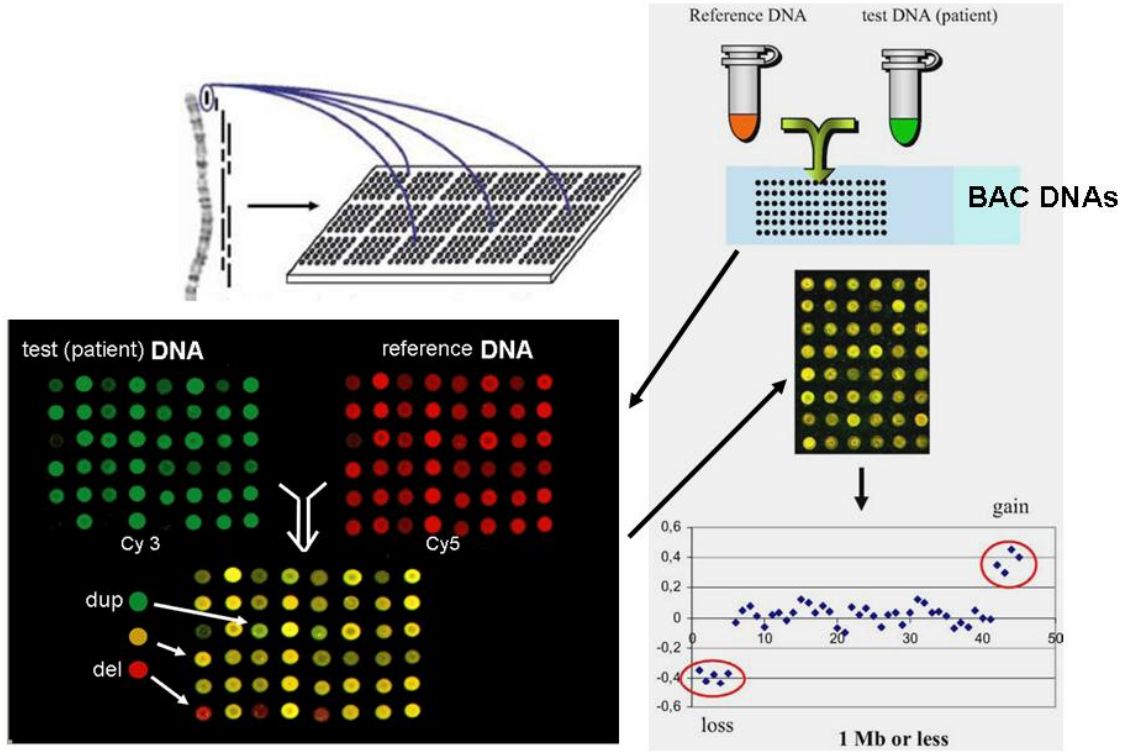

Figure 4. **BAC clones based array CGH.** The genomic DNA of a patient (test DNA) is labelled by a fluorochrome (green Cy 3 in the Figure) and genomic DNA of a normal control subject (reference DNA) is labelled by a different fluorochrome (red Cy 5 in the Figure). The two DNAs are cohybridised on an array grid of mapped genomic DNA fragments (BAC clones) spotted on a glass slide. The fluorescence is captured using a scanner. The fluorescence ratio is measured by a software and presented in graphic form. Copy number is proportional to the fluorescent [test/reference] ratios. In the Figure, the diploid status is presented in yellow, a genomic duplication in the patient (test) DNA is marked in green, while deletions are coloured in red. Genomic gains or losses are plotted on charts, and can be traced back to their genomic loci, chromosome, and physical position. Dup: duplication, del: deletion, Mb: Megabase.

The resolution of array CGH depends on the distance between the interrogating probes mapped on the array grid, and it is limited by the number of clones that can be deposited on the array. BAC-based array CGH was traditionally developed with a coverage of approximately 1 clone per Mb. [173]

It has been proposed that a combined approach of conventional karyotyping, FISH of the subtelomeric regions of the chromosomes, and array CGH would lead to an aetiological diagnosis in about 20% of patients with DD/MCA. [178] The percentage of submicroscopic rearrangements among individuals with unexplained DD exceeds that of microscopically visible alterations. [178] An overall incidence of 20% submicroscopic copy number changes was confirmed in a cohort of 140 patients, selected on the basis of a complex clinical phenotype including DD/MCA and dysmorphic facial features and a normal routine cytogenetic karyotype, studied by array CGH. [179] Excluding subtelomeric rearrangements, clinically relevant interstitial submicroscopic imbalances were identified in 8% of patients. Taking into consideration all reported studies, the authors concluded that array CGH screening, with a resolution of at least 1 Mb, could detect a de novo intrachromosomal alteration in at least 8.8% patients with DD/MCA. [179] In addition, three patients were identified to harbour a mosaicism for a structural chromosome rearrangement. One of them showed monosomy 7 in as little as 7% of the cells, confirming that array CGH also allows the detection of low grade mosaicism. [180]

The resolution limit of array CGH, as defined by the smallest pathogenic CNV identified, was set at approximately 0.25 Mb. [181]

1.4.2. Oligonucleotide Based Arrays

A disadvantage of BAC arrays is that they contain repetitive human DNA sequences, which cause a cross hybridisation, translating into a background noise in the hybridisation. The use of a blocking reagent like Cot-1 DNA, 50-300 bp DNA enriched for repetitive sequences, in the hybridisation solution suppresses nonspecific hybridisation. Even then, though, the signal-to-noise ratio still suffers from background noise. [173] Oligonucleotide arrays have the advantage that they can be chosen to be free of repetitive sequences, and provide high quality results due to a robust signal-to-

background ratio. [111, 173, 182] In these platforms, oligonucleotide probes are immobilised as arrays on a flat surface of glass or silica, and the oligonucleotides typically range in size from 20 to 80 nucleotides. [173, 183] High-density synthetic oligonucleotide arrays are capable of identifying genome wide aberrations at high resolution. [184] The array technology has, therefore, shifted from BAC-based array CGH, containing genomic clones at 1 Mb intervals, towards higher resolution array platforms that use oligonucleotides. [111, 182, 185]

1.4.3. Single Nucleotide Polymorphism (SNP) Arrays

High-density whole genome SNP array is a high-throughput technique that allows interrogation of hundreds of thousands up to millions of SNPs in a single assay. The SNP mapping technology makes use of oligonucleotide arrays to genotype genome-wide SNPs. [173, 184, 186, 187] The principles of the methodology are described in Figure 5.

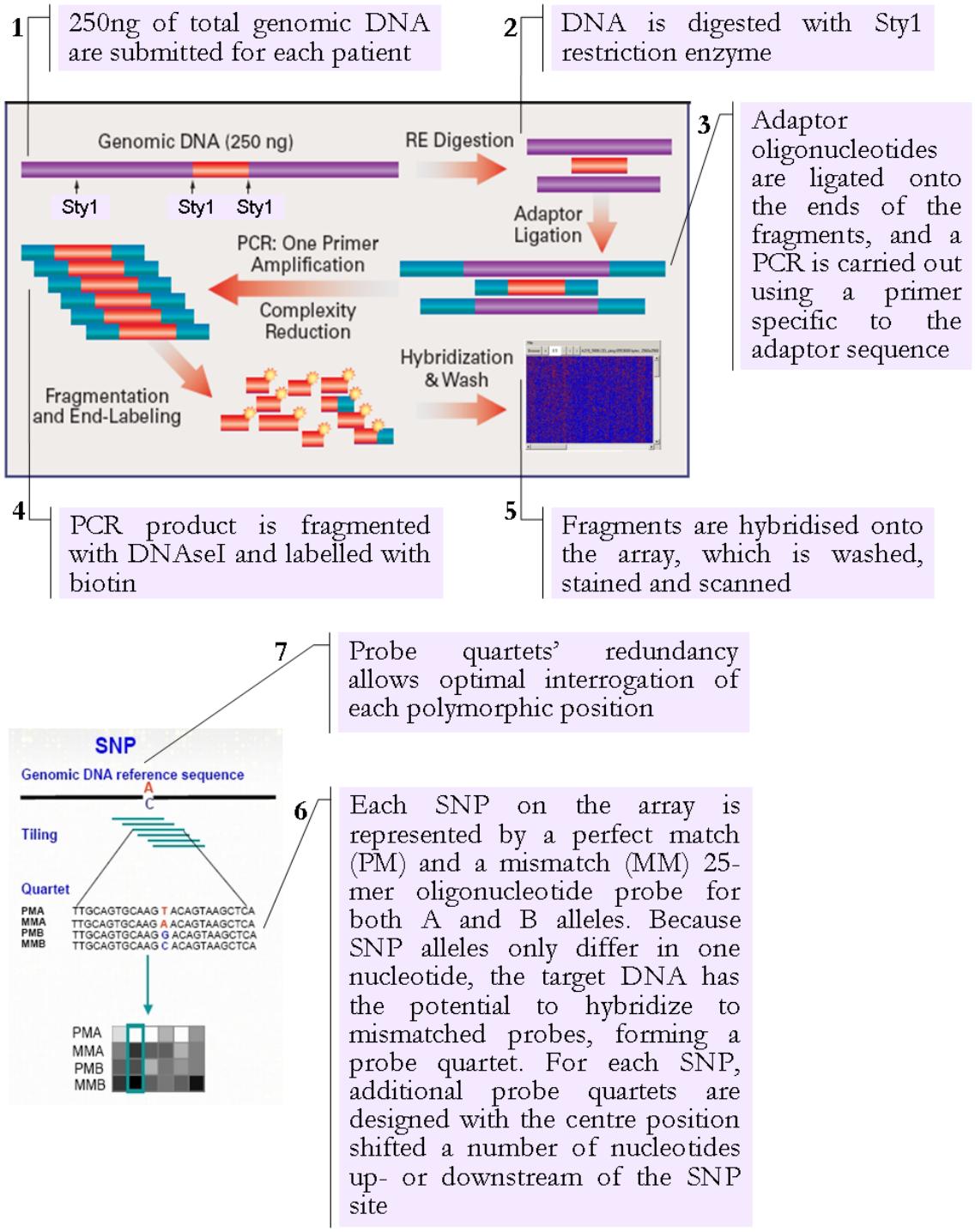

Figure 5. **Affymetrix oligonucleotide-based SNP mapping array.** In SNP genotyping platforms, oligonucleotides are used to interrogate the whole genome at unprecedented resolution. SNPs on the mapping arrays are selected based on reproducibility and physical distribution across the genome. [111, 185] Oligonucleotides are specific to known SNPs. Contrary to array CGH, a reference DNA from a control subject is not required, as the SNP map of a DNA reference dataset, like HapMap, can be utilised. [173] Each SNP on the array is interrogated by a set of probes that are each 25-nucleotide long. A probe is designed to be complementary, or very nearly

complementary, to the DNA sequence harbouring the SNP site. Because SNP alleles only differ in one nucleotide, the hybridization conditions for all probes on the array allow for the target DNA to hybridize to mismatched probes. Therefore, each 25-mer oligonucleotide probe is either a perfect match (PM; perfectly complementary to one of the SNP alleles), or a mismatch (MM; identical to a perfect match probe except that the centre base is altered so as to be perfectly complementary to neither allele). The purpose of the MM probe is to measure background noise and evaluate specificity in binding. [186] A number of additional probe quartets are designed on both strands, sense and antisense, with the centre position shifted a number of nucleotides up- or downstream of the SNP site. This is to provide data redundancy when interrogating each SNP region. [188] DNAseI: deoxyribonuclease I, PCR: polymerase chain reaction, RE: restriction enzyme; PMA: Perfect Match allele A, MMA: Mismatch allele A, PMB: Perfect Match allele B, MMB: Mismatch allele B.

The combination of SNP database, like HapMap, and high-density SNP array allows the use of SNPs as informative polymorphic markers for Mendelian hereditary diseases, complex traits and common disorders. [189] The copy number of any given genomic region containing the SNP can be inferred by the SNP genotyping and CNVs can be detected by differences in hybridisation intensity. [130, 190, 191] Array platforms that combine genomic copy number quantification and SNP genotyping offer the opportunity to perform genome-wide studies that might detect disease susceptibilities related either to a CNV or a SNP. [130, 173] A summary of the characteristics of the different SNP array products in the Affymetrix genotyping range is given in Table 2. [192]

	100K	**500K**	**SNP 5.0**	**SNP 6.0**
Restriction enzyme	XbaI and HindIII	NspI and StyI	NspI and StyI	NspI and StyI
Number of SNPs	116,204	500,568	500,568	906,600
Median distance between markers	8.5 kb	2.5 kb	2.5 kb	<700 bp
Average heterozygosity for each SNP	0.3	0.3	0.31	26.7-28.5% depending on population

Table 2. **Differences between Affymetrix SNP array platforms.**

SNP arrays have applications in copy number variation and whole genome association studies. The power of SNP arrays to interrogate a significant proportion of human genetic variation has facilitated genome-wide association studies where DNA samples of large numbers of affected (cases) and unaffected (controls) individuals are interrogated. The data are mined for statistically significant differences in allele frequencies between the two groups. [186] In common human pathologies, such as coronary artery disease or diabetes, the associated variant/genotype is putatively either a disease predisposition allele or in linkage disequilibrium with such an allele. [193, 194]

Genome-wide SNP genotyping on oligonucleotide platforms can be used for discovery and mapping of CNVs in the human genome with a virtually unlimited resolution, and their association with clinical phenotypes. [173, 187, 190] With the highest resolution platforms, SNP array analysis should theoretically detect all known syndromes with CNV aetiology as well as new ones. [111, 122, 181]

While other array-based methods, like array CGH, can detect only genomic gains or losses, the approach of combining genotypes and copy number estimation in SNP array technology has the additional advantage of detecting chromosomal abnormalities that do not alter copy number, but that can play an important role in pathology, such as copy number neutral loss of heterozygosity (LOH) and uniparental disomy (UPD). [173, 184, 186]

LOH is a form of allelic imbalance that can result from the complete loss of an allele or from an increase in copy number of one allele relative to the other, resulting in regions of LOH with or without copy number change, respectively. [187] Copy number neutral LOH can be due to UPD. [184]

UPD represents an allelic imbalance when one allele is deleted leading to reduplication or amplification of the other parental allele. This results in genomic regions with homozygous SNP calls but a copy number of two or higher. [186] UPD can be pathological when the wild-type allele (e.g. maternal) is missing and two copies of a mutant allele (e.g. paternal) are present, or due the imbalance of an imprinted gene, that is expressed differently when inherited by one parent or the other. [195]

Moreover, SNP arrays use genotype data to determine the molecular origin of UPD, as well as the parent of origin of a deletion or duplication that has arisen de novo. [184, 196]

Finally, the high resolution of SNP array provides more precise breakpoint definition

and disease loci mapping, which allows subtle phenotypic heterogeneity to be distinguished at a molecular level. [184]

1.4.4. Known and Emerging Syndromes

In a cohort of 100 children with idiopathic MR, and normal results of standard karyotype analysis, chromosome imbalances were found in 11 patients by use of whole genome 100K SNP array. De novo deletions, as small as 178 kb, were detected in 8 patients, de novo duplications, as small as 1.1 Mb, in 2 cases, and one instance of previously undetected mosaic trisomy of chromosome 9 was also recorded. [197] Similar results were obtained, utilising the same SNP array platform, in a group of 104 unselected patients with idiopathic MR. The genome-wide screening detected deletions as small as 20 kb, when covered by at least 3 SNPs, and duplications as small as 150 kb, when covered by at least 6 SNPs. Overall, putative disease-causing or de novo aberrations were detected in 9.1% of patients, and the detection rate was stated to be independent from clinical pre-selection of patients. [152] Previously undetected de novo chromosomal deletions were also identified in a small cohort of children with MCA, who had had a normal high-resolution karyotype and subtelomeric FISH analysis, by means of genome-wide 100K SNP array. [198]

Multiple commercially available SNP array platforms, including the Affymetrix 250K SNP NspI array and the Affymetrix 250K SNP StyI array, were used to detect CNVs in 318 patients with MR/MCA. Abnormalities were found in 22.6% of patients, including 6 CNVs that overlapped known microdeletion/duplication syndromes, 8 CNVs that overlapped recently described emerging syndromes (3q29 microduplication syndrome, 3 cases of 16p11.2 microdeletion syndrome, 2 cases of 16p13.11 microduplication syndrome, 22q11 duplication syndrome, and 22q11.2 distal deletion syndrome), 63 potentially pathogenic CNVs (in 52 patients), and two mosaic trisomies for an entire chromosome. The authors proposed a novel diagnostic approach for patients with MR/MCA, by first analysing each patient by means of SNP array instead of conventional karyotyping. [181]

The Affymetrix 500K SNP array platform was utilised in a study of 100 patients with idiopathic intellectual disability of unknown cause and their unaffected parents. Pathogenic genomic imbalances were found in 16 out of 100 patients. The same authors

had previously screened a cohort of 100 children with idiopathic DD by means of lower-resolution 100K SNP array, and pathogenic genomic imbalance had been found in 11 of them. Ten out of these 11 patients, together with 44 more patients from the same study, were included in the second cohort screened by 500K SNP array, and re-tested. The 500K SNP array platform identified all 10 previously detected pathogenic genomic copy number changes and at least one additional pathogenic CNV, that had not been detected with the 100K SNP array platform. Many benign CNVs were also detected during the screening with the 500K SNP array platform. [199]

A similar comparison, between two separate array platforms with different resolution, was performed in the study of 70 patients affected by idiopathic MR and dysmorphic features. In order to reduce the number of false positives, parameters were set to filter the results and consider only imbalances greater than 75 kb in size. In the comparison, the higher-resolution Affymetrix 6.0 SNP array platform confirmed its increased ability to detect small CNVs, and disclosed potentially pathogenic CNVs in 6% of patients, that had not been identified during the study with the lower-density oligonucleotide array. [200]

1.4.5. Disease Gene Mapping

Three unrelated patients with severe psychomotor retardation, epilepsy or febrile seizures, muscular hypotonia and variable brain and minor anomalies showed de novo interstitial microdeletions involving 5q14.3-q15. Molecular karyotyping, by means of Affymetrix 100K SNP array and Illumina 550K SNP array, allowed to identify and refine 3 overlapping deletions measuring 5.7, 3.9 and 3.6 Mb, respectively. The boundaries and sizes of the deletions in the three patients were different, but an overlapping region of around 1.6 Mb in 5q14.3 was defined, which harboured 5 genes. Amongst the 5 genes were: G protein-coupled receptor 98 (*GPR98*), a known epilepsy gene, and a second candidate gene, LysM, putative peptidoglycan-binding, domain containing 3 (*LYSMD3*), for the other central nervous system symptoms of the novel emerging 5q14.3 microdeletion syndrome. [201]

Chromosomal rearrangements have been detected in 5-10% of patients with autism spectrum disorder (ASD). Array CGH was utilised to test the hypothesis that de novo

CNV is associated with ASD, by screening the genomic DNA of patients, unaffected subjects, and their respective parents. De novo CNVs were found to be significantly associated with autism (P = 0.0005), and were identified in 12 out of 118 (10%) of patients with sporadic autism, in 2 out of 77 (3%) of patients with an affected first-degree relative, and in 2 out of 196 (1%) of controls. The authors concluded that de novo copy number mutations represent a significant risk factor for ASD. [202]

Further candidate chromosome regions and genes have been identified utilising high density SNP array platforms. In a cohort of 54 families with ASD patients, microcephalin 1 (*MCPH1*) gene copy number changes were detected in three patients, implicating *MCPH1* in chromosome band 8p23.1 as an ASD susceptibility gene. [203]

A large cohort of 996 individuals of European ancestry affected by ASD and their parents were genotyped with Illumina 1M SNP array and compared to 1,287 matched controls. The affected population was found to carry a higher number of rare (<1% frequency) CNVs than controls (1.19 fold, P = 0.012). Novel ASD loci that were affected by CNVs in cases and not in the control population were identified: SH3 and multiple ankyrin repeat domains 2 (*SHANK2*), synaptic RAS-GTPase-activating protein 1 (*SYNGAP1*) and discs large-associated protein 2 (*DLGAP2*), and the X-linked locus patched domain-containing protein 1 (*PTCHD1*). No CNVs affecting these candidate genes were found in an additional 3,677 European controls, implicating these rare genomic variants as ASD risk factors. [204]

LOH is a prominent characteristic of most human cancers. Two types of acquired LOH are observed in tumours: deletions and copy neutral UPD. In a study of 301 patients with haematological malignancies, 250K SNP array technology was applied to detect previously cryptic chromosomal changes, particularly UPD. Acquired UPD was shown to be a common chromosomal defect in myeloid malignancies, and mapping minimally overlapping segmental UPD regions has the potential to identify both known and novel pathogenic mutations. [205]

1.5. Hypothesis and Major Outcomes

The clinical data of a large number of children and adults who present with a pathology of the pituitary gland of unknown aetiology are entered into the database of endocrinological patients of the Great Ormond Street Hospital. Amongst them, a cohort of patients with a complex clinical phenotype, including MCA, dysmorphic features and impaired growth and development was selected to undergo a genome-wide screening of copy number changes with high-throughput high-resolution array-based technique.

Congenital hypopituitarism can be triggered by environmental insults, such as viral infections, vascular or degenerative damage, exposure to alcohol and/or drugs, and maternal age. Genetic mutations have been identified in genes responsible for pituitary development and function. However, only up to 10% of patients affected by hypopituitarism have recognised mutations in known genes. Novel genomic regions and candidate genes remain to be identified, the disruption of which is responsible for congenital pathology of the pituitary gland.

An analytical workflow was drawn up to screen the multiple CNVs detected in the cohort of patients. The presence of two pathogenic genomic imbalances, chromosome 6q terminal duplication and chromosome 11q terminal deletion, was confirmed in one patient, and the breakpoints were defined at high resolution. A previously undetected interstitial deletion of chromosome 22q was diagnosed in a patient with hypopituitarism and the complex cardiac malformation tetralogy of Fallot.

A further patient with the same association of hypopituitarism and tetralogy of Fallot harboured a submicroscopic rearrangement in the chromosome region 1p36.33. This CNV and three more regions of genomic imbalance, detected by SNP array in two patients, were assessed as potentially pathogenic CNVs.

Novel genes involved in the pathways of pituitary development are candidates for mutation screening by direct sequencing in larger cohorts of patients, in order to ascertain their prevalence and role in the aetiology and pathophysiology of hypopituitarism.

A nucleotide sequence variant, leading to a non-synonymous amino acid change, was identified in exon 2 of barH-like homeobox gene 2 (*BARX2*), that had not been reported before in the literature or in public databases. A non-sense mutation was found in exon 4 of *OTX2*, compatible with the clinical phenotype of the patient, that comprises of severe eye defects as well as pathology of the pituitary gland.

2. METHODS

2.1. Patients

At the moment of starting the project, the database of endocrinological patients seen at the Great Ormond Street Hospital and other national and international centres contained 1,697 index cases.

2.1.1. Patients Selected for High Resolution Genome-wide Copy Number Change Screening

A checklist of selection criteria was drawn up and applied to the clinical records contained in the database, in order to identify patients with a complex pituitary phenotype (i.e. associated with DD and/or MCA and/or dysmorphic features), who have the highest likelihood of harbouring submicroscopic chromosome imbalances. [171, 206, 207] The checklist was compiled on the basis of the results obtained by the study of the subtelomeric regions of the chromosomes, [171] and by screening with array CGH. [206, 207] A total of ten patients were selected, including two patients who were already known to carry individual chromosome 11q abnormalities.

A detailed pro-forma was designed for the project to be filled in for each patient included in the screening, with the aim of collecting consistent data across the whole cohort of patients under investigation. The patient pro-forma was divided into sections to log anamnestic, clinical, endocrinological and genetic information. Appendix A contains a copy of the *Patient Pro-forma*.

DNA samples were already stored for the majority of patients included in the database. In all cases, high resolution genome-wide copy number change screening was carried out on DNA extracted from fresh blood, as it has been shown in an array CGH

screening that clonal anomalies can arise in vitro in cultured cell lines. [208]

2.1.2. Patients Selected for Mutation Analysis.

A list of 72 patients with uncomplicated pituitary pathology, characterised by GHD and MRI evidence of a small pituitary gland and infundibulum and an ectopic posterior pituitary gland, were chosen to undertake mutation analysis in the novel candidate gene *BARX2*. One patient was already known to carry an apparently balanced chromosome translocation involving chromosome band 11q24.

A list of 35 patients with an association of pituitary and eye pathology, with or without DD and learning or behavioural difficulties, and/or MCA mainly of the brain and kidneys, were chosen to undertake mutation analysis in two novel candidate genes *BMP4* and *OTX2*. Three of these patients were also included in the high resolution genome-wide copy number change screening.

When a mutation was found in a patient, DNA samples extracted from fresh blood were obtained from both parents, and the status of the mutation was assessed by direct sequencing.

2.2. Affymetrix GeneChip 250K Sty1 Mapping Array

The Affymetrix GeneChip 250K Sty1 SNP mapping array was chosen to perform genome-wide copy number change analysis.

2.2.1. Quality Control of DNA

Two microliters (concentration: 250 ng/μl) of total genomic DNA were submitted for each patient. The integrity of each DNA sample was verified by electrophoresis on a 0.8% agarose gel before submission. A volume of 100 ml of 0.8% agarose gel was prepared by adding 0.8 grams of agarose to 100 ml of a 1.0X Tris/Borate/Ethylenediamineetracetic acid (EDTA) (TBE) solution, obtained by adding 1 volume (20 ml) of 5.0X TBE solution to 4 volumes (80 ml) of distilled water. The solution was swirled to mix, heated in a microwave for a total of 1 minute and 30 seconds, and cooled under tap water. Subsequently, 1.5 μl of 10 mg/ml ethidium bromide (EtBr) solution were added, and the solution was swirled to mix. The gel was poured into the tank with pre-inserted combs, and left to set for 45 minutes. The first well of each row of the gel was loaded with 4 μl of 100 bp DNA ladder. For each sample, 1 μl of DNA was added to 1 μl of Orange G loading buffer and mixed with 10 μl of double distilled water (ddH2O). For each sample, the total volume of 12 μl was split into two aliquots, 4 μl and 8 μl, and loaded onto the gel. The gel was submerged in 1.0X TBE buffer to run at 90-95 V (~60 mA), and eventually examined on the ultraviolet (UV) light-box.

2.2.2. Sample Processing with Affymetrix GeneChip 250K Sty1 Mapping Array

The DNA samples were processed at University College London Genomics by Kerra Pearce, using the Affymetrix GeneChip 250K Sty1 Mapping Array and reagents. The samples were processed according to the manufacturer's standard protocol. Briefly, 250 ng of total genomic DNA was digested with Sty1 restriction enzyme. Adaptor oligonucleotides were ligated onto the ends of the digested fragments. Three polymerase chain reactions (PCRs) per sample were carried out to amplify a subset of digested DNA, using a single primer specific to the adaptor oligonucleotide sequence. PCR conditions were optimised to preferentially amplify DNA fragments within an optimal set size range. The yield of the PCR amplification was evaluated by spectrophotometry, and the size distribution of the amplified fragment was validated by agarose gel

electrophoresis. Samples giving low yield or improper size distribution were re-amplified or eliminated. Negative controls containing no DNA were run during the digestion/ligation steps and for each PCR assay to monitor for potential external DNA contamination. The PCR-amplified product for each sample was purified and fragmented with deoxyribonuclease I (DNAseI). The resulting fragments were end-labelled with Biotin, and hybridised onto the 250K Sty1 Mapping arrays overnight. The arrays were washed and stained with a biotinylated antibody and Phycoerythrin-conjugated Streptavidin to produce an amplified fluorescent signal (using the Fluidics Station 450, Affymetrix). The arrays were scanned using the Scanner 3000 (Affymetrix). The raw fluorescent signal intensity measurements were extracted using the Affymetrix GeneChip Operating Software (GCOS) and the Affymetrix GeneChip Genotyping Software (GTYPE 4.1), to generate genotype calls (.DAT and .CEL files). [192] The optimal SNP genotype call rate for each experiment was set at ≥ 95%, with an acceptable threshold of 85%.

2.2.3. Copy Number Analysis

Upon receiving the .DAT and .CEL files, a copy number profile of the whole genome of each patient was produced using the GTYPE plug-in Affymetrix Copy Number Analysis Tool (CNAT 4.0). [192] For each patient, the genotype data was extracted into a .CPH file from the relevant .CEL file by running Batch Analysis in GTYPE 4.1. The analysis method used to determine genotype calls was a Dynamic Model (DM) based algorithm. [209]

2.2.4. Reference Subsets of the International HapMap Project Dataset

Two reference sets were built by downloading a subset of .CEL files from the international HapMap project Affymetrix GeneChip 500K Sty1 mapping array data bank. [210] The .CEL files were transferred into the GCOS/GTYPE framework, and the .CPH files were created as described above. At the time of this study, the international

HapMap project dataset on the Affymetrix GeneChip Sty1 arrays consisted of: 30 CEU trios (90 samples), 90 CHB and JPT individual samples, and 90 YRI individual samples. The two reference sets were built according to the CNAT 4.0 User Guide instructions for submicroscopic chromosome abnormalities testing. [211] Briefly, the size (n) of the reference set had to be $n \geq 25$; ethnicity-match was not mandatory for $n \geq 25$, while mixed gender reference sets had to be excluded. Sex-match was relevant to facilitate the interpretation of the results on chromosome X: when the reference set of all male samples was used, the denominator for the logarithmic (log) ratios on chromosome X was automatically set to 1 as the test sample was analysed against an haploid set for chromosome X. The reference sets were therefore created as follows: 22 CHB and JPT and 20 CEU individual male samples to test male patients, 23 CHB and JPT and 10 CEU individual female samples to test female patients. The copy number calculation was obtained by comparing the SNP intensities of the sample arrays against the intensity distribution of the reference sets, by running CNAT 4.0 Batch Analysis.

2.2.5. Batch Analysis Workflow Parameters

The CNAT 4.0 Batch Analysis Workflow was optimised for submicroscopic chromosome abnormalities detection. [211] Briefly, the probe-level normalisation was specified as median scaling, genomic smoothing (GS) lengths of both 0.1 and 0 Mb were utilised, a 5-State Hidden Markov Model (HMM) was applied to determine the prior value and estimate the SD of each copy number (CN) state (0-1-2-3-4). In particular, for a GS bandwidth equal to 0.1 Mb, the prior value was set uniformly at 0.2 for CN states 0 through 4, SD for CN state 2 was set at 0.07 and SD for CN states 0, 1, 3, 4 was set at 0.09; for a GS bandwidth equal to 0 Mb, the prior value was set uniformly at 0.2 for CN states 0 through 4, the SD for CN state 2 was set at 0.19 and SD for CN states 0, 1, 3, 4 was set at 0.25. The other user-tunable HMM parameter, transition decay length, was set at 0.1 Mb. The post-HMM processing option, adjust outliers, was switched off.

The software CNAT 4.0 is implemented with the University of California Santa Cruz (UCSC) genome browser. [212] At the time of performing this study, the UCSC genome browser was based on the March 2006 human reference sequence assembly by the National Center for Biotechnology Information (NCBI) Build 36.1. [213]

2.3. Genomic Sequencing

2.3.1. Primer Design

The primers were initially designed using the online tools provided by UCSC and/or NCBI. [212, 213] Subsequently, each pair of primers was manually adjusted after verification with Basic Local Alignment Search Tool (BLAST) from NCBI, [213] and, for *OTX2*, also by comparison with data published in the literature. [37, 40]

The primer pairs utilised for the PCR amplification of all coding exons, including intron-exon boundaries, of *BARX2*, *BMP4*, and *OTX2* are listed in Table 3, Table 4, and Table 5, respectively.

Exon	**Forward Primer**	**Reverse Primer**	**Product size (bp)**
1	5'-GCTACCCGCTCTCCTCC-3'	5'-TCCCTTAACTTAACCCTTCC-3'	448
2	5'-TGTCAGACAGACCTCAGCC-3'	5'-CCACAATGGGAGCAAGTC-3'	465
3	5'-AGCAGGATCCCATCTCTC-3'	5'-CCAAACTGCCAAATGGTC-3'	248
	5'-AGCAGGATCCCATCTCTCCTG-3'	5'-CCCAAACTGCCAAATGGTCCG-3'	248
4	5'-GCAACGTGAGGTTATACTGG-3'	5'-TTCTCTCCCTACTCTCCCTG-3'	425

Table 3. **Primer pairs used for genomic sequencing of *BARX2***. Two different sets of primers were used for exon 3.

Exon	**Forward Primer**	**Reverse Primer**	**Product size (bp)**
3	5'-CCCTCCATTTCTAGCCCTAA-3'	5'-GGGTTTGATGTAACCCGAAC-3'	582
4_1	5'-TAGGTTTCCCCTGCATAAGC-3'	5'-GCTTAGGGCTACGCTTGG-3'	642
4_2	5'-ATTAGCCGATCGTTACC-3'	5'-GTCCAGCTATAAGGAAGC-3'	590

Table 4. **Primer pairs used for genomic sequencing of *BMP4***. Exon 4 was covered by two sets of primers amplifying overlapping fragments of the whole exon.

Exon	Forward Primer	Reverse Primer	Product size (bp)
3	5'-CTCGCCTAGTCCGTGCTCT-3'	5'-GGAACAGGGTGTTGCATCC-3'	395
4	5'-CGGAAACGCCTATGACTGAGA-3'	5'-TTTCAAGCCTTCCTTCAGTCC-3'	325
5_1	5'-ACGGGAGCCATTCTTGTCCTTAAGG-3'	5'-CCCAAAGTAGGAAGTTGAGCCAGCA-3'	409
5_2	5'-TCTAGCACTTCAGTCCCGACCATTG-3'	5'-TGGCTAAAACTGGAATGTCCAGCCC-3'	536

Table 5. **Primer pairs used for genomic sequencing of *OTX2***. Exon 5 was covered by two sets of primers amplifying overlapping fragments of the whole exon.

2.3.2. Suspension and Aliquots of Primers

Primers were obtained dessicated and were resuspended in ddH2O according to the manufacturer instructions, to achieve a concentration of 1 µg/µl. The stock was divided into three aliquots, and one aliquot was utilised to prepare sub-aliquots of primers at concentrations of 50 ng/µl and 20 ng/µl, to be used in PCR and sequencing reactions, respectively.

2.3.3. DNA Aliquots

An aliquot of pre-extracted DNA sample from each patient and control (concentration: 250 ng/µl) was diluted in ddH2O with a dilution 1:10. To perform a PCR amplification, 2 µl of DNA of each sample were transferred onto a plate.

2.3.4. PCR Protocol

A quantity of 2.0 µl of genomic DNA, pre-extracted from fresh blood, from each patient was transferred onto a PCR plate, together with one control DNA sample.

The ingredients of the standard PCR reaction mix were added in the order listed in Table 6. Before the addition of the DNA Polymerase, the reaction mix was moved onto ice, together with the plate of DNA samples, and all subsequent work was conducted on ice. A volume of 23 µl of the PCR reaction mix was added to each 2 µl DNA sample on

the plate to reach a final reaction volume of 25 µl, and also to an empty well on the plate as a negative control for DNA contamination. The plate was covered with a plastic lid or tape pad.

Reaction Mix	**x 1 sample**	**Final concentration**
10X *Taq* Reaction buffer	2.5 µl	1X
50 mmol/l MgCl2	0.75 µl	1.5 mmol/l
2.0 mmol/l dNTPs	2.5 µl	200 µmol/l
Forward Primer	1.0 µl	50 ng/µl
Reverse Primer	1.0 µl	50 ng/µl
ddH2O	15.15 µl	
Taq DNA Polymerase	0.1 µl	
DNA	2.0 µl	
Final Reaction Volume	25 µl	

Table 6. **Standard PCR reaction mix.** dNTPs: deoxynucleoside triphosphates.

A quantity of 2.5 µl of the enhancing agent 10% dimethyl sulfoxide (DMSO) (final concentration 1%) was added to the PCR reaction mix to amplify exon 1 of *BARX2*. The PCR amplification of exon 2 of *BARX2* was performed either without or, preferentially, with the addition of 7.5 µl of the enhancing agent 5.0 mol/l Betaine (final concentration 1.5 mol/l). Both DMSO and Betaine act by inhibiting DNA secondary structures. In all cases, the volume of ddH2O was adjusted to reach the final reaction volume of 25 µl. The optimal PCR annealing temperatures determined for each pair of primers utilised in the study are listed in Table 7.

Exon	Annealing Temperature (°C)
BARX2	
1	54
2	60
3	60
4	57
BMP4	
3	58
4_1	58
4_2	60
OTX2	
3	60
4	60
5_1	60
5_2	60

Table 7. **PCR annealing temperatures.** Annealing temperatures for PCR amplification of all coding exons of *BARX2*, *BMP4*, and *OTX2*.

A total of 35 PCR programme cycles were run to amplify exons 1, 2 and 3 of *BARX2*, and all exons of *BMP4* and *OTX2*; 30 cycles were run for the PCR amplification of exon 4 of *BARX2*. The denaturation step of the PCR reaction was run at 94 ºC, and the elongation phase was run at 72 ºC, as described in Table 8.

Step	Temperature (ºC)	Running Time
1	94	4 min
2	94	30 s
3	annealing	30 s
4	72	30 s
go to 2	repeat 29 or 34 cycles	
5	72	2 min

Table 8. **Scheme of the PCR running programme.** The annealing temperature and the number of cycles changed for each pair of primers, as described in Table 7 and in the text.

To evaluate the yield of PCR amplification of each experiment, an aliquot of 5 µl of PCR product from each sample was mixed with an equal volume of tracking dye and loaded and run on a 1% agarose gel. A volume of 100 ml of 1% agarose gel was prepared as described above (paragraph 2.2.1.), by adding 1 gram of agarose to 100 ml of a 1.0X TBE solution.

2.3.5. Purification of PCR Products

PCR products were purified either with the ExoSAP method or with the microCLEAN single-reagent kit and protocol.

In the ExoSAP method, the ExoSAP master mix was made up by 1 µl of 20 U/µl Exonuclease I (ExoI), 2 µl of 1 U/µl Shrimp Alkaline Phosphatase (SAP) and 2.0 µl of ddH2O, to reach a final volume of 5 µl, that was added to an aliquot of 15 µl of PCR product. The ExoSAP master mix was prepared and kept on ice throughout the procedure. The ExoSAP programme was run in a thermal cycler at 37 ºC for 30 min, at 80 ºC for 15 min, and at 4 ºC for 10 s. The amount of DNA in the PCR product was quantified using a 1:20 dilution of the plasmid pGEM 32f(+). Ten microliters of a mix of 5 µl of diluted plasmid (initial DNA concentration of 200 ng/µl) and 5 µl of tracking dye were loaded in the first well of each row of a 2% agarose gel, producing a band with a content of DNA equal to 50 ng. The other wells of the gel were loaded with 10 µl of a mix of 5 µl of ExoSAP product and 5 µl of loading dye. The amount of DNA contained in each PCR product was determined by visual comparison with the plasmid pGEM 32f(+) band.

According to the microCLEAN single-reagent kit protocol, an equal volume of 3 µl of microCLEAN was added to 3 µl of PCR product, mixed by spinning for 10 s and vortexed briefly, and left to rest at room temperature for 5 minutes. Plates of PCR products were, subsequently, spun for 40 min at 50 Hz and temperature of around 21 ºC. The supernatant was removed by spinning the plate upside-down on a layer of tissue paper at 10 Hz for 1 min. Tubes containing PCR products were spun for 8 min at ~215 Hz and temperature of around 21 ºC. The supernatant was completely removed manually with a pipette.

2.3.6. Sequencing Reaction

Direct sequencing of *BARX2* was carried out using the BigDye Terminator v3.1 method for PCR products purified with the ExoSAP method, as follows. A quantity of 3 µl of each ExoSAP-PCR product was transferred into a well of a new sequencing plate (compatible with the MegaBace DNA Analysis System). The whole procedure was carried out on ice, and a quantity of 12 µl of the sequencing reaction mix was added to each well, to reach a final reaction volume of 15 µl. The sequencing reaction mix was made up with the reagents listed in Table 9.

Sequencing Mix	**x 1 sample**
BigDye Terminator v3.1	2.0 µl
5X Sequencing Buffer	3.0 µl
PCR Forward Primer (50 ng/µl)	1.0 µl
ddH2O	6.0 µl
ExoSAP-PCR product (DNA)	3.0 µl
Final Reaction Volume	15 µl

Table 9. **Sequencing reaction mix for *BARX2* following ExoSAP method.** Sequencing reaction mix for PCR products purified with the ExoSAP method.

The primer added to the sequencing mix was the same utilised in the PCR amplification of each exon of *BARX2*, at the same concentration of 50 ng/µl. In the sequencing reaction the forward primer was used for each exon of *BARX2*. One sequencing programme was used for all exons of *BARX2*, as outlined in Table 10.

Step	**Temperature (°C)**	**Running Time**
1	95	2 min
2	95	20 s
3	55	10 s
4	60	4 min
go to 2		repeat 34 cycles
5	20	2 min
6	4	Forever

Table 10. **Sequencing programme for *BARX2*.**

After running the sequencing programme, the PCR products were submitted to a desalting treatment with the Sephadex purification protocol. The MultiScreen Column Loader was loaded by completely filling the wells with Sephadex G-50. The excess of Sephadex G-50 was carefully collected by scraping the surface of the plate and put back in the container. A MultiScreen 96-well filter plate was placed on top of the filled Multi-Screen Column Loader and the two plates were flipped over, and the bottom of the Multi-Screen Column Loader was tapped firmly a few times (on average 3 times) to let all Sephedex powder fall out of the wells of the Multi-Screen Column Loader and into the wells of the MultiScreen 96-well filter plate. The Multi-Screen Column Loader was then removed. A volume of 300 µl of ddH2O was added to each well of the filter plate containing the Sephadex powder, the plate was wrapped in parafilm, and incubated at room temperature until the Sephedex powder inflated. The Sephadex filter plate was then weighed and spun for 5 min at 910 g and 4 ºC with the appropriate counterbalance, in order to pack the Sephadex column. The water tray was emptied. A volume of 150 µl of ddH2O was added to each well of the Sephadex filter plate, the plate was weighed, spun again for 5 min at 910 g and 4 ºC with the appropriate counterbalance, and emptied from the waste. The Thermowell wash plate was replaced with a new 96-well collection plate.

A volume of 10 µl of ddH2O was added to each sample in the sequencing plate, producing a final volume of 25 µl. The 25 µl samples from the sequencing plate were carefully added to the top of the packed column of Sephadex in the Sephadex filter plate, making sure to load the samples to the centre of the Sephadex column, without touching the column itself or loading along the wall of the well. The Sephadex filter block was weighed and spun for 5 min at 910 g and 4 ºC with the appropriate counterbalance. The Sephadex filter plate was removed, and the sample plate was dried and held at 4 °C until submission to sequencing with MegaBace DNA Analysis System.

Direct sequencing of *BARX2* was carried out using the BigDye Terminator v3.1 method for PCR products purified with the microCLEAN method, as follows. The whole procedure was carried out on ice. In order to cost-effectively decrease the volume of BigDye Terminator v3.1 utilised for each reaction, a BigDye Terminator v3.1 premix was prepared by adding 1 volume of BigDye Terminator v3.1 to 1 volume of 5X Sequencing Buffer and to 3 volumes of ddH2O. The final reaction volume was 5.0 µl

per sample. The BigDye Terminator v3.1 premix was used to make up the definitive sequencing reaction mix with the reagents listed in Table 11.

Sequencing Reaction Mix	**x 1 sample**
BigDye Terminator v3.1 premix	4.0 µl
PCR Primer (20 ng/µl)	1.0 µl
ddH2O	5.0 µl
Final Reaction Volume	10 µl

Table 11. **Sequencing reaction mix for *BARX2* following microCLEAN method.** Sequencing reaction mix for PCR products purified with microCLEAN.

The primers added to the sequencing mix were the same utilised in the PCR amplification of the exons of *BARX2*. In the sequencing reaction both forward and reverse primer were used for exons 2 and 3, while the forward primer only was used for the sequencing of exons 1 and 4. The primer concentration for the sequencing reaction was 20 ng/µl. A volume of 10 µl of the sequencing mix was added to each well of the plate of purified PCR products. One sequencing programme was used for all exons of *BARX2*, and for both the forward and reverse primer of exons 2 and 3. The sequencing programme is outlined in Table 12.

Step	**Temperature (°C)**	**Running Time**
1	96	1 min
2	96	30 s
3	56	15 s
4	60	4 min
go to 2	repeat 34 cycles	
5	20	2 min
6	4	Forever

Table 12. **Sequencing reaction programme for *BARX2*.** A lower concentration of both BigDye Terminator v3.1 enzyme and primer was utilised.

After running the sequencing programme, the PCR products were purified with a NaAc-EtOH precipitation mix, consisting of 2.0 µl of NaAc 3.0 mol/l, pH 5.2 and 50 µl of 100% EtOH, per sample. A volume of 50 µl of the precipitation mix was added to each

well of the sequence plate, the plate was sealed, vortexed gently, and left at room temperature for 20 min. Subsequently, the plate was weighed and spun with a counterbalance for 40 min at 67 Hz and temperature around 21 ºC. The supernatant was removed by emptying the plate into a sink. The PCR products were further washed by adding 50 µl of 70% EtOH into each well. The plate was weighed again and spun with a counterbalance for 10 min at 67 Hz and temperature around 21 ºC. The supernatant was removed by emptying the plate into a sink, and subsequently spinning the plate upside down on a layer of tissue paper for 1 min at 5 Hz. A volume of 10 µl of deionised formamide was added to each well, and the plate was sealed and stored in a fridge compartment until submission to sequencing with ABI 3730 DNA Analyser.

For the direct sequencing of *BMP4* and *OTX2*, both the BigDye Terminator v3.1 and the BigDye Terminator v1.1 protocols for PCR products purified with the microCLEAN method were utilised. The protocol designed for the sequencing reaction carried out with the BigDye Terminator v3.1 method was adjusted to the use of the BigDye Terminator v1.1, as shown in Table 13.

BigDye Terminator v1.1 Sequencing Reaction Mix	**x 1 sample**
BigDye Terminator v1.1	0.5 µl
5X Sequencing Buffer	1.5 µl
5.0 mol/l Betaine	2.0 µl
PCR Primer (20 ng/µl)	0.1 µl
ddH2O	5.9 µl
Final Reaction Volume	10 µl

Table 13. **BigDye Terminator v1.1 sequencing reaction mix.**

The primers added to either the BigDye Terminator v3.1 or BigDye Terminator v1.1 sequencing mix were the same ones utilised in the PCR amplification of the exons of *BMP4* and *OTX2*. In the sequencing reaction, both forward and reverse primer were used for all exons of both genes. The primer concentration was 20 ng/µl. A volume of 10 µl of the sequencing mix was added to each well of the plate of purified PCR products, and the same sequencing programme utilised for *BARX2* was used for both forward and reverse primer, for all exons of both *BMP4* and *OTX2* (Table 12). After

running the sequencing programme, the PCR products were purified with the NaAc-EtOH precipitation mix and protocol, as described above for *BARX2*.
When using the BigDye Terminator v3.1 method, a volume of 10 µl of deionised formamide was added to each well.
According to the BigDye Terminator v1.1 protocol, each PCR product was re-suspended in 10 µl of 1:10 dilution of 1X Tris-EDTA (TE) Buffer.
The plate was then sealed and stored in a fridge compartment until submission to sequencing with ABI 3730 DNA Analyser.

The genomic sequences of all exons of *BARX2*, *BMP4* and *OTX2* were analysed with the software Sequencher 4.7.

2.4. Restriction Digestion

A restriction enzyme digestion was performed following the identification of a nucleotide change in exon 4 of *OTX2* in one patient. The status of the mutation was assessed in 60 controls.

2.4.1. Selection of Restriction Enzyme

The online tool REBsites from the Restriction Enzyme data BASE - REBASE was utilised to identify the restriction enzyme for the digestion protocol. [214, 215] The restriction enzyme BfaI that cut, differentially, both the wild-type and the mutated sequence was selected; the cut in the wild-type sequence was used as a positive control of the restriction enzyme's activity. BfaI cleaved the wild-type sequence once and the mutated sequence twice. The predicted results and products of the two digestions are summarised in Table 14.

Length (bp)	5' Enzyme	5' Base	3' Enzyme	3' Base
wild-type				
208	BfaI	118	none	325
117	None	1	BfaI	117
mutation				
122	BfaI	204	none	325
117	None	1	BfaI	117
86	BfaI	118	BfaI	203

Table 14. **Predicted digests with the restriction enzyme BfaI.**

2.4.2. Restriction Digestion Protocol

Exon 4 of *OTX2* was amplified by PCR in 60 controls, following the protocols described above. The PCR products were transferred onto a plate, together with the samples of the patient in whom a mutation in exon 4 of *OTX2* had been identified by direct sequencing, and of both parents of the patient. The PCR fragments were purified with microCLEAN single-reagent kit utilising an equal volume of 5 µl of PCR product and 5 µl of microCLEAN reagent. At the end of the procedure, the pellet in each well was re-suspended in 5 µl of ddH2O, and left for 5 min at room temperature. The restriction digestion was carried out by adding 15 µl of a reaction master mix on top of the 5 µl of purified PCR product and mixing thoroughly avoiding the creation of air bubbles, to reach a final reaction volume of 20 µl, as shown in Table 15. The whole procedure was carried out on ice, until the time of starting the reaction.

Reaction Mix	x 1 sample	Final concentration
BfaI 5,000 U/ml	1 µl	5 U
10X NEBuffer 4	2 µl	1X
ddH2O	12 µl	
Purified PCR product	5 µl	
Final Reaction Volume	20 µl	

Table 15. **Restriction digestion reaction mix.**

The plate was incubated in a water bath at 37 ºC for 3 hours. The results of the restriction digestion were evaluated by electrophoresis on a 2% agarose gel. A volume of 100 ml of 2% agarose gel was prepared as described above (paragraph 2.2.1.), by adding 2 grams of agarose to 100 ml of a 1.0X TBE solution. An aliquot of 10 µl of restriction digestion product from each sample was mixed with a volume of 5 µl of tracking dye and loaded onto the gel. An aliquot of 10 µl of restriction digestion reaction mix without PCR product was loaded, with 5 µl of tracking dye, as a negative control for DNA contamination. A volume of 10 µl of PCR product from a control DNA sample, that did not undergo the restriction digestion, was also mixed with 5 µl of tracking dye and loaded onto the gel, as a negative control for restriction enzyme activity.

3. RESULTS

Patient Selection for CNV Analysis

Summary of results:

- A checklist of inclusion criteria was designed to select the patients to screen for genomic copy number changes by means of high-resolution SNP array;
- The patients were selected from the database of endocrinological patients of the Great Ormond Street Hospital. The clinical records were divided into groups according to the primary endocrinological diagnosis. Within each diagnostic group a separation was made between patients who presented with an isolated endocrinological pathology and patients with a complex clinical phenotype, in order to facilitate the application of the checklist;
- The evaluation of the database allowed the identification of a recurrent association between hypopituitarism and the rare cardiac malformation tetralogy of Fallot;
- A total of 10 patients were selected through the process to undergo whole genome testing for chromosome imbalances;
- Amongst the selected patients, one child and one young adult, both affected by severe hypopituitarism, were already known to carry an unbalanced and an apparently balanced rearrangement of chromosome 11q, respectively.

3.1. Checklist of Inclusion Criteria

In order to select the patients to be screened with high resolution genome-wide array, a list of inclusion criteria was compiled, and subsequently formalised into a checklist of selection criteria, presented in Table 16. The likelihood of harbouring a genomic copy number change increased with the number of criteria relevant to each patient and the overall score. A total score of at least 8 and the presence of at least one criteria from

section 4. (aside from 4. a) endocrinological disorders) were necessary for inclusion in the screening.

Checklist of Selection Criteria	**Score**
1. Family history	
a) non-consanguineous parents consanguineous parents	**0** **-1**
b) multiple miscarriages	**1**
c) 'chromosomal phenotype', mainly major congenital malformations, in a close relative	**2**
2. Apparently balanced chromosome translocation in a patient with an abnormal clinical phenotype	**6**
3. Known monogenic disease within a more complex clinical phenotype	**4**
4. Complex clinical phenotype including	
a) endocrinological disorders	**mandatory**
b) developmental delay/behavioural problems	**3**
c) microcephaly, growth abnormalities	**1**
d) major congenital anomalies of at least one organ and/or system unrelated to the pituitary gland and the brain (limbs and heart, in particular)	**3**
e) facial dysmorphic features (at least 2-3)	**1**
f) other clinical problems	**1**

Table 16. **Checklist of selection criteria.**

Developmental delay and mental retardation are the most common marker for the selection of patients to undergo screening for submicroscopic chromosome abnormalities. However, in the present study the essential inclusion criteria was the endocrinological disorder/s presented by each patient. The other inclusion criteria focused on the association of the endocrinological phenotype with indicators of a genomic imbalance as the aetiology.

1. a) An accurate family tree can usually confirm or rule out whether a genetically significant degree of consanguinity is present between the parents of a patient. This was relevant because parental consanguinity represents a risk factor for diseases with Mendelian autosomal recessive inheritance, rather than gene dosage imbalance due to

chromosomal submicroscopic abnormalities.

1. b) and c) A family history of recurrent miscarriages and/or a complex clinical phenotype in a close relative, similar to or different from the one presented by the patient under study, are suggestive of the presence of a balanced chromosome translocation in the family, that gave rise to a genomic imbalance and a pathological phenotype in the patient. The observation of a complex clinical phenotype in a close relative, different from the one shown by the patient, can be due to the concomitant presence of reciprocal derivative unbalanced chromosome translocations.

2) An abnormal clinical phenotype can be associated with an apparently balanced chromosome translocation (or other anomaly, e.g. inversion), defined by karyotyping on G-banding, and preferably at International System for human Cytogenetic Nomenclature (ISCN) +550. For patients who presented with such an association, and who were potential candidate for high resolution genome-wide copy number change screening, it was particularly important to obtain information regarding any other molecular cytogenetic investigation carried out (e.g. FISH of the subtelomeric regions of the chromosomes, sequential specific loci FISH). The results of these investigations, when available, were weighed into the selection process.

3) Patients with a recognised monogenic disease within a more complex clinical phenotype were considered to be ideal candidates for harbouring a submicroscopic chromosome imbalance. In fact, the patient's phenotype could arise from a contiguous gene syndrome including the gene responsible for the known diagnosed condition, as well as a novel candidate gene for the endocrinological phenotype and pathology of the pituitary gland.

4. a) The endocrinological phenotype of each patient was pivotal in guiding the selection process. All patients entered into the screening presented with variable degree and manifestations of pathology of the pituitary gland.

4. b) Variable degrees of DD, neurobehavioural problems and learning difficulties are the most common finding in patients with gene dosage imbalance, and were frequently associated with the endocrinological phenotype in the cohort of patients under study. DD and MCA represent the stronger markers that point towards the presence of a submicroscopic genome anomaly.

4. c) Apart from DD and MCA, growth abnormalities and microcephaly are considered common markers of a genetic aetiology and of gene dosage imbalance underlying the clinical phenotype of the patient. Growth abnormalities are also a strong indicator of

impaired function of the pituitary gland. Therefore, this aspect of the clinical phenotype of each patient was carefully considered.

4. d) The pituitary gland and the nervous system (brain) are tightly connected anatomically, embryologically, as well as functionally (in the neuro-endocrine system). Consequently, the combination of endocrinological and neurological symptoms, and underlying pituitary gland and brain malformations, is observed in several conditions. Therefore, the presence of major congenital malformation/s involving at least one other unrelated, distant organ and/or system was deemed necessary to define a complex clinical phenotype.

4. e) The thorough examination and detection of facial dysmorphic features in a patient can represent an useful instrument to guide the diagnosis. Also, the presence of a minimum number of 2-3 facial dysmorphic features, within a complex clinical phenotype, seems to increase the likelihood of identifying a genetic aetiology of the phenotype, as a submicroscopic genomic imbalance. The presence of dysmorphic features was evaluated in each patient, when the relevant information were available in the database, and, in particular, subsequently, when a patient could be examined in person.

4. f) Each clinical problem and aspect of the phenotype of each patient was taken into consideration during the selection process.

3.2. Database of Endocrinological Patients

All 1,697 clinical records included in the database of endocrinological patients were evaluated, and a list of 1,168 index cases was compiled, for whom sufficient information were available in the database. The index cases were subsequently divided into groups according to the primary endocrinological diagnosis. When information on the endocrinological phenotype of the patient were not available at the moment of starting the study, the clinical records were divided into groups according to the principal diagnosis suggestive of, or commonly associated with, an endocrinological disorder. A list of all primary diagnoses entered in the database and the relevant

number of patients are reported in Table 17, first and second columns. Within each diagnostic group, a separation was made between patients who presented with an isolated endocrinological or endocrine-related pathology, and patients who showed an association with other symptoms within a complex phenotype. Associations with environmental and/or acquired pathologies and/or multifactorial diseases observed in the general population (e.g. asthma) were not considered significant when defining a complex clinical phenotype. The numerical results of this subdivision are shown in Table 17, third column.

Primary diagnosis	**Number of patients**	**Patients with complex phenotype**
SOD	359	65
CPHD/panhypopituitarism (with or without structural anomalies of the pituitary gland)	304	48
IGHD	251	27
ONH	44	3
GHD (not better characterised)	28	1
Midline defects	18	12
Holoprosencephaly (HPE)	16	5
Short stature (not better characterised)	16	2
Miscellaneous pathology of pituitary gland (e.g. pituitary enlargement)	13	2*
Micro-/anophthalmia	8	4
HH	8	3
Thyroid gland pathology	7	-
Obesity	7	-
GH neurosecretory dysfunction (GHNSD)	5	-
Constitutional delay of growth and puberty (CDGP)	4	-
Cortisol deficiency	4	-
GHD associated to Fanconi anemia (FA)	4	-
Insulin-dependent diabetes mellitus (IDDM)	4	-
Sanjad-Sakati Syndrome	4*	-
Congenital adrenal hypoplasia (CAH)	3	-

Leri-Weill dyschondrosteosis	3*	-
Pancreas pathology	3	-
ACC	2	1
Ambiguous genitalia	2	-
DI	2	1
Ovary agenesis	2	-
Miscellaneous (e.g. absent uterus)	47	5
Total number of patients	**1168**	**179**

Table 17. **Numerical breakdown of the 1,168 index cases.** The clinical records included in the database of endocrinological patients were classified according to the primary diagnosis. The number of patients who presented with a complex clinical phenotype is also shown for each group. *Familial case; ACC: Agenesis of Corpus Callosum; CPHD: Combined Pituitary Hormone Deficiency; DI: Diabetes Insipidus; GH: Growth Hormone; GHD: Growth Hormone Deficiency; HH: Hypogonadotropic Hypogonadism; HPE: Holoprosencephaly; IGHD: Isolated Growth Hormone Deficiency; ONH: Optic Nerve Hypoplasia; SOD: Septo-Optic Dysplasia; -: no patients.

3.3. Association of Hypopituitarism with Tetralogy of Fallot

Amongst the 1,168 clinical records included in the database, six patients were identified who presented with the association of pathology of the pituitary gland and Tetralogy of Fallot (ToF). A list was compiled, and the summary of the symptoms associated with ToF in each one of these patients, together with their primary endocrinological diagnoses, is shown in Table 18.

ID	Primary diagnosis Other endocrinological symptoms	Other symptoms
5066	Midline defects (bilateral cleft lip and palate) HH	Anosmia
5135	DI Hypothyroidism, IUGR	Epilepsy, bilateral cleft lip and palate
5608	SOD CPHD	Bilateral aplasia of the retina
5745	IGHD	Midline defects
5859	CPHD	DD, tracheo-oesophageal fistula, laryngomalacia, duodenal web, known unbalanced karyotype: 46,XY,add(5)(q11.2).ish dup(5)(q22q11.2)(WCP5+)de novo; deceased
6168	CPHD Short stature, hypoplastic anterior pituitary	Exomphalos

Table 18. **Patients with hypopituitarism and Tetralogy of Fallot.** CPHD: Combined Pituitary Hormone Deficiency; DD: Developmental Delay; DI: Diabetes Insipidus; HH: Hypogonadotropic Hypogonadism; IGHD: Isolated Growth Hormone Deficiency; IUGR: Intrauterine Growth Retardation; SOD: Septo-Optic Dysplasia; ID: patient Identification number.

Patient 5859 was born from non-consanguineous parents, two weeks post-term, with a low birth weight of 2.4 kg. The patient unfortunately died at the age of 10 years. At birth, he had presented with ToF, that had required surgical intervention, a tracheo-oesophageal fistula, laryngomalacia, and duodenal web. Subsequently, he had shown DD and he had been diagnosed with hypopituitarism treated with GH, thyroxine and hydrocortisone. He was found to have a de novo partial inverted duplication of chromosome 5q.

On the basis of the preliminary information available in the database, the clinical phenotype of patient 5066 was deemed compatible with the diagnosis of Kallmann

syndrome. ToF had not been previously reported in Kallmann syndrome, however, congenital heart defect (CHD) is part of the clinical phenotype of this condition. The patient was, therefore, referred for further molecular cytogenetics analysis of the chromosome region Xp22.3 and the Kallmann syndrome interval gene 1 (*KALIG1*), in order to confirm or exclude the diagnosis, and was not considered to be a candidate for the screening with the 250K SNP array platform.

Four more cases of the association between variable degrees and manifestations of pathology of the pituitary gland and ToF were identified in the database of endocrinological patients: one patient had a primary endocrinological diagnosis of SOD with CPHD, one patient had a primary diagnosis of CPHD, one of IGHD, while one patient had DI and central hypothyroidism.

ToF is a complex and severe cardiac malformation presenting with the characteristic association of a ventricular septal defect (VSD), aorta overriding the VSD and right ventricle, pulmonary outflow tract stenosis and right ventricular hypertrophy. It constitutes ~10% of all CHD, and it has an incidence of 1/2500 newborns in the general population.

When only considering the patients without an aetiological diagnosis, the incidence of ToF in the database of endocrinological patients under study was of 4 over 1,168 index cases, equal to 1/292. This value is ~8.5 times greater than the one observed in the general population (1/2500). The cohort of endocrinological patients was pre-selected, and therefore biased, on the basis of the presence of pathology (versus the general population). However, the significant number of cases of association of ToF with hypopituitarism led to consider this recurrent association of interest for the high resolution genome-wide copy number screening with 250K SNP array platform.

3.4. Patient 6089 with Chromosome 11q Deletion Syndrome

Patient 6089 was born at term from non-consanguineous parents. At birth, he presented with bilateral cryptorchidism and skeletal malformations: hemi-vertebrae at multiple levels, multiple rib anomalies, including fusion of the right VII and VIII ribs, radial

shortening, short middle phalanx with clinodactyly; he also suffered from neonatal transient megakaryocytic thrombocytopenia. Subsequently, the patient presented with stature below the 3rd percentile, and severe GHD was diagnosed with undetectable levels of IGF1; an MRI targeted at evaluating the morphology of the pituitary gland demonstrated anterior pituitary hypoplasia, ectopic posterior pituitary, and absence of the rostrum of the corpus callosum. The patient responded extremely well to GH replacement therapy, and his growth velocity was restored to normal.

Patient 6089 carried a complex unbalanced chromosome rearrangement comprising of a partial terminal duplication of the long arm of chromosome 6, and a partial terminal deletion of chromosome 11q. His unbalanced karyotype was defined by routine cytogenetics as: 46,XY,del(11q24.2→qter) dup(6q25.3→qter)mat der. The chromosome imbalances derived from a maternal reciprocal translocation.

3.5. Patient 18905640 with Karyotype 46,XY,t(11q;22q)

A patient from China presented with panhypopituitarism, pituitary dwarfism with only scanty anterior pituitary tissue in a small sella turcica, and absent pituitary stalk, and carried an apparently balanced chromosome translocation between chromosomes 11q24 and 22q13, karyotype: 46,XY,t(11;22)(q24;q13). [216] At the age of 21 years, the patient did not show any sign of cognitive impairment. [Yang, personal communication] The chromosome translocation had been defined cytogenetically at low resolution; a DNA sample was obtained from this patient to perform 250K SNP array analysis, although no cell suspension for FISH analysis was available.

3.6. Clinical Details of the Patients Included in the CNV Analysis

The checklist of selection criteria was applied to each one of the 179 patients who presented with pathology of the pituitary gland within a complex clinical phenotype, and, therefore, a clinical history and symptoms compatible with the presence of an imbalance of multiple genes (contiguous gene syndrome).

Ten patients were eventually selected to undergo high resolution genome-wide copy number change screening, with the 250K SNP mapping array platform. Amongst them: 3 patients had a primary endocrinological diagnosis of IGHD, 2 patients had a diagnosis of SOD, 2 of CPHD/panhypopituitarism, 2 had growth deficiency and short stature, and 1 patient had DI. The clinical phenotypes of these patients, together with their primary endocrinological diagnoses, and the scores according to the checklist are reported in Table 19.

ID	Endocrinological phenotype	Other symptoms	Score
18905640	Panhypopituitarism, pituitary dwarfism: scanty anterior pituitary tissue in small sella turcica, absent pituitary stalk	Abnormal fusion of the humeral head and acromions bilaterally	**9**
4754	SOD, CPHD	Severe DD, gastro-intestinal malformation, myelodysplastic syndrome, facial dysmorphic features	**8**

4997	Growth deficiency, bilateral cryptorchidism	Severe prematurity (born at week 33 of gestation), DD, bilateral cleft lip and palate, bilateral epibulbar dermoids, right microphthalmia, micrognathia, multiple hemi and butterfly vertebrae, bilateral renal dysplasia, chronic renal failure, urethral multiplication, skin tags	**16**
5135	DI, central hypothyroidism, IUGR, post-natal growth deficiency	DD, epilepsy, ToF, bilateral cleft lip and palate	**10**
5608	SOD, GHD, TSHD	DD, ToF, bilateral aplasia of the retina and optic disc, hearing loss, facial dysmorphic features	**11**
5745	IGHD	DD, ToF, midline defects, facial dysmorphic features	**10**
6089	Severe GHD with undetectable levels of IGF1, short stature <3rd percentile, bilateral cryptorchidism, anterior pituitary hypoplasia, EPP, absence of the rostrum of the corpus callosum	Multiple skeletal malformations: hemi-vertebrae, fusion of the right VII and VIII ribs, radial shortening, short middle phalanx, clinodactyly, facial dysmorphic features, transient neonatal megakaryocytic thrombocytopenia	**9**
6110	Postnatal growth deficiency	Perinatal asphyxia, DD, microcephaly, cortical dysplasia, seizures, bilateral blepharophimosis, microphthalmia and coloboma, renal dysplasia, thrombocytopenia	**12**
6168	Hypopituitarism, hypoplastic anterior pituitary gland, short stature	DD, ToF, exomphalos	**9**

JD98	IGHD, hypoplastic anterior pituitary gland, short stature	Moderate DD, hypoplasia of the optic chiasma and left optic nerve, retinal rod-cone dystrophy, atrial septal defect, leg asymmetry, mild facial asymmetry and dysmorphic features, white forelock, hyper- and hypopigmented skin patches	**12**

Table 19. **Ten patients selected for high resolution genome-wide copy number change screening.** The endocrinological diagnosis, associated symptoms, and relevant scores according to the checklist are reported. CPHD: Combined Pituitary Hormone Deficiency; DD: Developmental Delay; DI: Diabetes Insipidus; EPP: Ectopic Posterior Pituitary; GHD: Growth Hormone Deficiency; IGF1: Insulin-like Growth Factor 1; IGHD: Isolated Growth Hormone Deficiency; IUGR: Intrauterine Growth Retardation; SOD: Septo-Optic Dysplasia; ToF: Tetralogy of Fallot; TSHD: Thyroid-Stimulating Hormone Deficiency; ID: patient Identification number. Patient 6089 had karyotype: 46,XY,del(11q24.2→qter) dup(6q25.3→qter)mat der. Patient 18905640 had karyotype: 46,XY,t(11;22)(q24;q13).

Patient 6089 was known to have an unbalanced karyotype comprising a partial terminal deletion of chromosome 11q. Because of the association between the chromosome anomaly and his complex phenotype, that included severe GHD and multiple anomalies of the pituitary gland's anatomy, this patient was selected for the screening for further investigation. Moreover, the presence of a known chromosome imbalance constituted a positive control during the optimisation and validation of the CNAT 4.0 Batch Analysis Workflow for the Affymetrix GeneChip 250K Sty1 Mapping Array.

Patient 4754 presented with an unique association of two severe and aetiologically unrelated pathologies, namely SOD and myelodysplastic syndrome (MDS), that had not been reported before in the literature, and that suggested the possibility of an underlying contiguous gene deletion/duplication syndrome.

Four patients, 5135, 5608, 5745 and 6168, presented with the association between hypopituitarism and ToF.

Three patients, 4997, 6110 and JD98, presented with complex phenotypes including growth defects, DD, eye pathology, and multiple congenital anomalies.

Patient 18905640 suffered from panhypopituitarism associated with minor skeletal defects, without cognitive impairment. The demonstration of an apparently balanced

chromosome translocation during routine karyotyping identified this patient as a candidate to harbour a submicroscopic imbalance in a candidate genomic region for pathology of the pituitary gland.

While the application of the checklist to the cohort of 179 patients with complex pituitary phenotypes was based on the preliminary information available in the database, for each one of the 10 patients eventually selected for the CNV screening, the standardised patient pro-forma designed for the project was filled in. Patients 5608, 6089 and JD98 were seen in person by the author. For patient 5135, complete and detailed clinical notes were made available to the author, and for patient 18905640 the patient pro-forma was filled in by his physician according to the author's instructions. For the other five patients, clinical information regarding each patient were made available to the author, however, the quantity and quality of the information varied with their source.

The cohort of patients selected for CN change screening on 250K SNP array platform was restricted to the number of ten. This poses limitations to the extrapolation of data, as discussed in chapter 6.4.

4. RESULTS

CNV Analysis

Summary of results:

- The 250K SNP array platform was utilised to perform genome-wide copy number change analysis in 10 patients with a complex clinical phenotype, including pathology of the pituitary gland;
- An analytical workflow was drawn to screen the multiple CNVs detected in the cohort of patients, and CNVs were detected in all patients;
- The presence of two pathogenic genomic imbalances, chromosome 6q terminal duplication and chromosome 11q terminal deletion, was confirmed in one patient, and the breakpoints were defined at high resolution;
- An interstitial deletion of chromosome 22q was diagnosed in a patient with hypopituitarism and tetralogy of Fallot;
- A submicroscopic rearrangement in the chromosome region 1p36.33 was found in a second patient with the association of hypopituitarism and tetralogy of Fallot; this CNV and three more genomic regions, affected by the presence of a CNV, were investigated as potential candidate regions for pathology in individual patients;
- Further 359 individual CNVs were assessed in terms of gene content, overlap with published databases of structural variations in the human genome, and for gene expression in the pituitary gland.

4.1. 250K SNP Array to Perform Genome-wide Copy Number Change Analysis

The Affymetrix GeneChip 250K Sty1 SNP mapping array contains probes for the detection of around 2.38×10^5 SNPs. Their genome-wide distribution allows for a large-scale genotype and copy number analysis.

The GTYPE 4.1 plug-in CNAT 4.0 software package, provided by Affymetrix, for CN analysis and graphical visualisation was chosen for the analysis of copy number profiles of all 10 patients selected for the screening. The CN profiles were initially assessed by visual inspection of the log2 Ratio and CN State plots of each autosome and chromosome X. Subsequently, the results of the interrogation of each SNP (i.e. the extrapolated copy number status, and statistic significance of the analysis) were also exported from CNAT 4.0 into Microsoft Excel spreadsheets for numerical analysis.

The whole genome profile of each one of the 10 patients was screened for regions with copy number smaller than 2, to indicate putative losses, and larger than 2, to indicate putative gains, applying the CNAT 4.0 batch analysis workflow with a genomic smoothing of 0.1 Mb (as detailed in paragraph 2.2.5.).

4.2. Ethical Approval and Informed Consent

The personal and clinical data of the patients included in the study are stored in compliance with the Data Protection Act 1998. The project has received full research ethical approval (revised in 2009).

A signed assent/consent form was obtained from each patient (and/or their legal guardians) included in the study. All participants received a patient/parents information sheet, detailing the aim of the study and the use of the participants' DNA sample to

study changes associated with the development and pathology of the pituitary gland. A copy of the information sheet is enclosed as Appendix B.

4.3. Analytical Workflow for the Screening of Multiple CNVs

The great majority of the CNVs found in the cohort of 10 patients were expected to represent genomic polymorphisms and not to be causative of the clinical phenotype presented by the patients under study. For the current project, a decisional workflow was designed by the author in order to filter the total of CNVs, and to identify the potentially pathogenic ones. The outline of the decisional process workflow is presented in Figure 6.

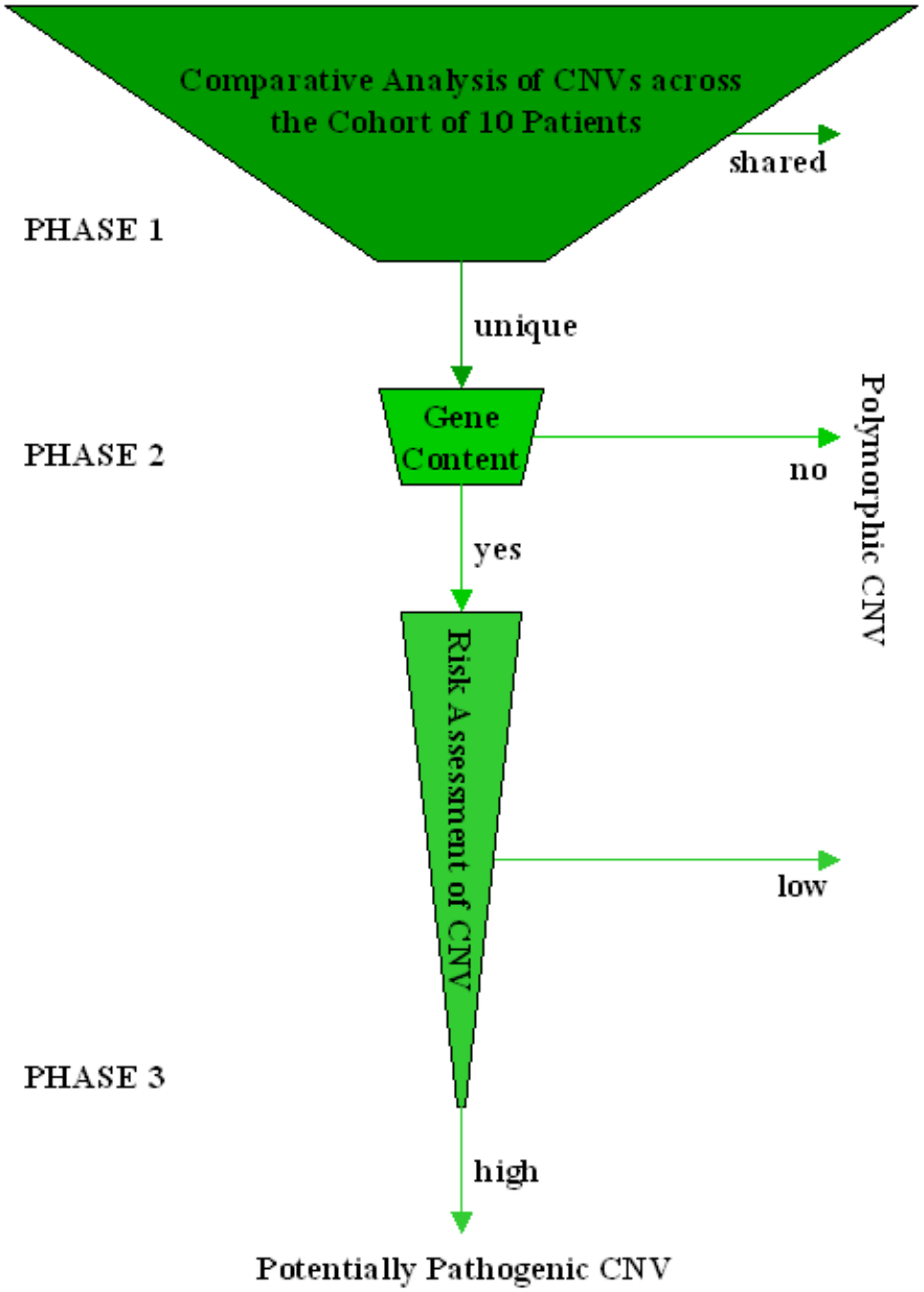

Figure 6. **Workflow of the decisional process.** The decisional process was divided into three phases: the width of the bases of each trapezium are approximately proportional to the number of CNVs that entered and exited each phase of the process; the height of each trapezium is approximately proportional to the timescale required by each one of the three phases the process was divided into.

For the first phase of the screening process, a Microsoft Excel spreadsheet was created for each chromosome (all autosomes and chromosome X) with the CN profile, exported from CNAT 4.0, of all 10 patients. The CN profiles were manually compared across the

whole cohort of 10 patients, and along the entire length of each chromosome, both visually and numerically, to identify CNVs *shared* by multiple patients.

A CNV was defined as *shared* when it fulfilled the following two criteria:

1) the percentage of overlap was equal or greater than 50% of the SNPs;
2) it was found in 2 or more patients, with at least 2 patients presenting with diverse established clinical diagnosis and/or non-overlapping clinical phenotypes.

When a CNV was present, in the same CN state, in only 2 patients with a degree of compatibility of their clinical phenotypes, the CNVs were further investigated in phase 2 of the process. Equally, when only 2 patients with unrelated clinical phenotypes carried a CNV involving the same SNPs but present in different CN states, i.e. CN 1 in one patient and CN 3 or CN 4 in the other patient, the CNVs were further investigated in phase 2 of the process.

Shared CNVs were considered not to be causative of the clinical phenotype in any individual patient, and were not investigated further.

The software CNAT 4.0 is implemented with the UCSC genome browser, and this tool was utilised in phase 2 of the process to assess the gene content of all unique CNVs. To this aim, the numerical output from Microsoft Excel spreadsheets was manually uploaded to UCSC genome browser to examine each CNV.

Although the absence of gene content within a CNV does not define a CNV as a benign (polymorphic) variant in the human population, the decision was made to utilise the criteria of presence versus absence of gene content within a CNV in the proposed decisional workflow. This decision was coherent with the selection of a cohort of patients with complex clinical phenotypes to undergo genome-wide CN screening, as such complex phenotypes, affecting the development of multiple organs, might reflect an underlying contiguous gene microdeletion/microduplication syndrome. The latter would be characterised by the dosage imbalance of two or more genes, including one relevant to the pituitary phenotype.

It is acknowledged that the rationale behind the criteria of phase 2 of the decisional workflow, however, poses a limitation to the identification of disruption of regulatory sequences and/or transcription units, which could lead to a pathological phenotype.

In phase 3 of the decisional process, each unique CNV was assessed in terms of overlap with published databases of genomic structural variations, and each known gene within

unique CNV was assessed in terms of gene function, gene pathways, protein domain/s, existing link to disease loci, known mutations, and gene expression in the pituitary gland.

4.4. SNP Genotype Call Rates

The first step in the screening with Affymetrix GeneChip 250K Sty1 SNP Mapping Array was the evaluation of the SNP genotype call rates, from the .DAT or .CEL file, performed by GTYPE 4.1. The overall performance of the assay is determined by the SNP call rate. The percentages of SNP call rate for all 10 patients included in the study are reported in Table 20; the mean value was 95.78%. Patient 6110 had a SNP call rate of 94.97%, considered to be not significantly different from the optimal cut-off of 95%. Patient 5745 had a SNP call rate of 90.55%, below the average, that was attributed to a less good quality of the DNA sample. This value is above the acceptable threshold of 85% and potential 'no calls' in regions of interest were taken into account during the analysis.

Patient ID	**SNP Call Rate %**
6089	97.02
18905640	96.70
JD98	97.46
5608	96.58
5135	96.07
4754	95.10
5745	90.55
6110	94.97
4997	96.55
6168	96.84

Table 20. **SNP call rates.** Percentage of SNP Call Rate for each one of the 10 patients studied with the Affymetrix GeneChip 250K Sty1 Mapping Array.

4.5. Detection of Multiple CNVs

The whole genome CN profile of each one of the 10 patients was initially assessed by visual inspection of the log2 Ratio and CN State plots of each chromosome. Subsequently, the CNAT 4.0 output for all SNPs of each autosome and chromosome X of each patient were exported to Microsoft Excel spreadsheets, and numerical analysis of the SNP CN state was performed. Tracks of CN profiles were also generated in CNAT 4.0 and exported to UCSC genome browser for purposes of visualisation and analysis.

A CNV was identified when at least two consecutive SNPs were present in CN state different from 2, applying the CNAT 4.0 batch analysis workflow with a genomic smoothing of 0.1 Mb (as detailed in paragraph 2.2.5.). The boundaries of the CNV were arbitrarily defined by the first and last SNP present in CN different from 2, with the aim of increasing specificity. However, it is acknowledged that the exclusion of the genomic regions lying between each boundary of the CNV, as defined, and the first neighbouring SNP in CN 2 decreased sensitivity and potentially led to loss of information. This limitation was taken into consideration during the analysis, and overcome by a revision of the CNV breakpoints when necessary.

A total of 3857 CNVs were found, involving all autosomes and chromosome X, and in all the patients.

4.5.1. Distribution of CNVs per Patient

CNVs were found in all patients, with a great variability in the number of CNVs per patient: the mean value was 386, with a SD of 133 (approximation of both mean and SD is to the nearest unity), while the range was [186 - 611]. No genomic regions in CN state equal to 0 (putative homozygous deletion) were detected in any of the 10 patients. The ratio of 2608 genomic gains, incorporating CN 3 and CN 4, to 1249 genomic losses, CN 1, was ~2:1. The breakdown of the number of different types of CNVs per patient is shown in Figure 7.

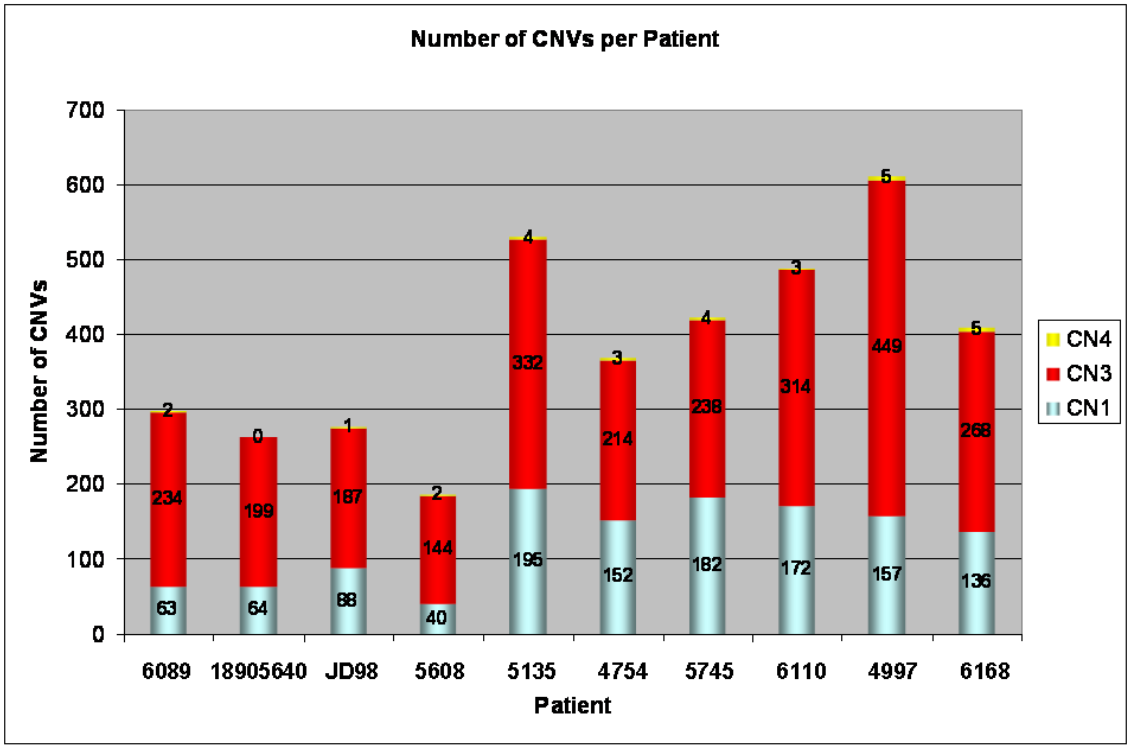

Figure 7. **Distribution of CNVs per patient.** Breakdown of the number of different types of CNVs in each one of the 10 patients in the cohort under study. CN: Copy Number.

4.5.2. Distribution of CNVs per Chromosome

CNVs were found in all chromosomes. Figure 8 represents the breakdown of different types of CNVs per each chromosome in the total of 10 patients. The mean value of CNVs per chromosome was 168 (SD = 130; approximation of both measurements to the nearest unity), while the range was [19 - 547]. The mean value of CNVs in CN 1 per chromosome was 54 versus 113 CNVs in CN 3 plus CN 4 per chromosome.

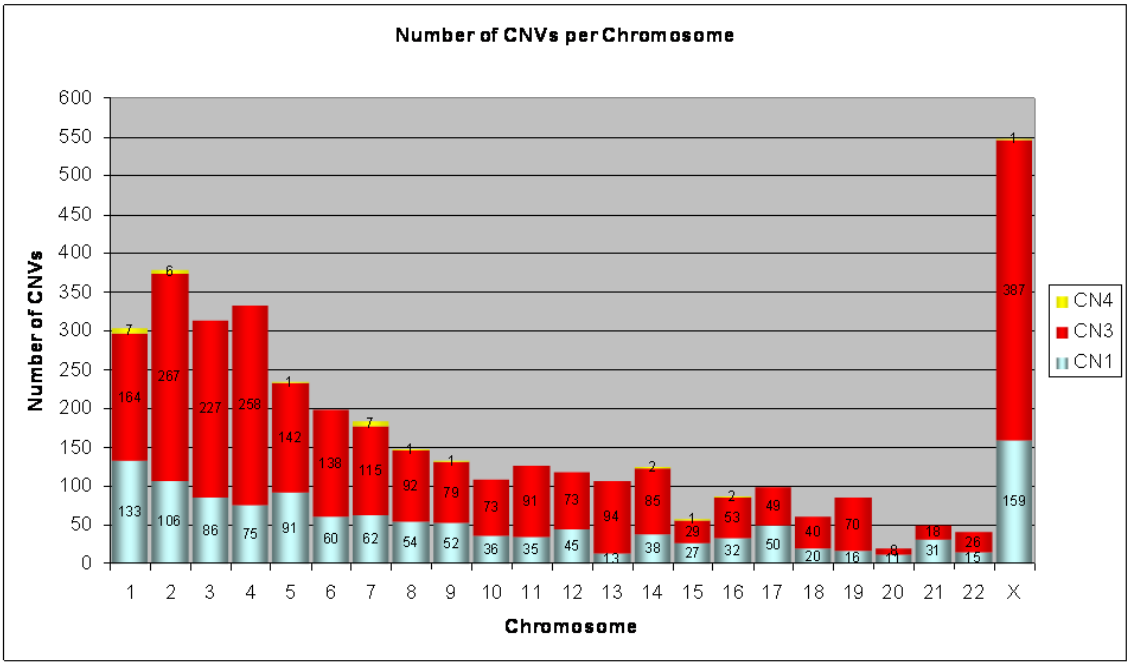

Figure 8. **Distribution of CNVs per chromosome.** Visual and numerical representation of the breakdown of the different types of CNVs per chromosome in the whole cohort of 10 patients. CN: Copy Number.

4.6. Distribution of Unique CNVs per Patient

The comparative analysis of the CN profiles across the whole cohort of 10 patients revealed that 3289 CNVs were shared (as defined in chapter 4.3.), and that only 568 (~15%), of the 3857 CNVs originally found in all autosomes and chromosome X, were unique to one patient. All unique CNVs were entered into phase 2 of the screening process, as potentially pathogenic genomic imbalances for that patient.

No genomic regions in CN state equal to 4 were detected in one patient only. The 568 unique CNVs showed a 1.2:1 ratio (approximated to one decimal place) of 306 genomic gains (CN 3) to 262 genomic losses (CN 1). The ratio demonstrated a relative increase in the number of genomic losses to genomic gains amongst the unique CNVs, when compared to the results (ratio ~2:1) calculated on the total number of CNVs.

Unique CNVs were found in all patients, with a mean value of 57 with a SD of 33

(approximation of both mean and SD is to the nearest unity). The range of variability in the number of unique CNVs per patient, [24 - 129], was smaller than what observed in the overall number of CNVs. The detailed breakdown of the number of different types of unique CNVs per patient is shown in Figure 9.

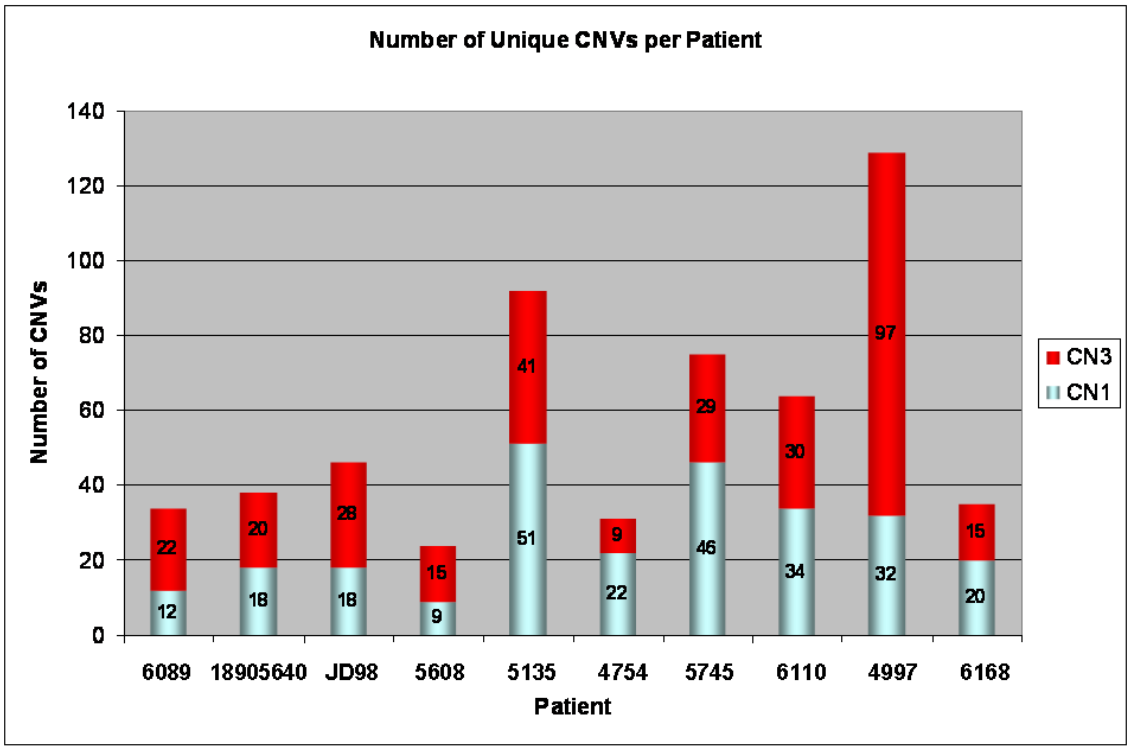

Figure 9. **Number of unique CNVs per patient.** Breakdown of the number of different types of unique CNVs for each one of the 10 patients in the cohort under study. CN: Copy Number.

Assessing the gene content of each unique CNV revealed that 202 unique CNVs did not contain any gene, while 366 (~64%), of the 568 unique CNVs originally found in all autosomes and chromosome X, contained at least one known gene. The 366 unique CNVs with a gene content showed a 1:1 ratio of 187 genomic gains (CN 3) to 179 genomic losses (CN 1). The ratio demonstrated a relative increase in the number of genomic losses to genomic gains amongst the unique CNVs containing at least one gene, when compared to the results (ratio 1.2:1 approximated to one decimal place) calculated on all unique CNVs.

Six categories were arbitrarily created to represent the distribution of the unique CNVs according to gene content: 0, 1, 2, 3, 4, 5 or more. The distribution of unique CNVs in gene content categories per CN state is presented in Figure 10.

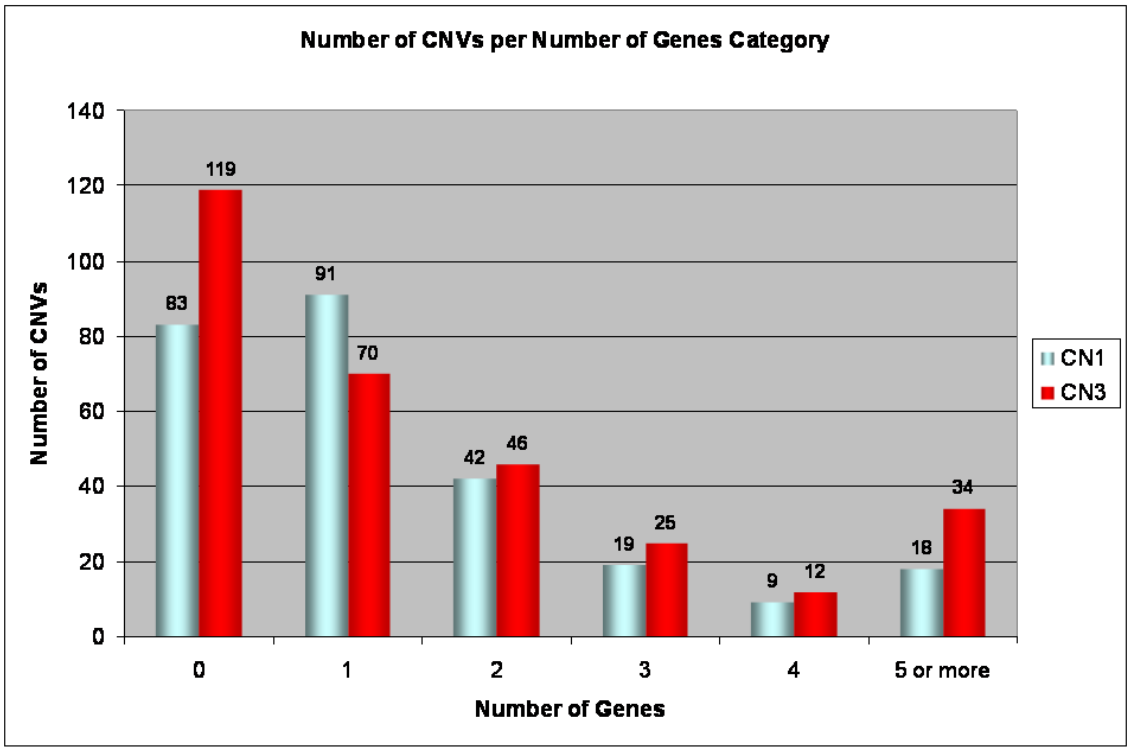

Figure 10. **Distribution of unique CNVs in number of genes categories.** The numbers of unique CNVs in CN state 1 and unique CNVs in CN state 3 belonging to each number of genes category are shown. CN: Copy Number.

Unique CNVs with gene content were found in all patients with a range of [12 - 92]. The numerical breakdown of the different types of unique CNVs with gene content per patient is shown in Figure 11.

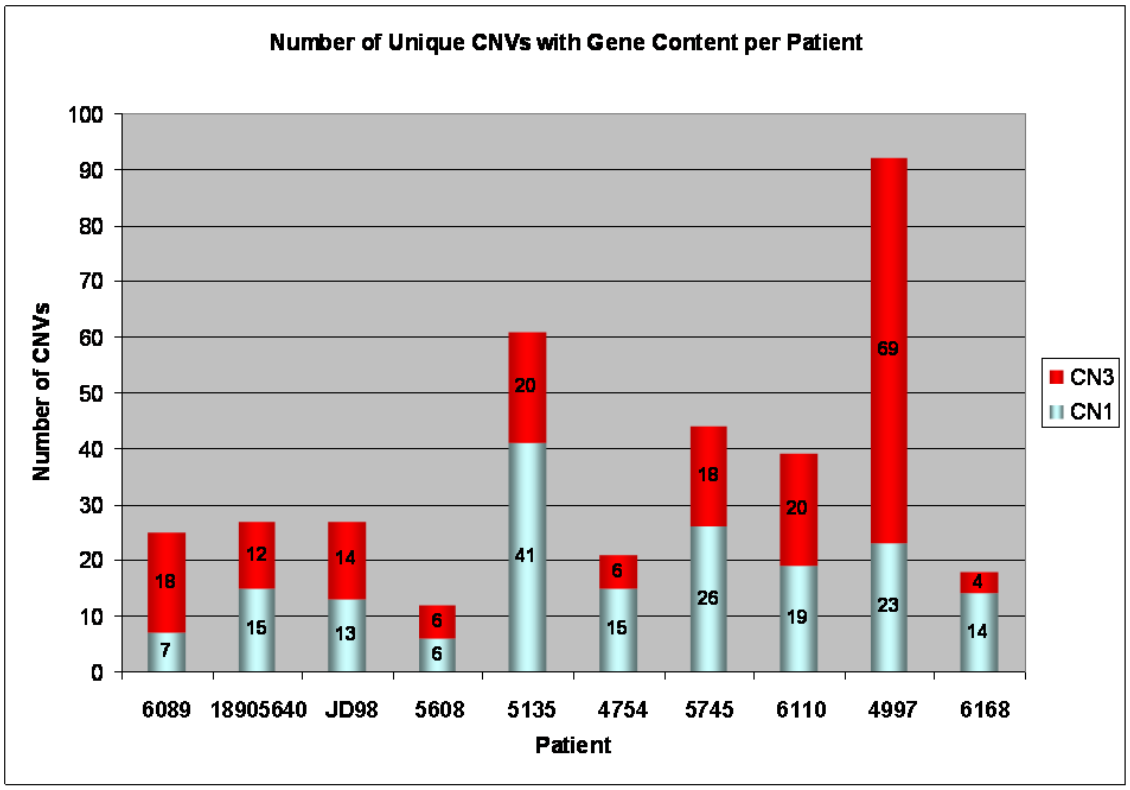

Figure 11. **Number of unique CNVs with gene content per patient.** Breakdown of the numbers of the two different types of unique CNVs, CN 1 and CN 3, containing at least one gene, for each one of the 10 patients in the cohort under study. CN: Copy Number.

4.7. Pathogenic Chromosome Imbalances

Pathogenic copy number changes were first identified by visual inspection of the log2 Ratio and CN State plots produced by CNAT 4.0. The DNA sample of patient 6089, who was known to harbour a complex chromosome rearrangement, was also utilised as a positive control to validate the CNAT 4.0 Batch Analysis parameters. The presence of two genomic imbalances was confirmed in patient 6089, and a further pathogenic chromosome interstitial deletion was diagnosed in patient 5135. The genomic imbalances harboured by the two patients underlie known contiguous gene deletion syndromes.

The breakpoints of the pathogenic genomic imbalances were refined by rerunning the

CNAT 4.0 batch analysis without genomic smoothing (GS = 0 Mb), and exporting the CNAT 4.0 output to Microsoft Excel spreadsheets for numerical analysis of the log2 Ratio and CN State of SNPs within and flanking the detected region of copy number change.

4.7.1. Chromosome 6q Terminal Duplication and Chromosome 11q Terminal Deletion

In patient 6089, the presence of both the partial terminal duplication of chromosome 6q and the partial terminal deletion of chromosome 11q was confirmed. The graphical output of CNAT 4.0 demonstrating the 6q duplication and the 11q deletion is shown in Figure 12 and Figure 13, respectively.

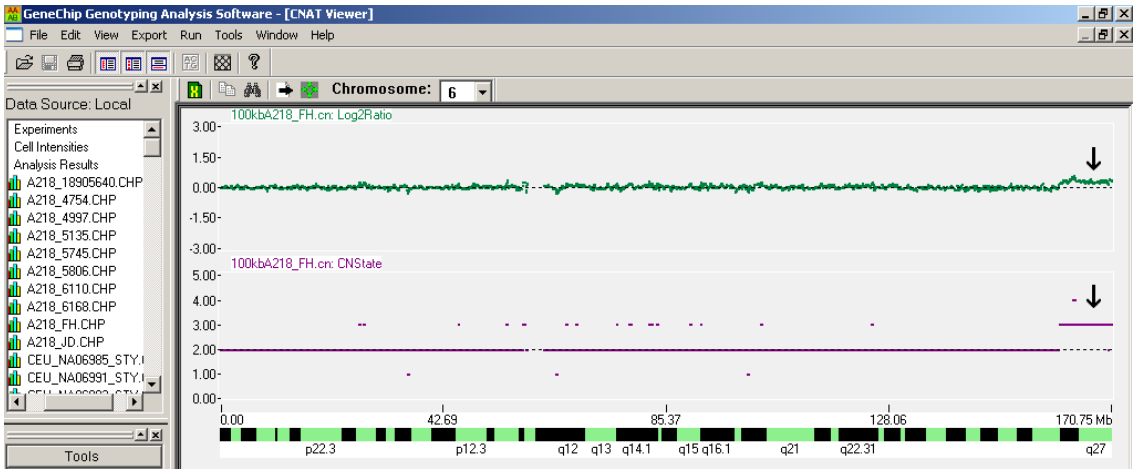

Figure 12. **Chromosome 6q duplication in patient 6089.** Graphical output of CNAT 4.0, from top to bottom log2 Ratio plot and Copy Number State plot of chromosome 6 of patient 6089, demonstrating the presence of a terminal duplication of the long arm of chromosome 6 (arrows).

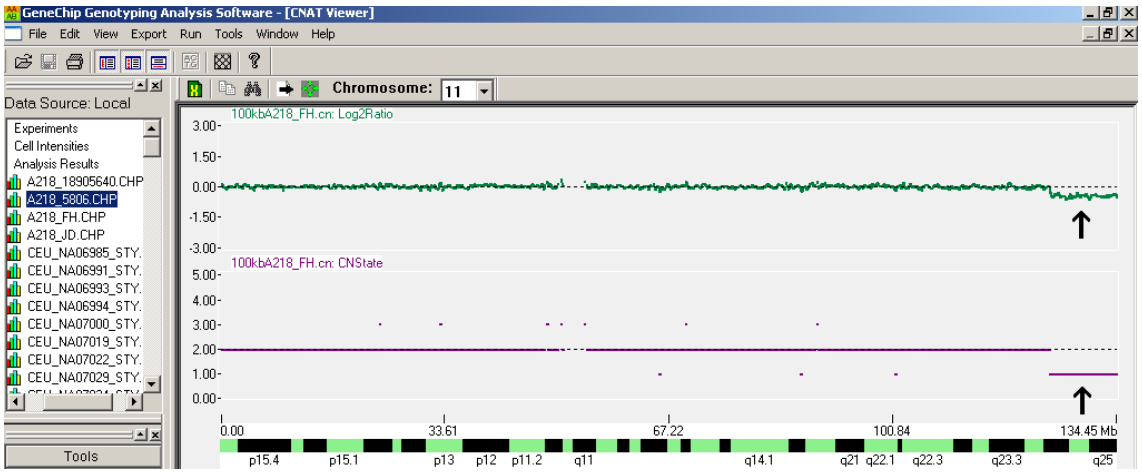

Figure 13. **Chromosome 11q deletion in patient 6089.** Graphical output of CNAT 4.0, from top to bottom log2 Ratio plot and Copy Number State plot of chromosome 11 of patient 6089, demonstrating the presence of a terminal deletion of the long arm of chromosome 11 (arrows).

The breakpoints of the two genomic imbalances were finely mapped within 29 kb and 26 kb intervals on chromosome 6q and chromosome 11q, respectively, as shown in Table 21. The size of both the 6q duplication and the 11q deletion was ~10 Mb.

Chromosome locus	**Breakpoint**	**SNP**	**Physical position**	**CN**
6q25.3	Terminal duplication	SNP_A-1951614	160,562,518	2
		SNP_A-1904727	160,591,490	3
11q24.2	Terminal deletion	SNP_A-2022234	124,370,133	2
		SNP_A-2275217	124,396,305	1

Table 21. **Breakpoints of the genomic imbalances in patient 6089.** CN: Copy Number.

According to clinical reports published in the literature of cases of trisomy 6q overlapping with the region duplicated in patient 6089, the terminal duplication of the long arm of chromosome 6 was deemed accountable for the skeletal malformations found in patient 6089. [217-219]

The partial deletion of the long arm of chromosome 11 is a clinically recognised syndrome characterised by DD, transient megakaryocytic thrombocytopenia (Paris-Trousseau syndrome), growth deficiency with length or height below the 5th percentile, cryptorchidism, congenital malformations and facial dysmorphic features. [220]

Clinical information on 108 Italian patients with del11q syndrome became available during the course of the project, [Mattina, personal communication; data not presented in this study] and upon revision we identified at least 14 patients who showed signs of pituitary function impairment (e.g. severe growth deficiency, lack of spontaneous pubertal development), supporting the existence of a novel gene involved in the pathology of the pituitary gland in patient 6089, and in del11q syndrome.

4.7.2. Chromosome 22q11.21 Interstitial Deletion

The screening with the Affymetrix GeneChip 250K Sty1 SNP Mapping Array revealed the presence of an interstitial deletion of chromosome 22q in patient 5135, as shown in Figure 14; the patient's karyotype was defined as 46,XY,del(22)(q11.21q11.21).

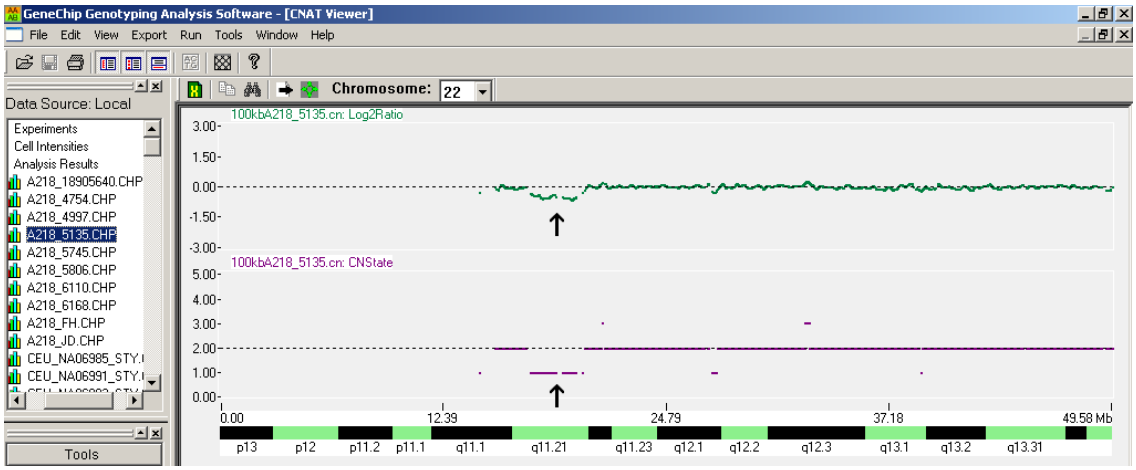

Figure 14. **Chromosome 22q deletion in patient 5135.** Graphical output of CNAT 4.0, from top to bottom log2 Ratio plot and Copy Number State plot of chromosome 22 of patient 5135, demonstrating the presence of an interstitial deletion of chromosome 22q (arrows).

The breakpoints of the genomic imbalance were refined by repeating the CN analysis with GS equal to 0 Mb, the telomeric breakpoint was finely mapped within a 42 kb interval, the centromeric breakpoint fell within a larger interval, between the two defining SNPs, of 258 kb, as shown in Table 22. The size of the deletion was 3 Mb.

Chromosome locus	Breakpoint	SNP	Physical position	CN
22q11.21	Centromeric	SNP_A-2200145	17,012,376	2
		SNP_A-4283311	17,270,967	1
22q11.21	Telomeric	SNP_A-2185542	20,303,319	1
		SNP_A-4277437	20,345,144	2

Table 22. **Breakpoints of the chromosome 22q11 interstitial deletion in patient 5135.** CN: Copy Number.

The breakpoints coincided with the two 22-specific low-copy repeats (LCR22s) that flank and facilitate the recurrence of the ~3 Mb microdeletion of 22q11.2. More than 85% of individuals with deletions in the 22q11.2 chromosome region carry the same ~3 Mb imbalance, that also overlapped the deletion in patient 5135. The presence of the interstitial deletion of chromosome 22q11.2 was independently confirmed by FISH with locus specific probe, and the karyotype of the patient was reported as: 46,XY.ish del(22)(q11.2q11.2)(D22S75-).

The patient's medical history and phenotype were reviewed by the author after the identification of the chromosome imbalance. Patient 5135 was born from non-consanguineous parents, at term with a low birth weight of 2.2 kg. At the age of 1 month, upon detection of severe hypernatremia, the diagnosis of central DI was made. The patient also suffered from central hypothyroidism, post-natal growth deficiency, DD, epilepsy, and presented with ToF, bilateral cleft lip and palate, absent thymus, small umbilical hernia, and facial dysmorphic features. At the age of 6 1/2 months, all auxological parameters, length, weight and head circumference, were below the 0.4th percentile. An MRI of the brain showed plagiocephaly, but no intracranial structural malformations and midline defects, nor anomalies of the anatomy of the pituitary gland. The patient successfully underwent surgery to repair his CHD, he developed recurrent respiratory infections, but his immunological profile showed that all values were within the normal ranges. Overall, the clinical phenotype of the patient was compatible with the diagnosis of del22q11.21 syndrome.

The association of 22q11.21 deletion syndrome and DI has never been reported in the literature. The deletion detected in our patient (including the 258 kb wide centromeric breakpoint interval) contained 42 characterised genes, but none of them had a known involvement in the pathology or development of the posterior or anterior pituitary gland.

Nine different chromosome loci associated with central DI have been mapped to seven different chromosomes. They include the locus, on chromosome 20p13, of isolated neurohypophyseal diabetes insipidus, as well as eight more loci of diseases that can present with central DI. The list of all known genomic loci associated with central DI is presented in Table 23. All nine loci were investigated for CN changes in patient 5135, but no CNVs were detected.

OMIM number	**Associated disease**	**Genomic locus**
#136760	Frontonasal Dysplasia 1; FND1 Frontonasal Dysplasia, included; FND, included	**1p21-p13**
#157170	Holoprosencephaly 2; HPE2	**2p21**
#182230	Septooptic Dysplasia Pituitary Hormone Deficiency, Combined, 5, included; CPHD5, included	**3p21.2-p21.1**
#604292	Ectrodactyly, Ectodermal Dysplasia, and Cleft Lip/Palate Syndrome 3; EEC3	**3q27**
#222300	Wolfram Syndrome 1; WFS1 Wolfram-Like Syndrome, Autosomal Dominant, included	**4p16.1**
#604928	Wolfram Syndrome 2; WFS2	**4q22-q24**
%129900	Ectrodactyly, Ectodermal Dysplasia, and Cleft Lip/Palate Syndrome 1; EEC1	**7q11.2-q21.3**
#611087	Polyhydramnios, Megalencephaly, and Symptomatic Epilepsy; PMSE	**17q23.3**
#125700	Diabetes Insipidus, Neurohypophyseal	**20p13**

Table 23. **List of known genomic loci of central DI.** The associated diseases and the relevant OMIM (Online Mendelian Inheritance in Man) numbers are also shown.

4.8. Potentially Pathogenic CNVs

Four more submicroscopic rearrangements were found in 3 patients, that were investigated as potentially having a disease-causing role in relation to the phenotype of

each patient. The CNVs were assessed by visual inspection of the log2 Ratio and CN State plots, and by numerical analysis of the SNP CN profiles exported into Microsoft Excel spreadsheets.

The limited size of the cohort of 10 patients and especially the absence of a cohort of controls have potentially posed limitations to the extrapolation and inference of data regarding the pathogenic versus polymorphic nature of CNVs detected by the screening, as also discussed in chapter 6.4.

4.8.1. Chromosome 22q12.3 Interstitial Deletion

Screening the whole genome profile of patient 18905640 for regions with smoothed copy number different from 2, applying the CNAT 4.0 batch analysis workflow with a genomic smoothing of 0.1 Mb, did not reveal any clearly pathogenic genomic imbalance by visual inspection of the log2 Ratio and CN State plots of each autosome and chromosome X. A total of 15 unique CNVs with gene content in CN 1 and a total of 12 unique CNVs with gene content in CN 3 were identified.

The patient was known to carry an apparently balanced chromosome translocation between chromosomes 11 and 22, defined, at low resolution routine karyotyping, as 46,XY,t(11;22)(q24;q13). One of the unique CNVs with gene content present in CN state 1 was located inside the chromosome band 22q12.3, compatible with the cytogenetic definition of the patient's translocation breakpoint at low resolution. CNAT 4.0 batch analysis with GS = 0 Mb was run, targeted to the genomic regions tentatively identified cytogenetically as the translocation breakpoints. The CN profiles were exported from CNAT 4.0 both to UCSC genome browser, for the purpose of visualisation, and to Microsoft Excel spreadsheets to allow the numerical analysis of the log2 Ratio and CN State of the SNPs covering the chromosome regions of interest.

The breakpoints of the CNV in CN state 1 identified in the chromosome region 22q12.3 were refined as shown in Table 24. The genomic imbalance had a size of 352 kb, including both the centromeric and the telomeric first flanking SNP in CN state 2. The centromeric and telomeric breakpoints were finely mapped within 21 kb and 3 kb intervals, respectively. Both breakpoints fell inside a coding gene. The CN profile of chromosomes 22q12.3 was exported to the UCSC genome browser as shown in Figure 15.

Chromosome locus	Breakpoint	SNP	Physical position	CN
22q12.3	Centromeric	SNP_A-2131773	35,050,725	2
		SNP_A-2102323	35,071,686	1
22q12.3	Telomeric	SNP_A-2301610	35,399,975	1
		SNP_A-1892611	35,403,134	2

Table 24. **Breakpoints of the chromosome 22q12.3 deletion in patient 18905640.** CN: Copy Number.

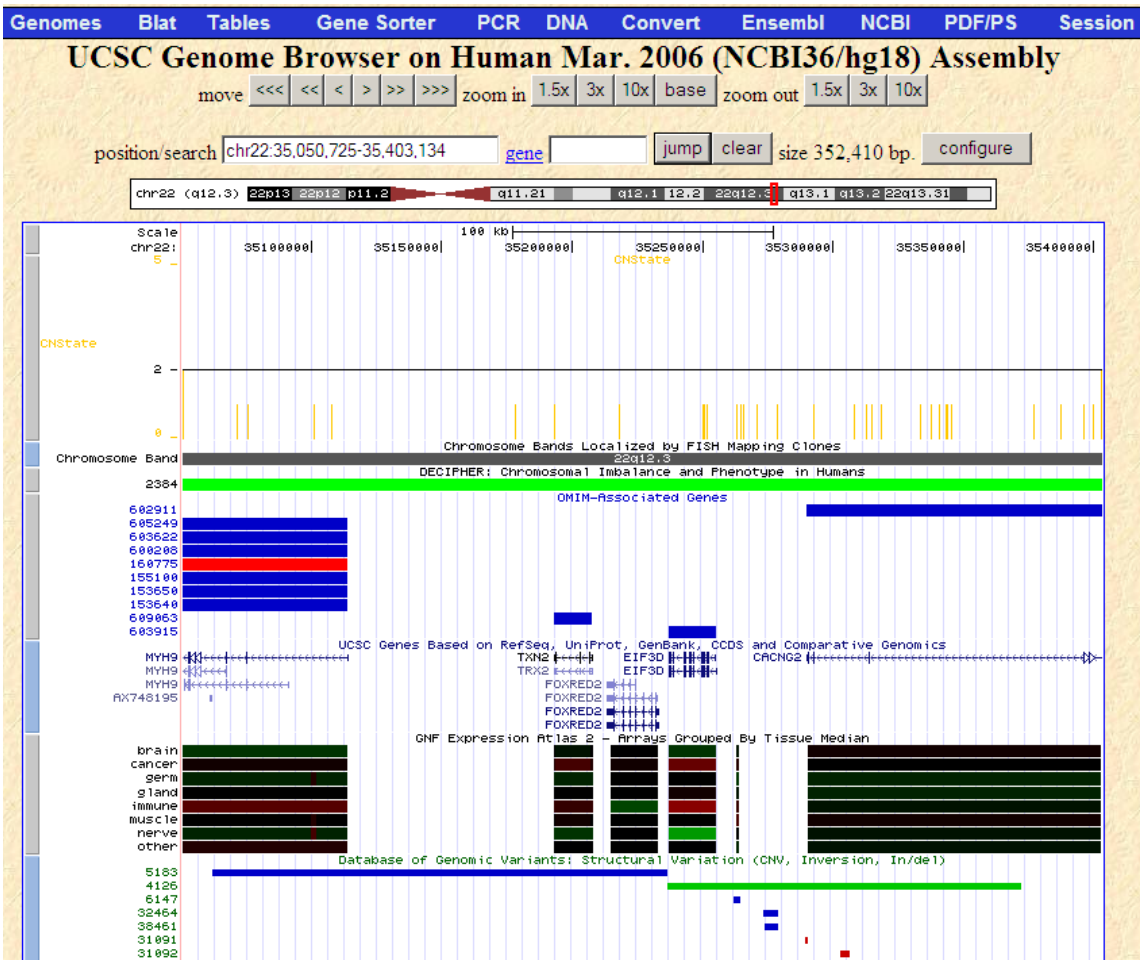

Figure 15. **Chromosome region 22q12.3 of patient 18905640 in UCSC genome browser.** Visualisation in UCSC genome browser of a custom track corresponding to the CN profile of chromosome region 22q12.3 of patient 18905640 exported from CNAT 4.0. The CNAT 4.0 batch analysis was run with GS = 0 Mb. From top to bottom: CNAT 4.0 CNState profile track, chromosome band localisation, overlapping genomic imbalances associated with a pathological phenotype in human entered in the database DECIPHER, OMIM loci, UCSC genes, tissue expression data according to GNF Gene Expression Atlas 2, overlapping genomic structural variants detected in healthy

individuals entered in the database of genomic variants (DGV). The two full (orange) bars at the extremities of the CNAT 4.0 CNState profile track represent the SNPs in CN state 2 flanking the genomic deletion, the half (orange) bars represent each SNP present in CN 1 inside the deletion. DECIPHER entry coloured green represents a duplication. OMIM-associated gene loci are represented by blue bars, OMIM-associated morbid loci are represented by red bars. The GNF Expression Atlas 2 data on seventy-nine human tissues are grouped by tissue median in eight arbitrary categories: a green bar indicates under-expression, a red bar indicates over-expression. The DGV entry coloured blue represents a genomic loss, the DGV entry coloured red represents a genomic gain, the DGV entry coloured green represents the presence of both genomic loss and genomic gain.

The genomic deletion, as present in patient 18905640, did not appear in the DGV, that catalogues documented structural variations and genomic polymorphisms in healthy individuals, and is interfaced with UCSC. However, it partly overlapped large genomic structural variants reported in the DGV. DECIPHER is an online database of (submicroscopic) chromosomal imbalances and clinical phenotypes in humans. [221] The entry corresponding to a chromosome imbalance overlapping the 22q12.3 deletion found in patient 18905640 referred to a male individual with agenesis or hypoplasia of the corpus callosum, cleft palate and midline cleft upper lip, hypospadias, small penis and VSD. However, the chromosome imbalance was a duplication, with a size of ~18 Mb, spanning from chromosome band 22q12.3 to 22q13.33.
The 22q12.3 deletion in patient 18905640 contained 5 characterised genes that are listed in Table 25, together with notes on their putative function, and expression in the pituitary gland.

Symbol	**Name**	**Function**	**Expression**
TXN2	Thioredoxin 2	Nuclear gene that encodes mitochondrial redox-active protein, may play a role in the regulation of mitochondrial membrane potential and against oxidant-induced apoptosis	-
FOXRED2	FAD-dependent oxidoreductase 2	Contains FAD-dependent oxidoreductase domain	+

EIF3D	Eukaryotic translation initiation factor 3, subunit D	Part of multiprotein complex that binds to the 40S ribosome, helps maintain the 40S and 60S subunits in a dissociated state, and promotes the binding of methionyl-tRNAi and mRNA	-
CACNG2	Calcium channel, voltage-dependent, gamma-2	Thought to stabilize the calcium channel in an inactive (closed) state	++
MYH9	Myosin heavy chain 9	Involved in cytokinesis, cell motility, and maintenance of cell shape	-

Table 25. **Genes located inside the 352 kb genomic deletion (22q12.3) of patient 18905640.** The expression in the pituitary gland is according to GNF Gene Expression Atlas 2; -: ratio <1, +: ratio slightly >1, ++: ratio moderately >1. FAD: Flavin Adenine Dinucleotide.

CACNG2. The telomeric breakpoint of the deletion, mapped within a 3 kb interval, fell inside the gene *CACNG2*. It has been observed that the phosphorylation of threonine (Thr)-321 of the *CACNG2* protein impairs its interaction with the genes discs large, drosophila, homolog of, 1 (*DLG1*) and *DLG4*; *DLG1* gene is deleted in the 3q29 microdeletion syndrome and is an autosomal homologue of an X-linked mental retardation gene, *DLG3*. [222] At the age of 21 years, patient 18905640 did not show any sign of cognitive impairment. [Yang, personal communication]

MYH9. Defects in *MYH9* have been found to underlie a large group of autosomal dominant allelic disorders that include: May-Hegglin anomaly (MHA), i.e. macrothrombocytopenia and leukocyte inclusions; Sebastian syndrome, characterised by macrothrombocytopenia and leukocyte inclusions different from MHA; Epstein syndrome, characterised by macrothrombocytopathy, sensorineural hearing loss and nephritis; Fechtner syndrome, that presents with the association of macrothrombocytopenia, leukocyte inclusions and Alport-like clinical features, i.e. sensorineural deafness, cataracts and nephritis; macrothrombocytopenia and progressive sensorineural hearing loss; Alport syndrome (i.e. ocular lesions, sensorineural hearing loss and nephritis) with macrothrombocytopenia; non-syndromic sensorineural deafness type 17, characterised by progressive hearing impairment and cochleosaccular degeneration. [223, 224] Individuals with mutations in the motor domain of *MYH9*

presented with severe thrombocytopenia and developed nephritis and deafness before the age of 40 years, while individuals with mutations in the tail domain had a much lower risk of non-congenital complications and significantly higher platelet counts. A genotype-phenotype correlation was established evaluating mutations in the four most frequently affected residues of *MYH9* (70% of cases): mutations at residue 1933 did not induce kidney damage or cataracts and caused deafness only in the elderly, those in position 702 resulted in severe thrombocytopenia and produced nephritis and deafness at a juvenile age, while alterations at residue 1424 or 1841 resulted in intermediate clinical phenotypes. [224] The symptoms caused by mutations of *MYH9* have age-dependant penetrance and variable expression.

The centromeric breakpoint of the 22q12.3 deletion in patient 18905640, mapped within a 21 kb interval, fell inside the *MYH9* gene; the deletion involved only the terminal 42 kb of *MYH9*, while two copies of most of its exons were preserved. A full blood count of patient 18905640, performed at the age of 19 years, only showed normocytic anaemia, and the patient did not show clinical signs of hearing impairment at the age of 21 years.

Overall, a causative relationship between the 352 kb deletion of chromosome region 22q12.3 and the hypopituitarism with anomalies of the anatomy of the pituitary gland in patient 18905640 could not be established. However, it remains possible that the deletion in the chromosome region 22q12.3 represents a loss of genomic material at the level of the translocation breakpoint.

4.8.2. Chromosome Region 11q24.2 Imbalance and *KIRREL3* Gene

Patient 18905640 had a severe pituitary phenotype overlapping with the one presented by patient 6089 with del11q syndrome. It was, therefore, hypothesised that the breakpoint of the translocation, carried by patient 18905640, in the genomic region 11q24 could affect a novel gene involved in the development and pathology of the pituitary gland, also underlying the pathogenesis of the hypopituitarism in del11q syndrome.

The ~10 Mb genomic region present in CN 1 in patient 6089 was screened for submicroscopic CN changes, potentially associated with the translocation breakpoint, in patient 18905640, by running the CNAT 4.0 batch analysis with GS = 0 Mb. Only one unique CNV with gene content was detected. The CNV was located in the chromosome region 11q24.2 and had an overall size of 52 kb, including both the centromeric and the telomeric first flanking SNP in CN state 2. Within the genomic imbalance, both a small deletion and a small duplication were present. The CNAT 4.0 batch analysis with GS = 0 Mb allowed to precisely define the breakpoints, as shown in Table 26.

Chromosome locus	**Breakpoint**	**SNP**	**Physical position**	**CN**
11q24.2	Centromeric	SNP_A-4302114	126,187,928	2
		SNP_A-4251263	126,191,973	1
11q24.2	Telomeric	SNP_A-2205137	126,233,398	3
		SNP_A-4295359	126,240,403	2

Table 26. **Breakpoints of the chromosome 11q24.2 rearrangement in patient 18905640.** The breakpoints were defined by numerical analysis of the SNP log2 Ratio and CN State by exporting the CNAT 4.0 output to a Microsoft Excel spreadsheet. CN: Copy Number.

The centromeric and telomeric breakpoints were finely mapped within 4 kb and 7 kb intervals, respectively. Both breakpoints fell inside a coding gene, kin of IRRE-like 3 (*KIRREL3*), that was the only gene involved in the 52 kb submicroscopic chromosome rearrangement. The CN profile of chromosomes 11q24.2 was exported to UCSC genome browser, as shown in Figure 16.

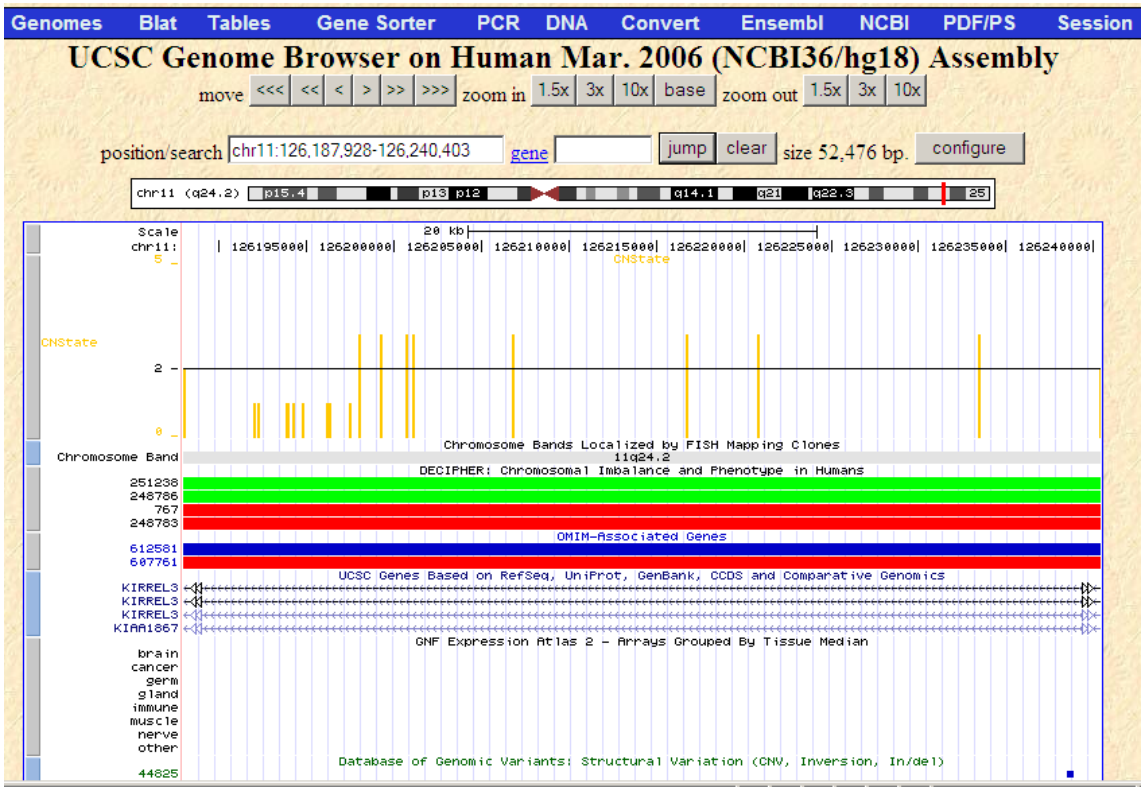

Figure 16. **Chromosome region 11q24.2 of patient 18905640 in UCSC genome browser.** Visualisation in UCSC genome browser of a custom track corresponding to the CN profile of chromosome region 11q24.2 of patient 18905640 exported from CNAT 4.0. The CNAT 4.0 batch analysis was run with GS = 0 Mb. From top to bottom: CNAT 4.0 CNState profile track, chromosome band localisation, overlapping genomic imbalances associated with a pathological phenotype in human entered in the database DECIPHER, OMIM loci, UCSC genes, overlapping genomic structural variants detected in healthy individuals entered in the database DGV. The two (orange) bars at the extremities of the CNAT 4.0 CNState profile track represent the SNPs in CN state 2 flanking the genomic imbalance, the half-height (orange) bars represent each SNP present in CN 1 (genomic deletion) and the 1.5-height (orange) bars represent each SNP present in CN 3 (genomic duplication) inside the submicroscopic chromosome rearrangement. DECIPHER entries coloured green represent a duplication, DECIPHER entries coloured red represent a deletion. OMIM-associated gene locus is represented by a blue bar, OMIM-associated morbid locus is represented by a red bar. No tissue expression data were available from GNF Gene Expression Atlas 2. The DGV entry coloured blue represents a genomic loss.

There was no significant overlap between the genomic imbalance detected in patient 18905640 and entries in the DGV. The four entries into the DECIPHER database,

corresponding to chromosome imbalances overlapping the rearrangement found in patient 18905640, referred to patients with very complex clinical phenotypes, with genomic imbalances ranging in size between 11 Mb and 27 Mb, and whose endocrinological phenotype was not known.

The submicroscopic chromosome rearrangement affected only the gene *KIRREL3*. *KIRREL3* is 576 kb in size, located between genomic positions 125,799,613 and 126,375,976, and contains 16 coding exons. The submicroscopic chromosome rearrangement and imbalance, present in patient 18905640, caused the loss of one copy of 5-9 kb and the gain of one copy of 35-42 kb within the last intron of the gene, as detailed in Table 27.

Chromosome locus	**SNP**	**Physical position**	**CN**
11q24.2	SNP_A-4302114	126,187,928	**2**
	SNP_A-4251263	126,191,973	**1**
11q24.2	SNP_A-2074406	126,197,407	**1**
	SNP_A-2087740	126,198,020	**3**
11q24.2	SNP_A-2205137	126,233,398	**3**
	SNP_A-4295359	126,240,403	**2**

Table 27. **CN profile of the 52 kb genomic rearrangement in 11q24.2 of patient 18905640.** Results of the numerical analysis of the SNP log2 Ratio and CN State by exporting the CNAT 4.0 output with GS = 0 Mb to a Microsoft Excel spreadsheet. The 52 kb genomic imbalance consists of both a genomic deletion (CN 1) and duplication (CN 3). CN: Copy Number.

KIRREL3 is located ~1.7 Mb centromeric to the gene friend leukemia virus integration 1 (*FLI1*), located in the chromosome region 11q24.3, identified as the candidate gene for the pathogenesis of Paris-Trousseau syndrome in 11q deletion syndrome. *KIRREL3* is a member of the nephrin-like protein family, which includes also *KIRREL* and *KIRREL2*. It encodes for a single-pass cell membrane protein. The cytoplasmic domains of these proteins interact with the C-terminus of podocin, and the genes are expressed in the kidney and specifically in podocytes of kidney glomeruli. Therefore, it has been hypothesised that *KIRREL3* could be involved in the hematopoietic supportive capacity of stroma cells. [225]

The genes *KIRREL* and *KIRREL2* have not been associated with human pathology,

while heterozygous missense mutations of *KIRREL3* have been found to be responsible of autosomal dominant mental retardation 4 (MRD4). Amongst the mutations, an amino acid substitution in a highly conserved residue within the cytoplasmic domain of the protein, caused by a mutation in exon 16 of the gene, was identified in a female patient with mild MR. [226] The clinical phenotype of patients with point mutations of *KIRREL3* seemed to consist of MR only, varying in degrees from mild to severe.

The detection of both a genomic deletion (CN 1) and duplication (CN 3) within the 52 kb genomic imbalance of chromosome 11q24.2 in patient 18905640 can be regarded as suggestive of the presence of a submicroscopic rearrangement of genomic material at the level of the chromosome translocation breakpoint. The 52 kb imbalance corresponds to a submicroscopic rearrangement affecting the last intron of *KIRREL3*. At the age of 21 years, patient 18905640 did not show any sign of cognitive impairment. However, genomic sequencing of *KIRREL3* in a large cohort of patients with isolated hypopituitarism and/or hypopituitarism associated with DD would have been necessary to clarify the potential contribution of *KIRREL3* to the pathology of the pituitary gland manifested by patient 18905640, as well as in 11q deletion syndrome, as discussed in paragraph 6.1.1.

4.8.3. Chromosome 1p36.33 Deletion

Patient 5608 presented with SOD, CPHD (GH, TSH and ACTH deficiency) and precocious puberty, associated with ToF. Other symptoms included: mild DD, hypotonia, bilateral aplasia of the optic disc and of the retina with severe visual impairment, hearing impairment, mild facial asymmetry and facial dysmorphic features. The CN change screening with Affymetrix GeneChip 250K Sty1 SNP Mapping Array with GS = 0.1 Mb identified a subtelomeric interstitial deletion of chromosome 1p36.33. The telomeric and centromeric breakpoints of the genomic imbalance were mapped by numerical analysis of the SNP log2 Ratio and CN State by running the CNAT 4.0 batch analysis with GS = 0 Mb, and exporting the output to a Microsoft Excel spreadsheet; the results are shown in Table 28.

Chromosome locus	Breakpoint	SNP	Physical position	CN
1p36.33	Telomeric	SNP_A-2118217	1,355,433	2
		SNP_A-1866065	1,468,016	1
1p36.33	Centromeric	SNP_A-1799863	1,878,229	1
		SNP_A-1908463	2,017,761	2

Table 28. **Breakpoints of the chromosome 1p36.33 deletion in patient 5608.** CN: Copy Number.

The telomeric and centromeric breakpoints fell within 112 kb and 139 kb intervals, respectively, while the size of the genomic deletion was 662 kb, including both the telomeric and the centromeric first flanking SNP in CN state 2. Because of the relatively large size of both, telomeric and centromeric, breakpoint intervals, a conservative approach was chosen: only SNPs in CN state 1 were taken into consideration for the purpose of mapping and defining the genomic deletion for further study. The deletion was, therefore, mapped between genomic physical positions 1,468,016-1,878,229, and the size of the deletion was 410 kb.

The 410 kb submicroscopic chromosome deletion detected in patient 5608 was not present in any other patient in the cohort under study, while it partly overlapped with the genomic imbalance that underlies the clinically recognised 1p36 microdeletion syndrome. Monosomy 1p36 deletion syndrome results from a heterozygous deletion of the most distal chromosomal band on 1p, and it is the most common terminal deletion in humans, with an estimated incidence of ~1/5000 births. [227] The clinical phenotype is characterised by DD, hypotonia, seizures, micro- and brachycephaly, growth deficiency, CHD, ophthalmologic findings, hearing loss and distinct facial dysmorphic features. [228-231] A detailed comparison between the complex clinical phenotype of patient 5608 and the most common symptoms of 1p36 deletion syndrome is shown in Table 29.

1p36 deletion syndrome (%)			Patient 5608
DD		100	+
Behavioural disorders		47	-
Microcephaly		65	-
Brachycephaly		65	+

Large anterior fontanel/delayed closure of anterior fontanel		77	n.d.
Seizures		44-72	-
CNS structural defects (e.g. cerebral atrophy, polymicrogyria, ACC)		88	SOD
Hypotonia		87-100	+
Growth retardation		n.d.	+
Hypothyroidism (with elevated TSH)		20	central
Hearing loss (mainly sensorineural)		82	+
Visual impairment (hypermetropia/myopia)		52-67	+
Visual inattentiveness		64	+
Cleft lip/palate, bifid uvula		17	+
CHD		66-71	+
Urogenital anomalies (e.g. cryptorchidism, hypospadias)		25-26	-
Camptodactyly		n.d.	+
Clinodactyly of the V finger		n.d.	+
Facial dysmorphic features:	**prominent forehead**	n.d.	-
	deep-set eyes	100	+
	asymmetric ears	n.d.	+
	posteriorly rotated/low-set ears	40	+
	flat nasal bridge	100	+

	midface hypoplasia	100	+
	long philtrum	100	+
	pointed chin	100	-

Table 29. **Comparison between the clinical symptoms of patient 5608 and 1p36 deletion syndrome.** The frequency given to each symptom of 1p36 deletion syndrome (expressed as percentage of patients displaying the symptom) was obtained by pooling the results of multiple screenings. [228-231] ACC: Agenesis of Corpus Callosum; CHD: Congenital Heart Defect; CNS: Central Nervous System; DD: Developmental Delay; SOD: Septo-Optic Dysplasia; TSH: Thyroid-Stimulating Hormone. +: present; -: absent; n.d.: not determined.

The diagnosis of 1p36 deletion syndrome is routinely achieved by locus specific FISH with at least two subtelomeric region probes, or by array CGH. The consensus FISH probes utilised for the detection of pathogenic deletions of 1p36 are: the telomere region-specific probes D1Z2-CEB108/T7 (SpectrumGreen, Vysis) and the more centromeric probe p58 containing the CDC2L1/2 locus (SpectrumOrange, Vysis). [231] However, it has also been suggested that, in cases with interstitial deletions and/or complex rearrangements, a targeted FISH approach with additional probes might be necessary. [229]

A cell line was obtained from a fresh blood sample of patient 5608, and FISH was performed with three locus specific probes for the subtelomeric region of chromosome 1p: CEB108/T7, D1Z2, and p58 (CDC2L1/CDC2L2), by Mr Rodger Palmer (Molecular Cytogenetics Section, Regional Cytogenetics Laboratory, Great Ormond Street Hospital NHS Trust). All three probes returned a positive hybridisation signal on the subtelomeric region of the short arm of both chromosomes 1.

The CN profile of chromosomes 1p36.33 of patient 5608 was exported from CNAT 4.0 to UCSC genome browser, for the purpose of visualisation. Data regarding the locus specific probes utilised for FISH analysis were superimposed on the UCSC graphical output for analytical purposes, as shown in Figure 17.

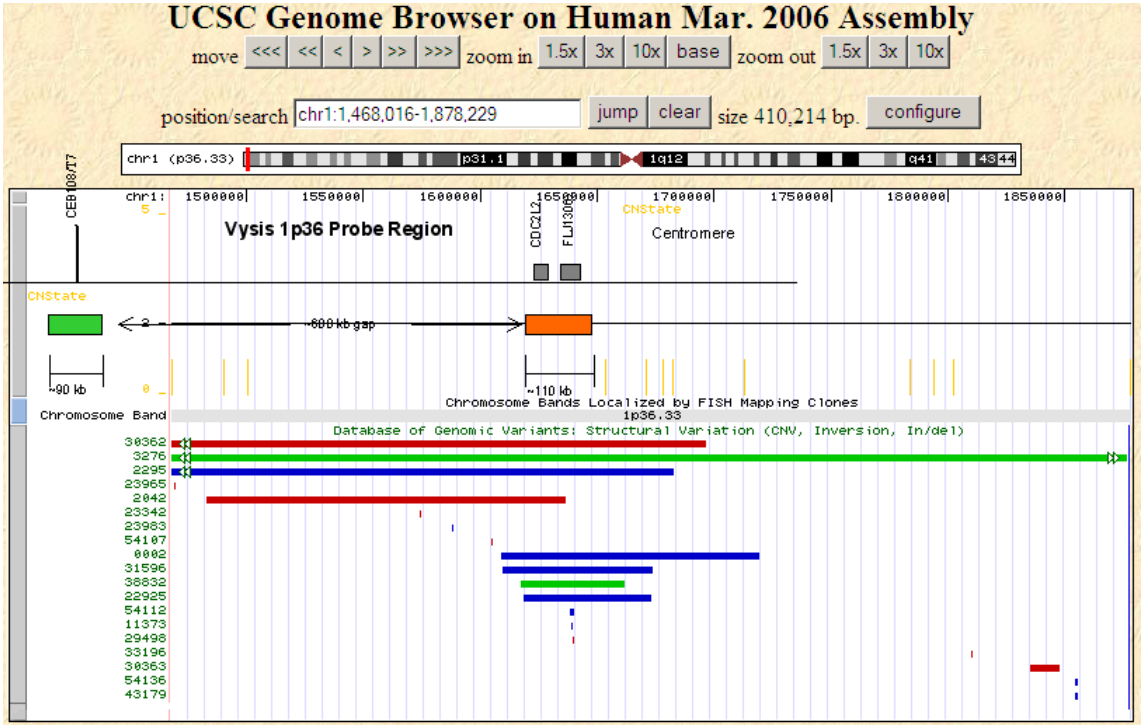

Figure 17. **Chromosome region 1p36.33 of patient 5608 in UCSC genome browser.** Visualisation in UCSC genome browser of a custom track corresponding to the CN profile of chromosomes 1p36.33 of patient 5608 exported from CNAT 4.0. The CNAT 4.0 batch analysis was run with GS = 0 Mb. The diagram of the Vysis 1p36 probe region covered by FISH was superimposed onto the UCSC graphical output. From top to bottom: diagram of the Vysis 1p36 Probe Region, CNAT 4.0 CNState profile track, chromosome band localisation, overlapping genomic structural variants detected in healthy individuals entered in the database DGV. The orange bars of the CNAT 4.0 CNState profile track represent each SNP present in CN state 1 within the genomic deletion. The DGV entry coloured blue represents a genomic loss, the DGV entry coloured red represents a genomic gain, the DGV entry coloured green represents the presence of both genomic loss and genomic gain. The positioning of the p58/CDC2L2 (orange) probe was arranged in the diagram according to the instructions supplied by the manufacturer (Abbott Molecular, Vysis) at the moment of performing FISH on the cell line of patient 5608.

The CEB108/T7-D1Z2 probes (green) hybridised to the subtelomeric region of both chromosomes 1p, consistently with the fact that the probes were telomeric to the distal breakpoint of the interstitial deletion of 1p36.33 detected in patient 5608, as defined by SNP mapping array.

The estimated gap between the telomeric and the more centromeric, p58

(CDC2L1/CDC2L2), FISH probes was 600 kb (according to the manufacturer). The p58 (CDC2L1/CDC2L2) probe was localised inside the chromosome CN 1 imbalance detected in patient 5608. The genomic deletion carried by patient 5608 was defined by 12 SNPs, on average 1 SNP per 34 kb. However, the SNPs were unevenly distributed, resulting in a 153 kb gap, between physical positions 1,500,664-1,653,691, where no SNP coverage was present. The probe p58 (CDC2L1/CDC2L2) that, according to manufacturer's data, is 110 kb in size fell inside the interval with lack of SNP coverage on the 250K Sty1 array. The chromosome imbalance in CN 1 detected in patient 5608 also involved a number of SNPs centromeric to the localisation of the probe p58 (CDC2L1/CDC2L2), that were not covered by the standard locus specific FISH.

Moreover, the 1p36.33 genomic region appeared to be rich in polymorphic structural variations, as reported by the DGV. Both duplications and deletions of the genomic locus where probe p58 (CDC2L1/CDC2L2) hybridises have been entered into the DGV as genomic variants.

The apparent discrepancy between the results of the Affymetrix GeneChip 250K Sty1 SNP Mapping Array and the locus specific FISH analysis could potentially reflect a complex rearrangement and genomic imbalance in the chromosome region 1p36.33 of patient 5608, as discussed in paragraph 6.2.2.

4.8.4. Chromosome 9q34.11 Interstitial Deletion

Patient 4754 presented with the unique association of two severe and aetiologically unrelated pathologies: SOD and MDS, that had not been reported before in the literature. The patient also suffered from severe DD, CPHD, and a gastro-intestinal malformation. The association of SOD and MDS was considered of particular interest, because it suggested that the complex phenotype of patient 4754 was due to a contiguous gene microdeletion/microduplication syndrome, and that the location of a known gene responsible for one of the two pathologies, i.e. MDS could potentially lead to the identification of a candidate chromosome region, and eventually a novel gene involved in the other aspect of the phenotype, namely SOD and CPHD.

A total of 104 entries were present in the database OMIM that referred to MDS. The great majority of them were not relevant to the investigation of the phenotype presented

by patient 4754 and its molecular bases, corresponding to fusion genes and somatic mutations, or were purposely excluded as no information was given about their genomic loci. The chromosome region 5q has a predominant role in the etiopathogenesis of MDS, as the deletion of all or part of the long arm of chromosome 5 is a frequent clonal chromosomal abnormality in MDS, especially the subtype refractory anaemia. Genes within the 5q common deleted region are candidates for MDS, and the CN profile of chromosome 5q of patient 4754 was screened for unique CNVs with gene content, and no CNVs were found.

Two more genomic loci were investigated: protein-tyrosine phosphatase, nonreceptor-type, 11 (*PTPN11*) and runt-related transcription factor 1 (*RUNX1*). The *PTPN11* gene is located in chromosome 12q24.1 and mutations in this gene are associated with a particular type of MDS, i.e. juvenile myelomonocytic leukemia (JMML), that constitutes approximately 30% of childhood cases of MDS. De novo germline heterozygous mutations of the gene have also been found in patients with features of Noonan syndrome and JMML. [232] The gene *RUNX1*, located on chromosome 21q22.3, encodes a hematopoietic transcription factor and heterozygous mutations of *RUNX1* cause an autosomal dominant, usually familial, platelet disorder with the development of acute myeloid malignancies. In one family, members of three generations presented with thrombocytopenia, hypospadias in males, umbilical hernia, and at least one member was diagnosed with MDS (characterised by progressive anaemia and neutropenia) at the age of 41 years. [233] No unique CNVs with gene content were detected at either genomic locus in patient 4754.

Eleven entries were present in the database OMIM that referred to SOD. Heterozygous mutations in the paired box gene 6 (*PAX6*), located in 11p13, are responsible for a wide spectrum of eye defects, including bilateral hypo- or aplasia and coloboma of the optic nerve, that overlap with the SOD spectrum. [234] The CN profile of patient 4754 was screened for unique CNVs with gene content at this genomic locus, as well as at selected genomic and morbid loci, that are known to be involved in hypopituitarism, listed in Table 1. No unique CNVs with gene content were detected at any of these genomic loci in patient 4754.

By cross referencing the lists of OMIM entries, no candidate chromosome region could be identified for the association of SOD with MDS. In order to try and identify a novel genomic locus for this unique association, the whole genome CN profile of patient

4754 was screened for unique CNVs with gene content after running the CNAT 4.0 batch analysis with GS = 0.1 Mb. An interstitial deletion of chromosome 9q34.11 was detected.

The centromeric and telomeric breakpoints of the genomic imbalance were mapped by numerical analysis of the SNP log2 Ratio and CN State by running the CNAT 4.0 batch analysis with GS = 0 Mb, and exporting the output to a Microsoft Excel spreadsheet; the results are shown in Table 30.

Chromosome locus	**Breakpoint**	**SNP**	**Physical position**	**CN**
9q34.11	Centromeric	SNP_A-1831060	129,365,085	2
		SNP_A-1783471	129,525,184	1
9q34.11	Telomeric	SNP_A-1887680	129,821,717	1
		SNP_A-4254903	129,841,977	2

Table 30. **Breakpoints of the chromosome 9q34.11 deletion in patient 4754.** CN: Copy Number.

The centromeric and telomeric breakpoints fell within 160 kb and 20 kb intervals, respectively. Because of the relatively large size of the centromeric breakpoint interval, a conservative approach was chosen: only SNPs in CN state 1 were taken into consideration for the purpose of mapping and defining the genomic deletion for further study. The deletion was, therefore, mapped between genomic physical positions 129,525,184-129,821,717, and the size of the deletion was 296 kb.

The 296 kb submicroscopic chromosome deletion detected in patient 4754 was not present in any other patient in the cohort under study, and it did not overlap with any chromosome rearrangement entered in the database DECIPHER nor in the DGV. The genomic deletion contained the whole length of the gene endoglin (*ENG*), that is 40 kb in size and the genomic locus of which maps between physical positions 129,617,112-129,656,868.

Heterozygous mutations of the *ENG* gene cause the autosomal dominant disorder hereditary hemorrhagic telangiectasia type 1 (HHT1). HHT1 is a vascular dysplasia leading to telangiectases and arteriovenous malformations of skin, mucosa, and viscera. The full clinical phenotype of the condition is characterised by: epistaxis and gastrointestinal bleeding, telangiectases on the mucosal surface of the tongue, lips, face, conjunctiva, ears and fingers, pulmonary arteriovenous malformations, cerebrovascular

malformations that can lead to intracranial haemorrhage, intrahepatic arteriovenous shunts associated with fibrosis and/or cirrhosis, retinal vascular malformations, and visceral involvement of other organs including kidneys, ovaries, spleen and lymph nodes. [235-237] HHT1 is highly penetrant, with at least one manifestation in 97% of patients, but penetrance is age-dependent. More than 90% of patients become symptomatic by the age of 21 years. In 62% of patients, a clinical diagnosis is achieved by the age of 16 years, with epistaxis being the presenting feature in 90% of cases; the mean age of onset of epistaxis is 12 years. [238-241]

Mutations of *ENG* disrupt the function of the encoded protein and cause pathology via haploinsufficiency. Therefore, the deletion of the entire *ENG* gene would have been likely to cause clinical symptoms of HHT1 in patient 4754.

Patient 4754 was born in 1988 and has crossed the mean age of onset of symptoms of HHT1. Unfortunately, the patient was lost to follow-up and it was not possible to obtain an updated clinical review of his phenotype. Several factors could have potentially prevented the diagnosis of HHT1 from being made in the patient, unless specifically sought, namely the age-dependent penetrance of HHT1 symptoms, the complex and severe clinical phenotype of the patient, and the presence of MDS that could have complicated the interpretation of episodes of haemorrhage.

To the author's knowledge, this would represent the first instance of the detection of the disruption of *ENG* on a SNP array platform. However, it would have been necessary to confirm the presence of the whole gene deletion of *ENG* by an independent molecular testing.

Finally, the confirmation of the deletion of *ENG* would warrant further investigation of the 9q34.11 chromosome region with the aim of identifying novel candidate genes for both MDS and SOD.

4.9. Risk Assessment of Unique CNVs

The interface of CNAT 4.0 with UCSC genome browser allowed to determine the gene content of each unique CNV, and the information available for each known gene: function, gene pathways, protein domain/s, existing link to OMIM disease loci, known

mutations and their mode of inheritance. In assessing gene parameters, particular attention was paid to the potential involvement of each gene in the development (e.g. gene pathways) and pathology (e.g. known OMIM loci) of the pituitary gland.

The interface with the UCSC genome browser was also utilised to check each unique CNV with gene content for gene expression in the pituitary gland, based on data from the GNF Gene Expression Atlas 2 of seventy-nine human tissues run over Affymetrix microarrays. Expression data in the pituitary gland were available for all but 5 genes within unique CNVs in CN state 1 and 4 genes within unique CNVs in CN state 3.

Finally, the UCSC genome browser was used to check each unique CNV with gene content against CNV databases for healthy individuals: the DGV and other databases of genomic structural variations interfaced with UCSC. The cumulative percentages of CNVs, divided into the two subtypes CN 1 and CN 3, that overlapped fully or partly or did not overlap with genomic imbalance/s already included in the DGV are reported in Figure 18.

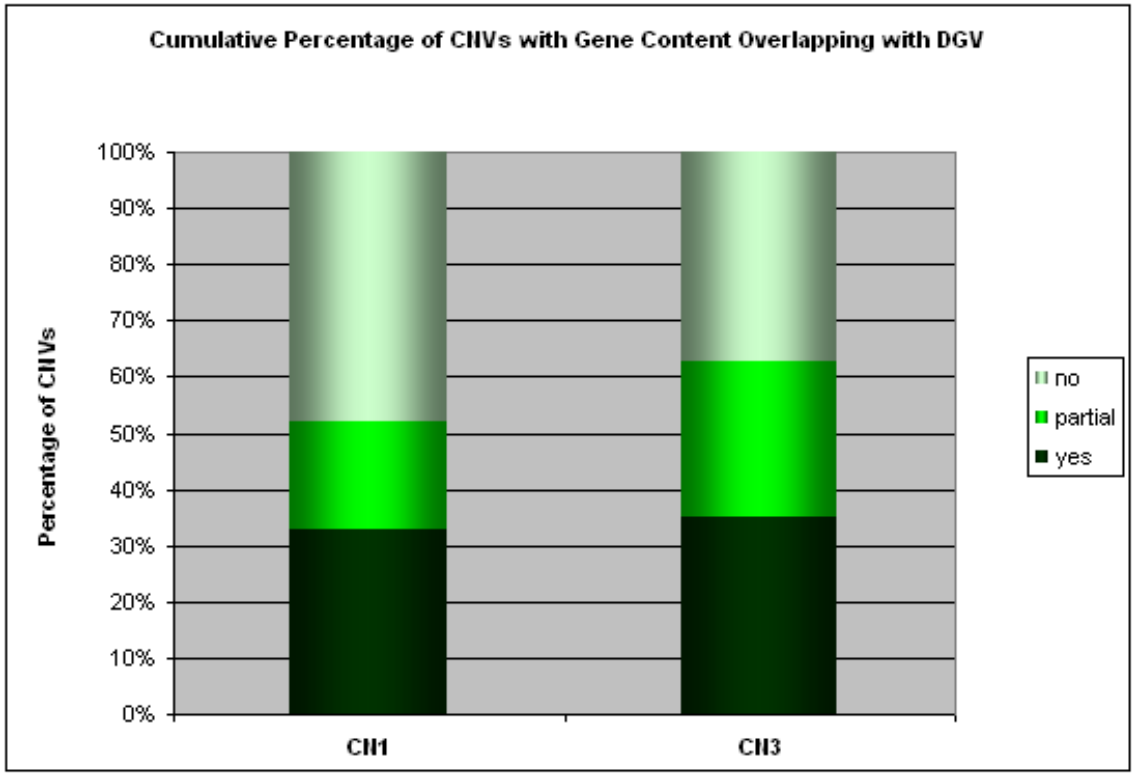

Figure 18. **Cumulative percentages of CNVs overlapping with the DGV.** The cumulative percentages of unique CNVs with gene content overlapping with genomic imbalance/s already included in the catalogue of the DGV are shown per each subtype of CNVs, CN 1 and CN 3. CN: Copy Number.

Overall, ~34% of unique CNVs with gene content overlapped with documented polymorphisms described in the DGV, and more than half (~57%) of unique CNVs with gene content overlapped at least partly (or fully) with genomic imbalances reported in the DGV. The number of CNVs in CN 3 that did not overlap with the DGV was lower than the number of CNVs in CN 1. Nearly half (48%) unique CNVs in CN 1 with gene content did not overlap with any genomic polymorphism included in the catalogue of the DGV; for unique CNVs in CN 3 with gene content, the percentage dropped to 37%.

Selected genomic loci that are known to be involved in hypopituitarism, listed in Table 1, were screened for CNVs in all patients under study, in order to rule out the presence of a contiguous gene genomic imbalance that included a gene already known to be involved in pituitary gland pathology. No CNVs overlapping with the selected morbid loci were identified in any of the patients, supporting the hypothesis that novel genomic regions and genes remain to be identified that play a role in pituitary development and function.

Equally, the small cohort of patients with the recurrent association of hypopituitarism and ToF, present in the database of endocrinological patients, proved to be genotypically heterogeneous, as no CNVs overlapping the previously identified 5q11.2→q22 duplication were detected. Four patients affected by variable degrees and manifestations of pathology of the pituitary gland and ToF were included in the screening with the 250K Sty1 SNP mapping array. In particular, the genomic region 5q11.2→q22 had been identified as a potential candidate chromosome locus, because a fifth patient 5859, unfortunately deceased, had been found to carry a de novo inverted duplication of chromosome 5q, 46,XY,add(5)(q11.2)dup(5)(q22q11.2). The chromosome region 5q11.2→q22 was screened for CN changes running the CNAT 4.0 batch analysis with GS = 0 Mb in all four patients, but no unique CNVs with gene content were detected.

4.10. Outcome of the Analytical Workflow for the Screening of Multiple CNVs

The decisional process workflow allowed to filter the total of 3857 CNVs initially found in the cohort of 10 patients, in order to identify the potentially pathogenic ones. The mean of CNVs per patient was reduced from 386 total CNVs per patient to 37 unique CNVs with gene content per patient. The decisional process tentatively catalogued gains (CN 3) as genomic polymorphisms more frequently than losses (CN 1), progressively increasing the ratio of CN 1 to CN 3 from 1:2 to 1:1. The outline of the outcome of the decisional process workflow is presented in Figure 19.

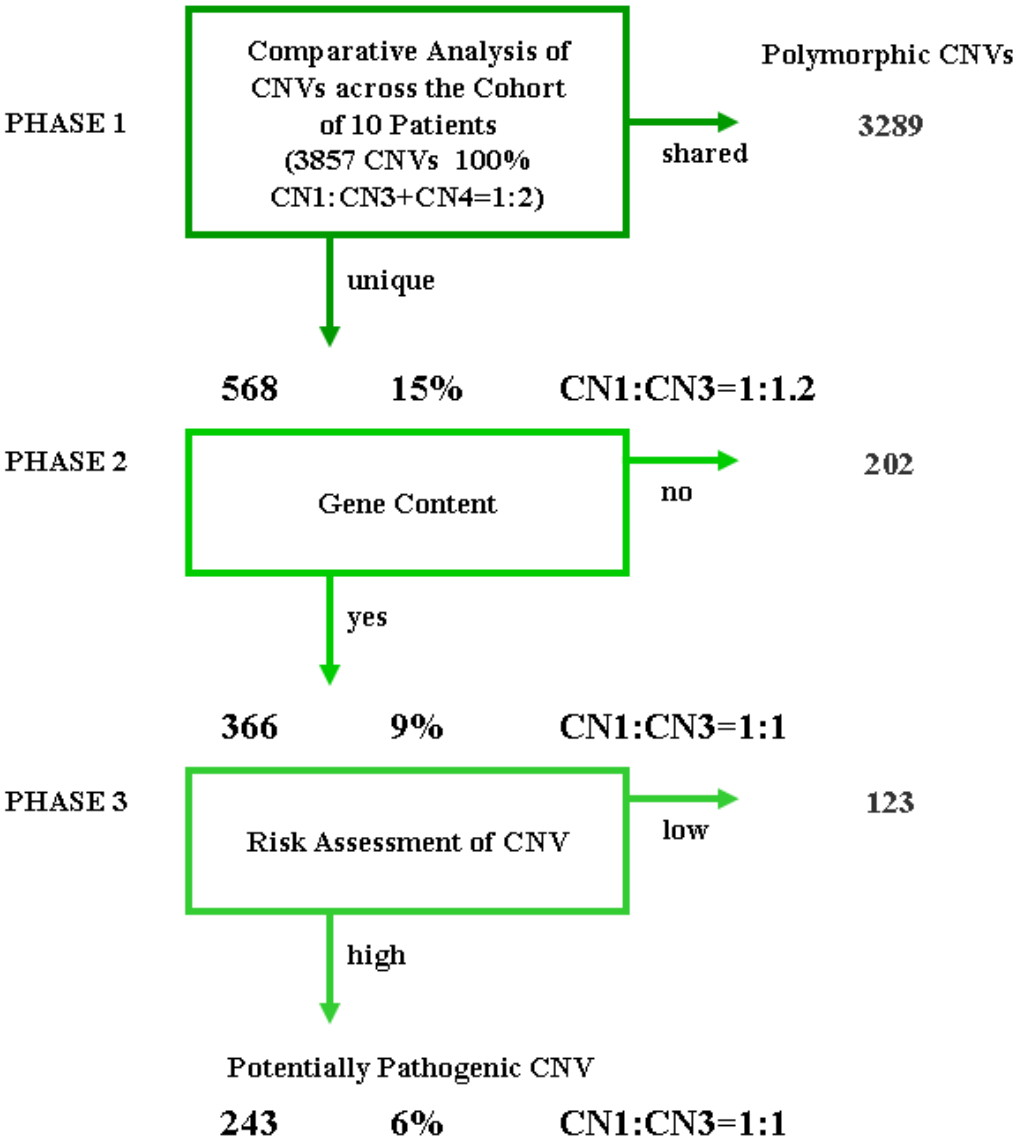

Figure 19. **Outcome of the analytical workflow for the screening of multiple CNVs.** The numbers and percentages of CNVs filtered in each phase of the decisional process are shown, together with the changing ratio of CNVs in CN 1 to CNVs in CN 3. CN: Copy Number.

The progressive increase of the CN 1:CN 3 ratio indicated that a higher percentage of unique CNVs in CN 3 than unique CNVs in CN 1 did not contain any gene. However, when only unique CNVs with presence of gene content were taken into consideration, the cumulative percentages of unique CNVs per CN state demonstrated that CNVs in CN 1 tended to hold fewer genes than CNVs in CN 3 (data shown in Figure 10).

The *shared* versus unique criteria utilised in the first phase of the decisional process, based on the comparative analysis of all CNVs across the whole cohort of 10 patients, allowed to reduce the total number of CNVs initially detected of ~85%. Overall, the

percentage of CNVs identified in the whole cohort of 10 patients gradually decreased from 100% to 6-9%, by applying the decisional workflow. The final percentage depends on the weight attributed to the comparison of the unique CNVs with gene content against the DGV, during phase 3 of the decisional process.

5. RESULTS

Candidate Gene Mutation Analysis

Summary of results:

- The gene *BARX2* was selected as a potential novel candidate gene for pituitary development and pathology, following a bioinformatic prediction targeting the chromosome region 11q24.2→qter affected by rearrangements in two patients included in the cohort under study, as well as in the del11q syndrome. Mutation analysis of *BARX2* was performed in a cohort of 71 selected patients;
- Two genes, that play a role in the embryological development of the pituitary gland, *OTX2* and *BMP4*, were screened for mutations in a cohort of 35 patients presenting with a complex pituitary and clinical phenotype;
- A nucleotide sequence variant, leading to a non-synonymous amino acid change, was identified in one patient in exon 2 of *BARX2*, that had not been reported before in the literature nor in public databases;
- A non-sense mutation was found in exon 4 of *OTX2*, compatible with the clinical phenotype of the patient that comprised of severe eye defects as well as pathology of the pituitary gland.

5.1. *BARX2*

BARX2 is a member of the homeobox gene family of transcription factors, its coding region spans approximately 14 kb and it is contained within 4 exons. The gene encodes a protein of 279 amino acids, with a homeodomain encompassing 60 amino acids (108-167), that works as transcriptional regulator via sequence-specific DNA binding. [242-244] *BARX2* is located on chromosome 11q24.3, ~560 kb telomeric to the gene *FLI1*, also located in the chromosome region 11q24.3. *FLI1* encodes a transcription factor that plays a role in megakaryopoiesis, and strong evidence has been collected that support its role in causing Paris-Trousseau syndrome in patients with 11q deletion syndrome.

[245, 246] Chromosome 11q deletion syndrome is a contiguous gene deletion disorder, but no candidate gene for the endocrinological phenotype has been identified.

The ~10 Mb terminal deletion of chromosome 11q in patient 6089 was identified as the candidate chromosome region to harbour the novel gene responsible for the severe pathology of the pituitary gland. Although this chromosome region proved to be gene-rich (it contained 134 characterised genes at the moment of conducting the study), a bioinformatic prediction was attempted. The bioinformatic prediction was performed using Gene Sorter from UCSC, targeting the 11q24.2→qter chromosome region, and interrogating a list of genes that were already known to be mutated in patients with pathology of the pituitary gland, namely *HESX1*, *LHX4*, *POU1F1* and *PROP1*. These genes were chosen because their mutations give rise to pathological conditions that have characteristics in common with what observed in patient 6089, in terms of clinical phenotype, morphology of the pituitary gland on MRI, and/or inheritance. Each one of these genes was input into Gene Sorter to look for genes with Pfam domain similarity and BLASTP protein homology. For all four genes, the search of a gene with Pfam domain similarity within the 11q24.2→qter chromosome region returned only one positive result: *BARX2*. The search for a gene, within the 11q24.2→qter chromosome region, with significant protein homology based on the BLASTP E-value gave a positive result only for two genes, *HESX1* and *PROP1*; in both cases the positive result was *BARX2*. The results, including the numerical values, of the bioinformatic prediction are summarised in Figure 20.

Gene	Phenotype	Inheritance	Search for	Pfam	BLASTP
HESX1	IGHD, CPHD, SOD; APH, EPP, absent infundibulum, ACC	R, D	?	BARX2	BARX2 7e-06
LHX4	CPHD, IGHD; small AP, EPP, cerebellar abnormalities	D	?	BARX2	-
POU1F1	GH, TSH, prolactin deficiencies; small or normal AP	R, D	?	BARX2	-
PROP1	GH, TSH, LH, FSH, prolactin deficiencies, evolving ACTH deficiency, early onset GH deficiency and growth retardation; small, normal or enlarged AP	R	?	BARX2	BARX2 0.003

Figure 20. **Results of the bioinformatic prediction targeted at the chromosome region 11q24.2→qter.** The bioinformatic prediction of a candidate gene in the 11q24.2→qter chromosome region was based on the similarity of the Pfam domain and the E-values of the BLASTP protein homology search. Both E-values, reported in the BLASTP column, were significantly smaller than 0.1 and, therefore, could be safely interpreted as the (null) probability that a match between the two proteins occurred by chance. ACC: Agenesis of Corpus Callosum; ACTH: Adrenocorticotrophic Hormone; AP: Anterior Pituitary; APH: Anterior Pituitary Hypoplasia; CPHD: Combined Pituitary Hormone Deficiency; EPP: Ectopic Posterior Pituitary; FSH: Follicle-Stimulating Hormone; GH: Growth Hormone; IGHD: Isolated Growth Hormone Deficiency; LH: Luteinizing Hormone; SOD: Septo-Optic Dysplasia; TSH: Thyroid-Stimulating Hormone. D: Dominant; R: Recessive.

The role of *BARX2* in the pathogenesis of the clinical phenotype of 11q deletion syndrome had been investigated previously in a small cohort of 9 patients affected by a specific symptom of the disease, isolated trigonocephaly, and no changes to the sequence of the gene had been identified. [242] Similarly, no etiologic mutations of *BARX2* coding sequence had been detected in 139 DNA samples from patients with ocular anomalies. [243] *BARX2* had not been previously studied by genomic sequencing in individuals with pathology of the pituitary gland.

5.2. *OTX2*

OTX2 is a member of the homeobox gene family and encodes a 289 amino acid protein, transcribed from a 5 kb genomic region that encompasses 3 coding exons, that acts as a transcription factor. The protein has a homeodomain, responsible for DNA binding, and C- and N-terminal transactivation domains, the activity of which relies on an intact homeodomain. The expression pattern of *OTX2* studied in early human embryos highlighted its prime role in eye morphogenesis, as well as demonstrating a role in hypothalamo-pituitary development. [103, 104] PCR-based human cDNA library screening identified *OTX2* expression in the pituitary gland and the hypothalamus, as well as in the whole foetal and adult brain, and the thalamus. [101-103] The expression of *OTX2* in the hypothalamus was associated with a transactivation function for the promoter of interstitial retinoid-binding protein (*IRBP*), involved in ocular function, as well as for the promoters of *GnRH1*, *POU1F1* and *HESX1*. [101, 102, 104]

Mutations of *OTX2* were first found to cause syndromic ano- microphthalmia and other ocular malformations by screening patients with a wide spectrum of eye defects, which ranged from bilateral anophthalmia to retinal dystrophy. [37] Heterozygous mutations in *OTX2* were identified in 11 affected individuals from 8 unrelated families. Eye defects were associated with intracranial and brain malformations (i.e. ACC, malformations of the hippocampus and septum pellucidum), DD (including severe), microcephaly, seizures, hearing loss, hypotonia and joint laxity. A normal-sized pituitary gland was documented in 4 patients, but no formal endocrinological investigations were performed. Heterozygous loss-of-function mutations occurred de novo in severely affected offspring in two families, while in two other families they were inherited from a gonosomal mosaic parent. In 4 additional families, reduced penetrance and variable expression were suggested. [37]

5.3. *BMP4*

The transcriptional unit of the human *BMP4* gene is encoded by 5 exons (of which 2 are coding exons) and spans approximately 7 kb. The gene encodes a 408 amino acid

protein that is a member of the bone morphogenetic protein family, which is part of the transforming growth factor-beta superfamily. In situ hybridisation in human embryos demonstrated expression of *BMP4* protein in the optic vesicle, the developing retina, the pituitary region and digits, and haploinsufficiency of *BMP4* was deemed a major candidate mechanism for abnormalities of the eyes (mainly ano- microphthalmia and retinal dystrophy), digits and brain, and for pathology of the pituitary gland. [247]

Genomic sequencing of *BMP4* first led to the identification of two familial heterozygous point mutations. In a family, where members of three generations suffered from anophthalmia-microphthalmia, iris and chorioretinal coloboma, retinal dystrophy of both rods and cones, mild DD, hypoplastic corpus callosum and polysyndactyly, a frameshift mutation, leading to a premature stop codon, was found. In a second family, a missense mutation in a highly conserved base of *BMP4* was associated with microphthalmia, sclerocornea, coloboma, DD, seizures, bilateral cryptorchidism, and brain and digital anomalies. In addition to the two pathogenic mutations, several low-penetrant variants were also identified in *BMP4*. [247]

5.4. Ethical Approval and Informed Consent

The personal and clinical data of the patients included in the study are stored in compliance with the Data Protection Act 1998. The project has received full research ethical approval (revised in 2009).

A signed assent/consent form was obtained from each patient (and/or their legal guardians) included in the study. All participants received a patient/parents information sheet, detailing the aim of the study and the use of the participants' DNA sample to study changes associated with the development and pathology of the pituitary gland. A copy of the information sheet is enclosed as Appendix B.

5.5. Selection Criteria of Patients for Mutation Analysis

The pituitary stalk carries the neural and vascular connections between the hypothalamus and the pituitary gland, and damage to the pituitary stalk results in both anterior and posterior pituitary dysfunction, although to a significantly variable extent. The presence or absence of an intact stalk or ectopic localisation of the posterior lobe on imaging is considered to be an important part of the description of the phenotype in pituitary dysfunction syndromes. Patients 6089 and 18905640, who carried a chromosome rearrangement of region 11q24 where *BARX2* is mapped, were both diagnosed with GHD and anterior pituitary hypoplasia; patient 6089 also presented with ectopic posterior pituitary, while absent pituitary stalk was diagnosed in patient 18905640. Therefore, a highly homogeneous cohort of 71 patients with isolated pituitary pathology were selected from the database of 1,168 index endocrinological patients, according to the following criteria: presence of GHD and MRI evidence of a small pituitary gland and infundibulum and an ectopic posterior pituitary gland.
Genomic sequencing of *BARX2* was carried out in all 71 patients and in patient 18905640.

A list of 35 patients presenting with the association of hypopituitarism and/or anatomical defects of the pituitary gland with eye pathology, ranging from anophthalmia-microphthalmia to retinal dystrophy, were chosen to undertake mutation analysis in the candidate genes *BMP4* and *OTX2*. The pituitary phenotype varied greatly in severity and manifestations, from short stature, IGHD, HH (with cryptorchidism and small/micro penis) to CPHD, small anterior pituitary, ectopic posterior pituitary, and SOD. Five patients (5238, 5328, 5984, 6222, JD98) included in the cohort selected for genomic sequencing of *BMP4* and *OTX2* had been identified during the review of the 1,168 clinical records included in the database of endocrinological patients, as they presented with the recurrent association between hypopituitarism and pathology of the retina. During the selection process, other aspects of the clinical phenotype were taken into consideration. DD and behavioural problems, congenital malformations of the brain (e.g. cortical atrophy), kidneys (e.g. renal hypoplasia) and digits (i.e. polydactyly) were

considered risk factors for the presence of mutations in *BMP4*, in particular. Sporadic instances of hearing loss and CHD were also recorded amongst the selected patients.

Three patients, who were included in the mutation analysis of *BMP4* and *OTX2*, were also included in the high resolution genome-wide CN change screening with the 250K SNP array platform. Patients 4997 and 6110 had complex and partly overlapping clinical phenotypes, including microphthalmia, growth deficiency, bilateral cryptorchidism (patient 4997 only, patient 6110 is female), DD and renal dysplasia; the third patient, JD98, had hypoplasia of the optic chiasm and left optic nerve, retinal rod-cone dystrophy, short stature, IGHD and hypoplastic anterior pituitary gland.

5.6. *BARX2* Sequence Variants

In patient 5907, a novel heterozygous missense mutation, c.280G>A, p.Ala-94-Thr (A94T), in exon 2 of *BARX2* was identified. Patient 5907 was a female born in 2000, from non-consanguineous parents, who suffered from panhypopituitarism (GH, TSH, ACTH deficiency and flat gonadotropin response) associated with an ectopic posterior pituitary gland and growth deficiency. She was receiving treatment with GH, thyroxine and hydrocortisone.

A DNA sample was obtained from both parents, and tested by direct sequencing for mutations in exon 2 of *BARX2*. The base substitution c.280G>A (p.A94T) was found, in the heterozygous state, in the father of the proband (sample number 6334); the mother (6335) showed a homozygous wild-type sequence. No information regarding the medical history of the proband's father were available. The mutation identified in patient 5907 and the results of the sequencing of the parental samples (6334, 6335) are shown in Figure 21.

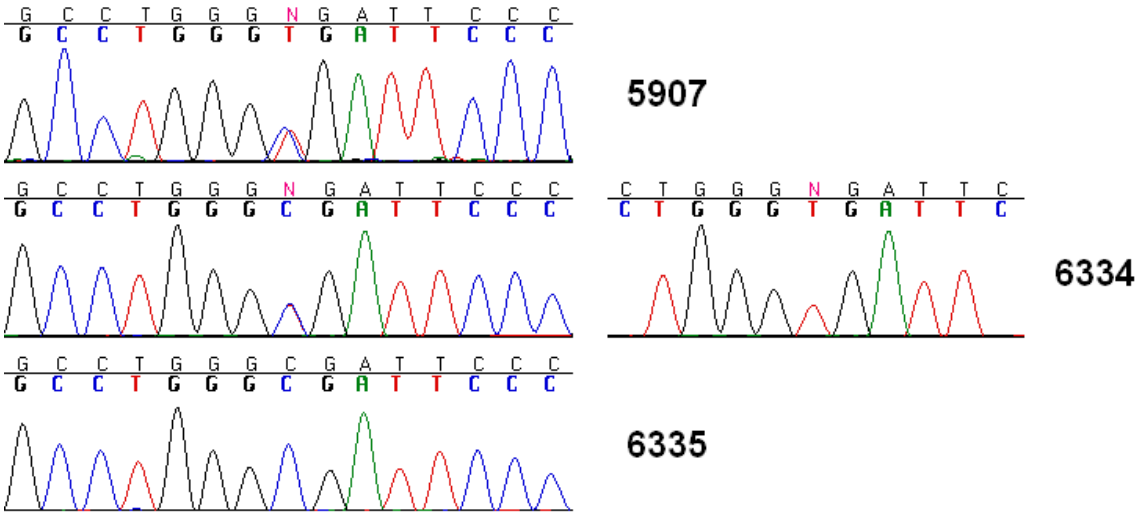

Figure 21. **Heterozygous mutation in exon 2 of *BARX2* in patient 5907 and her father (6334).** Detection of a heterozygous substitution (N) in exon 2 of *BARX2* in patient 5907 and her father (6334, left chromatogram). The mother (6335) has a homozygous wild-type sequence. In the picture, the reverse sequence is shown, and the mutant allele is represented as c.280C>T. For sample 6334, the sequence is also shown excluding allele 'C' to better visualise the presence of the mutant allele 'T' (right chromatogram).

The amino acid change A94T falls outside the conserved functional homeodomain (amino acids 108-167) of the protein encoded by *BARX2*. However, the substitution of the amino acid alanine with the bigger and polar amino acid threonine could potentially alter stoichiometry relationships. Figure 22 shows the conservation of the amino acid sequence including the one involved in the missense substitution.

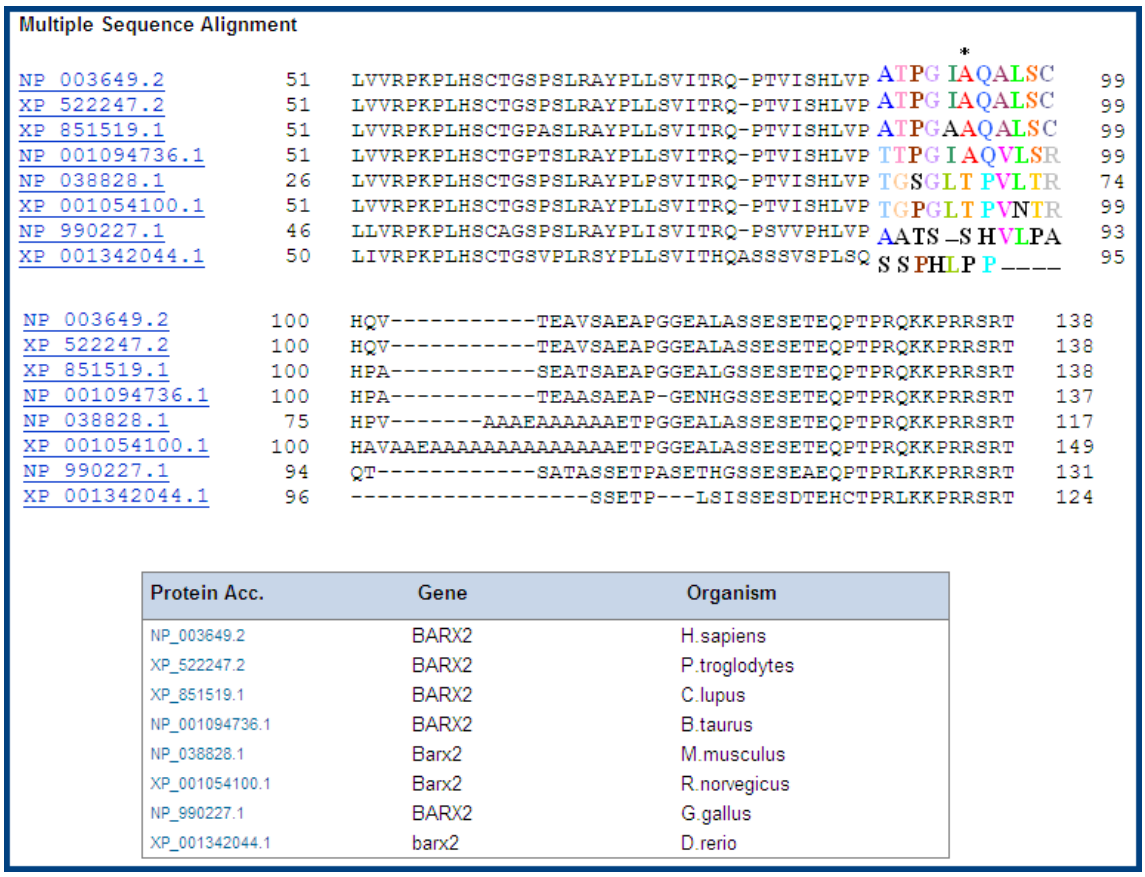

Figure 22. **Conservation of the amino acid residue affected by the *BARX2* mutation in patient 5907.** The multiple sequence alignment was generated by MUSCLE (multiple sequence comparison by log-expectation) version 3.6 from NCBI, showing gene conservation in Eutelostomi. The amino acid residue 94, affected by the mutation, is marked by an asterisk.

The amino acid residue 94 is conserved in 50% of the species, and the conservation appears to extend to a longer amino acid motif. The human 11 amino acid motif ATPGIAQALSC (containing at the centre the residue 94) is almost fully conserved in 50% of the species, while it is substituted by the motif TGxGLTPVxTR in 25% of the species. This pattern could reinforce the notion of a conserved stoichiometric relationship between the amino acid residues.

The mutation c.280G>A (A94T) had not been previously reported in the literature, nor in the public databases of the NCBI and of 1000 Genomes. The mutation had not been found in any of the 148 patients, affected by either trigonocephaly or eye pathology, included in previous mutation screenings of *BARX2*, nor it was found in any other one of the 71 patients included in the present screening.

Apart from the A94T mutation in exon 2, no other sequence changes were detected in the first three exons of *BARX2*. In exon 4, three different SNPs were detected, two of which had been reported before in the NCBI website, [213] while one was reported for the first time in this study. A fourth SNP was found in intron 3, five bases from the first coding nucleotide of exon 4. This intronic polymorphism had also been previously reported by NCBI. [213] Two of the SNPs were present in multiple patients, both in the heterozygous and homozygous state. The SNP newly identified in this study was detected in five patients. One SNP, in the coding region of exon 4, was present in one patient only. A summary of the identified SNPs, with the relevant numbers of occurrences in either the heterozygous or homozygous state, and allelic frequencies are presented in Table 31.

DNA change	**Protein change**	**Number of patients**		**Allelic frequency**	
		Het.	**Hom.**	**Present cohort**	**NCBI**
c.574-5C>T	-	25	7	0.271	0.428
c.609C>T	P203P	25	8	0.285	0.416
c.690T>G	G230G	5	-	0.035	-
c.755G>A	R252H	1	-	0.007	0.027

Table 31. **SNPs detected in intron 3 and exon 4 of *BARX2*.** All allelic frequencies refer to the non wild-type allele. The allelic frequencies calculated in the present cohort are approximated to three decimal places. Het.: heterozygous; Hom.: homozygous; -: not present.

The synonymous nucleotide change c.690T>G (G230G) had not been reported previously, and was found, in the heterozygous state, in five patients in the cohort under study. The missense amino acid change R252H had been reported previously in the NCBI website with an allelic frequency of 0.027 in the HapMap YRI population. One patient of probable African descent in the cohort under study presented the same missense SNP in the heterozygous state. A total of 24 patients carried both the c.574-5C>T SNP in intron 3 and the P203P synonymous change in exon 4 in the heterozygous state, and 7 patients carried both SNPs in the homozygous state. The concomitant presence and concordant state of these two polymorphisms in a total of 31 individuals indicated a linkage disequilibrium. Only two exceptions were recorded: in one instance, heterozygosity for the P203P SNP was accompanied by a homozygous wild-type sequence of the polymorphic position of intron 3; in the second case, the sequence of

patient 18905640 revealed the presence of the intronic polymorphism in the heterozygous state and the P203P SNP in the homozygous state.

The genomic sequencing of all exons and intron-exon boundaries of *BARX2* in patient 18905640 did not identify any other change, apart from the SNPs of intron 3 and exon 4 described above. The occurrence of a heterozygous polymorphism indicated the presence of two copies of *BARX2* at that genomic position. The results of the genomic sequencing did not suggest a disruption of a copy of *BARX2* in patient 18905640.

5.6.1. Conclusions regarding *BARX2* Mutation Analysis

The substitution c.280G>A is the only mutation leading to a non-synonymous amino acid change identified in the coding region of *BARX2* outside of exon 4. The relative positions of the identified mutation and SNPs are shown in Figure 23.

Figure 23. **Structure and sequence variants of *BARX2*.** The schematic representation highlights the relative positions of the identified mutation and SNPs.

The lack of clinical data regarding the father of patient 5907 complicated the interpretation of the results of the mutation analysis. Controls were not screened for the A94T mutation during the course of this study. However, this decision was justified by the availability of information from the whole cohort of 71 patients in the present study, 148 patients previously reported in the literature, and the NCBI and 1000 Genomes databases. According to these sources, the mutation A94T has been reported for the first time in this study, and, although its causal role in determining the endocrinological phenotype of patient 5907 could not be determined with certainty, the mutation's

frequency would fall below 1%. Functional studies of the variant protein would have helped in clarifying the role of the mutation and of *BARX2* in pituitary pathology. The lack of such contribution represents a limitation of this study.

The CNAT 4.0 batch analysis of the Affymetrix GeneChip 250K Sty1 SNP Mapping Array run with GS = 0 Mb allowed to verify the CN status of all SNPs covering *BARX2* in patient 18905640. The results were compared with the ones obtained, applying the same procedure, for patient 6089. A total of ten SNPs covered *BARX2*. The gene is 76 kb in size, which corresponded to an average of one SNP per ~8 kb, although the ten SNPs were not evenly distributed along the length of the gene. All SNPs were present in CN 1 in patient 6089, while they were present in CN 2 in patient 18905640, as shown in Figure 24.

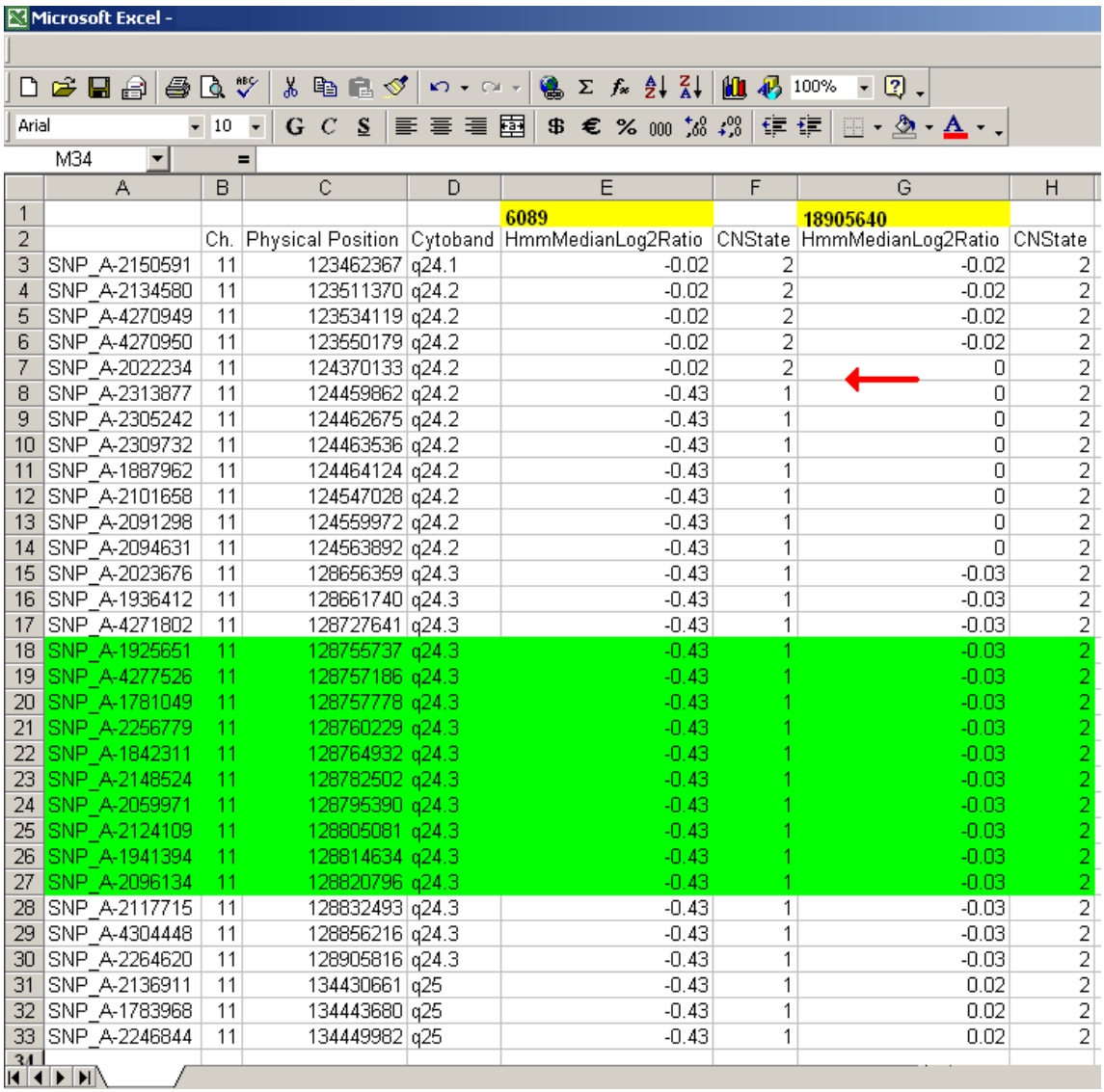

	A	B	C	D	E	F	G	H
1					6089		18905640	
2		Ch.	Physical Position	Cytoband	HmmMedianLog2Ratio	CNState	HmmMedianLog2Ratio	CNState
3	SNP_A-2150591	11	123462367	q24.1	-0.02	2	-0.02	2
4	SNP_A-2134580	11	123511370	q24.2	-0.02	2	-0.02	2
5	SNP_A-4270949	11	123534119	q24.2	-0.02	2	-0.02	2
6	SNP_A-4270950	11	123550179	q24.2	-0.02	2	-0.02	2
7	SNP_A-2022234	11	124370133	q24.2	-0.02	2	0	2
8	SNP_A-2313877	11	124459862	q24.2	-0.43	1	0	2
9	SNP_A-2305242	11	124462675	q24.2	-0.43	1	0	2
10	SNP_A-2309732	11	124463536	q24.2	-0.43	1	0	2
11	SNP_A-1887962	11	124464124	q24.2	-0.43	1	0	2
12	SNP_A-2101658	11	124547028	q24.2	-0.43	1	0	2
13	SNP_A-2091298	11	124559972	q24.2	-0.43	1	0	2
14	SNP_A-2094631	11	124563892	q24.2	-0.43	1	0	2
15	SNP_A-2023676	11	128656359	q24.3	-0.43	1	-0.03	2
16	SNP_A-1936412	11	128661740	q24.3	-0.43	1	-0.03	2
17	SNP_A-4271802	11	128727641	q24.3	-0.43	1	-0.03	2
18	SNP_A-1925651	11	128755737	q24.3	-0.43	1	-0.03	2
19	SNP_A-4277526	11	128757186	q24.3	-0.43	1	-0.03	2
20	SNP_A-1781049	11	128757778	q24.3	-0.43	1	-0.03	2
21	SNP_A-2256779	11	128760229	q24.3	-0.43	1	-0.03	2
22	SNP_A-1842311	11	128764932	q24.3	-0.43	1	-0.03	2
23	SNP_A-2148524	11	128782502	q24.3	-0.43	1	-0.03	2
24	SNP_A-2059971	11	128795390	q24.3	-0.43	1	-0.03	2
25	SNP_A-2124109	11	128805081	q24.3	-0.43	1	-0.03	2
26	SNP_A-1941394	11	128814634	q24.3	-0.43	1	-0.03	2
27	SNP_A-2096134	11	128820796	q24.3	-0.43	1	-0.03	2
28	SNP_A-2117715	11	128832493	q24.3	-0.43	1	-0.03	2
29	SNP_A-4304448	11	128856216	q24.3	-0.43	1	-0.03	2
30	SNP_A-2264620	11	128905816	q24.3	-0.43	1	-0.03	2
31	SNP_A-2136911	11	134430661	q25	-0.43	1	0.02	2
32	SNP_A-1783968	11	134443680	q25	-0.43	1	0.02	2
33	SNP_A-2246844	11	134449982	q25	-0.43	1	0.02	2

Figure 24. **Results of the CNAT 4.0 batch analysis of *BARX2* in patients 6089 and 18905640.** The numerical analysis of the SNP log2 Ratio and CN State was carried out by exporting the CNAT 4.0 output to a Microsoft Excel spreadsheet. The ten SNPs that covered *BARX2* are highlighted in green. The chromosome bands have been condensed for purpose of visualisation and to show also the fine definition of the breakpoint of the 11q deletion in patient 6089 by using SNP positions (red arrow). Ch: Chromosome; CNState: Copy Number State.

5.7. *OTX2* Mutation and Polymorphisms

In patient 5976 a novel heterozygous nonsense mutation, c.235G>T, p.E79X, in exon 4 of *OTX2* was identified. Patient 5976 was a female, born from non-consanguineous parents, who suffered from a bilateral severe eye defect in the spectrum of anophthalmia-microphthalmia and structural abnormalities of the pituitary gland demonstrated at the MRI.

A DNA sample was obtained from both parents, and tested by direct sequencing for mutations in exon 4 of *OTX2*. Both the father (sample number 6604) and the mother (sample number 6605) of the patient were found to be homozygous for the wild-type sequence. The mutation identified in patient 5976 and the results of the sequencing of the parental samples (6604, 6605) are shown in Figure 25.

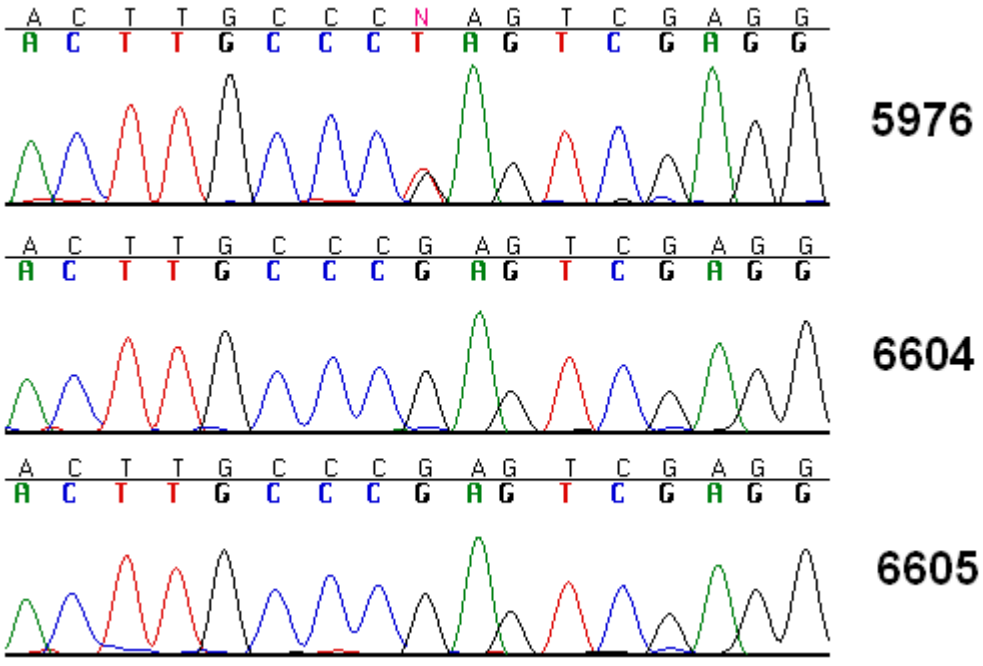

Figure 25. **Heterozygous mutation in exon 4 of *OTX2* in patient 5976.** Detection of a heterozygous c.235G>T substitution (N) in patient 5976; the patient's father (6604) and mother (6605) both showed homozygous wild-type sequences.

The E79X mutation had not been reported previously, it was not found in any other one of the 34 patients included in the screening, nor in 60 controls (120 chromosomes).

Figure 26 shows the results of the restriction enzyme digestion of patient 5976, both of her parents, and a sample of the controls.

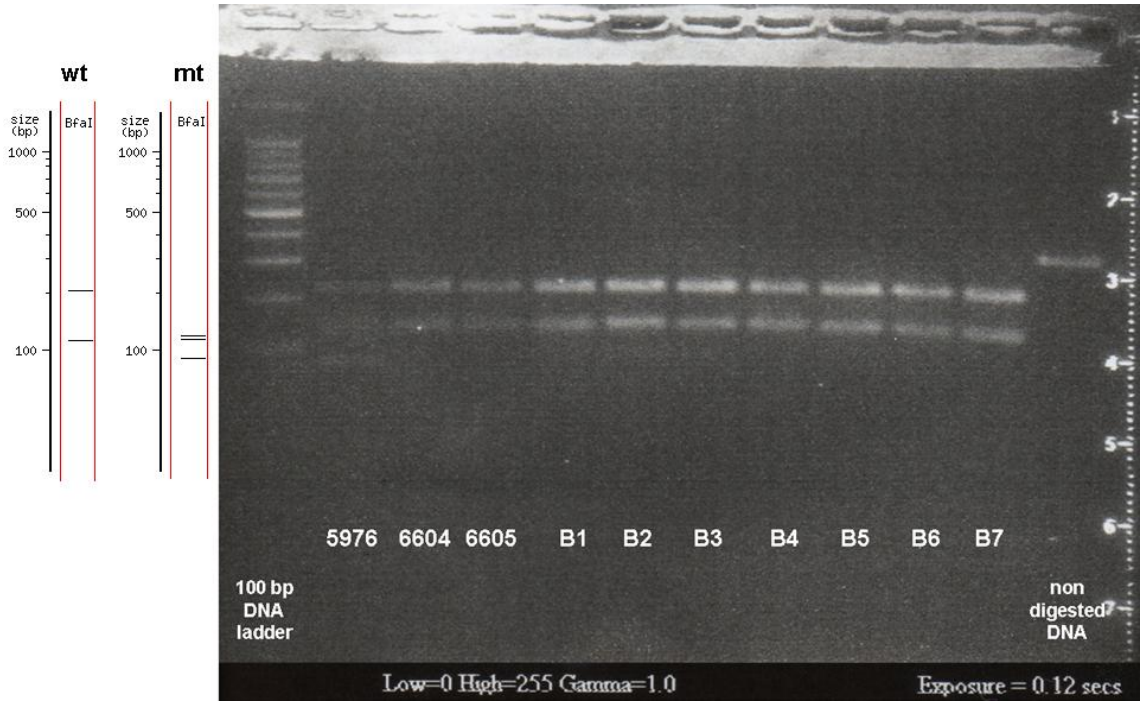

Figure 26. **Restriction digestion with the enzyme BfaI of mutation c.235G>T, p.E79X.** Patient 5976 carries the heterozygous mutation, and both alleles can be identified: the wild-type sequence is identified by the 208 bp product and the mutated allele is identified by the 86 bp band. Both parents of the patient (6604 and 6605) and seven controls (B1-B7) show the wild-type allele (restriction digestion products of 208 bp and 117 bp) only. An undigested PCR product of exon 4 of *OTX2* (size of 325 bp), from a control DNA sample, was loaded onto the gel as a negative control for restriction enzyme activity. The virtual run of the products of the restriction digestion of both the wild-type (wt) and the mutated (mt) alleles, performed by the REBsites tool, is shown on the left of the image.

The genomic sequencing of all exons and intron-exon boundaries of *OTX2* in all other patients did not identify any other mutation in the coding regions. One SNP located in intron 3 and one SNP in the 3' untranslated region (UTR), that had both been reported before in the NCBI database, were detected in 1 and 5 patients, respectively. The substitution c.97+12C>T in intron 3 was fond in 1 patient in the heterozygous state, corresponding to an allelic frequency in the present cohort of 0.028. The allelic frequency listed by NCBI was 0.036. [213] The c.870+10G>A SNP in the 3' UTR of the gene was detected in 4 patients in the heterozygous state and in 1 patient in the

homozygous state. This SNP was present in the NCBI database with an allelic frequency of 0.052, [213] while the allelic frequency calculated in the cohort under study was 0.171. All allelic frequencies refer to the non wild-type allele.

The mutation c.235G>T, leading to the insertion of a stop codon at the position of the amino acid residue 79 of *OTX2* in patient 5976, truncates the functional homeodomain of the protein and is, therefore, expected to abolish the DNA-binding ability and, consequently, the transactivation properties of the N- and C-terminal domains.
The pituitary pathology and the phenotype of patient 5976 are consistent with haploinsufficiency of the *OTX2* protein, as observed in other patients with severe mutations of *OTX2* and patients with deletions of the chromosome region 14q22-q23 (where *OTX2* is located), as discussed in chapter 6.7.

5.8. *BMP4* Mutation Analysis

The whole coding sequence (including intron-exon boundaries) of *BMP4* was screened for mutations in the 35 selected patients who presented with a complex clinical phenotype with the association of pituitary gland and eye pathology, and including brain, kidney and digit malformations. Genomic sequence analysis did not identify any pathogenic mutation in any of the patients.
A SNP in exon 4 of *BMP4*, previously reported by the NCBI with an allelic frequency of 0.461, [213] was found in the cohort under study. The nucleotide change c.455T>C, leading to the amino acid substitution p.V152A, was present in the heterozygous state in 13 patients, and in the homozygous state in 4 patients. The allelic frequency of the ‘C’ allele in the cohort under study was 0.6, while the frequency of the contig reference allele ‘T’ was 0.4.

6. DISCUSSION

6.1. CNVs and Candidate Genes Associated with Pituitary Pathology

Mutations in known genes involved in the development and function of the pituitary gland have been found to account for up to 10% of cases of congenital hypopituitarism. A list of these genes, the relevant clinical phenotypes and mode of inheritance is presented in Table 1. A non-sense mutation, not previously described, has been identified in the course of this project in one of these genes, *OTX2*.

In the search for novel genes for pituitary pathology, *BARX2* was considered a candidate because of its genomic position within the critical region for 11q deletion syndrome, and because of its protein homology and domain similarity with genes already known to be involved in pathology of the pituitary gland. *BARX2* had not been screened before for mutations in patients with isolated pathology of the pituitary gland. A large cohort of patients with a homogeneous clinical phenotype were selected from the database of endocrinological patients of the Great Ormond Street Hospital, and a nucleotide substitution, leading to a novel missense amino acid change, was detected in 1/72 patients. The sequence variation is not present in public databases nor in the literature.

In the same candidate genomic region, chromosome band 11q24.2, a submicroscopic genomic rearrangement was identified involving one gene only, *KIRREL3*, in one patient affected by panhypopituitarism and carrying an apparently balanced chromosome translocation 46,XY,t(11;22)(q24;q13).

A decisional workflow was designed to screen the CNVs identified in the cohort of 10 patients under study, and allowed to filter the total of 3857 CNVs initially detected, in order to reduce the mean of CNVs, that warranted further assessment, from 386 to 37 per patient. Two genomic imbalances, a terminal deletion of chromosome 11q and an interstitial deletion of chromosome 22q, were identified as the genetic cause of

pathology in two patients.

6.1.1. 11q Deletion Syndrome

The partial deletion of the long arm of chromosome 11 is a clinically recognised syndrome characterised by: DD in virtually 100% of patients (only two patients, with very small terminal deletions, did not show any sign of cognitive development impairment [Grossfeld, personal communication]), transient megakaryocytic thrombocytopenia (Paris-Trousseau syndrome), that tends to resolve spontaneously, with an age-dependent penetrance of 95-100%, growth deficiency with length or height below the 5th percentile in 68% of patients, unilateral or bilateral cryptorchidism in 58% of males (one instance of hypospadias was also reported), clinically significant heart malformations in at least 50% of patients, trigonocephaly (~30% of patients), pyloric stenosis (~15% of patients), hearing loss, and characteristic facial dysmorphic features. [220] In 8 (6 male and 2 female) patients with del11q syndrome and height <5th percentile, the levels of IGF1 were assessed, and found to be low in 4 out of the 8 patients; four male patients also showed cryptorchidism. These results implied that the cryptorchidism could represent a sign of underlying HH, and were interpreted as indicative of an overall pituitary gland dysfunction in del11q syndrome, with a critical region within the chromosome bands 11q24.2→qter. [220, 248] Only one case was described in the literature of a female patient who underwent a full endocrinological investigation. The patient had a 11q terminal deletion with breakpoint within band 11q23.3, and presented with severe growth deficiency with growth velocity at -9 SD, DD, CHD, and bilateral hearing loss. It was demonstrated that she suffered from both partial GHD and central hypothyroidism, and an MRI of the brain showed a small pituitary gland and infundibulum. Replacement therapy with GH and thyroxine restored her growth velocity to normal, but unfortunately the patient died of septic meningitis at the age of 2 years. [249, 250]

The clinical information on 108 Italian patients with del11q syndrome were reviewed by us during the course of the project, and revealed that at least 14 individuals had signs indicative of pituitary function impairment. The breakpoint of a terminal 11q deletion was finely mapped within a 26 kb interval between genomic positions 124,370,133-124,396,305 in patient 6089, who suffered from severe GHD, signs of HH, and

anatomical anomalies of the pituitary gland. Patient 18905640, affected by panhypopituitarism and severe structural abnormalities of the pituitary gland, carried an apparently balanced translocation involving chromosome band 11q24. Evidence has, therefore, been collected that supports the existence of an impaired function of the hypothalamo-pituitary axis in patients with 11q deletion syndrome, and the presence of a novel gene responsible for pituitary pathology.

Both *BARX2* and *KIRREL3* map within the 11q24.2→qter critical region for the endocrinological phenotype.
BARX2 was investigated in patient 18905640 both by means of genomic sequencing of all exons and intron-exon boundaries and for CN changes on the Affymetrix 250K Sty1 SNP array platform with CNAT 4.0 batch analysis run with GS = 0 Mb. All 10 SNPs covering *BARX2* were detected in CN 2, no mutations of its coding sequence were found, while one heterozygous SNP in intron 3 was detected that confirmed the presence of two copies of *BARX2* at that genomic position. However, a novel missense mutation of *BARX2* was identified in another patient, 5907, with isolated hypopituitarism, as further discussed in chapter 6.9.

In patient 18905640, two submicroscopic CNVs were identified in the genomic regions 11q24.2 and 22q12.3, respectively, corresponding to the sites of the patient's translocation breakpoints as defined by low resolution routine karyotyping. [216] The genomic imbalance in the region 11q24.2 was considered of particular interest, as it could have disrupted the gene involved in the etiopathogenesis of hypopituitarism in del11q syndrome. The 52 kb complex rearrangement in 11q24.2, comprising of both a deletion and a duplication, involved only one gene, *KIRREL3*.
KIRREL3 is expressed in the human foetal and adult brain, with variable levels of expression in different regions. [226, 251] Three different heterozygous missense mutations have been identified in five patients in highly conserved residues of the gene. All patients, four females and one male, suffered from MR varying in degrees from mild to severe. [226] Moreover, in a female patient with severe DD and an apparently balanced chromosome translocation t(11;16)(q24.2;q24), the chromosome 11 breakpoint junction sequence was demonstrated to map to intron 1 of *KIRREL3*, and the expression of *KIRREL3* was 45% lower in the patient than in two controls. The patient also showed a few additional clinical features: alternating exotropia, and minor dysmorphic features of the face, fingers and toes. [226] No additional chromosomal

rearrangements at or near the chromosomal breakpoints or unrelated to the translocation were detected by whole genome 250K Nsp1 array analysis. [226] Overall, alterations in *KIRREL3*, either alone or potentially in combination with other factors, are considered likely to play a role in DD. However, a definitive genotype-phenotype correlation has not yet been established. [226]

Genomic sequencing of *KIRREL3* has never been carried out in a cohort of patients with pathology of the pituitary gland, either isolated or in association with DD. The lack of such a pilot screening poses limits to the interpretation of the significance of the rearrangement detected within *KIRREL3* in patient 18905640, and, therefore, in del11q syndrome.

6.2. Genetic Basis for Complex Pituitary Diseases

The diagnosis of a pathogenic chromosomal imbalance or gene defect provides an explanation for the clinical symptoms of the patient, and potentially allows a more detailed prognosis and follow-up, as well as improved genetic counselling and definition of recurrence risks, benefiting the patients and their families.

The high resolution 250K SNP array allows a high resolution screening of CN changes of the whole genome, and more precise breakpoint mapping by using the SNP positions, which has the potential to detect submicroscopic CNVs and distinguish subtle phenotypic heterogeneity at a molecular level. [184] However, the uneven SNP coverage leads to variability in the scale of accuracy of breakpoint definition. In the author's experience breakpoint intervals, mapped by SNP position, have been found to be as large as 100-200 kb. Defining the size of a CNV by taking into consideration only the adjacent SNPs present in CN state different from 2 could increase specificity, while, on the contrary, including the flanking SNPs in CN state 2 as part of the CNV would increase sensitivity. In the current study, the first approach was generally preferred, in order to avoid the potential inclusion in a CNV of genes not covered by SNPs in the 250K Sty1 SNP array (e.g. chromosome 1p36.33 interstitial deletion in patient 5608; data presented in paragraph 4.8.3.) However, it is acknowledged that this approach

might have led to the loss of information pertaining an individual CNV, and exceptions were applied when the inclusion of the first flanking SNPs in CN 2 in the definition of the CNV did not influence the definition of the gene content (e.g. chromosome 22q12.3 interstitial deletion in patient 18905640; data presented in paragraph 4.8.1.).

In the course of this study, the assessment of the content of each CNV has been limited to coding genes, while the presence of regulatory sequences, within the region of genomic imbalance, was not specifically investigated. This approach poses limitations to the identification of pathologic genomic imbalances. However, complex pathology of the pituitary gland was investigated in this study under the hypothesis that genomic imbalances of multiple genes, in a contiguous gene syndrome, are likely to underlie complex clinical phenotypes. [181, 207]

A submicroscopic CNV in the chromosome region 1p36.33 was finely mapped and investigated as a potential candidate region for pathology in one patient, 5608, affetced by hypopituitarism and ToF.

6.2.1. Assessment of CNV Genomic Loci in Patients with Hypopituitarism and Tetralogy of Fallot

The revision of the database of endocrinological patients of the Great Ormond Street Hospital highlighted the recurrent association of hypopituitarism and ToF in six patients. Patient 5859, who unfortunately died at the age of 10 years, carried a large inverted duplication of chromosome 5q11.2-q22, patient 5066, on the basis of the revision of his clinical record, was referred for further molecular cytogenetic investigations with a suggested diagnosis of Kallmann syndrome. It could be argued that ToF represents the highest end of a spectrum of severity of CHD associated with pathology of the pituitary gland. However, ToF is a clinically and embryologically distinct cardiac malformation, [252, 253] and its incidence in the database of endocrinological patients was 1/292 versus 1/2500 in the general population. On these bases, the remaining four patients, presenting with this recurrent association, were included in the genome-wide copy number screening with the 250K SNP array platform. One pathogenic deletion of chromosome 22q11.21, and one genomic imbalance of chromosome 1p36.33 were identified. Although seemingly clinically

homogeneous this small group of six patients appeared to be genetically highly heterogeneous.

By means of high resolution CN change screening, patient 5135 was found to carry a 3 Mb deletion of the genomic region 22q11.21, with breakpoints that coincided with the LCR22s that flank and facilitate the recurrent 22q11.2 microdeletion.

Variable degrees of impairment of the function of the pituitary gland are a known feature of del22q11.21 syndrome. Amongst children between the ages of 1 and 15 years, with del22q11.2 syndrome, 41% showed a stature below the 5th percentile. Of them, 4 had a height significantly below the 5th percentile and low levels of IGF1 and IGFBP3. In three patients, GHD was confirmed and pituitary gland hypoplasia was documented at the MRI; two patients responded well to GH replacement therapy. [254] Hypoplastic pituitary gland was also observed amongst the CNS abnormalities in a cohort of 250 individuals (48% male and 52% female) with 22q11.2 deletion syndrome. [255] In a separate study, hypothyroidism was reported in 20% of adult patients with 22q11.2 deletion. [256]

Point mutations, leading to haploinsufficiency, of the gene *TBX1* (chromosome band 22q11.21) have been detected in individuals with a clinical phenotype overlapping the one of del22q11.21 syndrome, but without a chromosome deletion. Mutations in *TBX1* were aetiologically correlated to the physical anomalies in 22q11.21 deletion syndrome, while they did not seem to account for the CNS manifestations. [257, 258] According to the DGV, the 22q11.21 chromosome region is highly polymorphic, and a high number of CNVs overlapping the 22q11.21 deletion in patient 5135 was recorded. This observation could provide further evidence that only a few other genes, apart from *TBX1*, are involved in the pathogenesis of del22q11.21 syndrome. No candidate gene for the pathology of the pituitary gland has yet been identified in the chromosome region 22q11.21. Equally, there are no known genes involved in DI, or in the pathology of the anterior pituitary gland, in the whole of chromosome 22. The only instance of the association between DI and a genomic imbalance of chromosome 22q was the clinical report of a two-year-old female patient with 22q13.31 deletion syndrome, who presented with a complex phenotype including central DI, that was diagnosed at the age of 2 days and resolved at the age of 27 months. [259]

It has been demonstrated that the size of the 22q11.2 deletion remains unchanged during parent-to-child transmission, even though a great inter- and intrafamilial clinical variability is observed, making the genotype-phenotype correlation difficult. [260]

Patient 5135 harbours the common ~3 Mb deletion of 22q11.21; while hypothyroidism has been described in ~20% of patients with a similar genotype, the occurrence of DI had never been reported before. These findings contribute to the notion that a novel gene, potentially responsible for pathology of both the anterior and posterior pituitary gland, is localised in the genomic region 22q11.21.

Greenway et al. (2009) identified 10 genomic loci holding CNVs in subjects with non-syndromic ToF; the genomic positions in their study were based on the NCBI build 36.1. Recurrent CNVs were found at four loci: 1q21.1, 3p25.1, 7p21.3 and 22q11.2. CNVs at chromosome 1q21.1 were the most frequent, with a total of 4 duplications and 1 deletion, accounting for 1% of non-syndromic cases of ToF investigated. At six further loci, individual CNVs were detected, including one duplication in the chromosome region 4q22.1 that was absent in 2,265 controls. [261]

In patient 4997, in the present screening with 250K Sty1 SNP array, an unique genomic gain (CN 3) in chromosome 4q22.1 was identified that overlapped with the one detected by Greenway et al. (2009), and that was deemed to be pathogenic in their patient with isolated ToF. Greenway et al. (2009) identified a candidate gene for the ToF phenotype within the chromosome region 4q22.1: protein phosphatase, PP2C domain-containing, 1K (*PPM1K*), that encodes a phosphatase expressed in human right ventricular outflow tract tissues. [261] The same gene fell inside the region of genomic imbalance, and was therefore found to be duplicated, in patient 4997. Patient 4997 presented with a complex clinical phenotype of growth deficiency and bilateral cryptorchidism, severe DD, microphthalmia, bilateral cleft lip and palate, multiple hemi- and butterfly vertebrae, bilateral renal dysplasia and urethral multiplication, while echocardiography excluded the presence of CHD.

Although the findings from both studies derive from one patient only and do not provide conclusive evidence on the role of 4q22.1 microduplication in abnormal phenotypes, the severity of the clinical phenotype presented by patient 4997, and, at the same time, the lack of cardiac pathology, question the interpretation of the CNV in chromosome 4q22.1 as pathogenic in isolated ToF. These results caution against relying strictly on evidence of disease-derived CNVs and underscore the importance of genotype-phenotype correlation. An alternative explanation to the one proposed by Greenway et al. (2009) is that the microduplication of 4q22.1 constitutes a very rare genomic polymorphism.

6.2.2. SNP Mapping Array Assay in Monosomy 1p36

An interstitial deletion of chromosome region 1p36.33 was identified, by high resolution CN screening on 250K SNP array platform, in a patient who presented with features of monosomy 1p36 syndrome. Patient 5608 had SOD with midline clefting, coloboma of the optic nerve, associated with aplasia of the retina and ensuing severe visual impairment including myopia and visual inattentiveness. Instances have been reported in the literature of patients with 1p36 deletions and intracranial midline defects, including a 3-year-old girl in whom the MRI of the brain revealed periventricular nodular heterotopia and truncation of the rostrum of the corpus callosum, [262] and an 8-month-old girl with microcephaly in whom a brain MRI showed the presence of a midline malformation consisting of agenesis of the anterior commissure and rostral corpus callosum and partial agenesis of the septum pellucidum. [263] Coloboma of the optic nerve has also been reported in a minority of patients. [230] Interestingly, these structural defects of the CNS overlap with the ones observed in patient 5608 and are part of the SOD spectrum. Patient 5608 was diagnosed with CPHD, including TSH deficiency, and precocious puberty. In a cohort of patients with 1p36 deletion syndrome, 20% of patients were found to be affected by hypothyroidism. However, high levels of TSH were detected, implying a different nature (primary) of the hypothyroidism compared to patient 5608 (central). [231] Only a few patients reported in the literature were assessed for signs of precocious puberty. In a very small group of three patients, 2/3 (67%) cases of precocious puberty were identified. [228] Finally, patient 5608 presented with a complex and severe CHD, fulfilling the diagnosis of ToF. CHD are commonly observed in 1p36 deletion syndrome (66-71% of patients), and vary greatly in degrees of severity and manifestations. ToF has been estimated to represent the fourth most common CHD in 1p36 deletion syndrome. [230]

The size of 1p36 deletions giving rise to symptoms of the 1p36 deletion syndrome has been found to vary widely from <0.5 Mb to >10 Mb, and there is no single common breakpoint location. Of all deletions, 40% have breakpoints that occur 3.0-5.0 Mb from the telomere, and 67% are true terminal deletions. A much lower percentage (~7%) are interstitial deletion, retaining the 1p subtelomeric region, or a derivative chromosome 1 in which the 1p telomere has been replaced by another chromosome end. In fact, 33% of

genomic imbalances in 1p36 deletion syndrome result from complex rearrangements. [228-230] A review of the molecular basis of monosomy 1p36 identified four classes of rearrangements with no single common breakpoint: apparently simple terminal truncations, derivative unbalanced translocations, interstitial deletions, and complex rearrangements. Complex rearrangements included deletions with interrupted inverted duplications, large duplications and triplications with small terminal deletions, or more than one interstitial deletion on a single chromosome with normal intervening sequence. [228-230] Moreover, D1Z2 probe, estimated to map within 300 kb of the end of the chromosome on 1pterp36.33 (manufacturer's data) and that binds to a distal 1p hypervariable repeated sequence, was found not to be deleted in all del1p36 patients. Patients not deleted for the D1Z2 probe were assumed to have an interstitial deletion, within 1p36.3, that preserved the more telomeric region of the chromosome. [228]

The monosomy of 1p36 chromosome region is considered to be a contiguous gene deletion disorder, deriving from haploinsufficiency of multiple genes. However, it has been observed that individuals with the smaller deletions of chromosome 1p36 can present with most of the features associated with the 1p36 deletion syndrome, and no clear genotype-phenotype correlation has been identified. [230] In an attempt to establish genotype-phenotype correlations in monosomy 1p36, Redon et al. (2005) applied array CGH, using an overlapping clone microarray covering 99.5% of the euchromatic portion of chromosome 1, to six patients with clinical features characteristic of monosomy 1p36. They identified two patients who displayed very similar clinical findings (DD and facial dysmorphic features), but who had non-overlapping 1p36 deletions. [264] The authors suggested that monosomy 1p36 syndrome might be due to a positional effect of the 1p36 rearrangement, rather than haploinsufficiency of contiguous genes in the deleted region, and stressed the importance of correlating the clinical phenotype to FISH and molecular results, in order to draw conclusions. [264]

Patient 5608 presented with most of the physical features characteristic of monosomy 1p36 (Table 29), and a deletion with a minimal size of 410 kb in the chromosome region 1p36.33 was detected on the 250K SNP array platform. FISH with standard probes showed hybridisation of probe p58 (CDC2L1/CDC2L2) on both chromosomes 1 in patient 5608. Probe p58 appeared to be deleted in all patients with monosomy 1p36 syndrome. [228] However, both duplications and deletions of the genomic locus where probe p58 (CDC2L1/CDC2L2) hybridises have been entered into the DGV as genomic

variants (Figure 17), and the observation that the genomic region 1p36.33 appears to be highly polymorphic might support the notion that rearrangements of the subtelomeric region of the short arm of chromosome 1 are indeed complex in a significant proportion of patients.

Rosenfeld et al. (2010) reported five individuals with 200-823 kb overlapping deletions of proximal 1p36.33. The genomic imbalances were ascertained with oligonucleotide-based microarray analysis in four patients, and by BAC-based array CGH in patient 5. Metaphase FISH confirmed a deletion in patients 1-4, while FISH experiments were not performed in patient 5. All patients presented with features consistent with the monosomy 1p36 phenotype, namely, DD, behavioural problems, seizures, hypotonia and facial dysmorphic features. [265] The details of the genomic imbalances detected in this cohort of 5 patients with monosomy 1p36 are reported in Table 32, and compared with the findings in patient 5608 from the present study.

	Rosenfeld et al. (2010) [265]					Present study
	Patient 1	**Patient 2**	**Patient 3**	**Patient 4**	**Patient 5**	**Patient 5608**
Telomeric breakpoint physical position	1,713,510	1,656,080	1,713,510		1,419,309	1,468,016
Chromosome 1p36 Critical Region	1,912,154			1,737,827		1,878,229
Centromeric breakpoint physical position		1,924,811	2,336,237	2,171,157	2,242,269	
Deletion size (kb)	199	269	623	433	823	410

Table 32. **Comparison of genomic imbalances detected in patients with monosomy 1p36 and patient 5608.** The coordinates of the genomic positions defining the imbalances were given according to the NCBI build 36.1. The smallest region of deletion overlap amongst the 5 patients reported by Rosenfeld et al. (2010) is framed in grey. [265]

The smallest region of deletion overlap amongst the 5 patients reported by Rosenfeld et al. (2010) was 174 kb, and contained five genes. [265] Characterisation of small

deletions is important in contiguous gene deletion syndromes for narrowing critical intervals, and for the identification of causative or candidate genes for a feature or features of the phenotype. The deletion in patient 5608 significantly overlapped with the critical region identified by Rosenfeld et al. (2010). The discrepancy between the results of 250K SNP array and standard FISH analysis in patient 5608 opens different possible scenarios for interpretation. The findings of a deletion in chromosome 1p36 in patient 5608 could represent a false positive, or indeed the lack of SNP coverage on the 250K Sty1 array platform could have prevented the recognition of a complex rearrangement of chromosome region 1p36.33 in patient 5608, reflected in the hybridisation of the FISH probe in the region not covered by SNPs. Detection of smaller CNVs increases the interpretational challenge of distinguishing pathogenic CNVs from polymorphic ones, the incidence of which is ubiquitous and inversely proportional to size. [266]

In patients with clinical features of monosomy 1p36 and no genomic imbalances detected by FISH with standard probes, a targeted FISH approach with additional probes might be necessary to characterise interstitial deletions and/or complex rearrangements of the 1p36 genomic region. [228, 229] It is acknowledged that such approach could have been valuable also in understanding the nature and impact of the 1p36.33 genomic imbalance in patient 5608. Equally, the complexity in interpreting the results warrants the testing of parental samples and controls on the same, or comparable, SNP array platform.

6.3. Availability of Clinical and Genetic Data and Clinical Pre-Selection of Patients

In the database of endocrinological patients, the majority of records (1,168 index cases) carried sufficient clinical and genetic information to achieve a subdivision in primary diagnostic categories, and to allow a separation between patients who presented with a complex clinical phenotype and patients with an isolated pathology of the pituitary gland. The first group of patients included the candidates for the high resolution

genome-wide copy number change screening, the second group included the patients chosen for mutation analysis in the genes *BARX2*.

However, the quantity and quality of information available in the database for each patient varied significantly. The patient pro-forma was designed by the author with the aim of resolving this issue, and collecting a standardised and detailed description of the phenotype of each patient included in the screening. The availability of anamnestic and clinical data is crucial to the interpretation of the genetic findings, and will increase the diagnostic and analytical power of molecular genetic testing, and can be pivotal in addressing further screening and testing, as well as the clinical management and follow-up of patients. Similarly, the lack of clinical and anamnestic data can prevent high throughput techniques from reaching their full potential. The patient pro-forma has proven to be a valid instrument to link the clinical and genetic data when, logistically (e.g. geographic distance), a direct assessment of the patient/s was not possible.

In two instances, in the course of this project, the lack of availability of a medical history and/or of a follow-up have impacted on the efficacy of a genotype-phenotype correlation study. Both patient 5907 and her father (6334) carry the same sequence variant of *BARX2*; the absence of clinical information regarding individual 6334 prevented from establishing the segregation of the mutation with the clinical phenotype. In patient 4754, an interstitial deletion of chromosome 9q34.11 was detected that encompassed the whole of *ENG* gene. The patient was lost at follow-up and it was not possible to ascertain whether, at the age of 22 years, he showed signs of HHT1, and therefore to gain further insights into the potential role of the genomic imbalance into the etiopathogenesis of his complex clinical phenotype.

De Vries et al. (2005) observed that submicroscopic chromosome imbalances could be identified in 20% of patients with MR-MCA in a screening by array CGH, and stated that this detection rate reflected the improvement obtained by a pre-selection of patients, based on a careful clinical assessment of the MR-MCA phenotype, as well as additional symptoms, such as facial dysmorphic features and/or growth abnormalities. [178] On the contrary, the use of genome-wide array CGH in an unselected sample of patients was deemed likely to have a lower yield of micro-deletions/duplications. [178] Clinically pre-selected patients were include in the present genome-wide copy number change screening with high resolution 250K Sty1 SNP mapping array. The choice of patients was based on the evaluation of the clinical records in the database of

endocrinological patients, organised into diagnostic categories, and the application of a selection criteria checklist designed by the author for this project.

A criteria checklist for the clinical pre-selection of patients was first proposed to improve the study of the subtelomeric regions of the chromosomes with FISH probes. [171] It was constructed as a five item checklist comprising of: pre- and/or postnatal onset growth abnormalities, presence of at least two facial dysmorphic features, one or more non-facial dysmorphic feature and/or congenital abnormality, and family history of MR. [171] Subsequently, screenings carried out with array CGH were targeted at patients clinically pre-selected on the basis of similar and/or additional inclusion criteria, namely, behavioural problems, seizures, and clinical or radiological evidence of brain, trunk or limb anomalies. [206, 207] The checklist developed for the present study widened the spectrum of risk factors associated with the patient's family history (i.e. multiple miscarriages, similar or different congenital malformation/s in a close relative) that suggest the presence of a chromosome rearrangement, and took into consideration both inclusion and exclusion (i.e. parental consanguinity) criteria. Differently from previously proposed checklists, the list of selection criteria utilised in the current project included the presence of either a known apparently balanced chromosome translocation, that could be associated with cryptic rearrangements, [145, 147] or a recognised monogenic disease that, when present within a more complex clinical phenotype and associated with an endocrinological disorder, could potentially lead to the identification of a novel genomic locus for pathology of the pituitary gland.

6.4. Multiple CNVs Interpretational Challenge

Because of its high coverage of the human genome, the 250K Sty1 SNP array platform detected multiple CNVs across the whole genome of all patients investigated; in the great majority of cases these CNVs would represent genomic polymorphisms. The large extent of CNVs represents a background noise in the output of high resolution genome-wide genotyping arrays, and arguably it constitutes its major technical and interpretational challenge. [132, 176] Structural variants of DNA defined as CNVs

range in size between 1 kb and, usually, ~3 Mb. Typically, large-size CNVs (e.g. single BAC clone) were uncovered by array CGH, while smaller ones have been detected through SNP genotyping. [109, 132, 267] In the present study, 3857 CNVs were identified in the target cohort of 10 patients; one CNV with size of 3 Mb and two CNVs with a size of 10 Mb were demonstrated to be causal of the pathological phenotype of the patient.

Redon et al. (2006) released the first map of CNVs with size equal or larger than 1 kb in the human genome. They investigated genome-wide characteristics of CNVs in samples from four HapMap populations, utilising two platforms: Affymetrix GeneChip 500K Mapping array, and CGH with a whole genome tilepath (WGTP) array that comprised 26,574 large-insert clones representing 93.7% of the euchromatic portion of the human genome; two distinct relevant algorithms were applied. [109] The WGTP platform showed overestimation of CNV boundaries, as a CNV encompassing only a fraction of a clone would be reported as if the whole clone was involved. The average number of CNVs detected per sample was 24 for the 500K platform, and the mean size was 206 kb. Forty-three percent of all CNVs identified on one platform were replicated on the other, and approximately half of the CNVs were called in more than one individual. [109] Approximately equal numbers of deletions and duplications were identified on the WGTP platform, whereas deletions outnumbered duplications by approximately 2:1 on the 500K platform. Over half (58%) of the detected CNVs overlapped known genes, including known disease-related loci, but a significantly lower proportion of deletions than duplications (identified on the 500K platform) overlapped with the OMIM database. Thus, deletions appeared to be biased away from genes with respect to duplications. [109] When only CNVs that were recognised independently by at least two different methods to extract CNV information from Affymetrix SNP array data were taken into consideration, the frequency of copy number gains was 2.3-fold greater than the one of deletions. [130] Moreover, clinical experience has suggested that deletions have a higher likelihood of being pathogenic than duplications. [111, 199] Gene content appears a more reliable indicator for clinical significance compared with CNV size, such that small, gene-rich CNVs are more likely to be pathogenic than larger, gene-poor CNVs. [111] The analytical workflow applied in the present study progressively and consistently reduced, in each phase, the ratio of genomic gains to genomic losses. At the same time, the cumulative percentages of unique CNVs per CN state demonstrated that CNVs in CN 1 tended to hold less genes than CNVs in CN 3.

Shaikh et al. (2009) identified and assessed the CNVs in 2026 individuals: 1320 Caucasians (65.2%), 694 African-Americans (34.2%), and 12 Asian-Americans (0.6%). Overall, they detected a total of 54,462 CNVs, with an average of 27 CNVs per individual (range 4-79). Collectively, these CNVs spanned ~19.4% of the human genome. A majority of the CNVs detected (77.8%) were observed in more than one unrelated individual. The authors attributed the high rate of non-unique CNVs at least in part to the large study cohort. In fact, the relationship between non-unique CNV detection rate and sample size approaches a plateau as more samples are surveyed. [268] Moreover, it has been suggested that using local reference samples conveys the lowest noise in the test-over-reference intensity ratios for all SNPs used to identify CNVs. [269] The results presented in this study have been obtained on a cohort of 10 patients only assessed by genome-wide CN change screening of unpaired DNA samples, utilising a reference set built from data available from the HapMap collection. Increasing the number of tested DNA samples and introducing a group of controls would improve the extrapolation and inference of data regarding the pathogenic versus polymorphic nature of detected CNVs, allow to expand the local database of polymorphic CNVs, and, therefore, diminish the number of unique CNVs with gene content requiring individual risk assessment.

The challenge of interpreting vast amounts of information delivered by high resolution genome-wide CN screening techniques is particularly demanding in clinical diagnostic settings. It has been suggested that CNVs should be categorised into: clearly or likely to be pathogenic, likely to be benign, and of unknown clinical significance. [111] For CNVs that are initially catalogued as 'of unknown clinical significance', the availability of parental DNA samples can determine the origin, inherited versus *de novo*, of the CNV. A CNV that has been inherited from an unaffected parent is considered unlikely to be pathogenic, whereas a CNV that occurred de novo is considered more likely to be causally related to the patient's phenotype. However, exceptions could be found to this model, e.g. unmasked recessive mutations, imprinted genes and X-linked inheritance. [197] It has been argued that genome-wide testing is unwarranted when it is foreknown that parental samples will not be available for follow-up studies. [111] However, during the course of the presented project, the chromosome deletion 22q11.21 was identified in patient 5135, that represents an instance of a well characterised genomic microdeletion syndrome. The genomic imbalance was independently confirmed by FISH. Therefore,

genome-wide CN change screening on SNP array platform would retain the potential for identifying imbalances, that overlap critical regions of well-defined genomic disorders, for patients whose biological parents' DNA samples might not be available. The diagnosis would be beneficial to the clinical management and follow-up of the patient, and the replacement of sequential locus-specific testing for microdeletion and microduplication syndromes with genome-wide SNP array analysis has been proposed. [266] Moreover, even the knowledge that a CNV is inherited should be tempered with consideration of issues such as mosaicism, incomplete penetrance and variable expression. Also, apparently inherited CNVs may have different breakpoints, that would result in different functions or phenotypes in an affected child and healthy parents. [111]

Unique CNVs in one individual can be further assessed by cross-reference to catalogues of CNVs found in healthy (e.g. DGV) as well as affected (e.g. DECIPHER) individuals. However, the information related to a number of entries in the DGV are derived from CNV screening projects that used a single platform and were not validated, and lack precise breakpoint information. This raises issues regarding the reproducibility of those data. Moreover, considering age-dependent and incomplete penetrance disorders, it is possible that the lack of a clinical phenotype does not mirror the lack of presence of risk-alleles. [111] Similarly, the significance of a cross-reference to the catalogue of CNVs included in the database DECIPHER can be affected by the use of lower resolution platforms (like BAC-based array CGH) to generate the data, and, crucially, by the quantity and quality of clinical information available. [268] In the course of the presented study, in particular, the specificity of matches to phenotypes entered into the DECIPHER database needed to be thoroughly scrutinised, as information regarding the anatomy and function of the hypothalamus-pituitary gland axis are very rarely available or commented on. Therefore, the reference to the database DECIPHER was only utilised to evaluate supporting evidence of the pathogenicity of CNVs that had already been assessed within the decisional workflow.

6.5. Comparison of Analytical Workflow for Interpretation of CNV Significance

The workflow designed for the present study is compared to the ones proposed in three studies published in the literature. Gijsbers et al. (2009) suggested a novel diagnostic workflow for all (unselected) MR-MCA patients by first analysing every patient with high-density SNP array instead of conventional karyotyping. The SNP array approach should make targeted FISH and multiplex ligation-dependent probe amplification (MLPA) analysis redundant, and therefore the patient assessment workflow less time-consuming and more cost-effective. [181] Similarly, Bruno et al. (2009), presenting the first study describing the use of Affymetrix 250K Nsp1 SNP array for detection of pathogenic CNVs, aimed at investigating replacement of time-consuming, sequential locus-specific targeted testing for specific microdeletion and microduplication syndromes, using FISH or quantitative DNA tests, with genome screening using SNP array analysis, thus also improving the diagnostic yield in clinically pre-selected patients with DD-MCA. [266] Greenway et al. (2009) assessed the performance of high-resolution Affymetrix 6.0 array in detecting pathogenic CNVs in a cohort of patients affected by non-syndromic ToF. The results defined a minimum estimate of 10% of sporadic non-syndromic ToF cases resulting from de novo CNVs, however, this frequency was lower than the 25%-30% rate of de novo genomic imbalances observed in individuals with syndromic CHD. [261] A summary of the layout of each study is presented in Table 33, and compared with the one of the current project.

Affymetrix mapping array platform	**Software**	**Number of patients**	**Phenotype**	**CNV exclusion criteria**	**Mean CNVs /sample**	**Ref.**
250K Sty1	CNAT 4.0 Microsoft Excel	10	Pathology of pituitary gland	<2 adjacent SNPs	386	Present Study
250K Nsp1 250K Sty1^	CNAG 2.0	124	MR-MCA	CN 1: <5 adjacent SNPs or <150 kb; CN 3: <7 adjacent SNPs or <200 kb	3	[181]
250K Nsp1	CNAG 3.0 Microsoft Excel	117	MR-MCA	<7-10 adjacent SNPs with log2 ratio <-0.3 (CN 1) or >+0.3 (CN 3)*	4	[266]
6.0	Birdseye [270]	121	Non-syndromic ToF	CNV <20 kb	14#	[261]

Table 33. **Comparison of the layout of screenings of CNVs with SNP array.** ^Two different SNP array platforms were used in this study, only results relevant to the Affymetrix GeneChip 250K Nsp1 and 250K Sty1 arrays are taken into account; *7 SNPs for experiments with SD up to 0.20 and 10 SNPs for experiments with SD >0.20<0.26; #Chromosome X was excluded from the analysis. CN: Copy Number; MCA: Multiple Congenital Anomalies; MR: Mental Retardation; ToF: Tetralogy of Fallot; Ref.: Reference. CNAG: Copy Number Analyser for GeneChip. [271]

In all three referenced studies, exclusion criteria were applied in the phase of determining the operational definition of CNV. This conservative approach was adopted in order to minimise the number of false positive findings, and increase specificity. In the present study, no exclusion criteria were selected, in order to favour the sensitivity

of the test and minimise the risk of losing viable information about potentially clinically relevant CNVs, allowing the maximum flexibility in the further stages of the decisional process workflow.

The decisional processes for the screening of multiple CNVs, applied in the present and previous studies, are summarised in their 3 basic steps in Table 34. Each step corresponds to the removal of a number of CNVs from the total pool, based on the relevant criteria applied within each workflow.

	Present study	**[181]**	**[266]**	**[261]**
STEP 1	CNVs non-unique in the cohort of patients under study	CNVs present in the DGV and/or in-house reference set of 60 controls	CNVs present in the DGV and/or UCSC genome browser	Inherited CNVs
STEP 2	CNVs with no gene content	CNVs with no gene content	CNVs with no gene content	CNVs found in 2,265 control samples and/or reported in the literature [114]
STEP 3	CNVs with low pathogenic-risk	Inherited CNVs	CNVs with low pathogenic-risk	CNVs in individuals with CNV excess compared to the mean of the whole cohort

Table 34. **Three basic steps of the decisional process for the screening of multiple CNVs.** Each step indicates what class of CNVs were removed from the total pool, based on the relevant criteria applied at the corresponding stage within each decisional workflow.

Gijsbers et al. (2009) removed CNVs entered in the DGV and in their in-house reference set of 60 controls, when present in at least 3 individuals. [181] However, they did not define the criteria to establish an overlap between CNVs. Greenway et al. (2009) removed from the pool of potentially pathogenic CNVs, CNVs that shared at least 50%

overlap with 0.1% or more of control samples, as well as CNVs that matched previous reports in the literature. [261] The removal of CNVs shared across the cohort of 10 patients in the present study constituted the first step in the decisional workflow, and a CNV was defined as *shared* when it fulfilled stringent criteria.

The choice of utilising the presence in the DGV (and/or other genomic structural variant databases) as the sole criteria to catalogue CNVs as polymorphic can also be argued against. The information included in the DGV and similar databases need to be tempered with the knowledge and consideration of the following issues. The polymorphic genomic structural variants, and ensuing precision of breakpoint definition, can originate from lower resolution array platforms, such as array CGH platforms that contain large-insert BAC clones, which are on the order of 150 kb in size. Empirically, a significant copy number ratio change can be noted when a clone has gained or lost a copy of 25%-30% of its unique DNA sequences. This can lead to the potentially erroneous assumption that a CNV identified by a given clone on an array platform is the same CNV in another individual when identified by overlapping genomic sequence/s on another platform. [111] The population frequency of a previously reported CNV entered into databases and online catalogues can often be related to one individual only, and, crucially, the phenotypic characteristics of the comparison population often remain uncertain or unknown. [199] Therefore, it has been suggested that caution should be exercised when relying heavily on such databases like DGV to interpret the clinical significance of a CNV. This holds true especially for CNVs that have been reported only in a single individual. [111] Bruno et al. (2009) documented that polymorphisms described in the DGV accounted for 73% of the CNVs identified in their cohort, and they ruled out all the relevant CNVs in the first stage of the workflow. [266] The comparison with the DGV was used only in phase 3 of the workflow proposed in this study, during the risk assessment of CNVs, and did not represent an exclusion criteria alone. About 34% of unique CNVs with gene content overlapped with documented polymorphisms described in the DGV, and more than half (~57%) of unique CNVs with gene content overlapped at least partly (or fully) with genomic imbalances reported in the DGV. In the third and last phase of the decisional workflow, this criteria, if utilised alone, would have removed from further investigation only 3% of the total of CNVs initially identified, compared to the figure of 73% of CNVs excluded by Bruno et al. (2009) in the first stage of their workflow. [266]

The approach chosen for the present study was, instead, the creation in the first phase of the decisional workflow of a database of all non-unique CNVs detected, by

comparative analysis, in the cohort of patients derived from the database of endocrinological patients. This approach had the advantages of allowing to set stringent criteria for the definition of *shared* CNVs, and controlling the anamnestic and clinical data of all the individuals in whom the CNVs were detected. This method has been validated by subsequent observations that it minimises the potential of false positives due to platform-specific artefacts. [111, 268]

6.6. Genotype-Phenotype Correlation of *BARX2* Mutations

BARX2 was identified as a potential candidate gene for pathology of the pituitary gland following a bioinformatic prediction. Although the output of a bioinformatic prediction using Gene Sorter can be biased by the amount of information entered in the relevant databases, the calculation returned *BARX2* as the only gene fulfilling the input criteria.
A novel heterozygous A94T missense mutation was identified in exon 2 of *BARX2* in one patient (5907) who presented with a clinical phenotype comprising of panhypopituitarism and ectopic posterior pituitary gland. The amino acid change was not found in any other patient in the cohort under study, nor in any patient or control tested in previous screenings, [242, 243] but was present in the father of the proband.

In mice, the loss of *Barx2* appeared to cause a defect in the initiation and progression of hair follicle remodelling. [272] The *Barx2*-null mouse pups showed a minimal phenotype, they could be distinguished from the wild type pups only by their short whiskers, and about half were born with open eyelids. Later in life, adult mice had shorter hair than wild type mice. The heterozygous pups and adults appeared identical to the wild type animals. [272] However, expression studies of *Barx2* revealed a prominent activity throughout the development of the pituitary gland and associated structures. Early developmental expression of *Barx2* has been reported for embryonic day 9.5 (E9.5) to E12.5. [273] Localisation studies showed that expression of *Barx1* and *Barx2* overlap in the nervous system, particularly in the telencephalon, spinal cord and dorsal root ganglia. *Barx2* was also prominently expressed in the floor plate of the

midbrain. During craniofacial development *Barx1* and *Barx2* showed complementary patterns of expression whereas *Barx1* appeared in the mesenchime of the mandibular and maxillary processes, *Barx2* was observed in the ectodermal lining of the same tissues. [273] From E12.5, intense expression of *Barx2* was documented in the developing anterior pituitary gland in a spatial distribution resembling that of *Pit1* (*POU1F1*). [273] High levels of *Barx2* were confirmed in the Rathke's pouch after E13.5 by *in situ* hybridisation. [272] Therefore, while expression data would support a role of *Barx2* in pituitary gland development in mouse, the *Barx2*-null mice do not show an impairment of the pituitary function. Given the overlap between the expression patterns of *Barx1* and *Barx2*, it is possible that a degree of functional redundancy plays a role in avoiding the development of a pathological phenotype in *Barx2*-null mice, demonstrating the difficulties in extrapolating information from one organism to another.

Mutation analysis of *BARX2* had not been carried out before in a cohort of patients with pathology of the pituitary gland, however, *BARX2* was suggested as a potential candidate for the craniofacial features of 11q deletion syndrome. [242, 243] Although outside of the functional homeodomain of the *BARX2* protein, the A94T change is the only mutation identified in the coding region of *BARX2* outside of the C-terminal exon 4. The A94T mutation is located in exon 2, proximal to the functional homeodomain, and within a relatively conserved amino acid sequence of the protein. Indeed, *BARX2* appears to be conserved amongst species. The genomic sequencing of the 72 patients under study identified two SNPs of *BARX2*, the nucleotide substitution c.574-5C>T in intron 3 and the P203P synonymous change in exon 4, in a total of 31 patients in concordant heterozygous or homozygous state, with allelic frequencies 0.271 and 0.285, respectively. These observations suggested linkage disequilibrium, and only two exceptions were recorded. The same observation was made in a separate study, where an allelic frequency of 0.280 was calculated for both the intronic and exonic SNP. [210] The frequency of one missense mutation of *BARX2* detected in the whole cohort of 72 screened patients would indicate that the gene does not play a prominent role in the etiopathogenesis of isolated hypopituitarism and defects of the anatomy of the pituitary gland. However, it remains possible that the mutation is causally related to the clinical phenotype of patient 5907. The lack of anamnestic and clinical information regarding the father of patient 5907 prevented a genotype-phenotype correlation, and, in the absence of these information, functional studies of the effects of the A94T variant

should be undertaken to clarify the potential etiopathogenic role of *BARX2* mutation in pathology of the pituitary gland.

6.7. Genotype-Phenotype Correlation of *OTX2* Mutations

Patients have been reported in the literature with deletions of the long arm of chromosome 14 overlapping the genomic loci of *OTX2* and *BMP4*; a summary of the genotype-phenotype correlation of these genomic imbalances is presented in Table 35.

Chromosome deletion	**Sex**	**Age**	**Endocrine/pituitary phenotype**	**Other symptoms**	**Ref.**
del(14)(q22q23)	F	21 w (ga)	hypoplastic pituitary gland and stalk	bilateral anophthalmia, small cerebellum, hypoplastic kidneys	[274]
del(14)(q22.1q22.3)	M	4 y	growth deficiency, hypogonadism (bilateral cryptorchidism, micropenis), central hypothyroidism, suspected hypopituitarism	bilateral anophthalmia, DD, facial dysmorphic features	[275]

del(14)(q22.1q23.2)	F	21 m	small sella turcica, hypoplastic pituitary gland	bilateral anophthalmia, craniosynostosis, cervical vertebral anomalies, absent left auditory canal, facial asymmetry, microretrognathia, DD, cortical atrophy, hypotonia	[276]
del(14)(q22q23)	familial		- (normal anatomy of the pituitary gland)	uni- or bilateral anophthalmia, polydactyly	[277]
del(14)(q22q23)	M	5 y	hypoplastic pituitary gland, bilateral cryptorchidism	anophthalmia, DD, hypotonia, hearing loss, facial dysmorphic features, syndactyly	[278]
del(14)(q22.3q23.2)	F	n.r.	hypothyroidism	bilateral anophthalmia, partial ACC, DD	[247]

del(14)(q22.2q23.1)	M	7 y	APH, posterior pituitary not visualised, growth hormone deficiency, hypogonadism (bilateral cryptorchidism), neonatal hypoglycaemia	bilateral anophthalmia, partial ACC, severe DD, epilepsy, sleep disturbances, cerebellar vermis hypoplasia, microcephaly, hypotonia, mixed (conductive and sensorineural) hearing loss, recurrent otitis media, gastro-oesophageal reflux, scoliosis, high palate, bifid uvula, minor facial dysmorphic features	Patient 6137 and [247]
del(14)(q22.1q22.3)	F	1 y	- (normal anatomy of the pituitary gland)	bilateral congenital corneal opacity, DD, hypotonia, bilateral polysyndactyly	[279]

Table 35. **Genotype-phenotype correlation of 14(q22q23) genomic imbalances.** The endocrinological and/or pituitary phenotype and a summary of the other symptoms observed in each case are included. ACC: Agenesis of Corpus Callosum; APH: Anterior Pituitary Hypoplasia; DD: Developmental Delay; F: Female; M: Male; m: month/s; w: week/s; y: year/s; ga: gestational age (of foetus after premature termination of pregnancy); -: not present (the anatomy of the pituitary gland was investigated with brain MRI); n.r.: not reported. Ref.: Reference. Patient 6137 was included in the database of endocrinological patients under study.

The clinical phenotype associated with deletions of the chromosome region 14q22-q23 comprises of pathology of the eyes, CNS (particularly, DD, cerebellar hypoplasia, and hypotonia), digits, kidneys, as well as hearing loss and facial dysmorphic features. Hypopituitarism and anomalies of the anatomy of the pituitary gland have been

reported in most instances. Haploinsufficiency of genes, mapped within the chromosome region, was suggested as the likeliest mechanism of pathology. Four genes in particular were considered candidates, the hemizygous deletion of which could account for the clinical phenotype: *BMP4*, *OTX2*, *SIX1* and *SIX6*. [247, 278] In the present study, genomic sequencing of *BMP4* and *OTX2* was carried out in the same cohort of 35 patients with variable degree and manifestations of pathology of the pituitary gland, associated with defects of eyes, brain, kidneys and digits. The choice of the clinical phenotypes reflected the complex array of symptoms detected in patients with deletions of the chromosome region 14q22q23.

A novel heterozygous nonsense mutation, E79X, was identified in exon 4 of *OTX2* in a patient, 5976, with a bilateral severe eye defect in the spectrum of anophthalmia-microphthalmia, structural abnormalities of the pituitary gland and CPHD. The mutation lies within the homeodomain of the protein.

Twenty-five different heterozygous mutations of *OTX2* had been documented in previous studies, and are listed in Table 36, with a summary of the associated clinical phenotype and indication of their origin. [37, 38, 40, 280-286]

DNA mutation	**Protein mutation**	**Eye**	**Pituitary**	**Other**	**Origin**	**Ref.**
c.81delC	p.S28PfsX52	Mp	n.r.		p.m.	[37]
c.93C>G	p.Y31X	Mp	n.r.		De novo	[282]
c.106dupC	p.R36PfsX87	Mp	-		n.r.	[282]
c.117delCC	p.R39fsX86	Ap	-	DD	Mat. (healthy)	[37]
c.136dupA	p.T46NfsX84	Mp	-	Microcephaly, anteriorly placed anus	Pat.	[285]
c.214_217 delGCAC insCA	p.A72fsX86	Mp	-		n.r.	[280]
c.221_236 del16	p.K74fsX103	Mp/Ap	IGHD, APH, EPP	DD	n.r.	[280]

c.235G>T	p.E79X	Mp/Ap	CPHD, structural defects		De novo	5976
c.265C>G	p.R89G	Mp	-		De novo	[37]
c.265C>T	p.R89X	Ap	-		De novo	[286]
c.270A>T	p.R90S	Ap	IGHD, APH, EPP	DD	Pat.	[283]
c.289C>T	p.Q97X	Mp	n.r.		Pat.	[282]
c.295C>T	p.Q99X	Ap	n.r.		Pat. (healthy)	[37]
c.313C>T	p.Q105X	Ap	-	DD	De novo	[285]
c.371_372 delAG	p.E124EfsX135	Ap	n.r.	DD	Mat.	[282]
c.397C>A	p.P133T	Ap	n.r.		Pat. (healthy)	[37]
c.400C>G	p.P134A	Ap	n.r.	DD	De novo	[37]
c.402insC	p.L135fsX136	Ap	IGHD	DD, CP	De novo	[281]
c.405_406 insCT	p.S136fsX178	Ap	CPHD, APH, EPP	DD, Chiari defect	De novo	[38]
c.413C>G	p.S138X	RD	IGHD		De novo	[284]
c.456_457 delGAinsAT	p.W152X	Mp/Ap	CPHD	DD, microcephaly	De novo	[285]
c.464insGC	p.A155fsX177	Ap	-	DD, ACC	De novo	[37]
c.537T>A	p.Y179X	Mp	n.r.	DD	p.m.	[37]
c.553_556 dupTATA	p.S186IfsX187	Mp	APH, absent posterior pituitary	DD, microcephaly	De novo	[285]
c.562G>T	p.G188X	Mp	CPHD, APH, EPP	DD, seizures	n.r.	[280]

c.674A>G	p.N225S	-	CPHD, APH, EPP		n.r.	[40]

Table 36. **Heterozygous mutations in the *OTX2* gene.** The novel mutation identified in this study is highlighted in grey. Mp: microphthalmia; Ap: anophthalmia; RD: Retinal Dystrophy. APH: Anterior Pituitary Hypoplasia; CPHD: Combined Pituitary Hormone Deficiency; EPP: Ectopic Posterior Pituitary; IGHD: Isolated Growth Hormone Deficiency. ACC: Agenesis of Corpus Callosum; CP: Cleft Palate; DD: Developmental Delay. Mat: Maternal; Pat: Paternal; p.m.: parental mosaicism; -: absent; n.r.: not reported. Ref: Reference.

Together with point mutations, whole gene deletions of *OTX2* and microdeletions involving its genomic locus have been reported that led to a similar phenotype with the association of pituitary and eye defects. [280, 282, 287] In the course of this study, no genomic imbalances in the chromosome region 14q23.1 were detected, by high resolution CN change profiling with the 250K SNP array platform, in patients who presented with the association of pituitary gland and eye pathology. In patient 6137, who presented with bilateral anophthalmia, pituitary hypoplasia and CPHD, within a more complex clinical phenotype, a de novo interstitial deletion of chromosome 14(q22.2q23.1) was detected by array CGH, after specific loci MLPA deletion/duplication screening, MLPA and FISH screening with probes for the subtelomeric regions of the chromosomes, and genomic sequencing of the coding regions of *SOX2* had failed to identify any genomic imbalance or mutation.

The ocular phenotype of patients with mutations in *OTX2* is variable in severity; microphthalmia-anophthalmia is the most common symptom, but at least one case of isolated early onset retinal dystrophy has been reported, [284] and familial studies have shown that the penetrance of *OTX2* mutations is not complete. [37, 282, 283] An individual mutation in *OTX2* was also reported in a patient with CPHD and no ocular phenotype. [40] Similarly, heterozygous mutations of *OTX2* are associated with variable degrees and manifestations of pathology of the pituitary gland, although GHD, pituitary hypoplasia and ectopic posterior pituitary seem to occur with increased frequency. [280] Furthermore, a percentage of patients, carrying either a point mutation or a whole gene deletion, exhibit additional features, mainly brain anomalies, seizures and DD.

The c.235G>T mutation of *OTX2* reported in this study inserts the third most premature truncation of the protein homeodomain described to date, p.E79X. All three amino acid residues (valine 84, lysine 87, and asparagine 88) belonging to the homeodomain, and that have been demonstrated to have a critical role in DNA binding, are ablated by the mutation. [39] Functional analysis showed that the p.G188X-OTX2 protein localised to the nucleus, as did the wild-type protein, whereas the p.K74fsX103-OTX2 and p.A72fsX86-OTX2 proteins were incapable of localising to the nucleus. Transactivation analysis demonstrated that the p.K74fsX103-OTX2 and p.A72fsX86-OTX2 proteins had virtually no transactivation function, while the p.G188X-OTX2 protein had reduced (~50%) transactivation activity. [280] These observations confirm the severity of the c.235G>T mutation, that leads to the truncation of the protein homeodomain as early as at the amino acid residue 79 and to a complete loss-of-function. [39, 280]

Only one *OTX2* mutation, the amino acid missense change N225S, has been reported to date to act via a dominant-negative effect. This mutation occurred in a patient with CPHD and no ocular phenotype. [40] Despite the severity of the E79X mutation, patient 5976 did not present with any clinical symptom outside the eye and pituitary spectrum. At present, no genotype-phenotype correlation has been established between heterozygous mutations of *OTX2* and variable pituitary and clinical phenotypes. [280] The lack of a genotype-phenotype correlation strengthens the need for continuous endocrine follow-up of affected patients, throughout childhood and adolescence, since the clinical course cannot be anticipated. [283] Finally, patients with IGHD or CPHD and ocular malformations, together with genetic analysis for classic transcription factor genes involved in pituitary development and pathology (e.g. *PROP1*, *POU1F1*, *HESX1*, *SOX2*) should be tested also for the presence of mutations in *OTX2*.

References

1) Kelberman D, Rizzoti K, Lovell-Badge R, Robinson IC, Dattani MT.
Genetic regulation of pituitary gland development in human and mouse.
Endocr Rev. 2009 Dec;30(7):790-829. Review.

2) Mehta A, Dattani MT.
Developmental disorders of the hypothalamus and pituitary gland associated with congenital hypopituitarism.
Best Pract Res Clin Endocrinol Metab. 2008 Feb;22(1):191-206.

3) Cheung CC, Lustig RH.
Pituitary development and physiology.
Pituitary. 2007;10(4):335-50.

4) Pelletier G, Robert F, Hardy J.
Identification of human anterior pituitary cells by immunoelectron microscopy.
J Clin Endocrinol Metab. 1978;46:534-542.

5) Nussey SS, Whitehead SA.
Endocrinology An Integrated Approach.
Taylor & Francis. 2001.

6) Carter-Su C, Schwartz J, Smit LS.
Molecular mechanism of growth hormone action.
Annu Rev Physiol. 1996;58:187-207.

7) Veldhuis JD, Roemmich JN, Richmond EJ, Rogol AD, Lovejoy JC, Sheffield-Moore M, Mauras N, Bowers CY.
Endocrine control of body composition in infancy, childhood, and puberty.
Endocr Rev. 2005 Feb;26(1):114-46.

8) McFarland KC, Sprengel R, Phillips HS, Köhler M, Rosemblit N, Nikolics K, Segaloff DL, Seeburg PH.

Lutropin-choriogonadotropin receptor: an unusual member of the G protein-coupled receptor family.
Science. 1989 Aug 4;245(4917):494-9.

9) Matsumoto AM, Karpas AE, Paulsen CA, Bremner WJ.
Reinitiation of sperm production in gonadotropin-suppressed normal men by administration of follicle-stimulating hormone.
J Clin Invest. 1983;72:1005-1015.

10) Adashi EY.
Endocrinology of the ovary.
Hum Reprod. 1994;9:815-827.

11) Gimpl G, Fahrenholz F.
The oxytocin receptor system: structure, function, and regulation.
Physiol Rev. 2001;81:629-683.

12) Alatzoglou KS, Dattani MT.
Genetic forms of hypopituitarism and their manifestation in the neonatal period.
Early Hum Dev. 2009 Nov;85(11):705-12. Review.

13) Mehta A, Hindmarsh PC, Mehta H, Turton JP, Russell-Eggitt I, Taylor D, Chong WK, Dattani MT.
Congenital hypopituitarism: clinical, molecular and neuroradiological correlates.
Clin Endocrinol (Oxf). 2009 Sep;71(3):376-82.

14) Kelberman D, Dattani MT.
The role of transcription factors implicated in anterior pituitary development in the aetiology of congenital hypopituitarism.
Ann Med. 2006;38(8):560-77. Review.

15) Larsen WJ.
Human Embryology 3rd Edition.
Elsevier. 2001.

16) Moore KL and Persaud TVN.
The Developing Human Clinically Oriented Embryology 7th Edition.
W.B. Saunders Company. 2003.

17) Solov'ev GS, Bogdanov AV, Panteleev SM, Yanin VL.
Embryonic morphogenesis of the human pituitary.
Neurosci Behav Physiol. 2008 Oct;38(8):829-33.

18) Bazina M, Stefanović V, Bozanić D, Saraga-Babić M.
Ultrastructural and immunohistochemical characteristics of developing human pituitary gland.
Acta Histochem. 2007;109(5):366-76.

19) Schmook MT, Brugger PC, Weber M, Kasprian G, Nemec S, Krampl-Bettelheim E, Prayer D.
Forebrain development in fetal MRI: evaluation of anatomical landmarks before gestational week 27.
Neuroradiology. 2010 Jun;52(6):495-504.

20) Cheung CC, Lustig RH.
Pituitary development and physiology.
Pituitary. 2007;10(4):335-50.

21) Parkin JM.
Incidence of growth hormone deficiency.
Arch Dis Child. 1974;49:904-5.

22) Vimpani GV, Vimpani AF, Lidgard GP, Cameron EH, FarquharJW.
Prevalence of severe growth hormone deficiency.
Br Med J. 1977;2:427-30.

23) Thomas M, Massa G, Craen M, de Zegher F, Bourguignon JP, Heinrichs C, De Schepper J, Du Caju M, Thiry-Counson G, Maes M.
Prevalence and demographic features of childhood growth hormone deficiency in Belgium during the period 1986-2001.

Eur J Endocrinol. 2004;151:67-72.

24) Phillips JA 3rd, Cogan JD.
Genetic basis of endocrine disease. 6. Molecular basis of familial human growth hormone deficiency.
J Clin Endocrinol Metab. 1994 Jan;78(1):11-6. Review.

25) Patel L, McNally RJ, Harrison E, Lloyd IC, Clayton PE.
Geographical distribution of optic nerve hypoplasia and septo-optic dysplasia in Northwest England.
J Pediatr. 2006;148:85-8.

26) Tornqvist K, Ericsson A, Kallen B.
Optic nerve hypoplasia: Risk factors and epidemiology.
Acta Ophthalmol Scand. 2002;80:300-4.

27) Dattani MT.
Growth hormone deficiency and combined pituitary hormone deficiency: does the genotype matter?
Clin Endocrinol. 2005 63, 121-30.

28) Romero CJ, Nesi-França S, Radovick S.
The molecular basis of hypopituitarism.
Trends Endocrinol Metab. 2009 Dec;20(10):506-16. Review.

29) Kelberman D, Dattani MT.
Genetics of septo-optic dysplasia.
Pituitary. 2007;10(4):393-407. Review.

30) Kelberman D, Dattani MT.
Septo-optic dysplasia - novel insights into the aetiology.
Horm Res. 2008;69(5):257-65. Review.

31) Thomas PQ, Dattani MT, Brickman JM, McNay D, Warne G, Zacharin M,

Cameron F, Hurst J, Woods K, Dunger D, Stanhope R, Forrest S, Robinson IC, Beddington RS.
Heterozygous HESX1 mutations associated with isolated congenital pituitary hypoplasia and septo-optic dysplasia.
Hum Mol Genet. 2001 Jan 1;10(1):39-45.

32) Sobrier ML, Netchine I, Heinrichs C, Thibaud N, Vié-Luton MP, Van Vliet G, Amselem S.
Alu-element insertion in the homeodomain of HESX1 and aplasia of the anterior pituitary.
Hum Mutat. 2005 May;25(5):503.

33) Sobrier ML, Maghnie M, Vié-Luton MP, Secco A, di Iorgi N, Lorini R, Amselem S.
Novel HESX1 mutations associated with a life-threatening neonatal phenotype, pituitary aplasia, but normally located posterior pituitary and no optic nerve abnormalities.
J Clin Endocrinol Metab. 2006 Nov;91(11):4528-36.

34) Corneli G, Vivenza D, Prodam F, Di Dio G, Vottero A, Rapa A, Bellone S, Bernasconi S, Bona G.
Heterozygous mutation of HESX1 causing hypopituitarism and multiple anatomical malformations without features of septo-optic dysplasia.
J Endocrinol Invest. 2008 Aug;31(8):689-93.

35) McNay DE, Turton JP, Kelberman D, Woods KS, Brauner R, Papadimitriou A, Keller E, Keller A, Haufs N, Krude H, Shalet SM, Dattani MT.
HESX1 mutations are an uncommon cause of septooptic dysplasia and hypopituitarism.
J Clin Endocrinol Metab. 2007 Feb;92(2):691-7.

36) Carvalho LR, Woods KS, Mendonca BB, Marcal N, Zamparini AL, Stifani S, Brickman JM, Arnhold IJ, Dattani MT.
A homozygous mutation in HESX1 is associated with evolving hypopituitarism due to impaired repressor-corepressor interaction.
J Clin Invest. 2003 Oct;112(8):1192-201.

37) Ragge NK, Brown AG, Poloschek CM, Lorenz B, Henderson RA, Clarke MP, Russell-Eggitt I, Fielder A, Gerrelli D, Martinez-Barbera JP, Ruddle P, Hurst J, Collin JR, Salt A, Cooper ST, Thompson PJ, Sisodiya SM, Williamson KA, Fitzpatrick DR, van Heyningen V, Hanson IM.
Heterozygous mutations of OTX2 cause severe ocular malformations.
Am J Hum Genet. 2005 Jun;76(6):1008-22. Erratum in: Am J Hum Genet. 2005 Aug;77(2):334.

38) Tajima T, Ohtake A, Hoshino M, Amemiya S, Sasaki N, Ishizu K, Fujieda K.
OTX2 loss of function mutation causes anophthalmia and combined pituitary hormone deficiency with a small anterior and ectopic posterior pituitary.
J Clin Endocrinol Metab. 2009 Jan;94(1):314-9.

39) Chatelain G, Fossat N, Brun G, Lamonerie T.
Molecular dissection reveals decreased activity and not dominant negative effect in human OTX2 mutants.
J Mol Med. 2006 Jul;84(7):604-15.

40) Diaczok D, Romero C, Zunich J, Marshall I, Radovick S.
A novel dominant negative mutation of OTX2 associated with combined pituitary hormone deficiency.
J Clin Endocrinol Metab. 2008 Nov;93(11):4351-9.

41) Hagstrom SA, Pauer GJ, Reid J, Simpson E, Crowe S, Maumenee IH, Traboulsi EI.
SOX2 mutation causes anophthalmia, hearing loss, and brain anomalies.
Am J Med Genet A. 2005 Oct 1;138A(2):95-8.

42) Chassaing N, Gilbert-Dussardier B, Nicot F, Fermeaux V, Encha-Razavi F, Fiorenza M, Toutain A, Calvas P.
Germinal mosaicism and familial recurrence of a SOX2 mutation with highly variable phenotypic expression extending from AEG syndrome to absence of ocular involvement.
Am J Med Genet A. 2007 Feb 1;143(3):289-91.

43) Tziaferi V, Kelberman D, Dattani MT.
The role of SOX2 in hypogonadotropic hypogonadism.
Sex Dev. 2008;2(4-5):194-9. Review.

44) Kelberman D, Rizzoti K, Avilion A, Bitner-Glindzicz M, Cianfarani S, Collins J, Chong WK, Kirk JM, Achermann JC, Ross R, Carmignac D, Lovell-Badge R, Robinson IC, Dattani MT.
Mutations withinSox2/SOX2 are associated with abnormalities in the hypothalamo-pituitarygonadal axis in mice and humans.
J Clin Invest. 2006;116:2442-55.

45) Bakrania P, Robinson DO, Bunyan DJ, Salt A, Martin A, Crolla JA, Wyatt A, Fielder A, Ainsworth J, Moore A, Read S, Uddin J, Laws D, Pascuel-Salcedo D, Ayuso C, Allen L, Collin JR, Ragge NK.
SOX2 anophthalmia syndrome: 12 new cases demonstrating broader phenotype and high frequency of large gene deletions.
Br J Ophthalmol. 2007 Nov;91(11):1471-6.

46) Laumonnier F, Ronce N, Hamel BC, Thomas P, Lespinasse J, Raynaud M, Paringaux C, Van Bokhoven H, Kalscheuer V, Fryns JP, Chelly J, Moraine C, Briault S.
Transcription factor SOX3 is involved in X-linked mental retardation with growth hormone deficiency.
Am J Hum Genet. 2002 Dec;71(6):1450-5.

47) Woods KS, Cundall M, Turton J, Rizotti K, Mehta A, Palmer R, Wong J, Chong WK, Al-Zyoud M, El-Ali M, Otonkoski T, Martinez-Barbera JP, Thomas PQ, Robinson IC, Lovell-Badge R, Woodward KJ, Dattani MT.
Over- and underdosage of SOX3 is associated with infundibular hypoplasia and hypopituitarism.
Am J Hum Genet. 2005 May;76(5):833-49.

48) Roessler E, Du YZ, Mullor JL, Casas E, Allen WP, Gillessen-Kaesbach G, Roeder ER, Ming JE, Ruiz i Altaba A, Muenke M.
Loss-of-function mutations in the human GLI2 gene are associated with pituitary anomalies and holoprosencephaly-like features.

Proc Natl Acad Sci U S A. 2003 Nov 11;100(23):13424-9.

49) Netchine I, Sobrier ML, Krude H, Schnabel D, Maghnie M, Marcos E, Duriez B, Cacheux V, Moers A, Goossens M, Grüters A, Amselem S.
Mutations in LHX3 result in a new syndrome revealed by combined pituitary hormone deficiency.
Nat Genet. 2000 Jun;25(2):182-6.

50) Pfaeffle RW, Savage JJ, Hunter CS, Palme C, Ahlmann M, Kumar P, Bellone J, Schoenau E, Korsch E, Brämswig JH, Stobbe HM, Blum WF, Rhodes SJ.
Four novel mutations of the LHX3 gene cause combined pituitary hormone deficiencies with or without limited neck rotation.
J Clin Endocrinol Metab. 2007 May;92(5):1909-19.

51) Rajab A, Kelberman D, de Castro SC, Biebermann H, Shaikh H, Pearce K, Hall CM, Shaikh G, Gerrelli D, Grueters A, Krude H, Dattani MT.
Novel mutations in LHX3 are associated with hypopituitarism and sensorineural hearing loss.
Hum Mol Genet. 2008 Jul 15;17(14):2150-9.

52) Kristrom B, Zdunek AM, Rydh A, Jonsson H, Sehlin P, Escher SA.
A novel mutation in the LIM homeobox 3 gene is responsible for combined pituitary hormone deficiency, hearing impairment, and vertebral malformations.
J Clin Endocrinol Metab. 2009 Apr;94(4):1154-61.

53) Machinis K, Pantel J, Netchine I, Léger J, Camand OJ, Sobrier ML, Dastot-Le Moal F, Duquesnoy P, Abitbol M, Czernichow P, Amselem S.
Syndromic short stature in patients with a germline mutation in the LIM homeobox LHX4.
Am J Hum Genet. 2001 Nov;69(5):961-8.

54) Tajima T, Hattori T, Nakajima T, Okuhara K, Tsubaki J, Fujieda K.
A novel missense mutation (P366T) of the LHX4 gene causes severe combined pituitary hormone deficiency with pituitary hypoplasia, ectopic posterior lobe and a poorly developed sella turcica.

Endocr J. 2007 Aug;54(4):637-41.

55) Pfaeffle RW, Hunter CS, Savage JJ, Duran-Prado M, Mullen RD, Neeb ZP, Eiholzer U, Hesse V, Haddad NG, Stobbe HM, Blum WF, Weigel JF, Rhodes SJ.
Three novel missense mutations within the LHX4 gene are associated with variable pituitary hormone deficiencies.
J Clin Endocrinol Metab. 2008 Mar;93(3):1062-71.

56) Castinetti F, Saveanu A, Reynaud R, Quentien MH, Buffin A, Brauner R, Kaffel N, Albarel F, Guedj AM, El Kholy M, Amin M, Enjalbert A, Barlier A, Brue T.
A novel dysfunctional LHX4 mutation with high phenotypical variability in patients with hypopituitarism.
J Clin Endocrinol Metab. 2008 Jul;93(7):2790-9.

57) Turton JP, Mehta A, Raza J, Woods KS, Tiulpakov A, Cassar J, Chong K, Thomas PQ, Eunice M, Ammini AC, Bouloux PM, Starzyk J, Hindmarsh PC, Dattani MT.
Mutations within the transcription factor PROP1 are rare in a cohort of patients with sporadic combined pituitary hormone deficiency (CPHD).
Clin Endocrinol (Oxf). 2005 Jul;63(1):10-8.

58) Riepe FG, Partsch CJ, Blankenstein O, Mönig H, Pfäffle RW, Sippell WG.
Longitudinal imaging reveals pituitary enlargement preceding hypoplasia in two brothers with combined pituitary hormone deficiency attributable to PROP1 mutation.
J Clin Endocrinol Metab. 2001 Sep;86(9):4353-7.

59) Voutetakis A, Argyropoulou M, Sertedaki A, Livadas S, Xekouki P, Maniati-Christidi M, Bossis I, Thalassinos N, Patronas N, Dacou-Voutetakis C.
Pituitary magnetic resonance imaging in 15 patients with Prop1 gene mutations: pituitary enlargement may originate from the intermediate lobe.
J Clin Endocrinol Metab. 2004 May;89(5):2200-6.

60) Voutetakis A, Sertedaki A, Livadas S, Xekouki P, Bossis I, Dacou-Voutetakis C, Argyropoulou MI.
Pituitary size fluctuation in long-term MR studies of PROP1 deficient patients: A persistent pathophysiological mechanism?

J Endocrinol Invest. 2006 May;29(5):462-6.

61) Wu W, Cogan JD, Pfäffle RW, Dasen JS, Frisch H, O'Connell SM, Flynn SE, Brown MR, Mullis PE, Parks JS, Phillips JA 3rd, Rosenfeld MG.
Mutations in PROP1 cause familial combined pituitary hormone deficiency.
Nat Genet. 1998 Feb;18(2):147-9.

62) Reynaud R, Barlier A, Vallette-Kasic S, Saveanu A, Guillet MP, Simonin G, Enjalbert A, Valensi P, Brue T.
An uncommon phenotype with familial central hypogonadism caused by a novel PROP1 gene mutant truncated in the transactivation domain.
J Clin Endocrinol Metab. 2005 Aug;90(8):4880-7.

63) Fofanova O, Takamura N, Kinoshita E, Parks JS, Brown MR, Peterkova VA, Evgrafov OV, Goncharov NP, Bulatov AA, Dedov II, Yamashita S.
Compound heterozygous deletion of the PROP-1 gene in children with combined pituitary hormone deficiency.
J Clin Endocrinol Metab. 1998 Jul;83(7):2601-4.

64) Voutetakis A, Maniati-Christidi M, Kanaka-Gantenbein C, Dracopoulou M, Argyropoulou M, Livadas S, Dacou-Voutetakis C, Sertedaki A.
Prolonged jaundice and hypothyroidism as the presenting symptoms in a neonate with a novel Prop1 gene mutation (Q83X).
Eur J Endocrinol. 2004 Mar;150(3):257-64.

65) Kelberman D, Turton JP, Woods KS, Mehta A, Al-Khawari M, Greening J, Swift PG, Otonkoski T, Rhodes SJ, Dattani MT.
Molecular analysis of novel PROP1 mutations associated with combined pituitary hormone deficiency (CPHD).
Clin Endocrinol (Oxf). 2009 Jan;70(1):96-103.

66) Ward L, Chavez M, Huot C, Lecocq P, Collu R, Décarie JC, Martial JA, Van Vliet G.
Severe congenital hypopituitarism with low prolactin levels and age-dependent anterior pituitary hypoplasia: a clue to a PIT-1 mutation.

J Pediatr. 1998 Jun;132(6):1036-8. Review.

67) Turton JP, Reynaud R, Mehta A, Torpiano J, Saveanu A, Woods KS, Tiulpakov A, Zdravkovic V, Hamilton J, Attard-Montalto S, Parascandalo R, Vella C, Clayton PE, Shalet S, Barton J, Brue T, Dattani MT.
Novel mutations within the POU1F1 gene associated with variable combined pituitary hormone deficiency.
J Clin Endocrinol Metab. 2005 Aug;90(8):4762-70.

68) Vieira TC, Dias da Silva MR, Cerutti JM, Brunner E, Borges M, Arnaldi LT, Kopp P, Abucham J.
Familial combined pituitary hormone deficiency due to a novel mutation R99Q in the hot spot region of Prophet of Pit-1 presenting as constitutional growth delay.
J Clin Endocrinol Metab. 2003 Jan;88(1):38-44.

69) Snabboon T, Plengpanich W, Buranasupkajorn P, Khwanjaipanich R, Vasinanukorn P, Suwanwalaikorn S, Khovidhunkit W, Shotelersuk V.
A novel germline mutation, IVS4+1G>A, of the POU1F1 gene underlying combined pituitary hormone deficiency.
Horm Res. 2008;69(1):60-4.

70) Hendriks-Stegeman BI, Augustijn KD, Bakker B, Holthuizen P, van der Vliet PC, Jansen M.
Combined pituitary hormone deficiency caused by compound heterozygosity for two novel mutations in the POU domain of the Pit1/POU1F1 gene.
J Clin Endocrinol Metab. 2001 Apr;86(4):1545-50.

71) Salemi S, Besson A, Eblé A, Gallati S, Pfäffle RW, Mullis PE.
New N-terminal located mutation (Q4ter) within the POU1F1-gene (PIT-1) causes recessive combined pituitary hormone deficiency and variable phenotype.
Growth Horm IGF Res. 2003 Oct;13(5):264-8.

72) Carlomagno Y, Salerno M, Vivenza D, Capalbo D, Godi M, Mellone S, Tiradani L, Corneli G, Momigliano-Richiardi P, Bona G, Giordano M.

A novel recessive splicing mutation in the POU1F1 gene causing combined pituitary hormone deficiency.
J Endocrinol Invest. 2009 Sep;32(8):653-8.

73) Rainbow LA, Rees SA, Shaikh MG, Shaw NJ, Cole T, Barrett TG, Kirk JM.
Mutation analysis of POUF-1, PROP-1 and HESX-1 show low frequency of mutations in children with sporadic forms of combined pituitary hormone deficiency and septo-optic dysplasia.
Clin Endocrinol (Oxf). 2005 Feb;62(2):163-8.

74) Lamolet B, Pulichino AM, Lamonerie T, Gauthier Y, Brue T, Enjalbert A, Drouin J.
A pituitary cell-restricted T box factor, Tpit, activates POMC transcription in cooperation with Pitx homeoproteins.
Cell. 2001 Mar 23;104(6):849-59.

75) Ericson J, Norlin S, Jessell TM, Edlund T.
Integrated FGF and BMP signaling controls the progression of progenitor cell differentiation and the emergence of pattern in the embryonic anterior pituitary.
Development. 1998 Mar;125(6):1005-15.

76) Japón MA, Rubinstein M, Low MJ.
In situ hybridization analysis of anterior pituitary hormone gene expression during fetal mouse development.
J Histochem Cytochem. 1994 Aug;42(8):1117-25.

77) Gleiberman AS, Fedtsova NG, Rosenfeld MG.
Tissue interactions in the induction of anterior pituitary: role of the ventral diencephalon, mesenchyme, and notochord.
Dev Biol. 1999 Sep 15;213(2):340-53.

78) Sheng HZ, Zhadanov AB, Mosinger B Jr, Fujii T, Bertuzzi S, Grinberg A, Lee EJ, Huang SP, Mahon KA, Westphal H.
Specification of pituitary cell lineages by the LIM homeobox gene Lhx3.
Science. 1996 May 17;272(5264):1004-7.

79) Sloop KW, Meier BC, Bridwell JL, Parker GE, Schiller AM, Rhodes SJ.
Differential activation of pituitary hormone genes by human Lhx3 isoforms with distinct DNA binding properties.
Mol Endocrinol. 1999 Dec;13(12):2212-25.

80) Sobrier ML, Attié-Bitach T, Netchine I, Encha-Razavi F, Vekemans M, Amselem S.
Pathophysiology of syndromic combined pituitary hormone deficiency due to a LHX3 defect in light of LHX3 and LHX4 expression during early human development.
Gene Expr Patterns. 2004 Dec;5(2):279-84.

81) Thomas PQ, Johnson BV, Rathjen J, Rathjen PD.
Sequence, genomic organization, and expression of the novel homeoboxgene Hesx1.
J Biol Chem. 1995 Feb 24;270(8):3869-75.

82) Olson LE, Tollkuhn J, Scafoglio C, Krones A, Zhang J, Ohgi KA, Wu W, Taketo MM, Kemler R, Grosschedl R, Rose D, Li X, Rosenfeld MG.
Homeodomain-mediated beta-catenin-dependent switching events dictate cell-lineage determination.
Cell. 2006 May 5;125(3):593-605.

83) Olson LE, Dasen JS, Ju BG, Tollkuhn J, Rosenfeld MG.
Paired-like repression/activation in pituitary development.
Recent Prog Horm Res. 2003;58:249-61. Review.

84) Simmons DM, Voss JW, Ingraham HA, Holloway JM, Broide RS, Rosenfeld MG, Swanson LW.
Pituitary cell phenotypes involve cell-specific Pit-1 mRNA translation and synergistic interactions with other classes of transcription factors.
Genes Dev. 1990 May;4(5):695-711.

85) Fauquier T, Rizzoti K, Dattani M, Lovell-Badge R, Robinson IC.
SOX2-expressing progenitor cells generate all of the major cell types in the adult mouse pituitary gland.
Proc Natl Acad Sci U S A. 2008 Feb 26;105(8):2907-12.

86) Rizzoti K, Brunelli S, Carmignac D, Thomas PQ, Robinson IC, Lovell-Badge R.
SOX3 is required during the formation of the hypothalamo-pituitary axis.
Nat Genet. 2004 Mar;36(3):247-55.

87) Kelberman D, de Castro SC, Huang S, Crolla JA, Palmer R, Gregory JW, Taylor D, Cavallo L, Faienza MF, Fischetto R, Achermann JC, Martinez-Barbera JP, Rizzoti K, Lovell-Badge R, Robinson IC, Gerrelli D, Dattani MT.
SOX2 plays a critical role in the pituitary, forebrain, and eye during human embryonic development.
J Clin Endocrinol Metab. 2008 May;93(5):1865-73.

88) Quentien MH, Manfroid I, Moncet D, Gunz G, Muller M, Grino M, Enjalbert A, Pellegrini I.
Pitx factors are involved in basal and hormone-regulated activity of the human prolactin promoter.
J Biol Chem. 2002 Nov 15;277(46):44408-16.

89) Dasen JS, O'Connell SM, Flynn SE, Treier M, Gleiberman AS, Szeto DP, Hooshmand F, Aggarwal AK, Rosenfeld MG.
Reciprocal interactions of Pit1 and GATA2 mediate signaling gradient-induced determination of pituitary cell types.
Cell. 1999 May 28;97(5):587-98.

90) Tremblay JJ, Drouin J.
Egr-1 is a downstream effector of GnRH and synergizes by direct interaction with Ptx1 and SF-1 to enhance luteinizing hormone beta gene transcription.
Mol Cell Biol. 1999 Apr;19(4):2567-76.

91) Suh H, Gage PJ, Drouin J, Camper SA.
Pitx2 is required at multiple stages of pituitary organogenesis: pituitary primordium formation and cell specification.
Development. 2002 Jan;129(2):329-37.

92) Tremblay JJ, Goodyer CG, Drouin J.

Transcriptional properties of Ptx1 and Ptx2 isoforms.
Neuroendocrinology. 2000 May;71(5):277-86.

93) Bazina M, Vukojevic K, Roje D, Saraga-Babic M.
Influence of growth and transcriptional factors, and signaling molecules on early human pituitary development.
J Mol Histol. 2009 Aug;40(4):277-86.

94) Treier M, O'Connell S, Gleiberman A, Price J, Szeto DP, Burgess R, Chuang PT, McMahon AP, Rosenfeld MG.
Hedgehog signaling is required for pituitary gland development.
Development. 2001 Feb;128(3):377-86.

95) Hui CC, Slusarski D, Platt KA, Holmgren R, Joyner AL.
Expression of three mouse homologs of the Drosophila segment polarity gene cubitus interruptus, Gli, Gli-2, and Gli-3, in ectoderm- and mesoderm-derived tissues suggests multiple roles during postimplantation development.
Dev Biol. 1994 Apr;162(2):402-13.

96) Zhu X, Gleiberman AS, Rosenfeld MG.
Molecular physiology of pituitary development: signaling and transcriptional networks.
Physiol Rev. 2007 Jul;87(3):933-63. Review.

97) Sadler TW.
Susceptible periods during embryogenesis of the heart and endocrine glands.
Environ Health Perspect. 2000 Jun;108 Suppl 3:555-61. Review.

98) Kioussi C, Briata P, Baek SH, Rose DW, Hamblet NS, Herman T, Ohgi KA, Lin C, Gleiberman A, Wang J, Brault V, Ruiz-Lozano P, Nguyen HD, Kemler R, Glass CK, Wynshaw-Boris A, Rosenfeld MG.
Identification of a Wnt/Dvl/beta-Catenin --> Pitx2 pathway mediating cell-type-specific proliferation during development.
Cell. 2002 Nov 27;111(5):673-85.

99) Hayward P, Kalmar T, Arias AM.

Wnt/Notch signalling and information processing during development.
Development. 2008 Feb;135(3):411-24. Review.

100) Zhu X, Zhang J, Tollkuhn J, Ohsawa R, Bresnick EH, Guillemot F, Kageyama R, Rosenfeld MG.
Sustained Notch signaling in progenitors is required for sequential emergence of distinct cell lineages during organogenesis.
Genes Dev. 2006 Oct 1;20(19):2739-53.

101) Kurokawa D, Kiyonari H, Nakayama R, Kimura-Yoshida C, Matsuo I, Aizawa S.
Regulation of Otx2 expression and its functions in mouse forebrain and midbrain.
Development. 2004 Jul;131(14):3319-31.

102) Kurokawa D, Takasaki N, Kiyonari H, Nakayama R, Kimura-Yoshida C, Matsuo I, Aizawa S.
Regulation of Otx2 expression and its functions in mouse epiblast and anterior neuroectoderm.
Development. 2004 Jul;131(14):3307-17.

103) Larsen KB, Lutterodt MC, Møllgård K, Møller M.
Expression of the Homeobox Genes OTX2 and OTX1 in the Early Developing Human Brain.
J Histochem Cytochem. 2010 Jul;58(7):669-78.

104) Jean D, Bernier G, Gruss P.
Six6 (Optx2) is a novel murine Six3-related homeobox gene that demarcates the presumptive pituitary/hypothalamic axis and the ventral optic stalk.
Mech Dev. 1999 Jun;84(1-2):31-40.

105) Larsen KB, Lutterodt M, Rath MF, Møller M.
Expression of the homeobox genes PAX6, OTX2, and OTX1 in the early human fetal retina.
Int J Dev Neurosci. 2009 Aug;27(5):485-92.

106) Dattani MT.

DNA testing in patients with GH deficiency at the time of transition.
Growth Horm IGF Res. 2003 Aug;13 Suppl A:S122-9. Review.

107) Dattani M, Preece M.
Growth hormone deficiency and related disorders: insights into causation, diagnosis, and treatment.
Lancet. 2004 Jun 12;363(9425):1977-87. Review.

108) Kelberman D, Dattani MT.
Hypothalamic and pituitary development: novel insights into the aetiology.
Eur J Endocrinol. 2007 Aug;157 Suppl 1:S3-14. Review.

109) Redon R, Ishikawa S, Fitch KR, Feuk L, Perry GH, Andrews TD, Fiegler H, Shapero MH, Carson AR, Chen W, Cho EK, Dallaire S, Freeman JL, González JR, Gratacòs M, Huang J, Kalaitzopoulos D, Komura D, MacDonald JR, Marshall CR, Mei R, Montgomery L, Nishimura K, Okamura K, Shen F, Somerville MJ, Tchinda J, Valsesia A, Woodwark C, Yang F, Zhang J, Zerjal T, Zhang J, Armengol L, Conrad DF, Estivill X, Tyler-Smith C, Carter NP, Aburatani H, Lee C, Jones KW, Scherer SW, Hurles ME.
Global variation in copy number in the human genome.
Nature. 2006 Nov 23;444(7118):444-54.

110) Reymond A, Henrichsen CN, Harewood L, Merla G.
Side effects of genome structural changes.
Curr Opin Genet Dev. 2007;17:381-6.

111) Lee C, Iafrate AJ, Brothman AR.
Copy number variations and clinical cytogenetic diagnosis of constitutional disorders.
Nat Genet. 2007 Jul;39(7 Suppl):S48-54. Review.

112) Feuk L, Carson AR, Scherer SW.
Structural variation in the human genome.
Nat Rev Genet. 2006 Feb;7(2):85-97. Review.

113) Freeman JL, Perry GH, Feuk L, Redon R, McCarroll SA, Altshuler DM, Aburatani H, Jones KW, Tyler-Smith C, Hurles ME, Carter NP, Scherer SW, Lee C.
Copy number variation: new insights in genome diversity.
Genome Res. 2006 Aug;16(8):949-61. Review.

114) McCarroll SA, Kuruvilla FG, Korn JM, Cawley S, Nemesh J, Wysoker A, Shapero MH, de Bakker PI, Maller JB, Kirby A, Elliott AL, Parkin M, Hubbell E, Webster T, Mei R, Veitch J, Collins PJ, Handsaker R, Lincoln S, Nizzari M, Blume J, Jones KW, Rava R, Daly MJ, Gabriel SB, Altshuler D.
Integrated detection and population-genetic analysis of SNPs and copy number variation.
Nat Genet. 2008 Oct;40(10):1166-74.

115) Hastings PJ, Lupski JR, Rosenberg SM, Ira G.
Mechanisms of change in gene copy number.
Nat Rev Genet. 2009 Aug;10(8):551-64.

116) Iafrate AJ, Feuk L, Rivera MN, Listewnik ML, Donahoe PK, Qi Y, Scherer SW, Lee C.
Detection of large-scale variation in the human genome.
Nat Genet. 2004 Sep;36(9):949-51.

117) Sebat J, Lakshmi B, Troge J, Alexander J, Young J, Lundin P, Månér S, Massa H, Walker M, Chi M, Navin N, Lucito R, Healy J, Hicks J, Ye K, Reiner A, Gilliam TC, Trask B, Patterson N, Zetterberg A, Wigler M.
Large-scale copy number polymorphism in the human genome.
Science. 2004 Jul 23;305(5683):525-8.

118) Gu W, Zhang F, Lupski JR.
Mechanisms for human genomic rearrangements.
Pathogenetics. 2008 Nov 3;1(1):4.

119) Bailey JA, Yavor AM, Massa HF, Trask BJ, Eichler EE.
Segmental duplications: organization and impact within the current human genome project assembly.

Genome Res. 2001 Jun;11(6):1005-17.

120) Stankiewicz P, Inoue K, Bi W, Walz K, Park SS, Kurotaki N, Shaw CJ, Fonseca P, Yan J, Lee JA, Khajavi M, Lupski JR.
Genomic disorders: genome architecture results in susceptibility to DNA rearrangements causing common human traits.
Cold Spring Harb. Symp. Quant. Biol. 2003;68:445-54. Review.

121) Stankiewicz P, Lupski JR.
Genome architecture, rearrangements and genomic disorders.
Trends Genet. 2002;18:74-82.

122) Stankiewicz P, Lupski JR.
Structural variation in the human genome and its role in disease.
Annu Rev Med. 2010;61:437-55.

123) Weterings E, van Gent DC.
The mechanism of non-homologous end-joining: a synopsis of synapsis.
DNA Repair (Amst). 2004;3:1425-35.

124) Tanaka H, Yao MC.
Palindromic gene amplification: an evolutionarily conserved role for DNA inverted repeats in the genome.
Nat Rev Cancer. 2009;9:216-224.

125) Lee JA, Carvalho CM, Lupski JR.
A DNA replication mechanism for generating nonrecurrent rearrangements associated with genomic disorders.
Cell. 2007 Dec 28;131(7):1235-47.

126) Hastings PJ, Ira G, Lupski JR.
A microhomology-mediated break-induced replication model for the origin of human copy number variation.
PLoS Genet. 2009 Jan;5(1):e1000327. Review.

127) Zhang F, Khajavi M, Connolly AM, Towne CF, Batish SD, Lupski JR.
The DNA replication FoSTeS/MMBIR mechanism can generate human genomic, genic, and exonic complex rearrangements in humans.
Nat Genet. 2009 Jul;41(7):849-53.

128) Zhang F, Carvalho CMB, Lupski JR.
Complex human chromosomal and genomic rearrangements.
Trends Genet. 2009;25:298-307.

129) Conrad DF, Pinto D, Redon R, Feuk L, Gokcumen O, Zhang Y, Aerts J, Andrews TD, Barnes C, Campbell P, Fitzgerald T, Hu M, Ihm CH, Kristiansson K, Macarthur DG, Macdonald JR, Onyiah I, Pang AW, Robson S, Stirrups K, Valsesia A, Walter K, Wei J; Wellcome Trust Case Control Consortium, Tyler-Smith C, Carter NP, Lee C, Scherer SW, Hurles ME.
Origins and functional impact of copy number variation in the human genome.
Nature. 2010 Apr 1;464(7289):704-12.

130) Pinto D, Marshall C, Feuk L, Scherer SW.
Copy-number variation in control population cohorts.
Hum Mol Genet. 2007 Oct 15;16 Spec No. 2:R168-73. Review. Erratum in: Hum Mol Genet. 2008 Feb 1;17(3):166-7.

131) Stranger BE, Forrest MS, Dunning M, Ingle CE, Beazley C, Thorne N, Redon R, Bird CP, de Grassi A, Lee C, Tyler-Smith C, Carter N, Scherer SW, Tavaré S, Deloukas P, Hurles ME, Dermitzakis ET.
Relative impact of nucleotide and copy number variation on gene expression phenotypes.
Science. 2007 Feb 9;315(5813):848-53.

132) Feuk L, Marshall CR, Wintle RF, Scherer SW.
Structural variants: changing the landscape of chromosomes and design of disease studies.
Hum Mol Genet. 2006 Apr 15;15 Spec No 1:R57-66.

133) Reymond A, Henrichsen CN, Harewood L, Merla G.

Side effects of genome structural changes.
Curr Opin Genet Dev. 2007 Oct;17(5):381-6. Review.

134) Kleinjan DJ, van Heyningen V.
Position effect in human genetic disease.
Hum Mol Genet. 1998;7:1611-18.

135) Kleinjan DA, van Heyningen V.
Long-range control of gene expression: emerging mechanisms and disruption in disease.
Am J Hum Genet. 2005;76:8-32.

136) Cooper GM, Nickerson DA, Eichler EE.
Mutational and selective effects on copy-number variants in the human genome.
Nat Genet. 2007;39:S22-S29.

137) Takahashi N, Satoh Y, Kodaira M, Katayama H.
Large-scale copy number variants (CNVs) detected in different ethnic human populations.
Cytogenet Genome Res. 2008;123(1-4):224-33. Review.

138) Lupski J.
Genomic rearrangments and sporadic disease.
Nat Genet. 2007;39:S43-S47.

139) Lee C, Iafrate AJ, Brothman AR.
Copy number variation and clinical cytogenetics diagnosis of constitutional disorders.
Nat Genet. 2007;39:S48-S54.

140) Mills RE, Walter K, Stewart C, Handsaker RE, Chen K, Alkan C, Abyzov A, Yoon SC, Ye K, Cheetham RK, Chinwalla A, Conrad DF, Fu Y, Grubert F, Hajirasouliha I, Hormozdiari F, Iakoucheva LM, Iqbal Z, Kang S, Kidd JM, Konkel MK, Korn J, Khurana E, Kural D, Lam HY, Leng J, Li R, Li Y, Lin CY, Luo R, Mu XJ, Nemesh J, Peckham HE, Rausch T, Scally A, Shi X, Stromberg MP, Stütz AM, Urban AE, Walker JA, Wu J, Zhang Y, Zhang ZD, Batzer MA, Ding L, Marth GT, McVean G,

Sebat J, Snyder M, Wang J, Ye K, Eichler EE, Gerstein MB, Hurles ME, Lee C, McCarroll SA, Korbel JO; 1000 Genomes Project.
Mapping copy number variation by population-scale genome sequencing.
Nature. 2011 Feb 3;470(7332):59-65.

141) Ionita-Laza I, Rogers AJ, Lange C, Raby BA, Lee C.
Genetic association analysis of copy-number variation (CNV) in human disease pathogenesis.
Genomics. 2009 Jan;93(1):22-6. Review.

142) Zhang X, Snijders A, Segraves R, Zhang X, Niebuhr A, Albertson D, Yang H, Gray J, Niebuhr E, Bolund L, Pinkel D.
High-resolution mapping of genotype-phenotype relationships in cri du chat syndrome using array comparative genomic hybridization.
Am J Hum Genet. 2005 Feb;76(2):312-26.

143) Visser R, Gijsbers A, Ruivenkamp C, Karperien M, Reeser HM, Breuning MH, Kant SG, Wit JM.
Genome-Wide SNP Array Analysis in Patients with Features of Sotos Syndrome.
Horm Res Paediatr. 2010;73(4):265-274.

144) Osoegawa K, Vessere GM, Utami KH, Mansilla MA, Johnson MK, Riley BM, L'Heureux J, Pfundt R, Staaf J, van der Vliet WA, Lidral AC, Schoenmakers EF, Borg A, Schutte BC, Lammer EJ, Murray JC, de Jong PJ.
Identification of novel candidate genes associated with cleft lip and palate using array comparative genomic hybridisation.
J Med Genet. 2008 Feb;45(2):81-6.

145) De Gregori M, Ciccone R, Magini P, Pramparo T, Gimelli S, Messa J, Novara F, Vetro A, Rossi E, Maraschio P, Bonaglia MC, Anichini C, Ferrero GB, Silengo M, Fazzi E, Zatterale A, Fischetto R, Previderé C, Belli S, Turci A, Calabrese G, Bernardi F, Meneghelli E, Riegel M, Rocchi M, Guerneri S, Lalatta F, Zelante L, Romano C, Fichera M, Mattina T, Arrigo G, Zollino M, Giglio S, Lonardo F, Bonfante A, Ferlini A, Cifuentes F, Van Esch H, Backx L, Schinzel A, Vermeesch JR, Zuffardi O.

Cryptic deletions are a common finding in "balanced" reciprocal and complex chromosome rearrangements: a study of 59 patients.
J Med Genet. 2007 Dec;44(12):750-62.

146) Fauth C, Gribble SM, Porter KM, Codina-Pascual M, Ng BL, Kraus J, Uhrig S, Leifheit J, Haaf T, Fiegler H, Carter NP, Speicher MR.
Micro-array analyses decipher exceptional complex familial chromosomal rearrangement.
Hum Genet. 2006 Mar;119(1-2):145-53.

147) Gribble SM, Prigmore E, Burford DC, Porter KM, Ng BL, Douglas EJ, Fiegler H, Carr P, Kalaitzopoulos D, Clegg S, Sandstrom R, Temple IK, Youings SA, Thomas NS, Dennis NR, Jacobs PA, Crolla JA, Carter NP.
The complex nature of constitutional de novo apparently balanced translocations in patients presenting with abnormal phenotypes.
J Med Genet. 2005 Jan;42(1):8-16.

148) Rosenberg C, Knijnenburg J, Chauffaille Mde L, Brunoni D, Catelani AL, Sloos W, Szuhai K, Tanke HJ.
Array CGH detection of a cryptic deletion in a complex chromosome rearrangement.
Hum Genet. 2005 Apr;116(5):390-4.

149) Gijsbers AC, Bijlsma EK, Weiss MM, Bakker E, Breuning MH, Hoffer MJ, Ruivenkamp CA.
A 400kb duplication, 2.4Mb triplication and 130kb duplication of 9q34.3 in a patient with severe mental retardation.
Eur J Med Genet. 2008 Sep-Oct;51(5):479-87.

150) Talseth-Palmer BA, Bowden NA, Meldrum C, Nicholl J, Thompson E, Friend K, Liebelt J, Bratkovic D, Haan E, Yu S, Scott RJ.
A 1q44 deletion, paternal UPD of chromosome 2 and a deletion due to a complex translocation detected in children with abnormal phenotypes using new SNP array technology.
Cytogenet Genome Res. 2009;124(1):94-101.

151) Lupski JR.
Structural variation in the human genome.
N Engl J Med. 2007;356:1169-71.

152) Hoyer J, Dreweke A, Becker C, Göhring I, Thiel CT, Peippo MM, Rauch R, Hofbeck M, Trautmann U, Zweier C, Zenker M, Hüffmeier U, Kraus C, Ekici AB, Rüschendorf F, Nürnberg P, Reis A, Rauch A.
Molecular karyotyping in patients with mental retardation using 100K single-nucleotide polymorphism arrays.
J Med Genet. 2007 Oct;44(10):629-36.

153) van Ommen GJ.
Frequency of new copy number variation in humans.
Nature Genet. 2005;37:333-4.

154) International HapMap Consortium.
A haplotype map of the human genome.
Nature. 2005 Oct 27;437(7063):1299-320.

155) Sachidanandam R, Weissman D, Schmidt SC, Kakol JM, Stein LD, Marth G, Sherry S, Mullikin JC, Mortimore BJ, Willey DL, Hunt SE, Cole CG, Coggill PC, Rice CM, Ning Z, Rogers J, Bentley DR, Kwok PY, Mardis ER, Yeh RT, Schultz B, Cook L, Davenport R, Dante M, Fulton L, Hillier L, Waterston RH, McPherson JD, Gilman B, Schaffner S, Van Etten WJ, Reich D, Higgins J, Daly MJ, Blumenstiel B, Baldwin J, Stange-Thomann N, Zody MC, Linton L, Lander ES, Altshuler D; International SNP Map Working Group.
A map of human genome sequence variation containing 1.42 million single nucleotide polymorphisms.
Nature. 2001 Feb 15;409(6822):928-33.

156) Botstein D, Risch N.
Discovering genotypes underlying human phenotypes: past successes for mendelian disease, future approaches for complex disease.
Nat Genet. 2003;33:228-37.

157) Sabeti PC, Varilly P, Fry B, Lohmueller J, Hostetter E, Cotsapas C, Xie X, Byrne EH, McCarroll SA, Gaudet R, Schaffner SF, Lander ES; International HapMap Consortium, Frazer KA, Ballinger DG, Cox DR, Hinds DA, Stuve LL, Gibbs RA, Belmont JW, Boudreau A, Hardenbol P, Leal SM, Pasternak S, Wheeler DA, Willis TD, Yu F, Yang H, Zeng C, Gao Y, Hu H, Hu W, Li C, Lin W, Liu S, Pan H, Tang X, Wang J, Wang W, Yu J, Zhang B, Zhang Q, Zhao H, Zhao H, Zhou J, Gabriel SB, Barry R, Blumenstiel B, Camargo A, Defelice M, Faggart M, Goyette M, Gupta S, Moore J, Nguyen H, Onofrio RC, Parkin M, Roy J, Stahl E, Winchester E, Ziaugra L, Altshuler D, Shen Y, Yao Z, Huang W, Chu X, He Y, Jin L, Liu Y, Shen Y, Sun W, Wang H, Wang Y, Wang Y, Xiong X, Xu L, Waye MM, Tsui SK, Xue H, Wong JT, Galver LM, Fan JB, Gunderson K, Murray SS, Oliphant AR, Chee MS, Montpetit A, Chagnon F, Ferretti V, Leboeuf M, Olivier JF, Phillips MS, Roumy S, Sallée C, Verner A, Hudson TJ, Kwok PY, Cai D, Koboldt DC, Miller RD, Pawlikowska L, Taillon-Miller P, Xiao M, Tsui LC, Mak W, Song YQ, Tam PK, Nakamura Y, Kawaguchi T, Kitamoto T, Morizono T, Nagashima A, Ohnishi Y, Sekine A, Tanaka T, Tsunoda T, Deloukas P, Bird CP, Delgado M, Dermitzakis ET, Gwilliam R, Hunt S, Morrison J, Powell D, Stranger BE, Whittaker P, Bentley DR, Daly MJ, de Bakker PI, Barrett J, Chretien YR, Maller J, McCarroll S, Patterson N, Pe'er I, Price A, Purcell S, Richter DJ, Sabeti P, Saxena R, Schaffner SF, Sham PC, Varilly P, Altshuler D, Stein LD, Krishnan L, Smith AV, Tello-Ruiz MK, Thorisson GA, Chakravarti A, Chen PE, Cutler DJ, Kashuk CS, Lin S, Abecasis GR, Guan W, Li Y, Munro HM, Qin ZS, Thomas DJ, McVean G, Auton A, Bottolo L, Cardin N, Eyheramendy S, Freeman C, Marchini J, Myers S, Spencer C, Stephens M, Donnelly P, Cardon LR, Clarke G, Evans DM, Morris AP, Weir BS, Tsunoda T, Johnson TA, Mullikin JC, Sherry ST, Feolo M, Skol A, Zhang H, Zeng C, Zhao H, Matsuda I, Fukushima Y, Macer DR, Suda E, Rotimi CN, Adebamowo CA, Ajayi I, Aniagwu T, Marshall PA, Nkwodimmah C, Royal CD, Leppert MF, Dixon M, Peiffer A, Qiu R, Kent A, Kato K, Niikawa N, Adewole IF, Knoppers BM, Foster MW, Clayton EW, Watkin J, Gibbs RA, Belmont JW, Muzny D, Nazareth L, Sodergren E, Weinstock GM, Wheeler DA, Yakub I, Gabriel SB, Onofrio RC, Richter DJ, Ziaugra L, Birren BW, Daly MJ, Altshuler D, Wilson RK, Fulton LL, Rogers J, Burton J, Carter NP, Clee CM, Griffiths M, Jones MC, McLay K, Plumb RW, Ross MT, Sims SK, Willey DL, Chen Z, Han H, Kang L, Godbout M, Wallenburg JC, L'Archevêque P, Bellemare G, Saeki K, Wang H, An D, Fu H, Li Q, Wang Z, Wang R, Holden AL, Brooks LD, McEwen JE, Guyer MS, Wang VO, Peterson JL, Shi M, Spiegel J, Sung LM, Zacharia LF, Collins FS, Kennedy K, Jamieson R, Stewart J.

Genome-wide detection and characterization of positive selection in human populations.
Nature. 2007;449:913-8.

158) http://www.hapmap.org

159) International HapMap Consortium.
The International HapMap Project.
Nature. 2003;426:789-96.

160) Ahmadi KR, Weale ME, Xue ZY, Soranzo N, Yarnall DP, Briley JD, Maruyama Y, Kobayashi M, Wood NW, Spurr NK, Burns DK, Roses AD, Saunders AM, Goldstein DB.
A single-nucleotide polymorphism tagging set for human drug metabolism and transport.
Nat Genet. 2005;37:84-9.

161) Zeggini E, Rayner W, Morris AP, Hattersley AT, Walker M, Hitman GA, Deloukas P, Cardon LR, McCarthy MI.
An evaluation of HapMap sample size and tagging SNP performance in large-scale empirical and simulated data sets.
Nat Genet. 2005 Dec;37(12):1320-2.

162) de Bakker PI, Yelensky R, Pe'er I, Gabriel SB, Daly MJ, Altshuler D.
Efficiency and power in genetic association studies.
Nat Genet. 2005 Nov;37(11):1217-23.

163) Wellcome Trust Case Control Consortium.
Genome-wide association study of CNVs in 16,000 cases of eight common diseases and 3,000 shared controls.
Nature. 2010 Apr 1;464(7289):713-20.

164) Horton R, Gibson R, Coggill P, Miretti M, Allcock RJ, Almeida J, Forbes S, Gilbert JG, Halls K, Harrow JL, Hart E, Howe K, Jackson DK, Palmer S, Roberts AN, Sims S, Stewart CA, Traherne JA, Trevanion S, Wilming L, Rogers J, de Jong PJ, Elliott JF, Sawcer S, Todd JA, Trowsdale J, Beck S.
Variation analysis and gene annotation of eight MHC haplotypes: the MHC Haplotype Project.

Immunogenetics. 2008 Jan;60(1):1-18.

165) Zeggini E, Scott LJ, Saxena R, Voight BF, Marchini JL, Hu T, de Bakker PI, Abecasis GR, Almgren P, Andersen G, Ardlie K, Boström KB, Bergman RN, Bonnycastle LL, Borch-Johnsen K, Burtt NP, Chen H, Chines PS, Daly MJ, Deodhar P, Ding CJ, Doney AS, Duren WL, Elliott KS, Erdos MR, Frayling TM, Freathy RM, Gianniny L, Grallert H, Grarup N, Groves CJ, Guiducci C, Hansen T, Herder C, Hitman GA, Hughes TE, Isomaa B, Jackson AU, Jørgensen T, Kong A, Kubalanza K, Kuruvilla FG, Kuusisto J, Langenberg C, Lango H, Lauritzen T, Li Y, Lindgren CM, Lyssenko V, Marvelle AF, Meisinger C, Midthjell K, Mohlke KL, Morken MA, Morris AD, Narisu N, Nilsson P, Owen KR, Palmer CN, Payne F, Perry JR, Pettersen E, Platou C, Prokopenko I, Qi L, Qin L, Rayner NW, Rees M, Roix JJ, Sandbaek A, Shields B, Sjögren M, Steinthorsdottir V, Stringham HM, Swift AJ, Thorleifsson G, Thorsteinsdottir U, Timpson NJ, Tuomi T, Tuomilehto J, Walker M, Watanabe RM, Weedon MN, Willer CJ; Wellcome Trust Case Control Consortium, Illig T, Hveem K, Hu FB, Laakso M, Stefansson K, Pedersen O, Wareham NJ, Barroso I, Hattersley AT, Collins FS, Groop L, McCarthy MI, Boehnke M, Altshuler D.
Meta-analysis of genome-wide association data and large-scale replication identifies additional susceptibility loci for type 2 diabetes.
Nat Genet. 2008 May;40(5):638-45.

166) Nachman MW, Crowell SL.
Estimate of the mutation rate per nucleotide in humans.
Genetics. 2000;156:297-304.

167) McCarroll SA, Hadnott TN, Perry GH, Sabeti PC, Zody MC, Barrett JC, Dallaire S, Gabriel SB, Lee C, Daly MJ, Altshuler DM; International HapMap Consortium.
Common deletion polymorphisms in the human genome.
Nat Genet. 2006 Jan;38(1):86-92.

168) Hinds DA, Kloek AP, Jen M, Chen X, Frazer KA.
Common deletions and SNPs are in linkage disequilibrium in the human genome.
Nat Genet. 2006;38:82-5.

169) Locke DP, Sharp AJ, McCarroll SA, McGrath SD, Newman TL, Cheng Z, Schwartz S, Albertson DG, Pinkel D, Altshuler DM, Eichler EE.
Linkage disequilibrium and heritability of copy-number polymorphisms within duplicated regions of the human genome.
Am J Hum Genet. 2006 Aug;79(2):275-90.

170) Stevenson RE, Procopio-Allen AM, Schroer SJ, Collins JS.
Genetic syndromes among individuals with mental retardation.
Am J Med Genet. 2003 123A:29-32.

171) de Vries BB, White SM, Knight SJ, Regan R, Homfray T, Young ID, Super M, McKeown C, Splitt M, Quarrell OW, Trainer AH, Niermeijer MF, Malcolm S, Flint J, Hurst JA, Winter RM.
Clinical studies on submicroscopic subtelomeric rearrangements: a checklist.
J Med Genet. 2001 Mar;38(3):145-50.

172) de Vries BBA, Winter R, Schinzel A, van Ravenswaaij-Arts C.
Telomeres: a diagnosis at the end of chromosomes.
J Med Genet. 2003;40;385-398.

173) Beaudet AL, Belmont JW.
Array-based DNA diagnostics: let the revolution begin.
Annu Rev Med. 2008;59:113-29.

174) Aradhya S, Manning MA, Splendore A, Cherry AM.
Whole-genome array-CGH identifies novel contiguous gene deletions and duplications associated with developmental delay, mental retardation, and dysmorphic features.
Am J Med Genet A. 2007 Jul 1;143(13):1431-41.

175) Lu X, Shaw CA, Patel A, Li J, Cooper ML, Wells WR, Sullivan CM, Sahoo T, Yatsenko SA, Bacino CA, Stankiewicz P, Ou Z, Chinault AC, Beaudet AL, Lupski JR, Cheung SW, Ward PA.
Clinical implementation of chromosomal microarray analysis: summary of 2513 postnatal cases.
PLoS ONE. 2007 Mar 28;2(3):e327.

176) Shaffer LG, Bejjani BA, Torchia B, Kirkpatrick S, Coppinger J, Ballif BC.
The identification of microdeletion syndromes and other chromosome abnormalities: cytogenetic methods of the past, new technologies for the future.
Am J Med Genet C Semin Med Genet. 2007 Nov 15;145(4):335-45. Review.

177) Stankiewicz P, Beaudet AL.
Use of array CGH in the evaluation of dysmorphology, malformations, developmental delay, and idiopathic mental retardation.
Curr Opin Genet Dev. 2007 Jun;17(3):182-92. Review.

178) de Vries BB, Pfundt R, Leisink M, Koolen DA, Vissers LE, Janssen IM, Reijmersdal S, Nillesen WM, Huys EH, Leeuw N, Smeets D, Sistermans EA, Feuth T, van Ravenswaaij-Arts CM, van Kessel AG, Schoenmakers EF, Brunner HG, Veltman JA.
Diagnostic genome profiling in mental retardation.
Am J Hum Genet. 2005 Oct;77(4):606-16.

179) Menten B, Maas N, Thienpont B, Buysse K, Vandesompele J, Melotte C, de Ravel T, Van Vooren S, Balikova I, Backx L, Janssens S, De Paepe A, De Moor B, Moreau Y, Marynen P, Fryns JP, Mortier G, Devriendt K, Speleman F, Vermeesch JR.
Emerging patterns of cryptic chromosomal imbalances in patients with idiopathic mental retardation and multiple congenital anomalies: a new series of 140 patients and review of the literature.
J Med Genet. 2006 Aug;43(8):625-33.

180) Cheung SW, Shaw CA, Scott DA, Patel A, Sahoo T, Bacino CA, Pursley A, Li J, Erickson R, Gropman AL, Miller DT, Seashore MR, Summers AM, Stankiewicz P, Chinault AC, Lupski JR, Beaudet AL, Sutton VR.
Microarray-based CGH detects chromosomal mosaicism not revealed by conventional cytogenetics.
Am J Med Genet A. 2007 Aug 1;143(15):1679-86.

181) Gijsbers AC, Lew JY, Bosch CA, Schuurs-Hoeijmakers JH, van Haeringen A, den Hollander NS, Kant SG, Bijlsma EK, Breuning MH, Bakker E, Ruivenkamp CA.

A new diagnostic workflow for patients with mental retardation and/or multiple congenital abnormalities: test arrays first.
Eur J Hum Genet. 2009 Nov;17(11):1394-402.

182) Wicker N, Carles A, Mills IG, Wolf M, Veerakumarasivam A, Edgren H, Boileau F, Wasylyk B, Schalken JA, Neal DE, Kallioniemi O, Poch O.
A new look towards BAC-based array CGH through a comprehensive comparison with oligo-based array CGH.
BMC Genomics. 2007 Mar 29;8:84.

183) Matsuzaki H, Dong S, Loi H, Di X, Liu G, Hubbell E, Law J, Berntsen T, Chadha M, Hui H, Yang G, Kennedy GC, Webster TA, Cawley S, Walsh PS, Jones KW, Fodor SP, Mei R.
Genotyping over 100,000 SNPs on a pair of oligonucleotide arrays.
Nat Methods. 2004 Nov;1(2):109-11.

184) Slater HR, Bailey DK, Ren H, Cao M, Bell K, Nasioulas S, Henke R, Choo KHA, Kennedy GC.
High-resolution identification of chromosomal abnormalities using oligonucleotide arrays containing 116,204 SNPs.
Am J Hum Genet. 2005;77:709-26.

185) Zhang ZF, Ruivenkamp C, Staaf J, Zhu H, Barbaro M, Petillo D, Khoo SK, Borg A, Fan YS, Schoumans J.
Detection of submicroscopic constitutional chromosome aberrations in clinical diagnostics: a validation of the practical performance of different array platforms.
Eur J Hum Genet. 2008 Jul;16(7):786-92.

186) LaFramboise T.
Single nucleotide polymorphism arrays: a decade of biological, computational and technological advances.
Nucleic Acids Res. 2009 Jul;37(13):4181-93.

187) Rauch A, Rüschendorf F, Huang J, Trautmann U, Becker C, Thiel C, Jones KW, Reis A, Nürnberg P.

Molecular karyotyping using an SNP array for genomewide genotyping.
J Med Genet. 2004 Dec;41(12):916-22.

188) Lamy P, Andersen CL, Wikman FP, Wiuf C.
Genotyping and annotation of Affymetrix SNP arrays.
Nucleic Acids Res. 2006;34(14):e100.

189) Lam CW, Lau KC, Tong SF.
Microarrays for personalized genomic medicine.
Adv Clin Chem. 2010;52:1-18.

190) Cooper GM, Zerr T, Kidd JM, Eichler EE, Nickerson DA.
Systematic assessment of copy number variant detection via genome-wide SNP genotyping.
Nat Genet. 2008 Oct;40(10):1199-203.

191) Yau C, Holmes CC.
CNV discovery using SNP genotyping arrays.
Cytogenet Genome Res. 2008;123(1-4):307-12. Review.

192) http://www.affymetrix.com/

193) Samani NJ, Erdmann J, Hall AS, Hengstenberg C, Mangino M, Mayer B, Dixon RJ, Meitinger T, Braund P, Wichmann HE, Barrett JH, König IR, Stevens SE, Szymczak S, Tregouet DA, Iles MM, Pahlke F, Pollard H, Lieb W, Cambien F, Fischer M, Ouwehand W, Blankenberg S, Balmforth AJ, Baessler A, Ball SG, Strom TM, Braenne I, Gieger C, Deloukas P, Tobin MD, Ziegler A, Thompson JR, Schunkert H; WTCCC and the Cardiogenics Consortium.
Genomewide association analysis of coronary artery disease.
N Engl J Med. 2007;357:443-53.

194) Grayson BL, Smith ME, Thomas JW, Wang L, Dexheimer P, Jeffrey J, Fain PR, Nanduri P, Eisenbarth GS, Aune TM.
Genome-wide analysis of copy number variation in type 1 diabetes.
PLoS One. 2010 Nov 15;5(11):e15393.

195) Wilson M, Peters G, Bennetts B, McGillivray G, Wu ZH, Poon C, Algar E.
The clinical phenotype of mosaicism for genome-wide paternal uniparental disomy: two new reports.
Am J Med Genet A. 2008 Jan 15;146(2):137-48.

196) Talseth-Palmer BA, Bowden NA, Meldrum C, Nicholl J, Thompson E, Friend K, Liebelt J, Bratkovic D, Haan E, Yu S, Scott RJ.
A 1q44 deletion, paternal UPD of chromosome 2 and a deletion due to a complex translocation detected in children with abnormal phenotypes using new SNP array technology.
Cytogenet Genome Res. 2009;124:94-101.

197) Friedman JM, Baross A, Delaney AD, Ally A, Arbour L, Armstrong L, Asano J, Bailey DK, Barber S, Birch P, Brown-John M, Cao M, Chan S, Charest DL, Farnoud N, Fernandes N, Flibotte S, Go A, Gibson WT, Holt RA, Jones SJ, Kennedy GC, Krzywinski M, Langlois S, Li HI, McGillivray BC, Nayar T, Pugh TJ, Rajcan-Separovic E, Schein JE, Schnerch A, Siddiqui A, Van Allen MI, Wilson G, Yong SL, Zahir F, Eydoux P, Marra MA.
Oligonucleotide microarray analysis of genomic imbalance in children with mental retardation.
Am J Hum Genet. 2006 Sep;79(3):500-13.

198) Ming JE, Geiger E, James AC, Ciprero KL, Nimmakayalu M, Zhang Y, Huang A, Vaddi M, Rappaport E, Zackai EH, Shaikh TH.
Rapid detection of submicroscopic chromosomal rearrangements in children with multiple congenital anomalies using high density oligonucleotide arrays.
Hum Mutat. 2006 May;27(5):467-73.

199) Friedman J, Adam S, Arbour L, Armstrong L, Baross A, Birch P, Boerkoel C, Chan S, Chai D, Delaney AD, Flibotte S, Gibson WT, Langlois S, Lemyre E, Li HI, MacLeod P, Mathers J, Michaud JL, McGillivray BC, Patel MS, Qian H, Rouleau GA, Van Allen MI, Yong SL, Zahir FR, Eydoux P, Marra MA.
Detection of pathogenic copy number variants in children with idiopathic intellectual disability using 500 K SNP array genomic hybridization.

BMC Genomics. 2009 Nov 16;10:526.

200) Bernardini L, Alesi V, Loddo S, Novelli A, Bottillo I, Battaglia A, Digilio MC, Zampino G, Ertel A, Fortina P, Surrey S, Dallapiccola B.
High-resolution SNP arrays in mental retardation diagnostics: how much do we gain?
Eur J Hum Genet. 2010 Feb;18(2):178-85.

201) Engels H, Wohlleber E, Zink A, Hoyer J, Ludwig KU, Brockschmidt FF, Wieczorek D, Moog U, Hellmann-Mersch B, Weber RG, Willatt L, Kreiss-Nachtsheim M, Firth HV, Rauch A.
A novel microdeletion syndrome involving 5q14.3-q15: clinical and molecular cytogenetic characterization of three patients.
Eur J Hum Genet. 2009 Dec;17(12):1592-9.

202) Sebat J, Lakshmi B, Malhotra D, Troge J, Lese-Martin C, Walsh T, Yamrom B, Yoon S, Krasnitz A, Kendall J, Leotta A, Pai D, Zhang R, Lee YH, Hicks J, Spence SJ, Lee AT, Puura K, Lehtimäki T, Ledbetter D, Gregersen PK, Bregman J, Sutcliffe JS, Jobanputra V, Chung W, Warburton D, King MC, Skuse D, Geschwind DH, Gilliam TC, Ye K, Wigler M.
Strong association of de novo copy number mutations with autism.
Science. 2007 Apr 20;316(5823):445-9.

203) Ozgen HM, van Daalen E, Bolton PF, Maloney VK, Huang S, Cresswell L, van den Boogaard MJ, Eleveld MJ, van 't Slot R, Hochstenbach R, Beemer FA, Barrow M, Barber JC, Poot M.
Copy number changes of the microcephalin 1 gene (MCPH1) in patients with autism spectrum disorders.
Clin Genet. 2009 Oct;76(4):348-56.

204) Pinto D, Pagnamenta AT, Klei L, Anney R, Merico D, Regan R, Conroy J, Magalhaes TR, Correia C, Abrahams BS, Almeida J, Bacchelli E, Bader GD, Bailey AJ, Baird G, Battaglia A, Berney T, Bolshakova N, Bölte S, Bolton PF, Bourgeron T, Brennan S, Brian J, Bryson SE, Carson AR, Casallo G, Casey J, Chung BH, Cochrane L, Corsello C, Crawford EL, Crossett A, Cytrynbaum C, Dawson G, de Jonge M, Delorme R, Drmic I, Duketis E, Duque F, Estes A, Farrar P, Fernandez BA, Folstein

SE, Fombonne E, Freitag CM, Gilbert J, Gillberg C, Glessner JT, Goldberg J, Green A, Green J, Guter SJ, Hakonarson H, Heron EA, Hill M, Holt R, Howe JL, Hughes G, Hus V, Igliozzi R, Kim C, Klauck SM, Kolevzon A, Korvatska O, Kustanovich V, Lajonchere CM, Lamb JA, Laskawiec M, Leboyer M, Le Couteur A, Leventhal BL, Lionel AC, Liu XQ, Lord C, Lotspeich L, Lund SC, Maestrini E, Mahoney W, Mantoulan C, Marshall CR, McConachie H, McDougle CJ, McGrath J, McMahon WM, Merikangas A, Migita O, Minshew NJ, Mirza GK, Munson J, Nelson SF, Noakes C, Noor A, Nygren G, Oliveira G, Papanikolaou K, Parr JR, Parrini B, Paton T, Pickles A, Pilorge M, Piven J, Ponting CP, Posey DJ, Poustka A, Poustka F, Prasad A, Ragoussis J, Renshaw K, Rickaby J, Roberts W, Roeder K, Roge B, Rutter ML, Bierut LJ, Rice JP, Salt J, Sansom K, Sato D, Segurado R, Sequeira AF, Senman L, Shah N, Sheffield VC, Soorya L, Sousa I, Stein O, Sykes N, Stoppioni V, Strawbridge C, Tancredi R, Tansey K, Thiruvahindrapduram B, Thompson AP, Thomson S, Tryfon A, Tsiantis J, Van Engeland H, Vincent JB, Volkmar F, Wallace S, Wang K, Wang Z, Wassink TH, Webber C, Weksberg R, Wing K, Wittemeyer K, Wood S, Wu J, Yaspan BL, Zurawiecki D, Zwaigenbaum L, Buxbaum JD, Cantor RM, Cook EH, Coon H, Cuccaro ML, Devlin B, Ennis S, Gallagher L, Geschwind DH, Gill M, Haines JL, Hallmayer J, Miller J, Monaco AP, Nurnberger JI Jr, Paterson AD, Pericak-Vance MA, Schellenberg GD, Szatmari P, Vicente AM, Vieland VJ, Wijsman EM, Scherer SW, Sutcliffe JS, Betancur C.
Functional impact of global rare copy number variation in autism spectrum disorders.
Nature. 2010 Jul 15;466(7304):368-72.

205) Dunbar AJ, Gondek LP, O'Keefe CL, Makishima H, Rataul MS, Szpurka H, Sekeres MA, Wang XF, McDevitt MA, Maciejewski JP.
250K single nucleotide polymorphism array karyotyping identifies acquired uniparental disomy and homozygous mutations, including novel missense substitutions of c-Cbl, in myeloid malignancies.
Cancer Res. 2008 Dec 15;68(24):10349-57.

206) Schoumans J, Ruivenkamp C, Holmberg E, Kyllerman M, Anderlid BM, Nordenskjold M.
Detection of chromosomal imbalances in children with idiopathic mental retardation by array based comparative genomic hybridisation (array-CGH).
J Med Genet. 2005 Sep;42(9):699-705.

207) Shaw-Smith C, Redon R, Rickman L, Rio M, Willatt L, Fiegler H, Firth H, Sanlaville D, Winter R, Colleaux L, Bobrow M, Carter NP.
Microarray based comparative genomic hybridisation (array-CGH) detects submicroscopic chromosomal deletions and duplications in patients with learning disability/mental retardation and dysmorphic features.
J Med Genet. 2004 Apr;41(4):241-8.

208) Baptista J, Prigmore E, Gribble SM, Jacobs PA, Carter NP, Crolla JA.
Molecular cytogenetic analyses of breakpoints in apparently balanced reciprocal translocations carried by phenotypically normal individuals.
Eur J Hum Genet. 2005 Nov;13(11):1205-12.

209) Di X, Matsuzaki H, Webster TA, Hubbell E, Liu G, Dong S, Bartell D, Huang J, Chiles R, Yang G, Shen MM, Kulp D, Kennedy GC, Mei R, Jones KW, Cawley S.
Dynamic model based algorithms for screening and genotyping over 100 K SNPs on oligonucleotide microarrays.
Bioinformatics. 2005 May 1;21(9):1958-63.

210) http://hapmap.ncbi.nlm.nih.gov/downloads/raw_data/affy500k/

211) Affymetrix GeneChip® Chromosome Copy Number Analysis Tool (CNAT) – Version 4.0 User Guide. March 2006. Available at http://www.affymetrix.com/

212) http://genome.ucsc.edu/

213) http://www.ncbi.nlm.nih.gov/

214) http://rebase.neb.com/

215) Roberts RJ, Vincze T, Posfai J, Macelis D.
REBASE--enzymes and genes for DNA restriction and modification.
Nucleic Acids Res. 2007 Jan;35(Database issue):D269-70.

216) Yang CY, Chou CW, Chen SY, Cheng HM.

Anterior pituitary failure (panhypopituitarism) with balanced chromosome translocation 46,XY,t(11;22)(q24;q13).
Zhonghua Yi Xue Za Zhi (Taipei). 2001 Apr;64(4):247-52.

217) Cappon SL, Duncan AM, Khalifa MM.
Interstitial 6q duplication in an adult male without growth delay or severe mental retardation.
Med Sci Monit. 2000 May-Jun;6(3):581-5.

218) Henegariu O, Heerema NA, Vance GH.
Mild "duplication 6q syndrome": a case with partial trisomy (6)(q23.3q25.3).
Am J Med Genet. 1997 Feb 11;68(4):450-4. Review.

219) Titomanlio L, Giurgea I, Baumann C, Elmaleh M, Sachs P, Chalard F, Aboura A, Verloes A.
A locus for sacral/anorectal malformations maps to 6q25.3 in a 0.3 Mb interval region.
Eur J Hum Genet. 2006 Aug;14(8):971-4.

220) Grossfeld PD, Mattina T, Lai Z, Favier R, Jones KL, Cotter F, Jones C.
The 11q terminal deletion disorder: a prospective study of 110 cases.
Am J Med Genet A. 2004 Aug 15;129(1):51-61.

221) https://decipher.sanger.ac.uk/

222) Tarpey P, Parnau J, Blow M, Woffendin H, Bignell G, Cox C, Cox J, Davies H, Edkins S, Holden S, Korny A, Mallya U, Moon J, O'Meara S, Parker A, Stephens P, Stevens C, Teague J, Donnelly A, Mangelsdorf M, Mulley J, Partington M, Turner G, Stevenson R, Schwartz C, Young I, Easton D, Bobrow M, Futreal PA, Stratton MR, Gecz J, Wooster R, Raymond FL.
Mutations in the DLG3 gene cause nonsyndromic X-linked mental retardation.
Am J Hum Genet. 2004 Aug;75(2):318-24.

223) Pecci, A., Canobbio, I., Balduini, A., Stefanini, L., Cisterna, B., Marseglia, C., Noris, P., Savoia, A., Balduini, C. L., Torti, M.

Pathogenetic mechanisms of hematological abnormalities of patients with MYH9 mutations.
Hum. Molec. Genet. 14: 3169-3178, 2005.

224) Pecci A, Panza E, Pujol-Moix N, Klersy C, Di Bari F, Bozzi V, Gresele P, Lethagen S, Fabris F, Dufour C, Granata A, Doubek M, Pecoraro C, Koivisto PA, Heller PG, Iolascon A, Alvisi P, Schwabe D, De Candia E, Rocca B, Russo U, Ramenghi U, Noris P, Seri M, Balduini CL, Savoia A.
Position of nonmuscle myosin heavy chain IIA (NMMHC-IIA) mutations predicts the natural history of MYH9-related disease.
Hum Mutat. 2008 Mar;29(3):409-17.

225) Sellin, L.; Huber, T. B.; Gerke, P.; Quack, I.; Pavenstadt, H.; Walz, G.
NEPH1 defines a novel family of podocin interacting proteins.
FASEB J. 17: 115-117, 2003.

226) Bhalla, K.; Luo, Y.; Buchan, T.; Beachem, M. A.; Guzauskas, G. F.; Ladd, S.; Bratcher, S. J.; Schroer, R. J.; Balsamo, J.; DuPont, B. R.; Lilien, J.; Srivastava, A. K.
Alterations in CDH15 and KIRREL3 in patients with mild to severe intellectual disability.
Am J Hum Genet. 2008;83:703-13.

227) Heilstedt HA, Ballif BC, Howard LA, Kashork CD and Shaffer LG.
Population data suggest that deletions of 1p36 are a relatively common chromosome abnormality.
Clin Genet 2003: 64: 310–316.

228) Shapira SK, McCaskill C, Northrup H, Spikes AS, Elder FFB, Reid Sutton V, Korenberg JR, Greenberg F, Shaffer LG.
Chromosome 1p36 Deletions: The Clinical Phenotype and Molecular Characterization of a Common Newly Delineated Syndrome.
Am. J. Hum. Genet. 61:642–650, 1997.

229) Heilstedt HA, Ballif BC, Howard LA, Lewis RA, Stal S, Kashork CD, Bacino CA, Shapira SK, Shaffer LG.

Physical Map of 1p36, Placement of Breakpoints in Monosomy 1p36, and Clinical Characterization of the Syndrome.
Am. J. Hum. Genet. 72:1200–1212, 2003.

230) Gajecka M, Mackay KL, Shaffer LG.
Monosomy 1p36 deletion syndrome.
Am J Med Genet C Semin Med Genet. 2007 Nov 15;145C(4):346-56. Review.

231) Battaglia A, Hoyme HE, Dallapiccola B, Zackai E, Hudgins L, McDonald-McGinn D, Bahi-Buisson N, Romano C, Williams CA, Brailey LL, Zuberi SM, Carey JC.
Further delineation of deletion 1p36 syndrome in 60 patients: a recognizable phenotype and common cause of developmental delay and mental retardation.
Pediatrics. 2008 Feb;121(2):404-10. Erratum in: Pediatrics. 2008 May;121(5):1081. Braley, Lisa L [corrected to Brailey, Lisa L].

232) Tartaglia M, Niemeyer CM, Fragale A, Song X, Buechner J, Jung A, Hahlen K, Hasle H, Licht JD, Gelb BD.
Somatic mutations in PTPN11 in juvenile myelomonocytic leukemia, myelodysplastic syndromes and acute myeloid leukaemia.
Nat Genet. 2003;34:148-50.

233) Arepally G, Rebbeck TR, Song W, Gilliland G, Maris JM, Poncz M.
Evidence for genetic homogeneity in a familial platelet disorder with predisposition to acute myelogenous leukemia (FPD/AML).
Blood. 1998;92:2600-2.

234) Azuma N, Yamaguchi Y, Handa H, Tadokoro K, Asaka A, Kawase E, Yamada M.
Mutations of the PAX6 gene detected in patients with a variety of optic-nerve malformations.
Am J Hum Genet. 2003;72:1565-70.

235) Brant AM, Schachat AP, White RI.
Ocular manifestations in hereditary hemorrhagic telangiectasia (Rendu-Osler-Weber disease).

Am J Ophthal. 1989;107:642-6.

236) Fulbright RK, Chaloupka JC, Putman CM, Sze GK, Merriam MM, Lee GK, Fayad PB, Awad IA, White RI Jr.
MR of hereditary hemorrhagic telangiectasia: prevalence and spectrum of cerebrovascular malformations.
Am J Neuroradiol. 1998;19:477-84.

237) Garcia-Tsao G, Korzenik JR, Young L, Henderson KJ, Jain D, Byrd B, Pollak JS, White RI Jr.
Liver disease in patients with hereditary hemorrhagic telangiectasia.
New Eng J Med. 2000;343:931-6.

238) Plauchu H, de Chadarevian JP, Bideau A, Robert JM.
Age-related clinical profile of hereditary hemorrhagic telangiectasia in an epidemiologically recruited population.
Am J Med Genet. 1989;32:291-7.

239) Porteous MEM, Burn J, Proctor SJ.
Hereditary haemorrhagic telangiectasia: a clinical analysis.
J Med Genet. 1992;29:527-30.

240) Aassar OS, Friedman CM, White RIJr.
The natural history of epistaxis in hereditary hemorrhagic telangiectasia.
Laryngoscope. 1991;101:977-80.

241) Faughnan ME, Palda VA, Garcia-Tsao G, Geisthoff UW, McDonald J, Proctor DD, Spears J, Brown DH, Buscarini E, Chesnutt MS, Cottin V, Ganguly A, Gossage JR, Guttmacher AE, Hyland RH, Kennedy SJ, Korzenik J, Mager JJ, Ozanne AP, Piccirillo JF, Picus D, Plauchu H, Porteous ME, Pyeritz RE, Ross DA, Sabba C, Swanson K, Terry P, Wallace MC, Westermann CJ, White RI, Young LH, Zarrabeitia R.
International Guidelines for the Diagnosis and Management of Hereditary Hemorrhagic Telangiectasia.
J Med Genet. 2011 Feb;48(2):73-87.

242) Krasner A, Wallace L, Thiagalingam A, Jones C, Lengauer C, Minahan L, Ma Y, Kalikin L, Feinberg AP, Jabs EW, Tunnacliffe A, Baylin SB, Ball DW, Nelkin BD.
Cloning and chromosomal localization of the human BARX2 homeobox protein gene.
Gene. 2000 May 30;250(1-2):171-80.

243) Hjalt TA, Murray JC.
The human BARX2 gene: genomic structure, chromosomal localization, and single nucleotide polymorphisms.
Genomics. 1999 Dec 15;62(3):456-9.

244) http://pfam.sanger.ac.uk/

245) Wenger SL, Grossfeld PD, Siu BL, Coad JE, Keller FG, Hummel M.
Molecular characterization of an 11q interstitial deletion in a patient with the clinical features of Jacobsen syndrome.
Am J Med Genet A. 2006 Apr 1;140(7):704-8.

246) Raslova H, Komura E, Le Couédic JP, Larbret F, Debili N, Feunteun J, Danos O, Albagli O, Vainchenker W, Favier R.
FLI1 monoallelic expression combined with its hemizygous loss underlies Paris-Trousseau/Jacobsen thrombopenia.
J Clin Invest. 2004 Jul;114(1):77-84.

247) Bakrania P, Efthymiou M, Klein JC, Salt A, Bunyan DJ, Wyatt A, Ponting CP, Martin A, Williams S, Lindley V, Gilmore J, Restori M, Robson AG, Neveu MM, Holder GE, Collin JR, Robinson DO, Farndon P, Johansen-Berg H, Gerrelli D, Ragge NK.
Mutations in BMP4 cause eye, brain, and digit developmental anomalies: overlap between the BMP4 and hedgehog signaling pathways.
Am J Hum Genet. 2008 Feb;82(2):304-19.

248) Haghi M, Dewan A, Jones KL, Reitz R, Jones C, Grossfeld P.
Endocrine abnormalities in patients with Jacobsen (11q-) syndrome.
Am J Med Genet A. 2004 Aug 15;129(1):62-3.

249) Pivnick EK, Velagaleti GV, Wilroy RS, Smith ME, Rose SR, Tipton RE, Tharapel AT.
Jacobsen syndrome: report of a patient with severe eye anomalies, growth hormone deficiency, and hypothyroidism associated with deletion 11 (q23q25) and review of 52 cases.
J Med Genet. 1996 Sep;33(9):772-8. Review.

250) Michaelis RC, Velagaleti GV, Jones C, Pivnick EK, Phelan MC, Boyd E, Tarleton J, Wilroy RS, Tunnacliffe A, Tharapel AT.
Most Jacobsen syndrome deletion breakpoints occur distal to FRA11B.
Am J Med Genet. 1998 Mar 19;76(3):222-8.

251) Nagase T, Nakayama M, Nakajima D, Kikuno R, Ohara O.
Prediction of the coding sequences of unidentified human genes. XX. The complete sequences of 100 new cDNA clones from brain which code for large proteins in vitro.
DNA Res. 2001;8:85-95.

252) Goor DA, Lillehei CW.
Embryology of the heart in congenital malformation of the heart.
New York: Grune and Stratton; 1975. pp. 79-90.

253) Van Praagh R, Van Praagh S, Nebesar RA, Muster AJ, Sinha SN, Paul MH.
Tetralogy of Fallot: underdevelopment of the pulmonary infundibulum and its sequelae.
Am J Cardiol. 1970 Jul;26(1):25-33.

254) Weinzimer SA, McDonald-McGinn DM, Driscoll DA, Emanuel BS, Zackai EH, Moshang T.
Growth hormone deficiency in patients with 22q11.2 deletion: expanding the phenotype.
Pediatrics. 1998; 101: 929–32.

255) McDonald-McGinn DM, Kirschner R, Goldmuntz E, Sullivan K, Eicher P, Gerdes M, Moss E, Solot C, Wang P, Jacobs I, Handler S, Knightly C, Heher K, Wilson M,

Ming JE, Grace K, Driscoll D, Pasquariello P, Randall P, Larossa D, Emanuel BS, Zackai EH.
The Philadelphia story: the 22q11.2 deletion: report on 250 patients.
Genet Couns. 1999; 10: 11–24.

256) Bassett AS, Chow EW, Husted J, Weksberg R, Caluseriu O, Webb GD, Gatzoulis MA.
Clinical features of 78 adults with 22q11 Deletion Syndrome.
Am J Med Genet A. 2005 Nov 1;138(4):307-13.

257) Gong W, Gottlieb S, Collins J, Blescia A, Dietz H, Goldmuntz E, McDonald-McGinn DM, Zackai EH, Emanuel BS, Driscoll DA, Budarf ML.
Mutation analysis of TBX1 in non-deleted patients with features of DGS/VCFS or isolated cardiovascular defects.
J Med Genet. 2001; 38: E45.

258) Yagi H, Furutani Y, Hamada H, Sasaki T, Asakawa S, Minoshima S, Ichida F, Joo K, Kimura M, Imamura S, Kamatani N, Momma K, Takao A, Nakazawa M, Shimizu N, Matsuoka R.
Role of TBX1 in human del22q11.2 syndrome.
Lancet. 2003;362:1366-73.

259) Barakat AJ, Pearl PL, Acosta MT, Runkle BP.
22q13 deletion syndrome with central diabetes insipidus: a previously unreported association.
Clin Dysmorphol. 2004 Jul;13(3):191-4.

260) McDonald-McGinn DM, Tonnesen MK, Laufer-Cahana A, Finucane B, Driscoll DA, Emanuel BS, Zackai EH.
Phenotype of the 22q11.2 deletion in individuals identified through an affected relative: cast a wide FISHing net!
Genet Med. 2001; 3: 23–9.

261) Greenway SC, Pereira AC, Lin JC, DePalma SR, Israel SJ, Mesquita SM, Ergul E, Conta JH, Korn JM, McCarroll SA, Gorham JM, Gabriel S, Altshuler DM,

Quintanilla-Dieck Mde L, Artunduaga MA, Eavey RD, Plenge RM, Shadick NA, Weinblatt ME, De Jager PL, Hafler DA, Breitbart RE, Seidman JG, Seidman CE.
De novo copy number variants identify new genes and loci in isolated sporadic tetralogy of Fallot.
Nat Genet. 2009 Aug;41(8):931-5.

262) Neal J, Apse K, Sahin M, Walsh CA, Sheen VL.
Deletion of chromosome 1p36 is associated with periventricular nodular heterotopia.
Am J Med Genet. 2006;140A:1692-5.

263) Rudnik-Schoneborn S, Zerres K, Hausler M, Lott A, Krings T, Schuler HM.
A new case of proximal monosomy 1p36, extending the phenotype.
Am J Med Genet. 2008;146A:2018-22.

264) Redon R, Rio M, Gregory SG, Cooper RA, Fiegler H, Sanlaville D, Banerjee R, Scott C, Carr P, Langford C, Cormier-Daire V, Munnich A, Carter NP, Colleaux L.
Tiling path resolution mapping of constitutional 1p36 deletions by array-CGH: contiguous gene deletion or ‘‘deletion with positional effect’’ syndrome?
J Med Genet 2005;42:166-71.

265) Rosenfeld JA, Crolla JA, Tomkins S, Bader P, Morrow B, Gorski J, Troxell R, Forster-Gibson C, Cilliers D, Hislop RG, Lamb A, Torchia B, Ballif BC, Shaffer LG.
Refinement of causative genes in monosomy 1p36 through clinical and molecular cytogenetic characterization of small interstitial deletions.
Am J Med Genet A. 2010 Aug;152A(8):1951-9.

266) Bruno DL, Ganesamoorthy D, Schoumans J, Bankier A, Coman D, Delatycki M, Gardner RJ, Hunter M, James PA, Kannu P, McGillivray G, Pachter N, Peters H, Rieubland C, Savarirayan R, Scheffer IE, Sheffield L, Tan T, White SM, Yeung A, Bowman Z, Ngo C, Choy KW, Cacheux V, Wong L, Amor DJ, Slater HR.
Detection of cryptic pathogenic copy number variations and constitutional loss of heterozygosity using high resolution SNP microarray analysis in 117 patients referred for cytogenetic analysis and impact on clinical practice.
J Med Genet. 2009 Feb;46(2):123-31.

267) Reymond A, Henrichsen CN, Harewood L, Merla G.
Side effects of genome structural changes.
Curr Opin Genet Dev. 2007 Oct;17(5):381-6. Review.

268) Shaikh TH, Gai X, Perin JC, Glessner JT, Xie H, Murphy K, O'Hara R, Casalunovo T, Conlin LK, D'Arcy M, Frackelton EC, Geiger EA, Haldeman-Englert C, Imielinski M, Kim CE, Medne L, Annaiah K, Bradfield JP, Dabaghyan E, Eckert A, Onyiah CC, Ostapenko S, Otieno FG, Santa E, Shaner JL, Skraban R, Smith RM, Elia J, Goldmuntz E, Spinner NB, Zackai EH, Chiavacci RM, Grundmeier R, Rappaport EF, Grant SF, White PS, Hakonarson H.
High-resolution mapping and analysis of copy number variations in the human genome: a data resource for clinical and research applications.
Genome Res. 2009 Sep;19(9):1682-90.

269) McMullan DJ, Bonin M, Hehir-Kwa JY, de Vries BB, Dufke A, Rattenberry E, Steehouwer M, Moruz L, Pfundt R, de Leeuw N, Riess A, Altug-Teber O, Enders H, Singer S, Grasshoff U, Walter M, Walker JM, Lamb CV, Davison EV, Brueton L, Riess O, Veltman JA.
Molecular karyotyping of patients with unexplained mental retardation by SNP arrays: a multicenter study.
Hum Mutat. 2009 Jul;30(7):1082-92.

270) Korn JM, Kuruvilla FG, McCarroll SA, Wysoker A, Nemesh J, Cawley S, Hubbell E, Veitch J, Collins PJ, Darvishi K, Lee C, Nizzari MM, Gabriel SB, Purcell S, Daly MJ, Altshuler D.
Integrated genotype calling and association analysis of SNPs, common copy number polymorphisms and rare CNVs.
Nat Genet. 2008 Oct;40(10):1253-60.

271) Nannya Y, Sanada M, Nakazaki K, Hosoya N, Wang L, Hangaishi A, Kurokawa M, Chiba S, Bailey DK, Kennedy GC, Ogawa S.
A robust algorithm for copy number detection using high-density oligonucleotide single nucleotide polymorphism genotyping arrays.
Cancer Res. 2005 Jul 15;65(14):6071-9.

272) Olson LE, Zhang J, Taylor H, Rose DW, Rosenfeld MG.
Barx2 functions through distinct corepressor classes to regulate hair follicule remodeling.
Proc Nat Acad Sci. 2005;102:3708-13.

273) Jones FS, Kioussi C, Copertino DW, Kallunki P, Holst BD, Edelman GM.
Barx2, a new homeobox gene of the Bar class, is expressed in neural and craniofacial structures during development.
Proc Nat Acad Sci. 1997;94:2632-7.

274) Bennett CP, Betts DR, Seller MJ.
Deletion 14(q22-q23) associated with anophthalmia, absent pituitary, and other abnormalities.
J Med Genet. 1991;28:280-1.

275) Elliott J, Maltby EL, Reynolds B.
A case of deletion 14(q22.1q22.3) associated with anophthalmia and pituitary abnormalities.
J Med Genet. 1993;30:251-2.

276) Lemyre E, Lemieux N, Decarie JC, Lambert M.
Del(14)(q22.1q23.2) in a patient with anophthalmia and pituitary hypoplasia.
Am J Med Genet. 1998;77:162-5.

277) Ahmad ME, Dada R, Dada T, Kucheria K.
14q(22) deletion in a familial case of anophthalmia with polydactyly.
Am J Med Genet. 2003;120A:117-22.

278) Nolen LD, Amor D, Haywood A, St. Heaps L, Willcock C, Mihelec M, Tam P, Billson F, Grigg J, Peters G, Jamieson RV.
Deletion at 14q22-23 indicates a contiguous gene syndrome comprising anophthalmia, pituitary hypoplasia, and ear anomalies.
Am J Med Genet. 2006;140A:1711-8.

279) Hayashi S, Okamoto N, Makita Y, Hata A, Imoto I, Inazawa J.

Heterozygous deletion at 14q22.1-q22.3 including the BMP4 gene in a patient with psychomotor retardation, congenital corneal opacity and feet polysyndactyly.
Am J Med Genet A. 2008 Nov 15;146A(22):2905-10.

280) Dateki S, Kosaka K, Hasegawa K, Tanaka H, Azuma N, Yokoya S, Muroya K, Adachi M, Tajima T, Motomura K, Kinoshita E, Moriuchi H, Sato N, Fukami M, Ogata T.
Heterozygous orthodenticle homeobox 2 mutations are associated with variable pituitary phenotype.
J Clin Endocrinol Metab. 2010 Feb;95(2):756-64.

281) Dateki S, Fukami M, Sato N, Muroya K, Adachi M, Ogata T.
OTX2 mutation in a patient with anophthalmia, short stature, and partial growth hormone deficiency: functional studies using the IRBP, HESX1, and POU1F1 promoters.
J Clin Endocrinol Metab. 2008; 93:3697–3702.

282) Wyatt A, Bakrania P, Bunyan DJ, Osborne RJ, Crolla JA, Salt A, Ayuso C, Newbury-Ecob R, Abou-Rayyah Y, Collin JR, Robinson D, Ragge N.
Novel heterozygous OTX2 mutations and whole gene deletions in anophthalmia, microphthalmia and coloboma.
Hum Mutat. 2008;29:E278–E283.

283) Ashkenazi-Hoffnung L, Lebenthal Y, Wyatt AW, Ragge NK, Dateki S, Fukami M, Ogata T, Phillip M, Gat-Yablonski G.
A novel loss-of-function mutation in OTX2 in a patient with anophthalmia and isolated growth hormone deficiency.
Hum Genet. 2010 Jun;127(6):721-9.

284) Henderson RH, Williamson KA, Kennedy JS, Webster AR, Holder GE, Robson AG, FitzPatrick DR, van Heyningen V, Moore AT.
A rare de novo nonsense mutation in OTX2 causes early onset retinal dystrophy and pituitary dysfunction.
Mol Vis. 2009 Nov 21;15:2442-7.

285) Schilter KF, Schneider A, Bardakjian T, Soucy J-F, Tyler RC, Reis LM, Semina EV.
OTX2 microphthalmia syndrome: four novel mutations and delineation of a phenotype.
Clin Genet. 2011;79:158–68.

286) Gonzalez-Rodriguez J, Pelcastre EL, Tovilla-Canales JL, Garcia-Ortiz JE, Amato-Almanza M, Villanueva-Mendoza C, Espinosa-Mattar Z, Zenteno JC.
Mutational screening of CHX10, GDF6, OTX2, RAX and SOX2 genes in 50 unrelated microphthalmiaeanophthalmiaecoloboma (MAC) spectrum cases.
Br J Ophthalmol. 2010;94:1100-4.

287) Balikova I, De Ravel T, Ayuso C, Thienpont B, Casteels I, VillaverdeC, Devriendt K, Fryns JP, Vermeesch JR.
High frequency of submicroscopic chromosomal deletions in patients with idiopathic congenital eye malformations.
Am J Ophthal. Epub 2010 Nov 25.

Appendix A

Patient Pro-forma

Patient's NAME: **SEX: M F**
DATE of BIRTH: **DATE of EXAMINATION:**
HOSPITAL/CONSULTANT:
HOSPITAL No.:

Mother's NAME: **DATE of BIRTH:**
Father's NAME: **DATE of BIRTH:**

1) Family history

recurrent miscarriages: **No** **Yes**
If Yes, details:

mental retardation: **No** **Yes**
If Yes, details:

congenital malformations: **No** **Yes**
If Yes, details:

cancer: **No** **Yes**
If Yes, details:

known genetic conditions: **No** **Yes**
If Yes, details:

Parent consanguinity: **No** **Yes**
If Yes, degree and relationship within the family tree:

Family tree

2) Normal pregnancy and delivery? **Yes** **No**
If No, details:

Week of gestation at birth:

Delivery:

maternal smoking: **No** **Yes**
If Yes, details:

maternal alcohol **No** **Yes**
If Yes, details:

APGAR score at 1': 5':

3) Normal psychomotor development? **Yes** **No**
If No, details:

Degree and profile of cognitive delay (including scale used for assessment, and age at assessment):

Normal brain MRI? **Yes** **No**
If No, details:

Date of examination:

Normal EEG? **Yes** **No**
If No, details:

Date of examination:

Other neurological symptoms? **No** **Yes**
If Yes, details:

Other investigations? **No** **Yes**
If Yes, details:

4) Clinical examination

At birth
Current

Length/height:
Weight:
Head circumference:

Head and Neck

Head shape:

Hair/eyebrows/eyelashes:

Eyes/palpebral fissures/eye distance:

Ears:

Nose:

Philtrum:

Mouth/lips/gums/palate/tongue:

Teeth:

Chin:

Neck:

Bones, joints and muscles

Spine:

Thorax shape/ribs/intermamillary distance:

X-ray skeletal survey/other skeletal anomalies:

Bone age:

Joints:

Muscles:

Hands and Feet

Hand lenght: cm Middle finger lenght: cm

Fingers and toes:

syndactyly If Yes, details:	**No**	**Yes**
camptodactyly If Yes, details:	**No**	**Yes**
clinodactyly If Yes, details:	**No**	**Yes**
broad thumb	**No**	**Yes**
broad hallux	**No**	**Yes**
sandal gap	**No**	**Yes**

Palmar and plantar creases/other ridges/pads:

Nails:

Skin

Are extensibility, trophic properties and vascular pattern normal? **Yes** **No**
If No, details:

Is body hair normally distributed? **Yes** **No**
If No, details:

Are skin spots (hyper- hypopigmented, etc) present? **No** **Yes**
If Yes, details:

Are keloids or other abnormal scar formation present? **No** **Yes**
If Yes, details:

Genital organs/perineal region

MALE

Penis:

Testicles/volume:

Scrotum:

FEMALE

External genitalia:

Anal orifice:

Internal organs

Normal echocardiography? **Yes** **No**
If No, details:

Date of examination:

Normal abdominal echography? **Yes** **No**
If No, details:

Date of examination:

Other investigations? **No** **Yes**
If Yes, details:

5) Endocrinological examination

Mid Parental Height:

Spontaneous Puberty: **Yes** **No**

VISUAL ACUITY
Right Eye: Left Eye:
Right Optic Disc: Left Optic Disc:

ERG (date: / /):

VER (date: / /):

Other Ophthalmological Features:

Free Thyroxine:

Basal TSH: TRH Test Peak TSH:

Basal Prolactin: TRH Test Peak Prolactin:

GH Provocation Test Type:

Peak GH:

Basal Cortisol: Peak Cortisol On Synacthen:

Basal LH: Peak LH On LHRH:

Basal FSH: Peak FSH On LHRH:

Diabetes Insipidus: **Yes** **No**

Any Other Endocrine Results:

Hydrocortisone Treatment (Age):

Thyroxine Treatment (Age):

GH Treatment (Age):

DDAVP Treatment (Age):

Sex Steroids (Age):

Zoladex Treatment (Age):

Type Of Neuroimaging:

Results:

Final Diagnosis:

6) Genetic testing

Candidate Genes to be Tested for the Endocrinological Phenotype:

ISCN +550 karyoptye:

Subtelomeric FISH:

Other tests:

Patient DNA Sample No.:

Source of DNA (fresh blood, cell culture, etc.):

Appendix B

Title of Project: GENETIC ANALYSIS OF CHILDREN WITH FOREBRAIN, EYE AND/OR PITUITARY DEFECTS

Investigator: **Professor M.T. DATTANI**

We would like to invite your child to take part in our research study. Before you decide we would like you to understand why the research is being done and what it would involve for you and your child. One of our team will go through the information sheet with you and answer any questions you have. We would suggest that this should take about 10 minutes Talk to others about the study if you wish. Ask us if there is anything that is not clear. Take time to decide whether or not you wish to take part. Thank you for reading this.

Introduction

The pituitary gland in the brain makes a number of chemicals called hormones that help children grow and develop normally. In some children who do not grow well, the pituitary gland may not make growth hormone (GH) and/or other hormones. The gland may be very small or even absent. These children would need to be treated with the hormones that are missing. Occasionally, the small pituitary gland may be associated with abnormalities affecting the eyes and the brain; this is called septo-optic dysplasia or SOD.

We now know that the way your child's body changes and grows depends on the genetic material (called DNA, which is made up of thousands of genes) that your child has inherited from their parents. Changes within genes are the reason why we are all very different to each other. Normally, your child has two copies of a gene, one that comes to them from their father and one that comes to them from their mother. Sometimes a change within a gene that your child gets from his/her parents can lead to a medical condition. So far, we only know some of the genes that are important for normal pituitary development.

The aim of the study

In this study, we aim to study the genes controlling the development of the brain and pituitary gland. We have recently found that changes in a number of genes are associated with a small pituitary gland and a lack of growth hormone (GH) in some of our patients. We now want to look at children with these conditions in more detail and to examine their DNA for abnormalities in these and other genes that are important for the normal development of the brain. We hope that this will help us to understand why children suffer from these particular conditions.

Why is the study being done?

This study will help us to understand why children develop abnormalities of the forebrain, eyes and pituitary gland. Additionally, we will gain further insights into the complex development of these structures. Knowledge of the exact genetic mechanism for the underlying disease will enable us to make an earlier diagnosis in further affected children from the same family, and also to offer ante-natal diagnosis in certain cases. This will reduce the complications that could potentially arise in children with these disorders. Finally, understanding these conditions will enable us to find the best ways of making the diagnosis ie using the best tests available so that the diagnosis can be made with minimal discomfort to the patient.

How is the study being done?
We need to take a small blood sample (2 teaspoonfuls) from your child. To minimise discomfort, we will perform the blood test using local anaesthetic cream prior to collection of blood. Genetic material (DNA) will then be extracted from the blood, and full genetic analysis will be performed on these samples. The blood test will be performed by a member of the Paediatric Endocrinology team at Great Ormond Street Children's Hospital during one of your child's visits to the hospital. Only a single sample of blood is required for the study. Where possible, the blood sample will be taken at the same time as other tests of pituitary gland function which may need to be performed on your child from time to time in the out-patient clinic. If a change (mutation) is found within one of the genes that are important for pituitary development, then further blood samples may be required from your child and the rest of your family. However, the requirement for these samples will be discussed in detail with you and your family.

What will happen to the blood sample after it is taken?
The blood sample will be processed by members of Professor Dattani's team and stored without your child's name or details on it. Only Professor Dattani and the doctors who are directly involved in your child's medical care will be able to identify the sample by using a password protected database. This study is ongoing and the sample will not therefore be destroyed unless you ask for it to be destroyed. Ethical approval for this study to be ongoing will be asked for at regular intervals. The blood sample will remain in the Institute of Child Health (attached to Great Ormond Street Hospital); it will not be sent anywhere else.

What are the risks and discomfort?
No risk to your child can be foreseen. There is discomfort from a single needle prick for blood sampling, but this will be minimised by using local anaesthetic cream.

What are the potential benefits?
This study may help us to understand why your child has developed their problems. Additionally, we may be able to make the diagnosis earlier in future children who may have the condition, and where one child in the family already has the disorder, we may be able to make a diagnosis before birth in future pregnancies. An improved understanding of these conditions will help us to find the best ways of making the diagnosis i.e. using the best tests available so that the diagnosis can be made with minimal discomfort to the child. Some of these genes are associated with a changing (evolving) picture, with more hormonal abnormalities appearing with time. If that is the case, then we will be in a better position to anticipate these abnormalities once we have the genetic information and hence we will be able to diagnose the problem more rapidly.

Who will have access to the case/research records?
Only the researchers and a representative of the Research Ethics Committee will have access to the data collected during the study. We will tell people what we have learned in the study in reports and publications, but nobody will learn anything personal about your child, or any other child, by reading these reports or publications. The use of some types of personal information is safeguarded by the Data Protection Act 1998 (DPA). The DPA places an obligation on those who record or use personal information, but also gives rights to people about whom information is held. If you have any questions about data protection, contact the Data Protection officer via the switchboard on 020 7405 9200 extension 5217. We will also inform your general practitioner that you will be

taking part in this study.

What are the arrangements for compensation?
The project has been approved by an independent research ethics committee (Chelsea and Westminster) who believe that it is of minimal risk to you. However, research can carry unforeseen risks and we want you to be informed of your rights in the unlikely event that any harm should occur as a result of taking part in this study.

This research is covered by a compensation scheme which may apply in the event of any significant harm resulting to your child from involvement in the study. Under this scheme, it would not be necessary for you to prove fault. You also have the right to claim damages in a court of law. This would require you to prove fault on the part of the Hospital/Institute and/or any manufacturer involved.

Does my child have to take part in this study?
No. If you decide, now or at a later stage, that your child does not wish to participate in this research project, that is entirely your right, **and will not in any way prejudice any present or future treatment.**

Who is organizing and funding the study?
The study is being funded by the Wellcome Trust and a number of other charities.

Who do I speak to if problems arise?
Please contact Professor Dattani directly with any problems relating to the study.
If you have any complaints about the way in which this research project has been, or is being conducted, please, in the first instance, discuss them with the researcher. If the problems are not resolved, or you wish to comment in any other way, please contact the Chairman of the Research Ethics Committee, by post via the Research and Development Office, Institute of Child Health, 30 Guilford Street, London WC1N 1EH, or if urgent, by telephone on 0207 905.2620, and the Committee administration will put you in contact with him.

Researcher who will have contact with the family
Professor Mehul Dattani, Professor of Paediatric Endocrinology

Address of Researcher
Developmental Endocrinology Research Group, Clinical and Molecular Genetics Unit, UCL Institute of Child Health, 30 Guilford Street, London, WC1N 1EH.
Telephone: 020 7905 2657
Message Pager via GOSH switchboard.